[AMERICAN JOURNAL OF SCIENCE, VOL. 276, FEBRUARY, 1976, P. 97-240]

American Journal of Science

FEBRUARY 1976

THEORETICAL PREDICTION OF THE THERMODYNAMIC PROPERTIES OF AQUEOUS ELECTROLYTES AT HIGH PRESSURES AND TEMPERATURES. III. EQUATION OF STATE FOR AQUEOUS SPECIES AT INFINITE DILUTION

HAROLD C. HELGESON and DAVID H. KIRKHAM

Department of Geology and Geophysics, University of California, Berkeley, California 94720

ABSTRACT. Calculation of the electrostatic properties of H_2O as a function of solvent density permits controlled extrapolation to infinite dilution of apparent molal volumes of aqueous electrolytes at high pressures and temperatures. Extrapolations of this kind were carried out for 19 electrolytes with the aid of the molal analog of the Redlich-Meyer equation and published density measurements at 20 bars and temperatures from 25° to 200°C. Isobaric regression of the partial molal volumes at infinite dilution ($\bar{V}^\circ$) and corresponding isothermal standard partial molal compressibilities ($-(\partial\bar{V}^\circ/\partial P)_T$) as a function of temperature with a simple equation of state providing for the intrinsic volume of the electrolyte, electrostriction collapse of the solvent structure, and ion solvation affords close representation of experimental data at both high and low pressures and temperatures. The solvation contribution to the electrostriction volume loss is represented in the model by the classical Drude-Nernst equation, and the electrostriction collapse term by an asymptotic function of temperature, which is linear in pressure. The Drude-Nernst equation was evaluated using the electrostatic properties of H_2O to compute effective electrostatic radii of solvated ions from semiempirical relations providing for reduced orientational polarizability of H_2O molecules in the solvation shells about cations. Prediction of the change in $\bar{V}^\circ$ with increasing pressure as a function of temperature indicates that the extremum in the curve representing the isobaric dependence of $\bar{V}^\circ$ on temperature at low pressures gives way to a sigmoid configuration above ~ 1 to 2 kb. This behavior results from additive contributions consisting of an intrinsic volume (which is independent of pressure and temperature), a negative volume change attending local collapse of the solvent structure (which may be either a positive or negative function of temperature, depending on the pressure), and a negative volume of solvation (which becomes exponentially more negative as temperature increases and the dielectric constant of H_2O decreases). Both negative terms exhibit a positive dependence on pressure at low temperatures, but the isothermal pressure derivative of the collapse volume (which is independent of pressure) decreases (and becomes negative in the case of 1:1 electrolytes) as temperature increases. In contrast, the pressure dependence of the solvation term increases exponentially with increasing temperature, which causes the standard partial molal compressibility to maximize with increasing temperature at constant pressure. At high temperatures, the volumetric and electrostatic properties of the solvent cause $\bar{V}^\circ$, $(\partial\bar{V}^\circ/\partial T)_P$, and $-(\partial\bar{V}^\circ/\partial P)_T$ to become large negative numbers and approach $-\infty$ at the critical point for H_2O. Data currently available permit calculation of the standard partial molal properties of electrolytes and ionic species at temperatures and pressures to 600°C and 5 kb. The requisitive coefficients can be obtained by regression of isobaric low-temperature data and/or estimated from correlation algorithms. High pressure/temperature values of $\bar{V}^\circ$, $(\partial\bar{V}^\circ/\partial T)_P$, and $(\partial\bar{V}^\circ/\partial P)_T$ are given in tables and diagrams to facilitate geologic application of the equation of state, which can be used to compute the relative stabilities of minerals in hydrothermal systems.

INTRODUCTION

Integration of geologic observations with theoretical calculations describing equilibrium and mass transfer among minerals and aqueous

electrolyte solutions is a requisite for understanding metasomatic processes responsible for mineralogic changes in rocks. The purpose of this communication is to derive thermodynamic equations and coefficients for computing the relative standard partial molal properties of the aqueous species involved in these processes.

The occurrence of mineralogic changes in most igneous, sedimentary, and metamorphic rocks is a manifestation of the important role played by sea water, interstitial brines, meteoric water, or hydrothermal vein solutions in geochemical processes. Because few thermodynamic data are available for such solutions at high pressures and temperatures, calculation of the extent to which electrolytes interact with minerals under these conditions requires a comprehensive equation of state for aqueous species as well as predictive equations for the thermodynamic/electrostatic properties of the solvent. The first paper in this series (Helgeson and Kirkham, 1974a) is concerned with the latter equations, some of which were used in the second contribution (Helgeson and Kirkham, 1974b) to compute Debye-Hückel parameters for activity coefficients and the partial molal properties of electrolytes at high pressures and temperatures.[1] These calculations permit accurate interpretation of density and compressibility data, which are used in the present communication to formulate a general equation of state for computing the standard thermodynamic properties of aqueous species at pressures and temperatures to 5 kb and 600°C.

The standard state adopted in this study is one of unit activity of aqueous species in a hypothetical one (mean) molal solution. Accordingly, activity coefficients approach unity at infinite dilution at all pressures and temperatures, as does the activity of the solvent.

NOTATION

a	— Gibson-Tait coefficient in equation (2).
$\hat{a}$	— empirical correlation coefficient in equations (121) through (125).
a_1, a_2, a_3, a_4	— equation of state coefficients for an electrolyte.
$a_{1,j}, a_{2,j}, a_{3,j}, a_{4,j}$	— equation of state coefficients for the conventional properties of the jth ion.
a_{H_2O}	— activity of H_2O.

[1] Several errors in parts I and II (Helgeson and Kirkham, 1974a and b, respectively) have come to our attention since publication. The value of R shown in table 1 of part I as 8.31424 joules mole^{-1} (°K)$^{-1}$ should read 8.31440 joules mole^{-1} (°K)$^{-1}$. The captions of tables 36 and 37 in part I should be interchanged, as should the signs preceding the last two terms on the right side of equation (60) in part II. Equation (73) in part II should be replaced by

$$\begin{aligned}\bar{E}x_2 - \bar{E}x^\circ_2 &= \left(\frac{\partial \bar{V}_2}{\partial T}\right)_P - \left(\frac{\partial \bar{V}^\circ_2}{\partial T}\right)_P \\ &= 2.303\nu R\left(\left(\frac{\partial \log \gamma_\pm}{\partial P}\right)_T + T\left(\frac{\partial\left(\frac{\partial \log \gamma_\pm}{\partial P}\right)_T}{\partial T}\right)_P\right) \\ &= \frac{\bar{V}_2 - \bar{V}^\circ_2}{T} + 2.303\nu RT\left(\frac{\partial\left(\frac{\partial \log \gamma_\pm}{\partial P}\right)_T}{\partial T}\right)_P\end{aligned}$$

å	— ion size parameter in the Debye-Hückel equation.
$\hat{a}_j$	— proportionality constant in equation (62A).
a_1^*, a_2^*	— empirical correlation coefficients in equation (72).
abs	— superscript indicating an absolute thermodynamic property.
aq, aqueous	— subscripts denoting the aqueous state.
A	— distance in ångström units (1A = 10^{-10}m).
A+	— general representation of a cation.
A_γ	— Debye-Hückel limiting law parameter for activity coefficients defined by equation (48).
A_V	— Debye-Hückel limiting law parameter for partial molal volumes defined by equation (52).
b	— Gibson-Tait coefficient in equations (2) and (3).
b_1^*, b_2^*	— empirical correlation coefficients in equation (73).
b_γ	— empirical activity coefficient parameter in equation (56).
b_V	— empirical partial molal volume parameter defined by equation (57e).
b'_V	— empirical partial molal volume parameter in equations (53) and (55).
b^*_V	— empirical partial molal volume parameter in equations (58), (59), and (60).
B_γ	— Debye-Hückel parameter for activity coefficients defined by equation (56A).
B_V	— Debye-Hückel parameter for partial molal volumes defined by equation (57D).
c	— subscript denoting solvent collapse.
c_l	— empirical coefficient in the *l*th term of equation (55).
C_{H_2O}	— density function for H_2O defined by equation (6).
$\bar{C}^\circ_P$	— standard partial molal third law heat capacity (eq 42).
$\bar{C}^\circ_{P,T}$, $\bar{C}^\circ_{P,r,T}$	— standard partial molal heat capacity of an electrolyte at the subscripted pressure and temperature.
$\Delta\bar{C}^\circ_{P,c}$	— standard partial molal third law heat capacity of solvent collapse (eq 34).
$\bar{C}^\circ_{P,i}$	— standard intrinsic partial molal third law heat capacity (eq 36).
$\Delta\bar{C}^\circ_{P,s}$	— standard partial molal third law heat capacity of solvation in an aqueous phase (eq 21).
d, disordered	— subscripts denoting a disordered state.
e	— electronic charge (4.80298 esu).
e	— subscript denoting electrostriction.
$\bar{E}^\circ_x$	— standard partial molal expansibility (eq 41).
$\Delta\bar{E}^\circ_{x,c}$	— standard partial molal expansibility of solvent collapse (eq 33).

$\Delta\bar{E}^{\circ}_{x,e}$ — standard partial molal expansibility of electrostriction (eq 41).

$\bar{E}^{\circ}_{x,i}$ — standard intrinsic partial molal expansibility (eq 36).

$\Delta\bar{E}^{\circ}_{x,n}$ — sum of the standard intrinsic partial molal expansibility and the standard partial molal expansibility of solvent collapse (eq 34).

$\Delta\bar{E}^{\circ}_{x,s}$ — standard partial molal expansibility of solvation in an aqueous phase (eq 20).

$\bar{E}^{\circ}_{x,j}$, $\bar{E}^{\circ}_{x,j}{}^{abs}$ — conventional and absolute standard partial molal expansibility of the *j*th ion.

$\Delta\bar{E}^{\circ}_{x,c,j}$, $\Delta\bar{E}^{\circ}_{x,c,j}{}^{abs}$ — conventional and absolute standard partial molal expansibility of solvent collapse for the *j*th ion.

$\Delta\bar{E}^{\circ}_{x,e,j}$, $\Delta\bar{E}^{\circ}_{x,e,j}{}^{abs}$ — conventional and absolute standard partial molal expansibility of electrostriction for the *j*th ion.

$\bar{E}^{\circ}_{x,i,j}$, $\bar{E}^{\circ}_{x,i,j}{}^{abs}$ — conventional and absolute standard intrinsic partial molal expansibility of the *j*th ion.

$\Delta\bar{E}^{\circ}_{x,n,j}$, $\Delta\bar{E}^{\circ}_{x,n,j}{}^{abs}$ — conventional and absolute counterparts of the sum of the standard intrinsic partial molal expansibility of the *j*th ion and its standard partial molal expansibility of solvent collapse.

$\Delta\bar{E}^{\circ}_{x,s,j}$, $\Delta\bar{E}^{\circ}_{x,s,j}{}^{abs}$ — conventional and absolute standard partial molal expansibility of solvation (in an aqueous phase) for the *j*th ion.

g, gas — subscripts denoting the gas state.

ΔG_s — Gibbs free energy of solvation.

$\Delta\bar{G}^{\circ}_{s,j}$, $\Delta\bar{G}^{\circ}_{s,j}{}^{abs}$ — conventional and absolute standard partial molal Gibbs free energy of solvation (in an aqueous phase) for the *j*th ion.

ΔG_1 — Gibbs free energy of transfer for an ion from an aqueous disordered state to a vacuum.

ΔG_2 — Gibbs free energy of transfer for an ion from a vacuum to an aqueous ordered state.

$\bar{G}^{\circ}_{P,T}$, $\bar{G}^{\circ}_{P_r,T}$ — standard partial molal Gibbs free energy of an electrolyte at the subscripted pressure and temperature.

$\bar{H}^{\circ}_{P,T}$, $\bar{H}^{\circ}_{P_r,T}$ — standard partial molal enthalpy of an electrolyte at the subscripted pressure and temperature.

h — subscript denoting hydration of an ion from the gas state.

i — subscript designating intrinsic properties.

I — molal ionic strength of an electrolyte solution ($I=\frac{1}{2}\sum_j m_j Z_j^2$).

j — subscript index for ions.

K — equilibrium constant.

K° — "complete" equilibrium constant defined by equation (5).

k — average hydration number defined by equation (9).
l — integer index in equation (55).
m — molality.
M — molarity.
$\mathbf{M}$ — atomic mass (molecular weight).
$\mathbf{M}_j$ — atomic mass of the jth ion.
$\mathbf{M}_w$ — atomic mass of H_2O (18.0153 g mole^{-1}).
n_w — number of moles of H_2O in solution.
N — Born function defined by equation (25).
N° — Avogadro's number (6.02252×10^{23} mole^{-1}).
p_n — absolute percent of $\bar{V}°$ attributable to $\Delta\bar{V}°_n$ (defined by eq 95).
P — pressure in bars or kilobars.
P_e — "effective" pressure in the Gibson-Tait equation (eq 2).
P_r — reference pressure (1 bar).
Q — Born function defined by equation (17).
$Q_{e,j}$ — electronic multiplicity of the ground state for the jth ion.
$r_{d,j}$ — radius of the jth ion in the aqueous disordered state.
$r_{e,j}$ — effective electrostatic radius of the jth ion at infinite dilution.
$r_{i,j}$ — intrinsic radius of the jth ion at infinite dilution.
$r_{o,j}$ — distance from the center of the jth ion to the outer limit of its influence on the orientational polarizability of the H_2O dipoles in its solvation shell.
$r_{x,j}$ — crystal radius of the jth ion.
$r_{x,+}$ — crystal radius of a cation.
$r_{x,-}$ — crystal radius of an anion.
R — gas constant (1.98719 therm cal mole^{-1} (°K)$^{-1}$ or 83.14241 cm^3 bar mole^{-1} (°K)$^{-1}$).
$\bar{S}°$ — standard partial molal third law entropy (eq 41).
$\Delta\bar{S}°_c$ — standard partial molal third law entropy of solvent collapse (eq 33).
$\bar{S}°_i$ — standard intrinsic partial molal third law entropy (eq 36).
$\Delta\bar{S}°_s$ — standard partial molal third law entropy of solvation in an aqueous phase (eq 20).
$\bar{S}°_{P,T}$, $\bar{S}°_{P_r,T}$ — standard partial molal third law entropy of an electrolyte at the subscripted pressure and temperature.
$\bar{S}°_j$, $\bar{S}°_j{}^{abs}$ — conventional and absolute standard partial molal third law entropy of the jth ion (eq 66).
$\Delta\bar{S}°_{c,j}$, $\Delta\bar{S}°_{c,j}{}^{abs}$ — conventional and absolute standard partial molal third law entropy of solvent collapse for the jth ion (eq 69).

$\Delta\bar{S}^\circ_{h,j}$ — conventional standard partial molal third law entropy of hydration (from the gas state) for the *j*th ion (eq 70).

$\bar{S}^\circ_{j,gas}$ — standard partial molal third law entropy of the *j*th ion in the gas state (eq 71).

$\bar{S}^\circ_{i,j}$, $\bar{S}^\circ_{i,j}{}^{abs}$ — conventional and absolute standard intrinsic partial molal third law entropy of the *j*th ion (eq 69).

$\Delta\bar{S}^\circ_{n,j}$, $\Delta\bar{S}^\circ_{n,j}{}^{abs}$ — conventional and absolute counterparts of the sum of the standard intrinsic partial molal third law entropy of the *j*th ion and its standard partial molal third law entropy of solvent collapse (eq 68).

$\Delta\bar{S}^\circ_{s,j}$, $\Delta\bar{S}^\circ_{s,j}{}^{abs}$ — conventional and absolute standard partial molal third law entropy of solvation (in an aqueous phase) for the *j*th ion.

s — subscript denoting solvation in an aqueous solution.

sat, saturation — designation of liquid/vapor equilibrium for H_2O.

S_V — Debye-Hückel limiting law parameter for apparent molal volumes defined by equation (51).

S^*_V — empirical parameter in the molal equivalent of the Masson equation (eq 44).

T — temperature in °K.

T_r — reference temperature (298.15°K).

U — Born function defined by equation (22).

u,v — solvation parameters in reaction (8) and equation (9).

V_{soln} — volume of an electrolyte solution.

$\bar{V}$ — partial molal volume.

$\bar{V}^\circ$ — standard partial molal volume (eq 1).

$\Delta\bar{V}^\circ_c$ — standard partial molal volume of solvent collapse (eq 12).

$\bar{V}^\circ_d$ — standard partial molal volume of disorder.

$\Delta\bar{V}^\circ_e$ — standard partial molal volume of electrostriction (eq 10).

$\bar{V}^\circ_i$ — standard intrinsic partial molal volume (eq 11).

$\Delta\bar{V}^\circ_n$ — sum of the standard intrinsic partial molal volume and the standard partial molal volume of solvent collapse (eq 12).

$\Delta\bar{V}^\circ_s$ — standard partial molal volume of solvation in an aqueous phase (eq 10).

$\bar{V}^\circ_w$, $\bar{V}^\circ$, $\bar{V}^\circ_{H_2O}$ — specific volume or standard partial molal volume of H_2O in $cm^3\ g^{-1}$ or $cm^3\ mole^{-1}$, respectively.

$\bar{V}^\circ_x$ — standard partial molal volume of a crystalline solid.

$\bar{V}^\circ_{x,i,j}$ — standard intrinsic partial molal crystal volume of the *j*th ion.

$\Delta\bar{V}^\circ$ — standard partial molal volume of dissociation.

$\bar{V}^\circ_{II}$ — standard partial molal volume of a solvation shell about an ion.

$\bar{V}^\circ_j$ $\bar{V}^{\circ abs}_j$ — conventional and absolute standard partial molal volume of the jth ion.

$\Delta\bar{V}^\circ_{c,j}$, $\Delta\bar{V}^{\circ abs}_{c,j}$ — conventional and absolute standard partial molal volume of solvent collapse for the jth ion.

$\Delta\bar{V}^\circ_{e,j}$, $\Delta\bar{V}^{\circ abs}_{e,j}$ — conventional and absolute standard partial molal volume of electrostriction for the jth ion.

$\bar{V}^\circ_{i,j}$, $\bar{V}^{\circ abs}_{i,j}$ — conventional and absolute standard intrinsic partial molal volume of the jth ion.

$\Delta\bar{V}^\circ_{n,j}$, $\Delta\bar{V}^{\circ abs}_{n,j}$ — conventional and absolute counterparts of the sum of the standard intrinsic partial molal volume of an ion and its standard partial molal volume of solvent collapse.

$\Delta\bar{V}^\circ_{s,j}$, $\Delta\bar{V}^{\circ abs}_{s,j}$ — conventional and absolute standard partial molal volume of solvation (in an aqueous phase) for the jth ion.

V^*_P — molal volume of an electrolyte in the liquid state at pressure P.

w — solvation parameter in reaction (8) and equation (9).

W — Born function defined by equation (23).

Y — Born function defined by equation (64).

Z_j — charge on the jth ion.

Z_+ — charge on a cation.

Z_- — charge on an anion.

a — ionic strength function defined by equation (59A).

a^* — ionic strength function defined by equation (57G).

$\bar{\beta}^\circ$, $\bar{\beta}^\circ_{H_2O}$ — coefficient of isothermal compressibility of H_2O.

β^* ($\mathring{a}B_\gamma I^{1/2}$) — ionic strength function defined by equation (57H).

$\gamma_\pm$ — mean ionic activity coefficient of an electrolyte.

$\Gamma_{Z,j}$ — radius additivity parameter for the jth ion (eq 61).

Γ_+ — radius additivity parameter for a cation (eq 61A).

Γ_- — radius additivity parameter for an anion (eq 61A).

Δ — finite difference

ε, ε_{H_2O} — dielectric constant of H_2O.

η — Born constant defined by equation (14).

θ — structural temperature corresponding to one of the equation of state coefficients for an electrolyte (eq 26).

θ_j — structural temperature corresponding to one of the conventional equation of state coefficients for the jth ion.

$\bar{\kappa}^\circ$ — standard partial molal compressibility (eq 43).

$\Delta\bar{\kappa}^\circ_c$ — standard partial molal compressibility of solvent collapse (eq 37).

$\Delta\bar{\kappa}^\circ_e$ — standard partial molal compressibility of electrostriction (eq 43).

$\Delta\bar{K}^{\circ}_{i}$ — standard intrinsic partial molal compressibility (eq 36).

$\Delta\bar{K}^{\circ}_{n}$ — sum of the standard intrinsic partial molal compressibility and the standard partial molal compressibility of solvent collapse (eq 37).

$\Delta\bar{K}^{\circ}_{s}$ — standard partial molal compressibility of solvation in an aqueous phase (eq 24).

$\bar{K}^{\circ}_{j}$, $\bar{K}^{\circ}_{j}{}^{abs}$ — conventional and absolute standard partial molal compressibility of the jth ion.

$\Delta\bar{K}^{\circ}_{c,j}$, $\Delta\bar{K}^{\circ}_{c,j}{}^{abs}$ — conventional and absolute standard partial molal compressibility of solvent collapse for the jth ion.

$\Delta\bar{K}^{\circ}_{e,j}$, $\Delta\bar{K}^{\circ}_{c,j}{}^{abs}$ — conventional and absolute standard partial molal compressibility of electrostriction for the jth ion.

$\bar{K}^{\circ}_{i,j}$, $\bar{K}^{\circ}_{i,j}{}^{abs}$ — conventional and absolute standard intrinsic partial molal compressibility of the jth ion.

$\Delta\bar{K}^{\circ}_{n,j}$, $\Delta\bar{K}^{\circ}_{n,j}{}^{abs}$ — conventional and absolute counterparts of the sum of the standard intrinsic partial molal compressibility of the jth ion and its standard partial molal compressibility of solvent collapse.

$\Delta\bar{K}^{\circ}_{s,j}$, $\Delta\bar{K}^{\circ}_{s,j}{}^{abs}$ — conventional and absolute partial molal compressibility of solvation (in an aqueous phase) for the jth ion.

Λ — ionic strength function defined by equation (57B).

ν — number of moles of ions (mole of solute)$^{-1}$.

ν_j — number of moles of the jth ion (mole of solute)$^{-1}$.

ν_+ — number of moles of cations (mole of solute)$^{-1}$.

ν_- — number of moles of anions (mole of solute)$^{-1}$.

ξ — equation of state coefficient for an electrolyte at constant pressure (eq 29).

ξ_j — conventional equation of state coefficient for the jth ion at constant pressure.

$\bar{\rho}^{\circ}$, $\bar{\rho}^{\circ}_{w}$, $^{\circ}_{H_2O}$ — density of H_2O in g cm^{-3}.

ρ_{soln} — density of an electrolyte solution in g cm^3.

σ — equation of state coefficient for an electrolyte at constant pressure (eq 28).

σ_j — conventional equation of state coefficient for the jth ion at constant pressure.

$\sigma(I^{1/2})$ — ionic strength function defined by equation (59B).

$\sigma^*(\mathring{a}B_\gamma I^{1/2})$ — ionic strength function defined by equation (57H).

ϕ_V — apparent molal volume of an electrolyte (eq 45).

ψ — electrolyte parameter defined by equation (57C).

ω — Born coefficient for an electrolyte defined by equation (19).

ω_j, $\omega_j{}^{abs}$ — conventional and absolute Born coefficients for the jth ion (eqs 15 and 115).

REVIEW OF THEORETICAL CONCEPTS

A multitude of theoretical models has evolved over the past two hundred years to account for the decrease in volume and compressibility resulting from addition of an electrolyte to water. The spectrum ranges from Tamman's (1893, 1895) internal pressure theory and the Drude-Nernst concept of electrostriction volume loss (Drude and Nernst, 1894) to structural models of molecular interaction (Bernal and Fowler, 1933; Frank and Robinson, 1940; Frank and Wen, 1957; Frank, 1963, 1965; Desnoyers and others, 1969) and interstitial disorder (Stokes and Robinson, 1957; Glueckauf, 1965; Curthoys and Mathiesen, 1970) such as Gurney's (1953) cosphere model (Friedman and Krishnan, 1973), the spherical cavity theory (Hepler, 1957), and Benson and Copeland's (1963) free volume model. These and many more have been summarized by Kavanaugh (1964), Samoilov (1965), Rosseinsky (1965), Conway (1966), Conway and Barradas (1966), Wicke (1966), Desnoyers and Jolicoeur (1969), Horne (1969), Vaslow (1972), Millero (1971, 1972a), Franks (1973), Kay (1973), and others in reviews and critiques of the observations and conclusions responsible for modern theories of ion-solvent interaction.

Partial molal volume at infinite dilution.—Because ionic interaction is negligible at infinite dilution, the standard thermodynamic properties of aqueous electrolytes are controlled by the interaction of ions with solvent dipoles. Following Hepler (1957), Noyes (1964), Glueckauf (1965), Pankhurst (1969), and others, the standard partial molal volume ($\bar{V}°$) of an electrolyte can be viewed as the sum of an intrinsic volume component ($\bar{V}°_i$) and an electrostriction term ($\Delta\bar{V}°_e$); that is,[2]

$$\bar{V}° = \bar{V}°_i + \Delta\bar{V}°_e \qquad (1)$$

The intrinsic volume of an electrolyte is commonly taken to be proportional to the volume of its crystalline counterpart ($\bar{V}°_x$) with either a theoretical or empirical proportionality constant, which may or may not be assigned a dependence on ion radius (Couture and Laidler, 1956; Hepler, 1957; Mukerjee, 1961; Conway, Verrall, and Desnoyers, 1965, 1966; Curthoys and Mathieson, 1970). Other approaches invoke the assumption that the intrinsic volume of an ion is proportional to the cube of the sum of its crystal radius and a semiempirical or theoretical constant (for example, see Noyes, 1964; Glueckauf, 1965; Pankhurst, 1969; Millero, 1972a). The constant is added to the crystal radius (r_x) to account for the observation that $\bar{V}°_i$ for an aqueous ion is much larger than the volume of a sphere with radius r_x, which has led to separation of $\bar{V}°_i$ into two additive components, $\bar{V}°_x$, and a disorder term ($\bar{V}°_d$) representing random close packing and disordered void space (Stokes and Robinson, 1957; Conway, Desnoyers, and Smith, 1964; Conway, Verrall, and Desnoyers, 1965, 1966; Glueckauf, 1965; King, 1969).

The electrostriction volume term in equation (1) corresponds to the volume loss associated with local collapse of the solvent structure and

[2] Other models include an additional "caged" term in equation (1) to provide explicitly for structural contributions (Millero, 1972a).

simultaneous solvation of the solute species. Solvated species are regarded by Samoilov (1972) as statistical entities which have physical significance only in the context of the residence time for any given nearest neighbor configuration. The nature of these configurations is highly disputed.

A myriad of structural theories has evolved to account for the thermodynamic properties of water and aqueous electrolytes (Franks, 1972; Eisenberg and Kauzmann, 1969; Frank, 1966, 1972; Horne, 1969; Barker and Henderson, 1972; Greyson and Snell, 1970), but most agree that water is (at least in part) a tetrahedrally coordinated liquid at low temperatures with a relatively open structure stabilized by hydrogen bonding (Bernal and Fowler, 1933; Gurney, 1953; Frank, 1958, 1972; Frank and Wen, 1957). The spatial and temporal integrity of the structure and the nature of H_2O polymerization is the central issue of debate among advocates of continuum theories (Kell, 1972) and mixture models (Davis and Jarzynski, 1972) of water structure (Franks, 1972; Ben-Naim, 1973). Various cluster schemes (Frank and Wen, 1957; Frank, 1966; Frank and Quist, 1961) and dipole association models have been proposed. One of these is the pyramidal $H_9O_4^+$ complex, which consists of three H_2O dipoles in primary coordination about the hydronium ion (H_3O^+) with a secondary coordination shell of loosely held and more disoriented water dipoles (Wicke, Eigen, and Ackermann, 1954; Eigen and De Maeyer, 1959). Increasing temperature apparently leads to changes in the average coordination number caused by disruption of the secondary solvation shells (Gurney, 1953; Wicke, Eigen, and Ackerman, 1954).

Upon addition of an electrolyte to water, short-range order among the solvent molecules is destroyed in the vicinity of the ions by local collapse of the water structure, which permits H_2O dipoles to orient in primary and more disordered secondary coordination shells about the aqueous species (Bockris, 1949; Samoilov, 1957, 1965; Duncan and Kepert, 1959). The local disruption of hydrogen bonding among the solvent dipoles by ion-solvent interaction is accompanied by a decrease in entropy as well as volume. Numerous models of ion hydration have been proposed (Kavanaugh, 1964; Samoilov, 1965; Bockris, Saluja, and Madan, 1970; Bockris and Saluja, 1972; Friedman and Krishnan, 1973), and repeated attempts have been made to describe the process in terms of electrostatic theory. In most such models the electrostriction volume loss is represented by the partial derivative of the Born (1920) equation (as corrected by Bjerrum, 1929) with respect to pressure at constant temperature, which corresponds to the Drude-Nernst equation (Drude and Nernst, 1894). Calculation of $\Delta\bar{V}^\circ_e$ with this expression requires the assumption that both the solvent and solute are incompressible, which is not the case in aqueous electrolytes. Nevertheless, the electrostriction entropy or volume loss for many aqueous species can be correlated with Z^2/r_x or similar charge/radius parameters in modified forms of the Drude-Nernst equation (Laidler and Pegis, 1957; Curthoys and Mathieson, 1970). Several attempts have been made to calculate $\Delta\bar{V}^\circ_e$ from electrostatic theory (Frank, 1955) assuming spherical symmetry of ions in a dimensionless dielectric con-

tinuum (Padova, 1963; Whalley, 1963; Benson and Copeland, 1963), but in most cases the theoretical models yield unreasonably large values of $\Delta\bar{V}^\circ_e$ owing to inadequate provision for dielectric saturation, void space, molecular size, and structural discontinuities in the calculations. Efforts to take account of these factors (Noyes, 1962; Desnoyers, Verrall, and Conway, 1965; Dunn, 1974) have been only partly successful.

Ionization as a function of pressure.—Relatively few equations of state for aqueous species have been proposed, other than those pertaining to ionization reactions. Volume changes accompanying ion dissociation, electrolytic conductance, and ionization as a function of pressure and temperature have been reviewed by Hamman (1963) and more recently by Gancy (1972), Brummer and Gancy (1972), Helper and Woolley (1973), Olofsson and Hepler (1975), and Hemmes (1972). Early calculations of the pressure dependence of the partial molal volumes of aqueous electrolytes employed the Gibson-Tait equation (Gibson, 1935, 1938), which is based on Tamman's internal pressure theory (Tamman, 1893) and Tait's empirical observations on the H.M.S. Challenger (Tait, 1889). The Gibson-Tait equation for the partial molal volume of an electrolyte at a given concentration and temperature can be written as

$$\bar{V}_P = V^*_P - \left(\frac{a}{b + P_e + P}\right)\frac{dP_e}{dm} \tag{2}$$

where $\bar{V}_P$ stands for the partial molal volume of the electrolyte at the subscripted pressure, V^*_P refers to the molal volume of the pure solute in the liquid state at the same pressure, P_e is an effective pressure which is independent of total pressure but dependent on concentration, m represents molality, and a and b are constants. Owen and Brinkley (1941) employed a modification of the Gibson-Tait equation to formulate an equation of state for the ionization of aqueous electrolytes, which leads to

$$RT \ln(K_P/K_1) = -\Delta\bar{V}^\circ_1 (P-1) + \Delta\bar{\kappa}^\circ_1 \left((b+1)(P-1) - (b+1)^2 \ln\left(\frac{b+P}{b+1}\right)\right) \tag{3}$$

where K_P represents the dissociation constant for a given species at the pressure of interest, K_1 is the corresponding dissociation constant at one bar, $\Delta\bar{V}^\circ_1$ stands for the standard partial molal volume of dissociation at one bar, b is again a constant (= 2996 bars for aqueous solutions at 25°C), and

$$\Delta\bar{\kappa}^\circ_1 = -\left(\frac{\partial\Delta\bar{V}^\circ}{\partial P}\right)_T \tag{4}$$

at 1 bar.

The Gibson-Tait equation leaves much to be desired for general application in solution chemistry. Comparative calculations and experimental measurements indicate that Owen and Brinkley's approach fails to predict accurately the pressure dependence of dissociation constants for acetic acid, H_2O, and other aqueous species (Hamman, 1963).

Several alternatives to equation (3) have been proposed on the basis of the low temperature/pressure behavior of log K for various species. Unfortunately, the slight dependence of many ionization constants on pressure at low temperatures and the relatively large uncertainties (which are of comparable magnitude to the low-temperature pressure dependence of log K) inherent in their experimental determination relegate most of the alternatives to the status of first order approximations. For example, measurements of the pressure dependence of the dissociation constants of H_2S, H_2CO_3, H_3PO_4, H_2SO_3, benzoic acids, and other species at temperatures ranging from 25° to 65°C (Ellis, 1959, 1963; Ellis and Anderson, 1961; Clark and Ellis, 1960; Hamman, 1963) reveal only slight changes in the standard partial molal volume of dissociation with increasing pressure. It might be assumed on this basis that $\Delta\bar{\kappa}°$ or even $\Delta\bar{V}°$ can be regarded as a pressure-independent variable in calculating ionization constants at high pressures and temperatures without introducing serious errors in predicted values of log K. However, extensive comprehensive and systematic conductance and potentiometric measurements at high pressures and temperatures (Noyes, 1907; Noyes, Kato, and Sosman, 1910; Franck, 1956a,b,c; 1961, 1973; Holzapfel and Franck, 1966; Ritzert and Franck, 1968; Hartmann and Franck, 1969; Renkert and Franck, 1969; Mangold and Franck, 1969; Quist and others, 1963; Quist, Marshall, and Jolley, 1965; Quist and Marshall, 1966, 1968a,b,c,d, 1969; Dunn and Marshall, 1969; Quist, 1970; Whitfield, 1972; Tödheide, 1972; Lown, Thirsk and Lord Wynne-Jones, 1968, 1970; Lown and Thirsk, 1972) leave little doubt that such is not the case.

Lown, Thirsk, and Lord Wynne-Jones (1970) assume in a first approximation that the standard partial molal compressibility of ionization is independent of pressure. Although this assumption yields adequate representation of the low temperature/pressure dependence of the dissociation constant of acetic acid as well as that of H_2O (Millero, Hoff, and Kahn, 1972; Olofsson and Hepler, 1975), it is inconsistent in principle with electrostatic theory and recent measurements of the dielectric constant of H_2O (Heger, ms), which require the standard partial molal compressibilities of aqueous species to be functions of both pressure and temperature.

An alternate approach has been taken by Quist and Marshall (1968a) and more recently by North (1973) which is based on Franck's (1956a,b,c; 1961) early observation that values of log K derived from isothermal conductance data for a large number of electrolytes at high pressures and temperatures can be regarded as linear functions of the logarithm of the density of the solvent. This observation, which is also true for H_2CO_3, CH_3COOH, benzoic acids, and other species at low temperatures and pressures (fig. 1), requires the standard partial molal volume of ionization ($\Delta\bar{V}°$) to be proportional to the product of temperature (T) and the coefficient of isothermal compressibility of the solvent ($\bar{\beta}°_{H_2O}$). In a series of papers, Quist and Marshall (1968a) and Marshall (1968, 1969, 1970, 1972) suggest that the proportionality between $\Delta\bar{V}°$ and $\bar{\beta}_{H_2O}T$ is a funda-

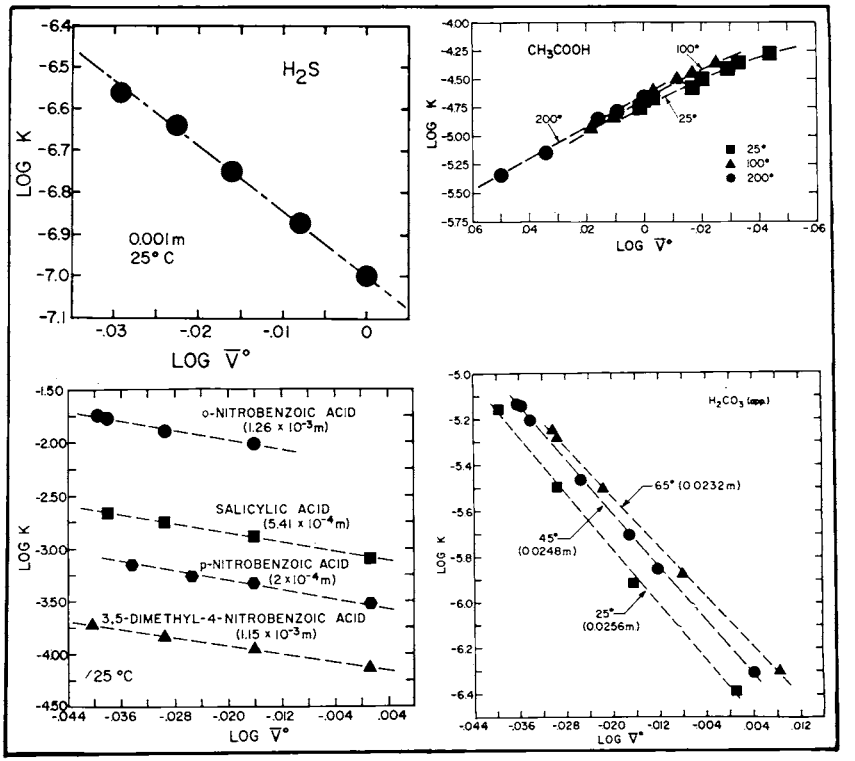

Fig. 1. Standard molal dissociation constant of CH_3COOH in H_2O and apparent molal dissociation constants of four benzoic acids, H_2S, and $H_2CO_{3(apparent)}$ in aqueous solutions of constant concentration as a function of the logarithm of the specific volume of the solvent ($\bar{V}°$) at constant temperature. The values of $\bar{V}°$ were computed from equations given by Helgeson and Kirkham (1974a). The symbols represent data reported by Ellis (1959), Clark and Ellis (1960), Ellis and Anderson (1961), and Lown, Thirsk, and Lord Wynne-Jones (1970).

mental relation and generalize their observation by advocating the concept of a complete equilibrium constant (K°), which is defined by first designating $(\partial \ln K/\partial \ln \rho_{H_2O})_T$ as an average hydration number (k) representing the net change in solvation attending ionization. The complete equilibrium constant is then related to its conventional counterpart (K) by

$$K° = K\, C_{H_2O}{}^{-k} \tag{5}$$

where

$$C_{H_2O} = 55.51\overline{\rho}°_{H_2O} \tag{6}$$

Hence,

$$\Delta\bar{V}° = -kRT\overline{\beta}°_{H_2O} \tag{7}$$

By adopting a standard state in which $a_{H_2O} = C_{H_2O}$, K° becomes the equilibrium constant for a dissociation reaction of the form

$$AB(H_2O)_u + kH_2O \rightleftharpoons A(H_2O)_v{}^+ + B(H_2O)_w{}^- \tag{8}$$

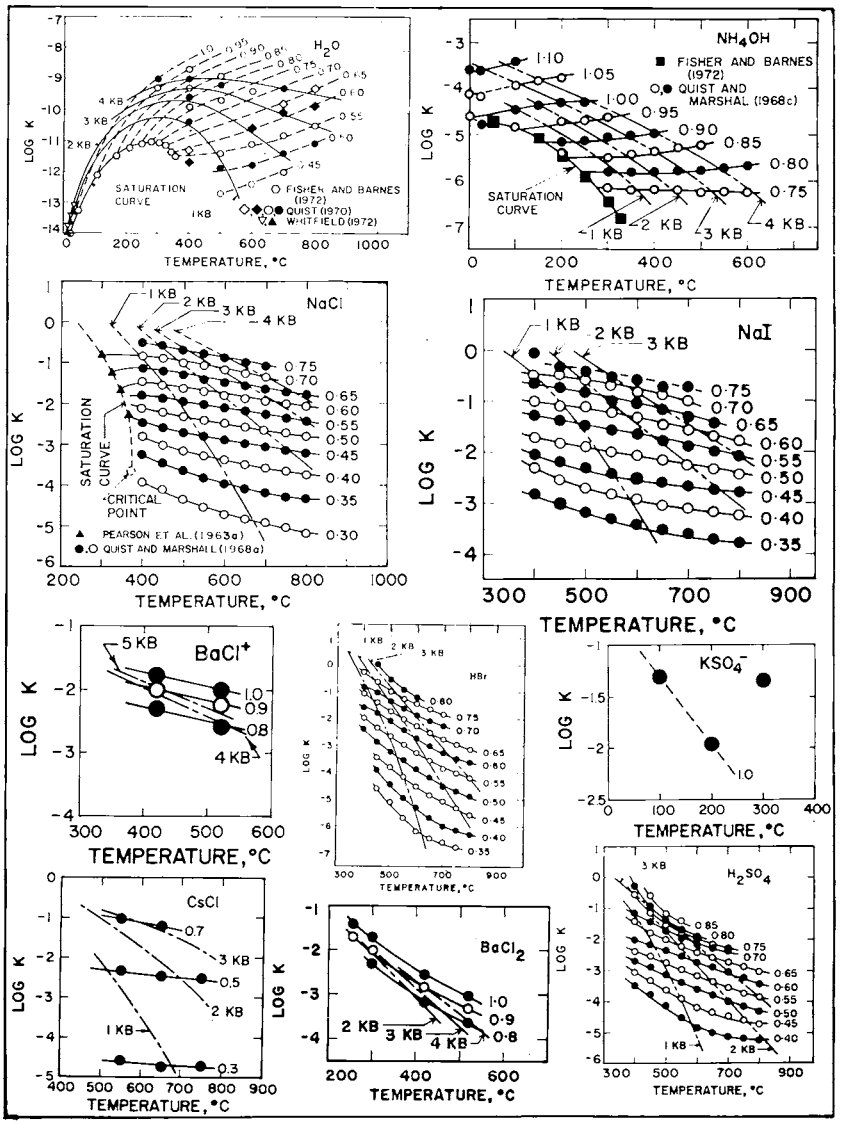

Fig. 2. Standard molal activity product constant of H_2O and standard molal dissociation constants of NaCl, NaI, HBr, H_2SO_4, CsCl, NH_4OH, $BaCl^+$, $BaCl_2$, and KSO_4^- in H_2O as a function of temperature at constant density of H_2O (labeled in g cm^{-3}) or constant pressure (labeled in kb). The isobars were plotted with the aid of equations given by Helgeson and Kirkham (1974a). The symbols represent data reported by Quist (1970), Fisher and Barnes (1972), Whitfield (1972), Pearson, Copeland, and Benson (1963a), Quist and Marshall (1968a, b, and c), Dunn and Marshall (1969), Quist, Marshall and Jolley (1965), Franck (1961), Ritzert and Franck (1968), and Quist and others (1963).

where

$$k = v + w - u \tag{9}$$

For many (but not all) electrolytes, the average hydration number defined by Marshall appears to be independent of temperature. By regarding the partial molal volume of an aqueous ion as the sum of the intrinsic volume of the species and the volume of its hydration shell ($\bar{V}^\circ_{II}$), Marshall (1970) rationalizes equation (7) by arguing that the intrinsic volume of ionization and $(\partial\Delta\bar{V}^\circ_{II}/\partial P)_T$ are essentially zero, which requires $\Delta\bar{V}^\circ$ to be a function only of the pressure–volume–temperature properties of the solvent. Although the observations leading to equation

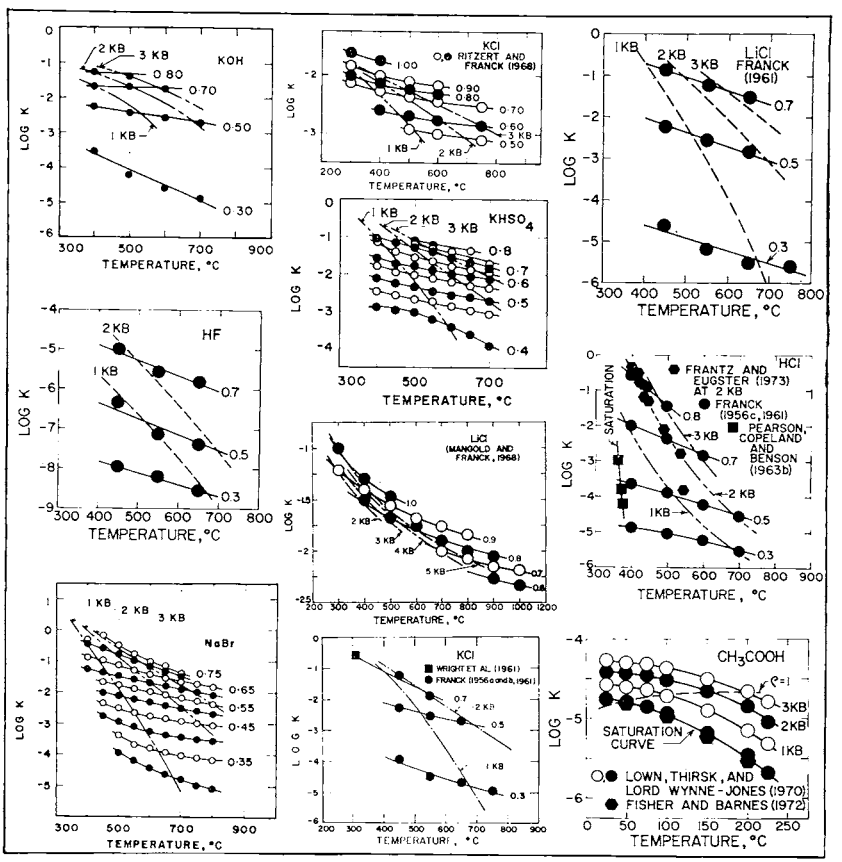

Fig. 3. Standard molal dissociation constants of $KHSO_4$, KOH, NaBr, HCl, KCl, HF, CH_3COOH, and LiCl in H_2O as a function of temperature at constant density of H_2O (labeled in g cm^{-3}) or constant pressure (labeled in kb). The isobars were plotted with the aid of equations given by Helgeson and Kirkham (1974a). The symbols represent data reported by Quist and Marshall (1966, 1968d), Franck (1956a, b, and c, 1961); Pearson, Copeland and Benson, 1963b); Frantz and Eugster (1973); Ritzert and Franck (1968), Wright, Lindsay, and Druga (1961), Lown, Thirsk, and Lord Wynne-Jones (1970), Fisher and Barnes (1972), and Mangold and Franck (1969).

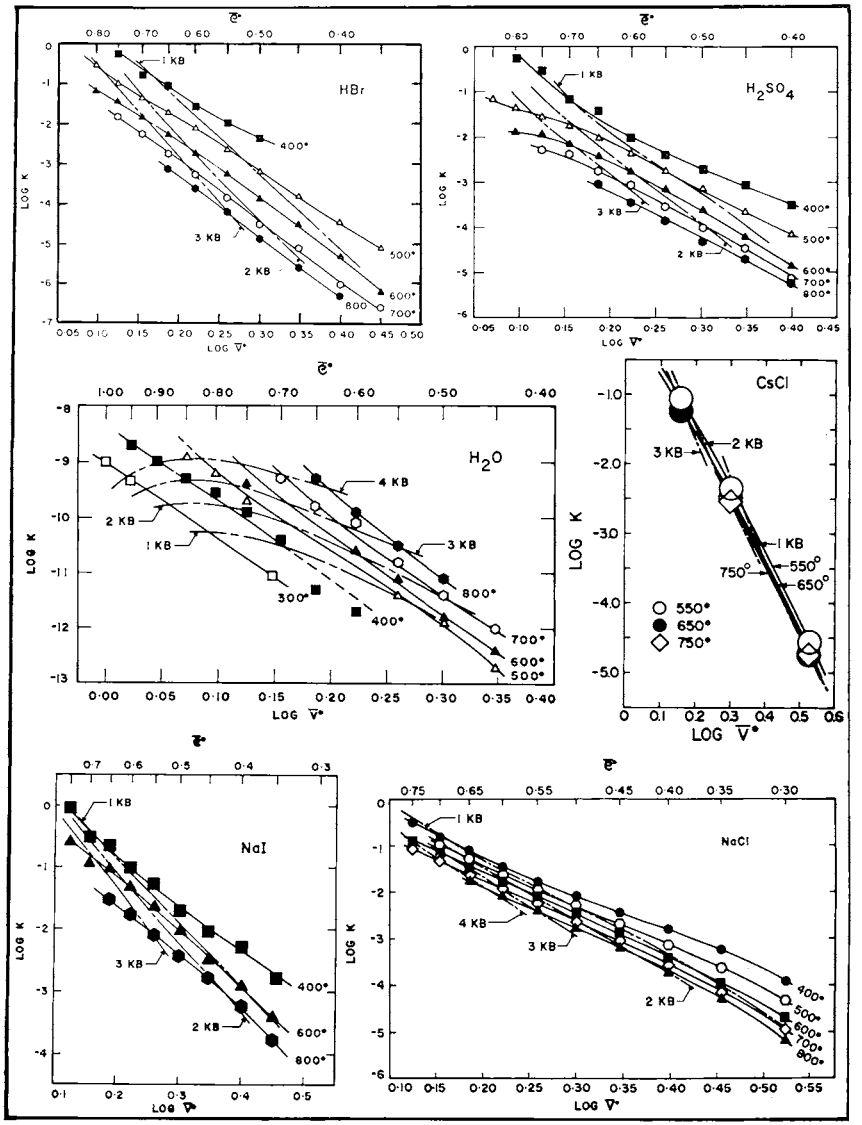

Fig. 4. Standard molal activity product constant of H_2O and standard molal dissociation constants of NaCl, NaI, HBr, H_2SO_4, and CsCl in H_2O as a function of the logarithm of the specific volume of H_2O ($\bar{V}^\circ$) at constant temperature (labeled in °C) or pressure (labeled in kb). The values of $\bar{V}^\circ$ and $\bar{\rho}^\circ$ (the density of H_2O) were computed from equations given by Helgeson and Kirkham (1974a). The symbols represent data reported by Quist (1970), Quist and Marshall (1968a and b), Quist, Marshall, and Jolley (1965), Franck (1961), and Dunn and Marshall (1969).

(7) are consistent with scaled particle theory (Lucas, 1973), and the approach yields dissociation constants in close agreement with those derived from conductance measurements at high pressures and temperatures, its general validity as a fundamental relation suitable for extrapolating experimental data is open to serious question, both from the point of view of solvation (Matheson, 1969) and electrostatic theory (Gilkerson, 1970).

Careful analysis of the high pressure/temperature log K values published by Franck, Quist, Marshall, and their coworkers as a function of log $\bar{\rho}^{\circ}_{H_2O}$ reveals that the linear relation of log K to log C_{H_2O} is not well

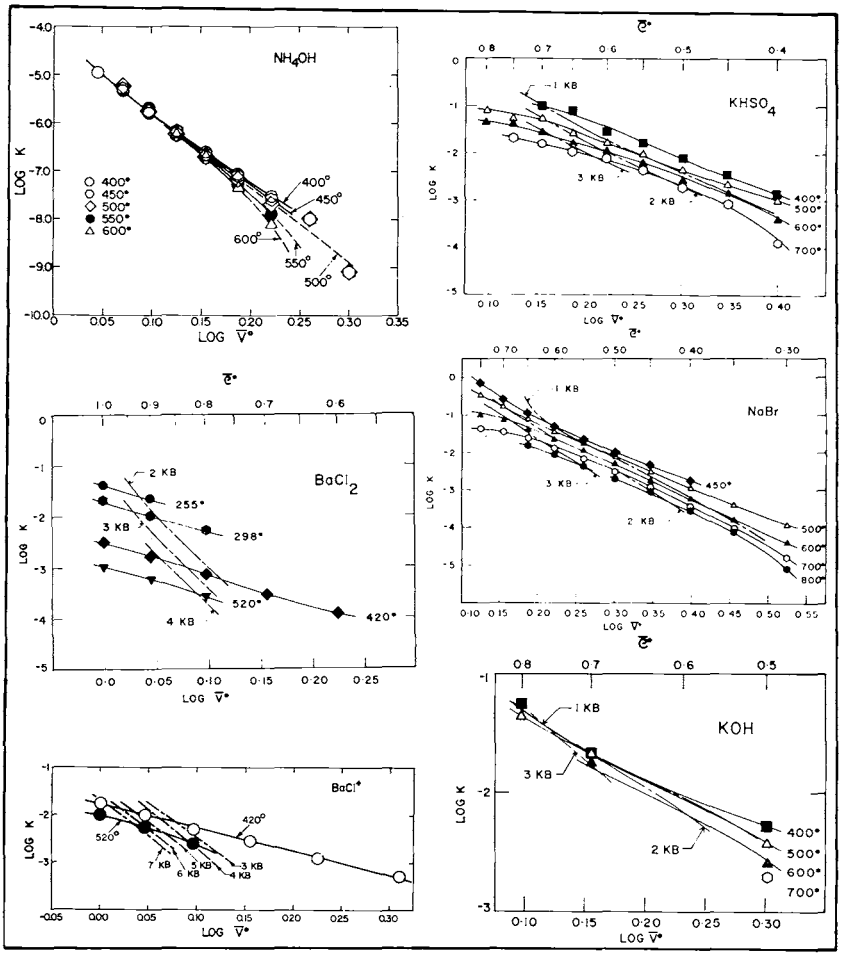

Fig. 5. Standard molal dissociation constants of NH_4OH, $BaCl^+$, $BaCl_2$, $KHSO_4$, KOH, and NaBr in H_2O as a function of the logarithm of the specific volume of H_2O ($\bar{V}^{\circ}$) at constant temperature (labeled in °C) or pressure (labeled in kb). The values of $\bar{V}^{\circ}$ and $\bar{\rho}^{\circ}$ (the density of H_2O) were computed from equations given by Helgeson and Kirkham (1974a). The symbols represent data reported by Ritzert and Franck (1968), Quist and Marshall (1966, 1968d) and Franck (1956c, 1961).

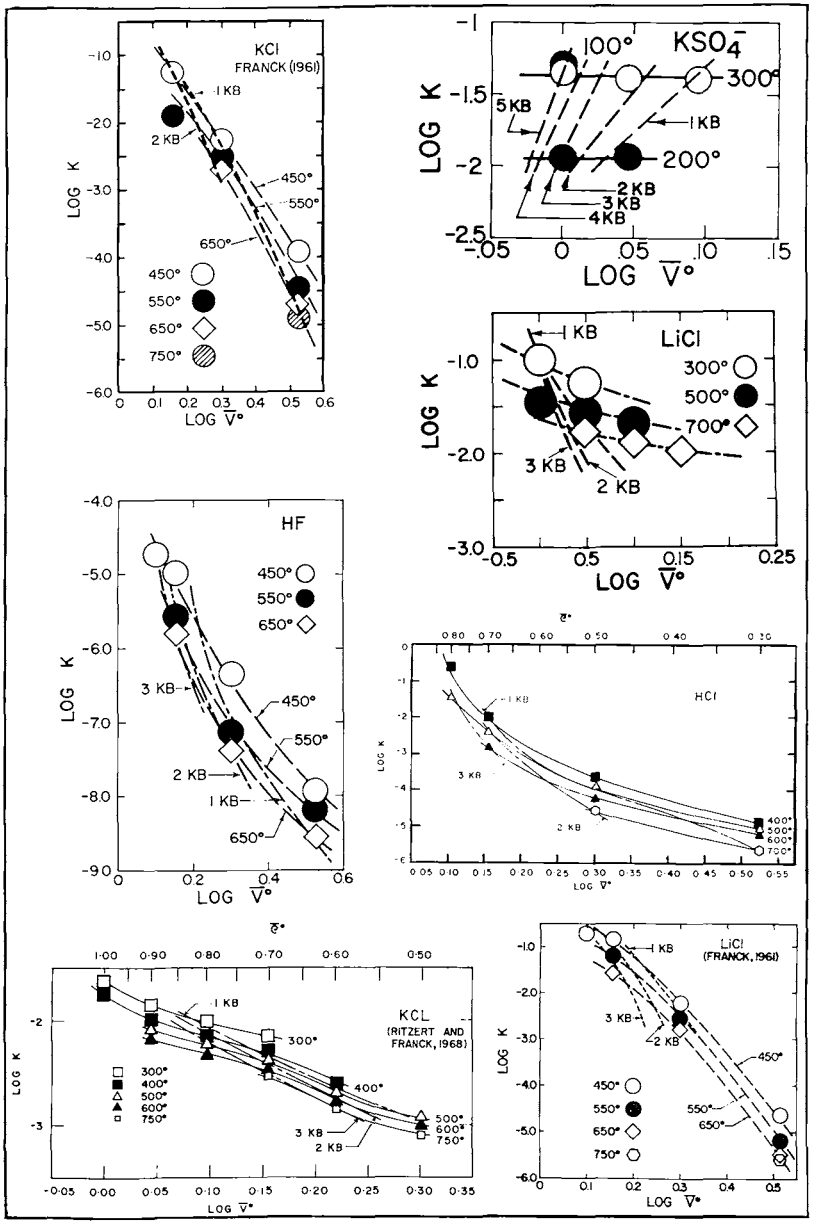

Fig. 6. Standard molal dissociation constants of HCl, KCl, HF, KCl, LiCl, and KSO_4^- in H_2O as a function of the logarithm of the specific volume of H_2O ($\bar{V}°$) at constant temperature (labeled in °C) or pressure (labeled in kb). The values of $\bar{V}°$ and $\bar{\rho}°$ (the density of H_2O) were computed from equations given by Helgeson and Kirkham (1974a). The symbols represent data reported by Franck (1956a, b, and c, 1961), Ritzert and Franck (1968), Mangold and Franck (1969), and Quist and others (1968).

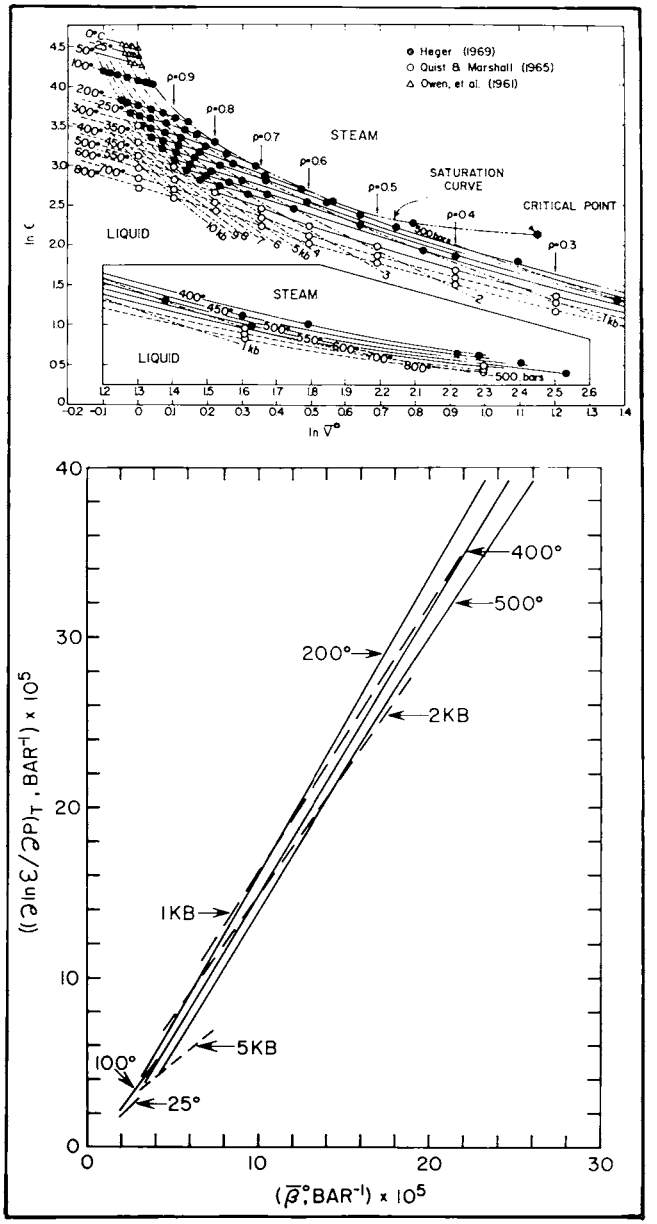

Fig. 7. Logarithm of the dielectric constant of H_2O (ε) as a function of the logarithm of the specific volume of H_2O ($\bar{V}°$) at constant temperature (labeled in °C) or pressure (labeled in bars or kb) and the partial derivative of ln ε with respect to temperature at constant pressure as a function of the coefficient of isothermal compressibility ($(-\partial \ln \bar{V}°/\partial P)_T$) of H_2O ($\bar{\beta}°$) at constant temperature (labeled in °C) or pressure (labeled in kb). The symbols and curves represent experimental data and/or computed values given by Oshry (ms), Owen and others (1961), Heger (ms), Quist and Marshall (1965), and Helgeson and Kirkham (1974a).

defined for $\bar{\rho}^\circ_{H_2O} \geq 0.6$ or $\bar{\rho}^\circ_{H_2O} \leq 0.4$, particularly for the 400° and 800°C isotherms. At densities > 0.6 or lower than 0.4, the distribution of data points indicates nonlinearity in the isotherms. Marshall considered these departures to be the result of experimental uncertainty, but the isochoric plots of the data against temperature in figures 2 and 3 suggest that the departures are systematic and probably real. The curves in these figures are consistent with those shown in figures 4 through 6 (and fig. 1, in the case of acetic acid) which (in contrast to the curves drawn through the experimental data by Marshall) are nonlinear functions of $\log \bar{\rho}^\circ_{H_2O}$.

Consideration of electrostatic theory and changes in the dielectric constant (ε) and thermodynamic properties of H_2O as functions of pressure and temperature implies that equation (7) is actually a quasi-identity arising from the linear relation (and near proportionality) of $(\partial \ln \varepsilon_{H_2O}/\partial P)_T$ to $\bar{\beta}^\circ_{H_2O}$ over wide ranges of pressure and temperature (fig. 7). As a consequence, the electrostriction volume of ionization, which is a function (see below) of $(\partial \ln \varepsilon_{H_2O}/\partial P)_T/\varepsilon$ (fig. 8), exhibits a near-linear dependence on $\bar{\beta}^\circ_{H_2O}T$. At high temperatures, where the electrostatic contribution to $\Delta\bar{V}^\circ$ is large, log K would thus be expected to exhibit a quasilinear relation to $\log \bar{\rho}^\circ_{H_2O}$. At low temperatures in the liquid phase region where $\bar{\rho}^\circ_{H_2O}$ approaches a linear dependence on pressure, the same relation (fig. 1) would be expected if the nonelectrostatic contribution to $\Delta\bar{V}^\circ$ is also a near-linear function of pressure. It is shown below that such appears to be the case.

The observations summarized in the preceding paragraph in no way detract from the utility of Marshall's approach, but they relegate equation (7) to the role of a predictive algorithm for certain species, pressures, and temperatures, rather than a fundamental relation of general applicability which can be used with confidence to formulate a comprehensive equation of state for aqueous electrolytes. Some of the dangers inherent in generalizing linear correlations of log K for one or another species with different properties of the solvent over restricted ranges of pressure and temperature (such as the electrostatic approach taken by Ryzhenko, ms) can be assessed by comparing the various curves in figure 9 with each other and with those shown in figures 1 and 4 through 6. It can be seen that the dissociation constant for H_2S, H_2CO_3, and acetic acid appear to be linear isothermal functions of both $1/\varepsilon_{H_2O}$ and $\log \bar{\rho}^\circ_{H_2O}$ (or $\log \bar{V}^\circ_{H_2O}$). It can also be seen that $\log K_{NaBr}$ and $\log K_{HBr}$ exhibit a quasilinear dependence on $\ln \varepsilon_{H_2O}$ from 450° to 500°C as well as a near-linear dependence on $\log \bar{V}^\circ_{H_2O}$ at constant (high) temperature. Despite the fact that Owen and Brinkley (1941) computed the pressure dependence of the dissociation constant for H_2O from equation (3), note that the results of the calculations exhibit a linear dependence on $1/\varepsilon_{H_2O}$ at 25°C (fig. 9).

Both theoretical and experimental observations indicate that none of the relations shown in figure 9 is definitive or generally applicable, nor are the standard partial molal volumes of aqueous electrolytes at low pressures and temperatures proportional to (or even linear functions of)

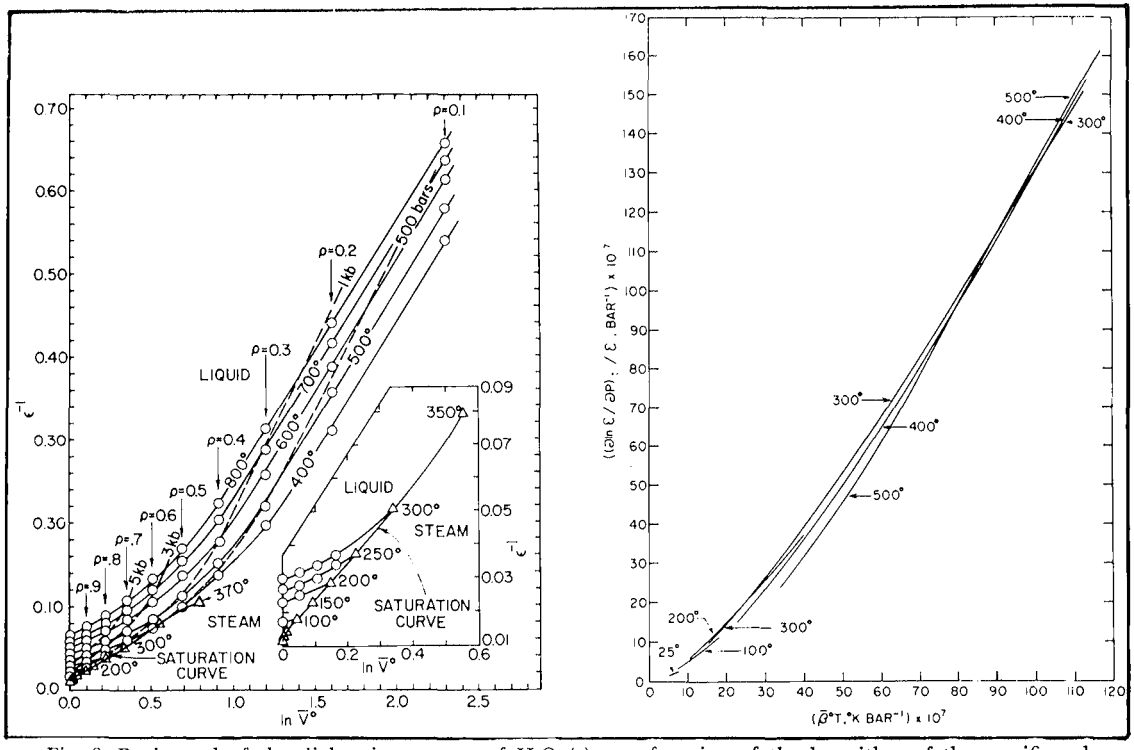

Fig. 8. Reciprocal of the dielectric constant of H_2O (ε) as a function of the logarithm of the specific volume of H_2O ($\bar{V}°$) at constant temperature (labeled in °C) or pressure (labeled in bars or kb) and the partial derivative of ε^{-1} as a function of the product of temperature and the coefficient of isothermal compressibility ($(-\partial \ln \bar{V}°/\partial P)_T$) of H_2O ($\bar{\beta}°$) at constant temperature (labeled in °C). The symbols and curves represent experimental data and/or computed values given by Oshry (ms), Owen and others (1961), Heger (ms), Quist and Marshall (1965), and Helgeson and Kirkham (1974a).

the product of temperature and the isothermal compressibility of H_2O as a function of temperature at constant pressure.

DERIVATION OF THE EQUATION OF STATE

Because the various factors contributing to the electrostriction volume loss are interdependent variables, they are not strictly separable as additive functions of pressure and temperature. Nevertheless, a general equation of state for aqueous electrolytes can be derived by describing the combined effect of these factors on $\bar{V}^\circ$ as the sum of the volume loss due to local collapse of the solvent structure ($\Delta\bar{V}^\circ_c$) and that attending the solvation process ($\Delta\bar{V}^\circ_s$); that is,

$$\Delta\bar{V}^\circ_e = \Delta\bar{V}^\circ_c + \Delta\bar{V}^\circ_s \tag{10}$$

which can be combined with equation (1) to give

$$\bar{V}^\circ = \bar{V}^\circ_i + \Delta\bar{V}^\circ_c + \Delta\bar{V}^\circ_s = \Delta\bar{V}^\circ_n + \Delta\bar{V}^\circ_s \tag{11}$$

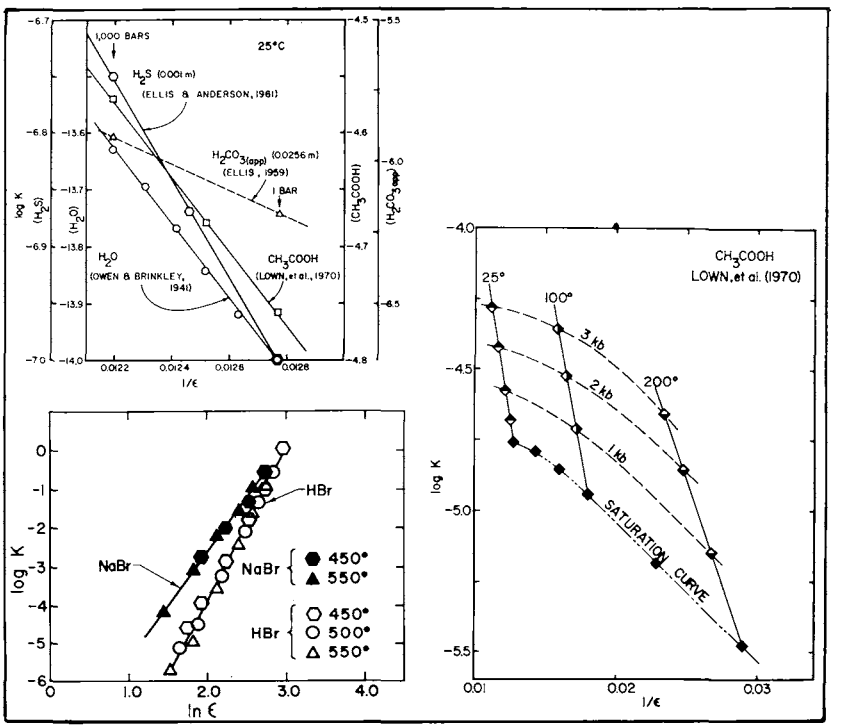

Fig. 9. Standard molal dissociation constants for NaBr and HBr in H_2O as a function of the logarithm of the dielectric constant of H_2O (ε), and the standard molal activity product constant of H_2O, standard molal dissociation constant of CH_3COOH, and apparent molal dissociation constants of H_2S and $H_2CO_{3(\text{apparent})}$ in aqueous solutions of constant concentration as a function of ε^{-1} at constant temperature (labeled in °C) and/or pressure (labeled in bars or kb). The values of ε were computed from equations given by Helgeson and Kirkham (1974a). The symbols represent data reported by Quist and Marshall (1968b and d), Ellis and Anderson (1961), Ellis (1959), Lown, Thirsk, and Lord Wynne-Jones (1970), and Owen and Brinkley (1941).

where

$$\Delta\bar{V}^\circ_n = \bar{V}^\circ_i + \Delta\bar{V}^\circ_c \tag{12}$$

The relative contributions of $\Delta\bar{V}^\circ_n$ and $\Delta\bar{V}^\circ_s$ to $\Delta\bar{V}_e$ as functions of temperature and pressure can be approximated by regarding $\Delta\bar{V}^\circ_s$ as the change in volume associated with solvation of idealized ions consistent with Debye-Hückel theory, the Born model, and the Drude-Nernst equation. All these relations are strictly applicable only to incompressible, unpolarizable, spherical ions in a homogeneous and continuous medium with a given dielectric constant, which requires the solvation shells about the ions to exhibit spherical symmetry. Although it has been demonstrated repeatedly that this simple model fails to account adequately for the entire electrostriction volume loss associated with ion-solvent interaction, restricted application of the Born model and continuum theory to the solvation process within an aqueous phase affords close approximation of experimental data (see below).

Electrostatic model of ion solvation.—The Born (1920) equation (as corrected by Bjerrum, 1929) can be written for the absolute standard partial molal Gibbs free energy of solvation ($\Delta\bar{G}^\circ_s{}^{abs}$) of the jth ion as[3]

$$\Delta\bar{G}^\circ_{s,j}{}^{abs} = \frac{N^\circ Z_j{}^2 e^2}{2r_{e,j}}\left(\frac{1}{\varepsilon} - 1\right) = \frac{\eta Z_j{}^2}{r_{e,j}}\left(\frac{1}{\varepsilon} - 1\right) = \omega_j{}^{abs}\left(\frac{1}{\varepsilon} - 1\right) \tag{13}$$

where N° stands for Avogadro's number (6.02252×10^{23} mole^{-1}), e represents the electronic charge (4.80298 esu), Z_j and $r_{e,j}$ correspond to the charge and effective electrostatic radius of the ion, ε is the dielectric constant of the solvent,

$$\eta = \frac{N^\circ e^2}{2} = 1.66027 \times 10^5 \text{ A cal. mole}^{-1}\ , \tag{14}$$

and

$$\omega_j{}^{abs} = \frac{\eta Z_j{}^2}{r_{e,j}} \tag{15}$$

Applications of the Born equation in solution chemistry have been criticized extensively in the chemical literature, largely because of ambiguities inherent in the choice of appropriate effective electrostatic radii and representation of the dielectric constant of the medium in the immediate vicinity of an ion. Measurements of the permittivities of electrolyte solutions as a function of frequency (Hasted, Ritson, and Collie, 1948; Haggis, Hasted, and Buchanan, 1952; Hasted and El Sabeh, 1953; Hasted and Roderick, 1958; Harris and O'Konski, 1957; Giese, Kaatz, and Pottel, 1970; Pottel, 1966; 1973) leave little doubt that the orientational polarizability of H_2O dipoles in the primary solvation shells about cations is reduced significantly by coordination. In contrast, those in the solvation shells about anions are loosely held and easily perturbed. If the

[3] All symbols representing thermodynamic properties of individual ions refer to the conventional properties unless indicated otherwise by the superscript "*abs*" for absolute.

dielectric constant in equation (13) is taken to be that of the bulk solvent, it follows that $r_{e,j}$ must take into account solvated H_2O dipoles with reduced orientational polarizability. Such provision is implicit in calculations of $r_{e,j}$ from experimental data using the dielectric constant of H_2O to represent that in the immediate vicinity of an ion (see below).

Although the Born equation is strictly applicable only to transfer of an ion from a vacuum to a dielectric medium, it can be applied to electrostriction solvation within an aqueous phase by regarding the Gibbs free energy of solvation (ΔG_s) as the sum of the change in the Gibbs free energy attending transfer of the ion to a vacuum from a disordered aqueous state (ΔG_1) and that associated with returning it to an ordered state (ΔG_2); that is, $\Delta G_s = \Delta G_1 + \Delta G_2$. The transfer process for a given ion (represented by A^+) is depicted schematically below:

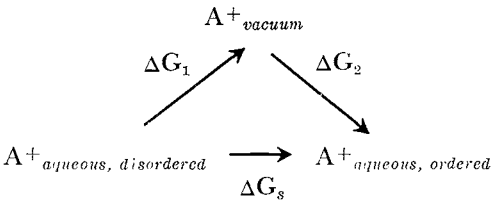

where $A^+_{aqueous,\ disordered}$ refers to the unsolvated ion in an aqueous state of disorder immediately after collapse of the solvent structure and $A^+_{aqueous,\ ordered}$ represents the solvated ion with oriented H_2O dipoles in primary and secondary coordination.

The solvation process is commonly identified in solution chemistry with transfer of an ion from a vacuum (or gas state) to an aqueous solvated state without explicit regard for local collapse of the solvent structure. Consequently, the Born theory, which contains no provision for electrostriction collapse, fails to describe adequately the transfer process. However, because contributions to the electrostriction volume loss by A^+_{vacuum} and local collapse of the solvent structure cancel in the transfer of an ion both to and from a vacuum (as depicted in the schematic diagram shown above), the Born theory is directly applicable to the process of ion solvation within an aqueous phase. No statistical or structural modification of the Born equation is thus required to represent $\Delta\bar{G}^\circ_{s,j}{}^{abs}$, which can be expressed in terms of the dielectric constant of the bulk solvent if provision for void space in the solvation shells, dielectric saturation, and the finite dimensions of the solvent dipoles are incorporated in $r_{c,j}$. The nonelectrical part of the electrostriction volume loss must then be incorporated in the model by providing separately for the collapse contribution to $\bar{V}^\circ$ (see below).

Although Latimer (1955) and others have suggested that the radius parameter in equations (13) and (15) should be treated as a function of temperature to rationalize observed correlations of entropy with ionic potential at 25°C, recent consideration of the temperature dependence of the thermodynamics of ion hydration from the gas state in terms of

continuum theory (Murray, Sen, and Cobble, in preparation) indicates that $r_{e,j}$ can be regarded safely as a temperature-independent parameter. If $r_{e,j}$ is also independent of pressure, differentiating equation (13) with respect to pressure at constant temperature leads to the Drude-Nernst equation; that is,

$$\left(\frac{\partial \Delta \bar{G}^\circ_{s,j}{}^{abs}}{\partial P}\right)_T = \Delta \bar{V}^\circ_{s,j}{}^{abs} = -\omega_j{}^{abs} Q \tag{16}$$

where $\Delta \bar{V}^\circ_{s,j}{}^{abs}$ refers to the absolute standard partial molal volume of solvation for the jth aqueous ion and

$$Q = \frac{1}{\varepsilon}\left(\frac{\partial \ln \varepsilon}{\partial P}\right)_T \tag{17}$$

for the solvent. For an electrolyte, equation (16) appears as

$$\Delta \bar{V}^\circ_s = \sum_j \nu_j \Delta \bar{V}^\circ_{s,j}{}^{abs} = -\omega Q \tag{18}$$

where

$$\omega = \eta \sum_j^{\nu} (\nu_j Z_j{}^2/r_{e,j}) = \sum_j^{\nu} \nu_j \omega_j{}^{abs} \tag{19}$$

in which ν_j stands for the number of moles of the jth ion in one mole of an electrolyte consisting of ν moles of ions.

In contrast to the present model, Noyes (1964) used the Drude-Nernst equation to represent $\Delta \bar{V}^\circ_e$ for large ions, and Benson and Copeland (1963) employed a modified version of the relation to describe $\Delta \bar{V}^\circ_e$ as an isothermal function of density. Hammann and Strauss (1955) sought to improve the applicability of the Drude-Nernst equation to $\Delta \bar{V}^\circ_e$ by removing the constraint of ion incompressibility from the Born model, which permits $r_{e,j}$ to be a pressure dependent variable. Although such modifications yield close approximations of $\Delta \bar{V}^\circ_e$ for certain species, none is generally applicable in solution chemistry owing to the failure of the Born theory to account for $\Delta \bar{V}^\circ_c$ and thus for all of $\Delta \bar{V}^\circ_e$. In the present study, $r_{e,j}$ is regarded as a pressure/temperature-independent parameter.

The first and second partial derivatives of equation (18) with respect to temperature at constant pressure can be written as

$$\Delta \bar{E}^\circ_{x,s} \equiv \left(\frac{\partial \Delta \bar{V}^\circ_s}{\partial T}\right)_P = -\left(\frac{\partial \Delta \bar{S}^\circ_s}{\partial P}\right)_T = -\omega U \tag{20}$$

and

$$\left(\frac{\partial \Delta \bar{E}^\circ_{x,s}}{\partial T}\right)_P = \left(\frac{\partial^2 \Delta \bar{V}^\circ_s}{\partial T^2}\right)_P = -\frac{1}{T}\left(\frac{\partial \Delta \bar{C}^\circ_{P,s}}{\partial P}\right)_T = -\omega W \tag{21}$$

where $\Delta\bar{E}^{\circ}_{x,s}$, $\Delta\bar{S}^{\circ}_{s}$, and $\Delta\bar{C}^{\circ}_{P,s}$ stand for the standard partial molal isobaric expansibility, third law entropy, and heat capacity of solvation of the electrolyte,, and U and W represent successive partial derivatives of equation (17) for the solvent, which can be written as

$$U \equiv \left(\frac{\partial Q}{\partial T}\right)_P = -\frac{1}{\varepsilon}\left(\left(\frac{\partial\left(\frac{\partial \ln \varepsilon}{\partial P}\right)_T}{\partial T}\right)_P - \left(\frac{\partial \ln \varepsilon}{\partial T}\right)_P \left(\frac{\partial \ln \varepsilon}{\partial P}\right)_T\right) \quad (22)$$

and

$$W \equiv \left(\frac{\partial^2 Q}{\partial T^2}\right)_P = \left(\frac{\partial U}{\partial T}\right)_P = \frac{1}{\varepsilon}\left(\left(\frac{\partial\left(\frac{\partial^2 \ln \varepsilon}{\partial T^2}\right)_P}{\partial P}\right)_T - 2\left(\frac{\partial \ln \varepsilon}{\partial T}\right)_P \left(\frac{\partial\left(\frac{\partial \ln \varepsilon}{\partial P}\right)_T}{\partial T}\right)_P - \left(\frac{\partial \ln \varepsilon}{\partial P}\right)_T \left(\frac{\partial^2 \ln \varepsilon}{\partial T^2}\right)_P + \left(\frac{\partial \ln \varepsilon}{\partial P}\right)_T \left(\frac{\partial \ln \varepsilon}{\partial T}\right)_P^2\right) \quad (23)$$

Analogous differentiation of equation (18) with respect to pressure at constant temperature leads to

$$\left(\frac{\partial \Delta\bar{V}^{\circ}_{s}}{\partial P}\right)_T = -\bar{\kappa}^{\circ}_{s} = -\omega N \quad (24)$$

where $\bar{\kappa}^{\circ}_{s}$ represents the standard partial molal compressibility of solvation of an electrolyte and

$$N \equiv \left(\frac{\partial Q}{\partial P}\right)_T = \frac{1}{\varepsilon}\left(\left(\frac{\partial^2 \ln \varepsilon}{\partial P^2}\right)_T - \left(\frac{\partial \ln \varepsilon}{\partial P}\right)_T^2\right) \quad (25)$$

for the solvent.

Values of Q, U, W, and N for H_2O have been computed for pressures and temperatures from 0° to 600°C and 0.001 to 5 kb (Helgeson and Kirkham, 1974a). These values were used in the present study to compute values of $r_{e,j}$ and the thermodynamic consequences of electrostriction solvation (see below).

Intrinsic volume and electrostriction collapse.—Comparison of the isobaric temperature dependence of Q with changes in the standard partial molal volume of electrolytes with increasing temperature at constant pressure suggests that $\Delta\bar{V}^{\circ}_{n}$ in equation (11) is a positive asymptotic

function of temperature at low pressures which can be described by the isobaric relation,

$$\Delta\bar{V}^{\circ}_{n} = \sigma + \frac{\xi T}{T-\theta} \tag{26}$$

where σ, ξ, and θ are temperature-independent coefficients characteristic of an electrolyte. From a theoretical standpoint, θ can be regarded as a structural temperature, a concept introduced by Bernal and Fowler (1933). In contrast to ω in the electrostriction solvation equations presented above, σ, ξ, and θ in equation (26) are not constrained by the model to be independent of pressure.

The pressure dependence of $\Delta\bar{V}^{\circ}_{n}$ can be expressed by differentiating equation (26) with respect to pressure at constant temperature, which yields

$$\begin{aligned}\left(\frac{\partial\Delta\bar{V}^{\circ}_{n}}{\partial P}\right)_{T} \equiv -\bar{\kappa}^{\circ}_{n} &= \left(\frac{\partial\sigma}{\partial P}\right)_{T} \\ &\quad + \frac{T}{T-\theta}\left(\frac{\partial\xi}{\partial P}\right)_{T} + \frac{\xi T}{(T-\theta)^{2}}\left(\frac{\partial\theta}{\partial P}\right)_{T} \\ &= \left(\frac{\partial\sigma}{\partial P}\right)_{T} + \frac{(\Delta\bar{V}^{\circ}_{n}-\sigma)}{\xi}\left(\frac{\partial\xi}{\partial P}\right)_{T} + \frac{(\Delta\bar{V}^{\circ}_{n}-\sigma)}{T-\theta}\left(\frac{\partial\theta}{\partial P}\right)_{T} \\ &= \left(\frac{\partial\sigma}{\partial P}\right)_{T} + \frac{(\Delta\bar{V}^{\circ}_{n}-\sigma)}{\xi}\left(\frac{\partial\xi}{\partial P}\right)_{T} + \frac{(\Delta\bar{V}^{\circ}_{n}-\sigma)^{2}}{\xi T}\left(\frac{\partial\theta}{\partial P}\right)_{T}\end{aligned} \tag{27}$$

Because σ, ξ, and θ are independent of temperature, their partial derivatives with respect to pressure at constant temperature are also independent of temperature. Trial and error regression of $-\bar{\kappa}^{\circ}$ and $\bar{V}^{\circ}$ data for electrolytes over a range of temperatures at constant pressure suggests that θ can be regarded as a pressure-independent parameter. For example, alternate fits of the sum of equations (24) and (27) to experimental values of $-\bar{\kappa}^{\circ}$ at one bar and a series of temperatures from 0° to 55°C with and without $(\partial\theta/\partial P)_{T}$ set to zero yield equally close fits of the data (within experimental uncertainty). In contrast, comparison of the coefficients obtained from these fits with those generated by regression of isobaric $\bar{V}^{\circ}$ data as a function of temperature with the sum of equations (18) and (26) indicates that both σ and ξ are pressure-dependent functions. The simplest approximation permitted by the data is given by

$$\sigma = a_{1} + a_{2}P \tag{28}$$

and

$$\xi = a_{3} + a_{4}P \tag{29}$$

where a_1, a_2, a_3, and a_4 are pressure/temperature-independent coefficients characteristic of a given electrolyte or species. As shown below, the con-

sequences of equations (28) and (29) are consistent with experimental observations at high pressures.

Combining equations (26), (28), and (29) results in

$$\Delta\bar{V}^{\circ}_{n} = a_1 + a_2 P + \frac{(a_3 + a_4 P)T}{T-\theta} \tag{30}$$

Taking account of equation (12) we can now write

$$\bar{V}^{\circ}_{i} = a_1 \tag{31}$$

and

$$\Delta\bar{V}^{\circ}_{c} = a_2 P + \frac{\xi T}{T-\theta} = a_2 P + \frac{(a_3 + a_4 P)T}{T-\theta} \tag{32}$$

from which it follows that

$$\Delta\bar{E}^{\circ}_{x,n} = \Delta\bar{E}^{\circ}_{x,c} \equiv \left(\frac{\partial\Delta\bar{V}^{\circ}_{c}}{\partial T}\right)_P = -\left(\frac{\partial\Delta\bar{S}^{\circ}_{c}}{\partial P}\right)_T = -\frac{\xi\theta}{(T-\theta)^2} = -\frac{(a_3 + a_4 P)\theta}{(T-\theta)^2} \tag{33}$$

and

$$\left(\frac{\partial\Delta\bar{E}^{\circ}_{x,n}}{\partial T}\right)_P = \left(\frac{\partial\Delta\bar{E}^{\circ}_{x,c}}{\partial T}\right)_P = \frac{\partial^2\Delta\bar{V}^{\circ}_{c}}{\partial T^2}_P = -\frac{1}{T}\left(\frac{\partial\Delta\bar{C}^{\circ}_{P,c}}{\partial P}\right)_T = \frac{2\theta\xi}{(T-\theta)^3} = \frac{2\theta(a_3 + a_4 P)}{(T-\theta)^3} \tag{34}$$

where $\Delta\bar{E}^{\circ}_{x,c}$, $\Delta\bar{S}^{\circ}_{c}$, and $\Delta\bar{C}^{\circ}_{P,c}$ refer to the standard partial molal isobaric expansibility, entropy, and heat capacity of collapse. The intrinsic standard partial molal volume ($\bar{V}^{\circ}_{i}$) is thus treated as a pressure/temperature independent parameter in the model, which means

$$\Delta\bar{\kappa}^{\circ}_{n} = \Delta\bar{\kappa}^{\circ}_{c} \tag{35}$$

and

$$\bar{E}^{\circ}_{x,i} \equiv \left(\frac{\partial\bar{V}^{\circ}_{i}}{\partial T}\right)_P = -\left(\frac{\partial\bar{S}^{\circ}_{i}}{\partial P}\right)_T = \left(\frac{\partial\bar{E}^{\circ}_{x,i}}{\partial T}\right)_P = \left(\frac{\partial^2\bar{V}^{\circ}_{i}}{\partial T^2}\right)_P = -\frac{1}{T}\left(\frac{\partial\bar{C}^{\circ}_{P,i}}{\partial P}\right)_T = \left(\frac{\partial\bar{V}^{\circ}_{i}}{\partial P}\right)_T = -\bar{\kappa}^{\circ}_{i} = 0 \tag{36}$$

where $\bar{E}^{\circ}_{x,i}$, $\bar{S}^{\circ}_{i}$, $\bar{C}^{\circ}_{P,i}$, and $\bar{\kappa}^{\circ}_{i}$ represent the standard intrinsic partial molal expansibility, entropy, heat capacity, and compressibility of the electrolyte. Because the actual variation of $\bar{V}^{\circ}_{i}$ with pressure and/or temperature is almost certainly slight (that is, negligible by comparison with changes in $\Delta\bar{V}^{\circ}_{c}$ and $\Delta\bar{V}^{\circ}_{s}$), the assumption represented by equation (36) should introduce insignificant error in the equation of state.

The standard partial molal compressibility of collapse ($\Delta\bar{K}^\circ_c$) is given by the partial derivative of equation (32) with respect to pressure at constant temperature; that is,

$$\left(\frac{\partial\Delta\bar{V}^\circ_c}{\partial P}\right)_T = \left(\frac{\partial\Delta\bar{V}^\circ_n}{\partial P}\right)_T = -\Delta\bar{K}^\circ_c = a_2 + \frac{a_4 T}{T-\theta} \qquad (37)$$

which is independent of pressure; that is, $(\partial^2\Delta\bar{V}^\circ_c/\partial P^2)_T = 0$. Combining equations (32) and (37) leads to

$$-\Delta\bar{K}^\circ_c = \frac{a_2(\xi - a_4 P)}{\xi} + \frac{a_4\Delta\bar{V}^\circ_c}{\xi} \qquad (38)$$

At constant pressure, equation (38) requires $\Delta\bar{K}^\circ_c$ to be a linear function of $\Delta\bar{V}^\circ_c$.

Partial molal volume, expansibility, and compressibility.—Taking account of equations (11), (18), (31), and (32), the composite equation of state for aqueous electrolytes at infinite dilution can be written as

$$\bar{V}^\circ = a_1 + a_2 P + \frac{(a_3 + a_4 P)T}{T-\theta} - \omega Q \qquad (39)$$

which is consistent with

$$\bar{V}^\circ = \sigma + \frac{\xi T}{T-\theta} - \omega Q \qquad (40)$$

where σ and ξ are given by equations (28) and (29). Similarly, from equations (20), (21), and (33) through (36) it follows that

$$\bar{E}^\circ_x \equiv \left(\frac{\partial\bar{V}^\circ}{\partial T}\right)_P = -\left(\frac{\partial\bar{S}^\circ}{\partial P}\right)_T = \Delta\bar{E}^\circ_{x,e}$$
$$= -\frac{\xi\theta}{(T-\theta)^2} - \omega U = -\frac{(a_3 + a_4 P)\theta}{(T-\theta)^2} - \omega U \qquad (41)$$

and

$$\left(\frac{\partial\Delta\bar{E}^\circ_{x,e}}{\partial T}\right)_P = \left(\frac{\partial\bar{E}^\circ_x}{\partial T}\right)_P = \left(\frac{\partial^2\bar{V}^\circ}{\partial T^2}\right)_P = -\frac{1}{T}\left(\frac{\partial\bar{C}^\circ_P}{\partial P}\right)_T$$
$$= \left(\frac{\partial\Delta\bar{E}^\circ_{x,e}}{\partial T}\right)_P = \frac{2\theta\xi}{(T-\theta)^3} - \omega W = \frac{2\theta(a_3 + a_4 P)}{(T-\theta)^3} - \omega W \qquad (42)$$

where $\bar{E}^\circ_x$, $\bar{S}^\circ$, and $\bar{C}^\circ_P$ refer to the standard partial molal expansibility and the third law entropy and heat capacity of an electrolyte, respectively. The standard partial molal compressibility is given by the sum of equations (24) and (37); that is

$$\left(\frac{\partial\bar{V}^\circ}{\partial P}\right)_T = -\bar{K}^\circ = -\Delta\bar{K}^\circ_e \equiv \left(\frac{\partial\Delta\bar{V}^\circ_e}{\partial P}\right)_T = a_2 + \frac{a_4 T}{T-\theta} - \omega N \qquad (43)$$

The coefficients in the equation of state and its partial derivatives can be evaluated for a given electrolyte by separate or combined regression of experimental values of $\bar{V}^\circ$ and $\bar{\kappa}^\circ$ as functions of temperature at constant pressure, which permits the validity of the equations to be assessed by comparing experimental observations of $\bar{V}^\circ$ at high pressures and/or temperatures with corresponding values predicted independently from the equation of state and fit coefficients obtained from regression of low temperature/pressure data. In addition to σ and ξ for a given pressure, isobaric regression of $\bar{V}^\circ$ as a function of temperature with equation (40) yields values of ω and θ (which are pressure-independent). Specifying these latter parameters or their theoretical counterparts in regression of corresponding $\bar{\kappa}^\circ$ data with equation (43) permits calculation of a_1 and a_3 from equations (28) and (29) using the values of a_2 and a_4 generated by regression of the compressibility data. Alternately, simultaneous regression of both $\bar{V}^\circ$ and $\bar{\kappa}^\circ$ values with equations (39) and (43) can be carried out to obtain values of a_1, a_2, a_3, a_4, θ, and ω. In either case the values of ω and other parameters obtained by regression can be compared with their theoretical counterparts (discussed below) to assess the uncertainty in the fit coefficients. However, the data from which these coefficients are derived must be highly accurate to insure reliable prediction of $\bar{V}^\circ$ at temperatures and pressures beyond the range represented by the experimental data. High-precision density data and accurate extrapolation of apparent molal volumes of electrolytes to infinite dilution are critical requisites for calculating dependable coefficients for the equation of state.

ANALYSIS OF DENSITY DATA

Relative densities of a large number of electrolytes have been measured by Ellis (1966, 1967, 1968) and Ellis and McFadden (1968, 1973) at concentrations from 0.05 m or 0.1 m to 0.5, 1.0, or 2.0 m (depending on the electrolyte) and temperatures from 25° or 50°C to 200°C at 20 bars. Ellis and McFadden computed partial molal volumes of the electrolytes at infinite dilution from their density data with the aid of the molal counterpart of the Masson (1929) equation; that is,

$$\phi_V = \bar{V}^\circ + S^*_V \, m^{1/2} \tag{44}$$

where S^*_V stands for the slope of the curve obtained by plotting the apparent molal volume of an electrolyte (ϕ_V) against $m^{1/2}$. The apparent molal volume of an electrolyte is related to the corresponding volume of a solution (V_{soln}) containing n_w moles of H_2O and n moles of solute by

$$\phi_V = \frac{V_{soln} - n_w \bar{V}^\circ_w}{n} = \frac{1}{m}\left(\frac{1000 + m\mathbf{M}}{\rho_{soln}}\right) - \frac{1000}{\bar{\rho}^\circ_w}\right) \tag{45}$$

where $\bar{V}^\circ_w$ refers to the standard partial molal volume of the solvent in cm^3 $mole^{-1}$, $\mathbf{M}$ is the molecular weight of the solute in g $mole^{-1}$, and ρ_{soln} and $\bar{\rho}^\circ_w$ stand for the density in g cm^3 of the solution and that of pure H_2O, respectively. All of the S^*_V values used by Ellis and McFadden to evaluate equation (57) were determined empirically from their experi-

mental data. However, in the case of $MgCl_2$, $CaCl_2$, $SrCl_2$, and $BaCl_2$, they employed nonlinear free-hand extrapolation of ϕ_V as a function of $m^{1/2}$ to obtain estimates of $\bar{V}°$.

As pointed out by Redlich and Rosenfeld (1931), the slope constant in the Masson equation should correspond to the Debye-Hückel limiting slope obtained by differentiating

$$\log \gamma_{\pm} = -A_\gamma |Z_+ Z_-| I^{1/2} \tag{46}$$

to give

$$\left(\frac{\partial \log \gamma_{\pm}}{\partial P}\right)_T = \frac{\bar{V} - \bar{V}°}{2.303 \nu RT} = -\left(\frac{\partial A_\gamma}{\partial P}\right)_T |Z_+ Z_-| I^{1/2} \tag{47}$$

where $\bar{V}$ denotes the partial molal volume of the electrolyte, $\gamma_{\pm}$ represents the mean ionic activity coefficient of an electrolyte consisting of ν moles of ions (mole of solute)$^{-1}$, Z_+ and Z_- stand for the charges on the cation and anion, respectively, I refers to ionic strength in molality units of concentration ($I = \nu|Z_+Z_-|m/2$), and A_γ is the Debye-Hückel limiting law parameter defined by

$$A_\gamma = \frac{1.824829238 \times 10^6 \, \bar{\rho}°^{1/2}}{(\varepsilon T)^{3/2}} \tag{48}$$

where ε again stands for the dielectric constant of H_2O. It follows from the first identity in equation (45) that

$$\bar{V} = \phi_V + m\left(\frac{\partial \phi_V}{\partial m}\right)_{P,T,n_w} \tag{49}$$

which can be combined with equation (44) and its partial derivative with respect to m to give

$$\bar{V} = \bar{V}° + \frac{3}{2} S^*_V \, m^{1/2} \tag{50}$$

If we now replace S^*_V with its theoretical counterpart (S_V) and combine equations (47) and (50) we can write

$$S_V \equiv -\frac{2}{3} A_V \left(\frac{\nu|Z_+Z_-|}{2}\right)^{3/2} \tag{51}$$

where

$$A_V \equiv -2(2.303)RT\left(\frac{\partial A_\gamma}{\partial P}\right)_T = 2.303RTA_\gamma\left(3\left(\frac{\partial \ln \varepsilon}{\partial P}\right)_T - \bar{\beta}°\right) \tag{52}$$

where $\bar{\beta}°$ stands for the coefficient of isothermal compressibility of H_2O ($(\partial \ln \bar{\rho}°/\partial P)_T$).

Despite the fact that the Debye-Hückel limiting law for $\log \gamma_{\pm}$ is theoretically applicable only at concentrations of the order of 0.01 m or less, the Masson equation has been found empirically to represent the

low-temperature concentration dependence of ϕ_V to much higher concentrations. However, the value of S^*_V obtained empirically rarely corresponds to the theoretical slope, S_V. The functional form of the concentration dependence of ϕ_V at low temperatures is thus insensitive to departures of $\bar{V}$ from the Debye-Hückel limiting law, which is manifested by differences in S^*_V and S_V. These differences, which increase with increasing temperature, commonly lead to erroneous values of $\bar{V}^\circ$ obtained from the Masson equation (Millero, 1972a).

Calculations and uncertainties.—To improve on Ellis and McFadden's extrapolation of apparent molal volumes to infinite dilution at 20 bars, values of ϕ_V were recomputed (eq 45) from their reported solution densities at temperatures from 25° or 50° to 200°C and those of H_2O taken from Kell and Whalley (1965) for temperatures from 25° to 150°C and Schmidt (1969) for 175° and 200°C.[4]

The ϕ_V values were then fit graphically to the molal counterpart of the Redlich-Meyer equation (Redlich and Meyer, 1964), which can be written as

$$\phi_V = \bar{V}^\circ + S_V\, m^{1/2} + b'_V\, m \tag{53}$$

where S_V is again the theoretical Debye-Hückel limiting slope, and b'_V is a coefficient characteristic of the electrolyte. The molal counterpart of the Redlich-Meyer equation requires $\phi_V - S_V m^{1/2}$ to exhibit a linear dependence on molality with slope b'_V and intercept $\bar{V}^\circ$. Plots of this kind (generated from the recalculated ϕ_V values) are depicted in figures 11 through 13 for the 19 electrolytes considered by Ellis and McFadden at 20 bars and 25° or 50° to 200°C. The values of S_V and A_V required for the calculations were computed from equations (51) and (52) with the aid of an equation of state for H_2O (Keenan and others, 1969) and its partial derivatives, which were used to calculate $\bar{\beta}^\circ$ and values of $(\partial \ln \varepsilon/\partial P)_T$ based on regression (Helgeson and Kirkham, 1974a) of dielectric constant data (Oshry, 1949; Owen and others, 1961; Heger, ms) at high pressures and temperatures. The results of the limiting slope calculations for 0° to 200°C at 20 bars (Helgeson and Kirkham, 1974b) are shown in table 1.

Graphic fits of $\phi_V - S_V m^{1/2}$ to m were performed in lieu of numerical regression in order to take adequate account of the relatively large uncertainties in the computed values of ϕ_V at the lower concentrations and to insure b'_V values that define a smooth function of temperature for each electrolyte. The latter constraint assures internal consistency and provides a basis for resolving ambiguities introduced in the $\phi_V - S_V m^{1/2}$ plots by the large relative uncertainty in corresponding values of ϕ_V and ρ_{soln}. The relative uncertainty of ϕ_V is a negative function of concentration defined by the partial derivative of equation (45) with respect to ρ_{soln} at

[4] In his earlier work, Ellis apparently used densities of H_2O taken from Dorsey (1940) to compute ϕ_V. Densities of HCl solutions, which were not published by Ellis and McFadden (1968), were obtained by written communication.

constant molality, which can be written in terms of finite differences ($\Delta\phi_V$ and $\Delta\rho_{soln}$) as

$$\Delta\phi_V = -\left(\frac{1000 + m\mathbf{M}}{m\ \rho_{soln}{}^2}\right)\Delta\rho_{soln} \tag{54}$$

It can be deduced from equation (54) that absolute errors in density are magnified in ϕ_V by more than $10^3/m$, so that densities of dilute solutions must be known to a precision of the order of 10 ppm or better to yield unambiguous values of ϕ_V.

Ellis and McFadden's experimental apparatus was designed to measure changes in solution density with increasing temperature relative to the solution density at 50°C. In most cases they used densities for 50°C (corrected to a pressure of 20 bars) reported in the International Critical Tables (1928) to convert their relative measurements to absolute values. Ellis and McFadden's measurements of absolute densities at 25° and 50°C

TABLE 1

Debye-Hückel limiting law coefficient for the partial molal volumes of aqueous electrolytes (A_V) in $cm^3\ kg^{1/2}\ mole^{-3/2}$ at 20 bars and temperatures from 0° to 200°C (Helgeson and Kirkham, 1974b)

T, °C	A_V	T, °C	A_V
0	2.327	105	6.353
5	2.396	110	6.765
10	2.467	115	7.208
15	2.544	120	7.686
20	2.630	125	8.202
25	2.728	130	8.759
30	2.836	135	9.361
35	2.958	140	10.011
40	3.091	145	10.715
45	3.239	150	11.478
50	3.400	155	12.305
55	3.576	160	13.203
60	3.767	165	14.179
65	3.974	170	15.242
70	4.198	175	16.401
75	4.440	180	17.668
80	4.702	185	19.054
85	4.985	190	20.575
90	5.289	195	22.248
95	5.618	200	24.091
100	5.972		

were limited to KF, NH_4ClO_4, $NaHCO_3$, and NaHS. The precision of the densities reported in the International Critical Tables is ± 5 ppm, except for $MgCl_2$, $CaCl_2$, $SrCl_2$, and $BaCl_2$, which are given to ± 50 ppm. However, the accuracy of the densities given in the International Critical Tables for 1:1 electrolytes is not comparable to the precision, especially in the dilute end of the concentration range. An example is shown in figure 10. The apparent molal volume of NaCl at 25°C and 20 bars (computed from the densities reported in the International Critical Tables) is plotted against $m^{1/2}$ in the upper diagram, and $\phi_V - S_V m^{1/2}$ is shown as a function of molality in the lower diagram. The dashed lines represent linear extrapolations of the two data points at the highest concentrations (which are the least uncertain). The slope of the dashed line in the upper diagram corresponds to the theoretical slope, S_V, and the intercept is equal to that of the dashed line in the lower diagram, which is consistent with the molal counterpart of the Redlich-Meyer equation. The intercepts are in close agreement with the value of $\bar{V}°$ for NaCl at 25°C and one bar (16.61 cm^3 $mole^{-1}$) reported by Millero (1972b). Because b'_V for NaCl at 25°C is small, either the Masson equation or its molal analog with the theoretical slope suffices to describe the concentra-

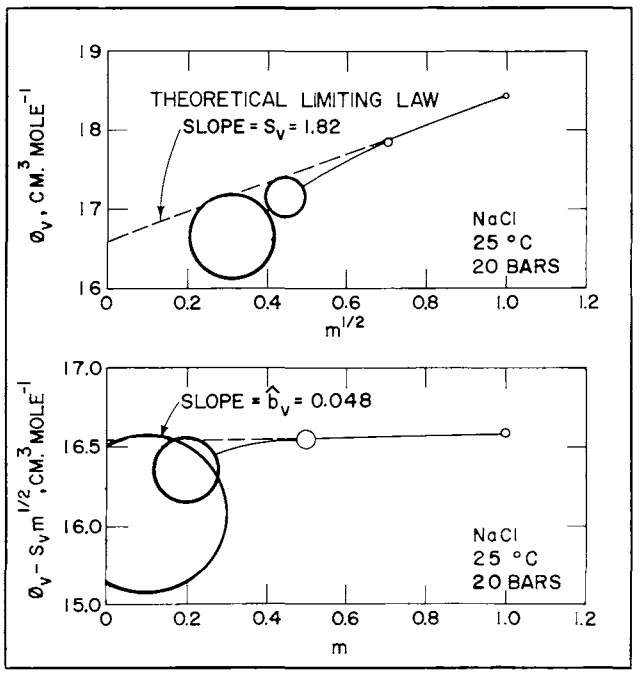

Fig. 10. Apparent molal volume (ϕ_V) of NaCl computed (eq 45) from densities of NaCl solutions reported in the International Critical Tables and that for H_2O taken from Kell and Whalley (1965) as a function of the square root of the molality (m) of NaCl (upper diagram) and the difference between ϕ_V and S_V $m^{1/2}$ (where S_V stands for the theoretical Debye-Hückel limiting slope computed (eq 51) from the appropriate value of A_V in table 1) as a function of m at 25 C and 20 bars.

tion dependence of ϕ_V in figure 10, but at higher temperatures this is no longer true. Note that a straight line drawn through all the points in the upper diagram would have a slope (S^*_V) of 2.1 and an intercept ($\bar{V}°$) of 16.2 cm^3 mole^{-1}, which would introduce an error of 0.4 cm^3 mole^{-1} in $\bar{V}°$. This error would be tripled if only the two data points for the more dilute concentrations were used for empirical application of the Masson equation. An uncertainty in ϕ_V corresponding to a precision of ± 5 ppm for the densities reported in the International Critical Tables would be of the order of 0.05 cm^3 mole^{-1} or less for the data points shown in figure 10. However, there can be little doubt that the actual uncertainty arising

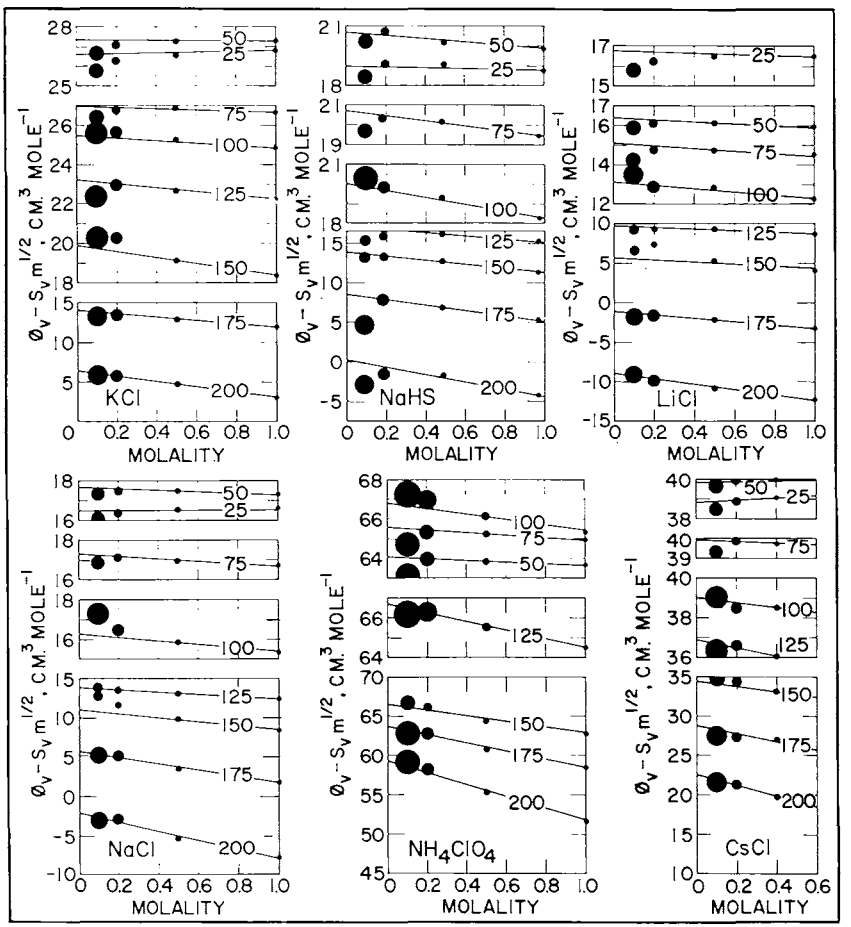

Fig. 11. Extrapolation plots against molality (m) of the difference between the apparent molal volume (ϕ_V) and $S_V\ m^{1/2}$ (where S_V stands for the theoretical Debye-Hückel limiting slope) for electrolytes at 20 bars and 25° to 200°C computed (eqs 45 and 51) from values of A_V in table 1, densities of H_2O given by Kell and Whalley (1965) and Schmidt (1969), and densities of electrolytes reported by Ellis (1968; written commun., 1970) and Ellis and McFadden (1972).

from inaccuracies in solution densities reported in the International Critical Tables is of the order represented by the size of the symbols in figure 10. For the most dilute data point, the minimum uncertainty is ± 0.5 cm^3 $mole^{-1}$ (± 3 percent), which is consistent with an uncertainty in the corresponding solution density of more than ± 50 ppm.

As a consequence of the experimental technique employed by Ellis and McFadden, errors in the International Critical Table densities responsible for discrepancies such as those apparent in figure 10 are inherent in the high temperature densities computed from the relative density measurements, which are themselves subject to additional uncertainty. The experimental uncertainties estimated by Ellis and McFadden range from ± 10 to ± 20 ppm at 50° and 75°C to ± 50 ppm at 175° and 200°C. Additional errors may arise from uncertainties in the density of the solvent. Possible errors in Kell and Whalley's (1965) densities of H_2O at 20 bars range from 6 ppm at 25°C to 21 ppm or less at 150°C. Densities of H_2O at 175° and 200°C are given by Schmidt (1969) to a precision of 50 ppm.

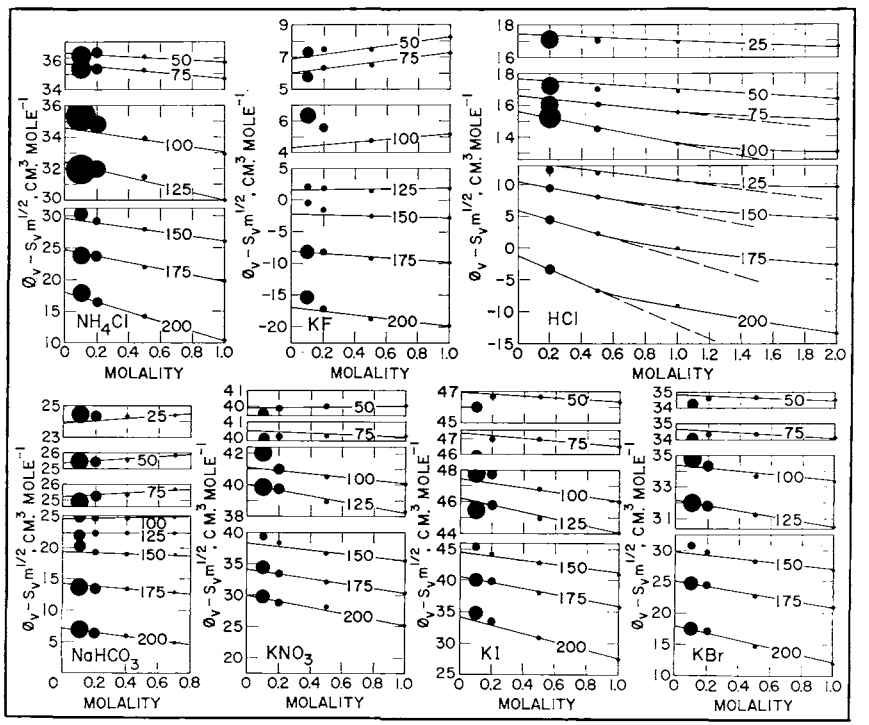

Fig. 12. Extrapolation plots against molality (m) of the difference between the apparent molal volume (ϕ_V) and S_V $m^{1/2}$ (where S_V stands for the theoretical Debye-Hückel limiting slope) for electrolytes at 20 bars and 25° to 200°C computed (eqs 45 and 51) from values of A_V in table 1, densities of H_2O given by Kell and Whalley (1965) and Schmidt (1969), and densities of electrolytes reported by Ellis (1967, 1968).

The minimum accumulated consequences of the uncertainties summarized above at $m = 0.1$ probably range from the order of $\pm$ 0.3 to $\pm$ 1.5 cm^3 mole^{-1} (depending on the electrolyte) at temperatures $\leq$ 75°C to approximately $\pm$ 1 to $\pm$ 2 cm^3 mole^{-1} at 200°C. As concentration increases, the minimum uncertainties decrease to values ranging from about $\pm$ 0.05 to $\pm$ 0.1 cm^3 mole^{-1} at $m = 1.0$ and temperatures $\leq$ 75°C, and $\pm$ 0.2 to $\pm$ 0.3 cm^3 mole^{-1} at $m = 1.0$ at 200°C. These overall uncertainties, which are conservative estimates, are approximated by the sizes of the symbols in figures 11 to 13.

Discussion.—It can be seen in figures 11 and 12 that equation (53) represents (within the limits of uncertainty) most of the experimental data for 1:1 electrolytes at all of the temperatures. A notable exception is HCl, which exhibits systematic departures from the molal counterpart of the Redlich-Meyer equation as temperature increases above 50°C at

TABLE 2

Empirical values of the molal b'_V parameter for aqueous electrolytes (eq 53) in cm^3 kg mole^{-2} at 20 bars and temperatures from 25° to 200°C. The numbers given in this table correspond to the slopes of the curves in figures 10 through 13[a]

Electrolyte	Temperature, °C							
	25	50	75	100	125	150	175	200
HCl	-0.50	-0.70	-1.10	-2.00	-3.13	-4.66	-7.50	-11.20
LiCl	-0.35	-0.58	-0.72	-0.84	-1.04	-1.43	-2.14	-3.40
NaCl	0.04	-0.44	-0.66	-0.90	-1.50	-2.55	-4.02	-5.80
KCl	0.16	-0.12	-0.36	-0.64	-1.00	-1.47	-2.18	-3.34
CsCl	0.60	0.20	-0.40	-1.10	-2.16	-3.60	-5.15	-6.78
NH_4Cl	-	-0.55	-0.94	-1.60	-2.46	-3.54	-5.15	-7.50
KBr	0.15[b]	-0.44	-0.63	-1.00	-1.70	-2.86	-4.33	-6.00
KF	-	1.40	1.28	0.92	0.28	-0.56	-1.64	-2.96
KI	-0.15[b]	-0.56	-0.90	-1.42	-2.24	-3.34	-4.85	-6.60
$NaHCO_3$	0.8	0.70	0.60	0.30	0.00	0.64	-1.70	-3.28
KNO_3	0.9[b]	0.10	-0.46	-1.03	-1.82	-2.78	-3.81	-4.92
NaHS	-0.12	-0.83	-1.33	-1.73	-2.08	-2.55	-3.35	-4.60
NH_4ClO_4	-0.2[b]	-0.40	-0.70	-1.30	-2.20	-3.60	-5.26	-7.20
$MgCl_2$	-	-5.0	-9.0	-16.0	-26.0	-39.4	-54.5	-71.0
$CaCl_2$	-1.0[b]	-4.0	-6.0	-11.0	-17.0	-27.0	-48.0	-79.0
$SrCl_2$	-	-6.2	-8.4	-13.2	-21.0	-33.2	-51.0	-71.0
$BaCl_2$	-3.0[b]	-5.0	-8.0	-12.8	-19.0	-29.3	-44.0	-62.0
Na_2SO_4	4.0	-2.0	-3.6	-6.4	-12.8	-22.0	-38.0	-68.0
K_2SO_4	-	-2.5	-4.5	-8.0	-13.0	-26.0	-44.0	69.6

[a]Where these curves are nonlinear, $\hat{b}_V$ corresponds to the slope in the dilute concentration range. [b]Extrapolated or interpolated from the curves in figures 14 and 15.

concentrations > 0.5 *m*. In a number of cases (for example, NaHS at 200°C), the experimental points for the dilute concentrations appear to be aberrant, suggesting larger experimental uncertainties than those estimated by Ellis and McFadden (and included in the overall minimum uncertainties represented by the sizes of the symbols in figs. 11 through 13). The spurious nature of these data points is confirmed by the fact that alternate values of b'_V corresponding to the slopes of curves drawn through them fail to define a smooth dependence of b'_V on temperature.

The 1:2 and 2:1 electrolytes represented by the curves in figure 13 exhibit behavior similar to that of HCl, that is, increasing departures from equation (53) with increasing temperature. Plots for the molar scale of concentration analogous to those in figure 13 exhibit similar departures from the Redlich-Meyer equation, which have also been noted for certain 2:1, 3:1, and 4:1 electrolytes at 25°C and 1 bar (Millero, 1972a). The dashed lines in figures 11 and 13 represent linear extensions of the segments of the curves in the dilute region of concentration. The slopes of the linear curves and dashed lines in figures 11 through 13 correspond to the molal b'_V values given in table 2 and plotted in figures 14 and 15. The intercepts of the linear curves and dashed lines correspond to the values of $\bar{V}^\circ$ shown in table 3.

Despite the fact that the low temperature b'_V values taken from the literature and plotted in figures 14 and 15 are consistent with the molar scale of concentration and derived from data at one bar, it can be seen that they are in close agreement with the molal values for 20 bars. Differences in b'_V introduced by the different scales of concentration are relatively small (within the uncertainty of the data) at low temperatures. The order of magnitude of these differences can be assessed with the aid of figure 16, where it can be seen that the difference in the two scales of concentration is of the order of 0.02 at 1.0 *m* and $\sim$ 0.01 at 0.5 *m*, which requires b'_V on the molar scale of concentration to be slightly larger than the corresponding molal b'_V. Consideration of the molal b'_V values in table 2 and figures 14 and 15 suggests that those for 1:1 electrolytes at low temperatures should be of the order of 0.05 or less smaller than the corresponding molar b'_V values, but for 1:2 and 2:1 electrolytes the difference should be $\sim$ 0.1 or less. It can be seen in figures 14 and 15 that these differences are within the uncertainty of the b'_V values and that the molal and molar values plotted in the diagrams are consistent with one another. The effect of a difference in pressure of 19 bars between the low-temperature b'_V values taken from the literature and those computed in the present study is also within the uncertainty of the data.

Owing to the relatively small magnitude of the b'_V values for 1:1 electrolytes at low temperatures, errors in b'_V have a minor effect on extrapolated values of $\bar{V}^\circ$ derived from the Redlich-Meyer equation or its molal analog. For the same reason, application of the Masson equation or its molal counterpart also affords close approximations of $\bar{V}^\circ$ at low temperatures. However, such is not the case for 1:2 and 2:1 electrolytes, nor for 1:1 electrolytes at high temperatures where b'_V becomes a rela-

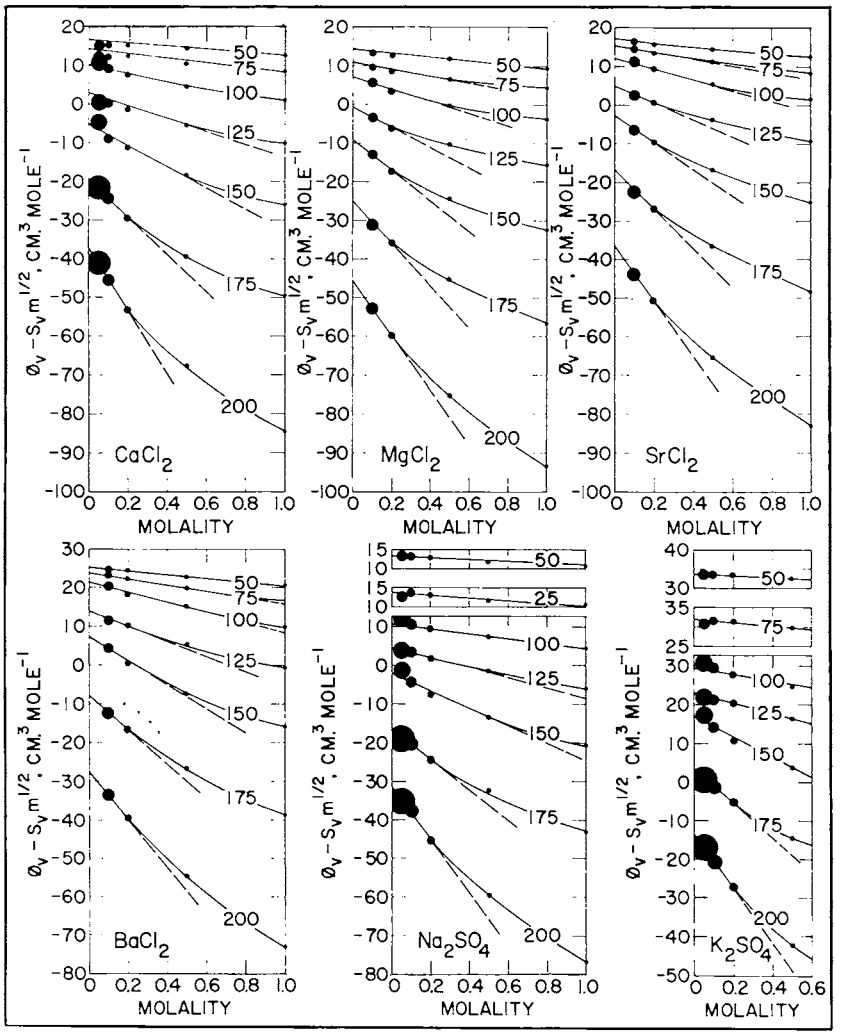

Fig. 13. Extrapolation plots against molality (m) of the difference between the apparent molal volume (ϕ_V) and $S_V\, m^{1/2}$ (where S_V stands for the theoretical Debye-Hückel limiting slope) for electrolytes at 20 bars and 25° to 200°C computed (eqs 45 and 51) from values of A_V in table 1, densities of H_2O given by Kell and Whalley (1965) and Schmidt (1969), and densities of electrolytes reported by Ellis (1966, 1968) and Ellis and McFadden (1972).

tively large negative number. As a consequence, the $\bar{V}°$ values given in table 3 differ to an increasing degree with increasing temperature from the corresponding values obtained by Ellis and McFadden from the molal analog of the Masson equation using the empirical parameter, S^*_V. The latter values are generally more positive than those in table 3. The differences for 1:1 electrolytes are of the order of 1 cm^3 $mole^{-1}$ or less at low temperatures, increasing to 2 or 3 cm^3 $mole^{-1}$ at 200°C. The corresponding differences for 1:2 and 2:1 electrolytes are $\sim$ 4 cm^3 $mole^{-1}$ or less at low temperatures and 8 to 11 cm^3 $mole^{-1}$ at 200°C.

Despite the fact that the nonlinear relation of molarity to molality as a function of concentration means that the molal and molar versions of the Redlich-Meyer equation cannot both give rise to linear curves like those in figure 11, uncertainties in the data and the slight departures

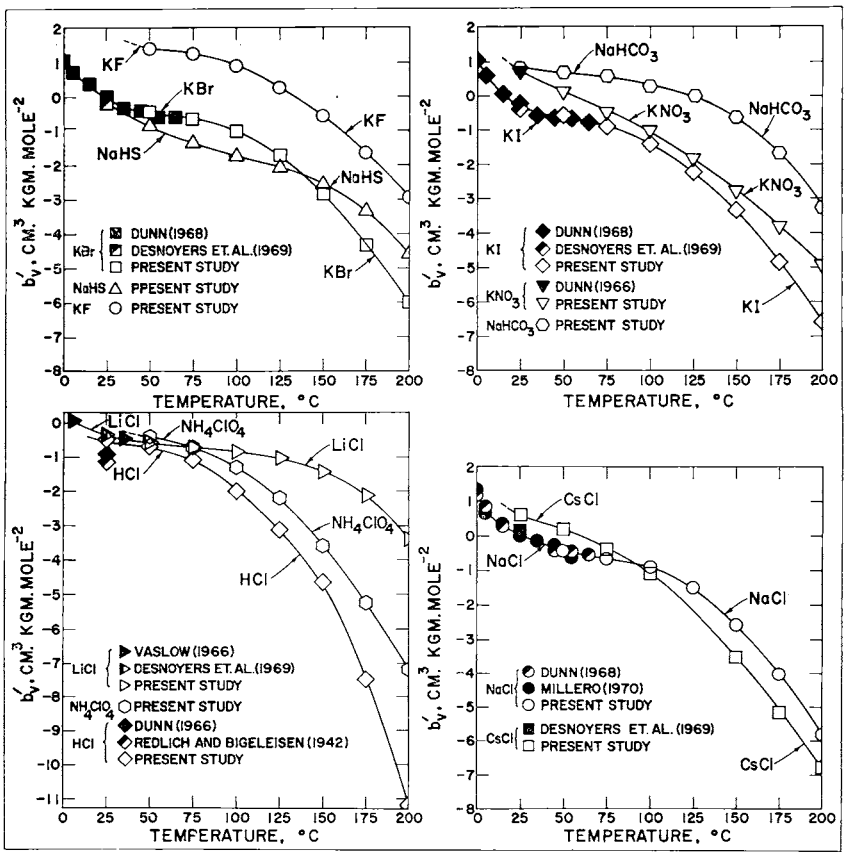

Fig. 14. Molal b'_V coefficients for various electrolytes (eq 53) as a function of temperature at 20 bars. Except for those taken from the literature (which are in cm^3 1 $mole^{-2}$), the values of b'_V (table 2) plotted above correspond to the slopes of the curves for the respective electrolytes in figures 11 through 13.

of molarity from molality at $m \leq 1$ preclude a nonlinear interpretation of the distribution of points in the dilute region of concentration on either scale. The departures from linearity at higher concentrations for HCl and those for the 1:2 and 2:1 electrolytes in figures 12 and 13 far exceed the effect of choosing one concentration scale over another. The molal scale is generally more convenient for geochemical calculations because changes in temperature and pressure affect the molar but not the molal scale of concentration.

Additional terms are required in the Redlich-Meyer equation to represent completely the nonlinear curves in figures 12 and 13, which can be described by an empirical power function of the form

$$\phi_V = \bar{V}^\circ + S_V m^{1/2} + b'_V m + \sum_{l=2} c_l m^l \qquad (55)$$

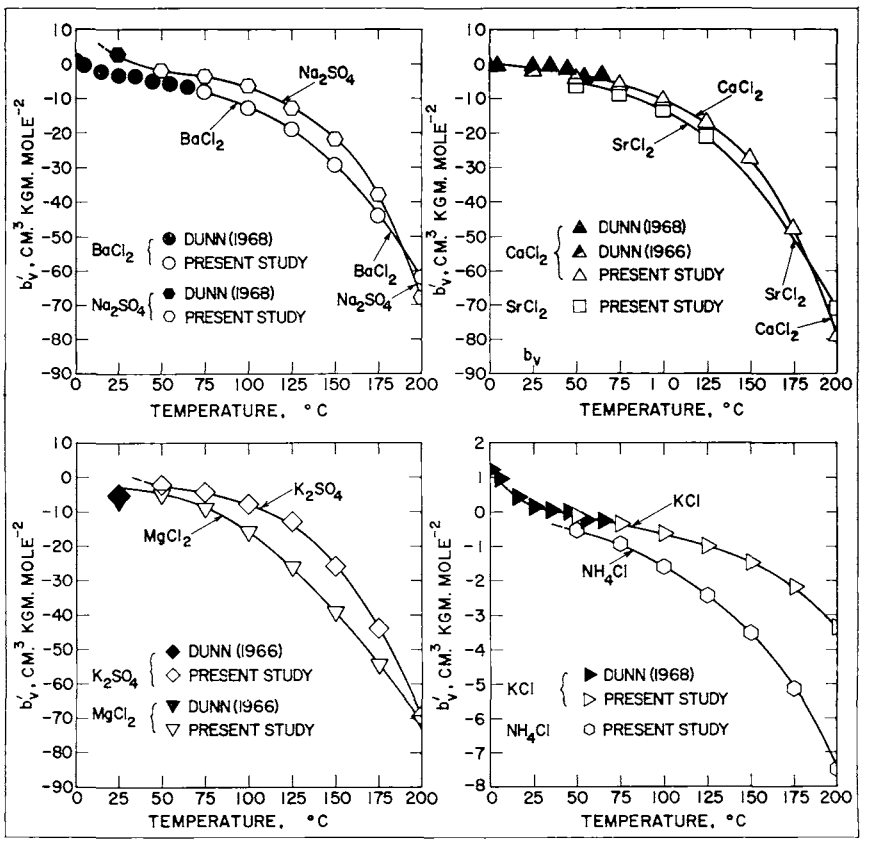

Fig. 15. Molal b'_V coefficients for various electrolytes (eq 53) as a function of temperature at 20 bars. Except for those taken from the literature (which are in cm^3 1 $mole^{-2}$), the values of b'_V (table 2) plotted above correspond to the slopes of the curves for the respective electrolytes in figures 11 through 13.

where c_l stands for the coefficients in the higher-order terms indexed on the interger l ($l = 2, 3 \ldots$.). However, such an approach is hardly warranted in view of the fact that the Redlich-Meyer equation is inconsistent with the extended Debye-Hückel equation commonly used to represent activity coefficients as a function of ionic strength (see below). Although this inconsistency leads to negligible errors in extrapolated values of $\bar{V}°$ (Helgeson and Kirkham, 1976), it precludes use of an extended Redlich-Meyer equation to interpret theoretically a nonlinear dependence of $\phi_V - S_V m^{1/2}$ on m at high concentrations.

The cause of the departure from linearity of the curves for HCl and the 1:2 and 2:1 electrolytes in figures 12 and 13 is almost certainly due to the fact that the Redlich-Meyer equation is inconsistent with

$$\log \gamma_{\pm} = -\frac{|Z_+ Z_-| A_\gamma I^{1/2}}{1 + \mathring{a} B_\gamma I^{1/2}} + b_\gamma I \qquad (56)$$

TABLE 3

Standard partial molal volumes of aqueous electrolytes in cm^3 $mole^{-1}$ at 20 bars and temperatures from 25° to 200°C computed from density data (Ellis, 1966, 1967, 1968; Ellis, written commun., 1970; Ellis and McFadden, 1968, 1972) and equations (45) and (53) together with values of A_V and b'_V taken from tables 1 and 2

Electrolyte	Temperature, °C							
	25	50	75	100	125	150	175	200
HCl	17.5	17.7	16.6	15.6	13.6	10.4	5.8	-1.2
LiCl	16.8	16.4	15.1	13.1	9.7	5.7	-1.2	-9.0
NaCl	16.55	17.7	17.3	16.3	13.9	11.1	5.7	-2.0
KCl	26.6	27.3	27.0	25.4	23.2	19.9	14.0	6.4
CsCl	38.8	39.9	39.9	39.0	36.9	34.4	28.6	22.5
NH_4Cl	-	36.2	35.6	34.6	32.4	29.6	24.7	17.9
KBr	-	34.8	34.6	34.4	32.1	29.6	25.0	18.1
KF	-	6.9	6.0	4.3	1.6	-2.3	-8.2	-17.0
KI	-	46.9	47.3	47.4	46.2	44.4	40.5	34.1
$NaHCO_3$	23.9	25.4	25.2	24.5	22.3	19.3	14.2	7.1
KNO_3	-	39.8	40.5	41.1	40.0	38.2	34.0	29.9
NaHS	18.9	20.7	20.7	20.0	17.2	13.8	8.5	0.2
NH_4ClO_4	-	64.1	65.6	66.8	66.7	65.6	63.6	59.2
$MgCl_2$	-	14.3	10.8	7.0	-0.8	-9.2	-25.0	-45.8
$CaCl_2$	-	16.7	14.1	10.0	3.0	-5.6	-19.6	-37.5
$SrCl_2$	-	17.2	15.2	12.0	5.0	-2.8	-16.6	-36.5
$BaCl_2$	-	25.3	23.8	21.2	14.0	7.4	-7.8	-27.2
Na_2SO_4	-	13.2	13.8	10.5	4.6	-2.0	-16.5	-31.5
K_2SO_4	-	33.4	32.0	29.8	23.0	16.7	3.0	-13.8

where å represents the ion size parameter, b_γ denotes a coefficient characteristic of the electrolyte, and B_γ stands for the molal Debye-Hückel coefficient defined by

$$B_\gamma \equiv \frac{50.29158649 \times 10^8 \overline{\rho}^{\circ 1/2}}{(\varepsilon T)^{1/2}} \tag{56A}$$

If å is regarded as a temperature/pressure-independent parameter, it follows from equation (56) that

$$\bar{V} = \bar{V}^\circ + \frac{\psi A_V I^{1/2}}{\Lambda} + \frac{\psi A_\gamma \text{å} B_V I}{\Lambda^2} + \frac{\nu b_V I}{2} \tag{57}$$

which is consistent with

$$\phi_V = \bar{V}^\circ + \psi A_V I^{1/2} a^* + 2\psi A_\gamma B_V \beta^*(\text{å} B_\gamma I^{1/2}) + \frac{\nu b_V I}{4} \tag{57A}$$

where

$$\Lambda = 1 + \text{å} B_\gamma I^{1/2} , \tag{57B}$$

$$\psi = \frac{\nu |Z_+ Z_-|}{2} , \tag{57C}$$

$$B_V = 2(2.303)RT \left(\frac{\partial B_\gamma}{\partial P}\right)_T , \tag{57D}$$

$$b_V = 2(2.303)RT \left(\frac{\partial b_\gamma}{\partial P}\right)_T , \tag{57E}$$

$$\beta^*(\text{å} B_\gamma I^{1/2}) = \frac{1}{\text{å}^3 B_\gamma^4 I}\left(\frac{\Lambda^2}{2} - 3\Lambda + \frac{1}{\Lambda} + 3 \ln \Lambda + 1.5\right) \tag{57F}$$

and

$$a^* = \frac{1}{\Lambda} - \frac{\sigma^*(\text{å} B_\gamma I^{1/2}}{3} \tag{57G}$$

where

$$\sigma^*(\text{å} B_\gamma I^{1/2}) = \frac{3}{\text{å}^3 B_\gamma^3 I^{3/2}}\left(\Lambda - \frac{1}{\Lambda} - 2 \ln \Lambda\right) \tag{57H}$$

If $\text{å} B_\gamma$ is set to unity, equation (56) reduces to the Guggenheim (1935) equation, which is consistent with

$$\bar{V} = \bar{V}^\circ + \frac{\psi A_V I^{1/2}}{1 + I^{1/2}} + \frac{\nu b^*_V I}{2} \tag{58}$$

and

$$\phi = \bar{V}^\circ + \psi A_V I^{1/2}\, a + \frac{\nu b^*_V I}{4} \tag{59}$$

where b^*_V represents the analog of b_V for $\mathring{a}B_\gamma = 1$ and

$$\alpha = \frac{1}{1 + I^{1/2}} - \frac{\sigma(I^{1/2})}{3} \tag{59A}$$

where

$$\sigma(I^{1/2}) = \frac{3}{I^{3/2}}\left(1 + I^{1/2} - \frac{1}{1 + I^{1/2}} - 2 \ln (1 + I^{1/2}) \right) \tag{59B}$$

Equation (59) is analogous to that commonly used to describe the concentration dependence of the apparent molal enthalpies of electrolytes.

Although equations (53), (57A), and (59) commonly yield nearly equivalent fits of experimental data, only equation (57A) is consistent with the behavior of activity and osmotic coefficients at high concentrations (Helgeson and Kirkham, in preparation). Owing to differences in the ionic strength functions in these expressions, alternate regression of density data with the three equations cannot yield the same numerical values of b'_V, b_V, and b^*_V. Nevertheless, in most circumstances all three lead to the same extrapolated value of $\bar{V}°$. Although equations (53) and (59) fail to represent adequately experimental values of ϕ_V for HCl, $BaCl_2$, $MgCl_2$, $CaCl_2$, and $SrCl_2$ at ionic strengths > 0.2 to 1 m (depending on the electrolyte), equation (57A) affords close fits of the data for these electrolytes at all temperatures and concentrations where ion association is negligible (Helgeson and Kirkham, in preparation). In the case of Na_2SO_4 and K_2SO_4, which are partly associated in all but dilute solutions, none of the equations suffices to represent experimental density data at high concentrations.

The success of equations (53) and (59) in representing the concentration dependence of ϕ_V for many electrolytes is a fortuitous consequence of the behavior of α and α^* as functions of ionic strength. For example, it can be shown that α is a near-linear function of $I^{1/2}$ from $I \approx 0.01$ to

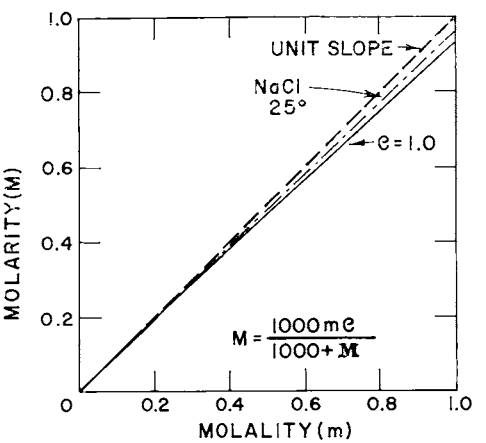

Fig. 16. Molarity of NaCl as a function of molality at 25°C.

TABLE 4

Summary of the Born solvation functions (eqs 17, 22, and 25) for $\Delta\bar{V}^{\circ}_{s}$, $-\Delta\bar{K}^{\circ}_{s}$, and $\Delta\bar{E}^{\circ}_{x,s}$ (eqs 18, 20, and 24) at temperatures from 0° to 200°C, 20 bars, and pressures corresponding to the vapor-saturation curve for H_2O (Helgeson and Kirkham, 1974a)

Temperature[d]	H_2O Saturation Pressures			20 Bars		
	Q[a] × 10^7	N[b] × 10^{10}	U[c] × 10^9	Q[a] × 10^7	N[b] × 10^{10}	U[c] × 10^9
0	5.373	-1.37	1.98	5.354	-1.37	1.81
5	5.476	-1.73	1.83	5.441	-1.70	1.73
10	5.569	-1.94	1.99	5.532	-1.90	1.93
15	5.676	-2.07	2.33	5.637	-2.02	2.28
20	5.807	-2.17	2.75	5.762	-2.11	2.71
25	5.952	-2.24	3.20	5.909	-2.18	3.17
30	6.123	-2.32	3.68	6.079	-2.25	3.65
35	6.321	-2.40	4.17	6.274	-2.33	4.13
40	6.542	-2.49	4.66	6.492	-2.42	4.62
45	6.787	-2.60	5.16	6.736	-2.53	5.12
50	7.058	-2.73	5.68	7.004	-2.65	5.63
55	7.355	-2.88	6.22	7.299	-2.80	6.15
60	7.679	-3.05	6.77	7.620	-2.96	6.70
65	8.032	-3.24	7.35	7.969	-3.15	7.27
70	8.414	-3.46	7.95	8.347	-3.37	7.86
75	8.828	-3.71	8.59	8.756	-3.61	8.49
80	9.274	-3.99	9.27	9.197	-3.88	9.15
85	9.754	-4.31	9.98	9.672	-4.19	9.85
90	10.027	-4.66	10.74	10.183	-4.53	10.60
95	10.828	-5.05	11.55	10.732	-4.92	11.40
100	11.426	-5.49	12.42	11.323	-5.34	12.25
105	12.069	-5.98	13.36	11.958	-5.82	13.16
110	12.760	-6.52	14.36	12.641	-6.35	14.15
115	13.503	-7.13	15.43	13.374	-6.94	15.20
120	14.301	-7.80	16.60	14.162	-7.60	16.34
125	15.159	-8.56	17.86	15.010	-8.34	17.58
130	16.083	-9.40	19.22	15.922	-9.16	18.92
135	17.076	-10.34	20.71	16.904	-10.08	20.37
140	18.146	-11.40	22.32	17.962	-11.11	21.96
145	19.299	-12.58	24.09	19.102	-12.27	23.69
150	20.543	-13.91	26.02	20.334	-13.57	25.59
155	21.886	-15.40	28.13	21.664	-15.03	27.67
160	23.337	-17.08	30.45	23.104	-16.68	29.96
165	24.908	-18.98	33.01	24.664	-18.54	32.48
170	26.609	-21.12	35.83	26.357	-20.66	35.28
175	28.455	-23.55	38.95	28.197	-23.06	38.38
180	30.460	-26.31	42.42	30.200	-25.79	41.83
185	32.642	-29.45	46.27	32.386	-28.92	45.68
190	35.020	-33.03	50.58	34.776	-32.51	49.99
195	37.617	-37.13	55.39	37.394	-36.64	54.85
200	40.457	-41.85	60.80	40.271	-41.42	60.33

[a] bar^{-1}. [b] bar^{-2}. [c] $bar^{-1}(°K)^{-1}$. [d] °C.

$I \approx 1$ which can be approximated by a linear curve with an intercept equal to 2/3 and a slope of −0.3. Under these circumstances, equation (59) reduces to

$$\phi_V = \bar{V}^\circ + \frac{2}{3}\psi A_V I^{1/2} + \frac{(\nu b^*_V - 0.6\psi A_V)I}{4} \qquad (60)$$

which is of the same form as equation (53). It is thus not surprising that both equations (53) and (59) yield similar fits of experimental data at ionic strengths from $\sim$ 0.01 to 1 m.

It can be seen in figures 14 and 15 that b'_V exhibits a negative sigmoid dependence on temperature. As temperature increases from 0°C, b'_V decreases to a decreasing degree and in many cases approaches a constant value in the vicinity of 75°C before decreasing to an increasing degree with further increase in temperature to 200°C. Although none of the curves in figures 14 and 15 exhibits an extremum, a maximum could in principle occur in the intermediate temperature range.

REGRESSION OF STANDARD PARTIAL MOLAL VOLUMES AND COMPRESSIBILITIES

Regression of the values of $\bar{V}^\circ$ computed above (table 3) and supplemental data taken from the literature (Millero, 1972b) with equation (40) and values of Q for 20 bars (table 4) produced the solid curves in figures 17 through 19 and the values of σ, ξ, θ, ω, and $\bar{V}^\circ$ in tables 5 and 6.[5] Despite the fact that the standard partial molal volumes taken from the literature (figs. 17-19) pertain to a pressure of 1 atm, they were included in the regression analysis with those for 20 bars because the effect of the low-temperature difference in pressure on the calculations is within the overall uncertainty of the experimental values of $\bar{V}^\circ$. Consideration of compressibility data indicates that the difference in pressure of 19 bars introduces corresponding differences in $\bar{V}^\circ$ at 0°C of $\sim$ 0.2 cm^3 mole^{-1} or less for 1:1 electrolytes and $\sim$ 0.4 cm^3 mole^{-1} or less for 1:2 and 2:1 electrolytes. These differences decrease by $\sim$ 50 percent as temperature increases to 80°C, which is the highest temperature for which values of $\bar{V}^\circ$ were taken from the literature. It can be seen in figures 17 through 19 that in most cases discrepancies of 0.2 or 0.4 cm^3 mole^{-1} or less are within the uncertainty in $\bar{V}^\circ$ represented by the distribution of low-temperature values reported by different experimentalists. The pressure corresponding to all the data points plotted in figures 17 through 19 can thus be regarded as 20 bars without introducing undue uncertainty in the regression analysis.

It can be seen in figures 17 through 19 that the solid regression curves closely represent most of the experimental data for all the electrolytes; that is, with the exception of a few aberrant data points (see below), they

[5] For convenience in thermodynamic calculations, all equation of state coefficients other than θ reported in this communication are expressed in units of cal mole^{-1}, cal mole^{-1} bar^{-1}, or cal mole^{-1} bar^{-2}, depending on the coefficient. They can be converted to cm^3 mole^{-1} or cm^3 mole^{-1} bar^{-1} by dividing the values given for the coefficients by 0.0239 cal bar^{-1} cm^{-3}.

fall within a few tenths or less of a cubic centimeter mole^{-1} of the experimental values of $\bar{V}°$. The dashed curves shown in these figures were generated by alternate regression calculations described below. In certain instances the low temperature data plotted in figures 17 through 19 exhibit considerable scatter, but many of the anomalous values are obvious, for example, those reported by Isono and Tamamushi (1967) for NaCl, NH_4Cl, LiCl, KCl, $CaCl_2$, KNO_3, and KI at 5°C and Longworth (1935) for NH_4Cl at 25°C. With the exception of such data, all pertinent values of $\bar{V}°$ reported in Millero's (1972b) compilation were included in the regression analysis. However, only those data that could be shown with clarity are plotted in figures 17 through 19.

Owing to the dearth of experimental data for NaHS, $NaHCO_3$, NH_4Cl, NH_4ClO_4, and KF at low temperatures, the solid regression curves

TABLE 5

Summary of fit coefficients generated by four-parameter regression of standard partial molal volume data for aqueous electrolytes as a function of temperature at 20 bars (table 3 and figures 17 through 19) with equation (40) and values of Q taken from table 4[a]

Electrolyte	σ[b]	ξ[b] × 10^2	θ[c]	ω[d] × 10^{-5}
HCl	0.57470	-1.04908	246.021	1.45598
LiCl	0.53676	-0.19629	265.894	1.90597
NaCl	0.71313	-4.91441	231.002	1.66657
KCl	0.94393	-4.66749	229.236	1.77206
CsCl	1.18964	-3.29960	238.839	1.47618
NH_4Cl	1.02147	-1.19867	253.658	1.41443
KBr	1.09274	-4.26475	235.074	1.43209
KF	0.31137	-0.25807	270.158	1.76960
KI	1.46843	-7.74993	224.364	1.24149
$NaHCO_3$	0.80604	-1.51700	271.390	1.49811
KNO_3	1.28600	-7.27381	229.662	1.08570
NaHS	0.74258	-2.51257	258.929	1.69838
NH_4ClO_4	3.72340	-155.02127	86.180	1.01991
$MgCl_2$	0.67424	-0.78332	259.056	4.37126
$CaCl_2$	0.74571	-0.95327	260.757	4.11265
$SrCl_2$	0.78206	-1.36880	259.613	4.04255
$BaCl_2$	1.17967	-8.43250	231.233	4.14943
Na_2SO_4	0.86258	-7.43877	237.790	3.70840
K_2SO_4	1.22095	-3.58823	252.781	3.68932

[a] The regression curves generated by the fits correspond to the solid curves in figures 17 through 19. [b] cal mole^{-1} bar^{-1}. [c] °K. [d] cal mole^{-1}.

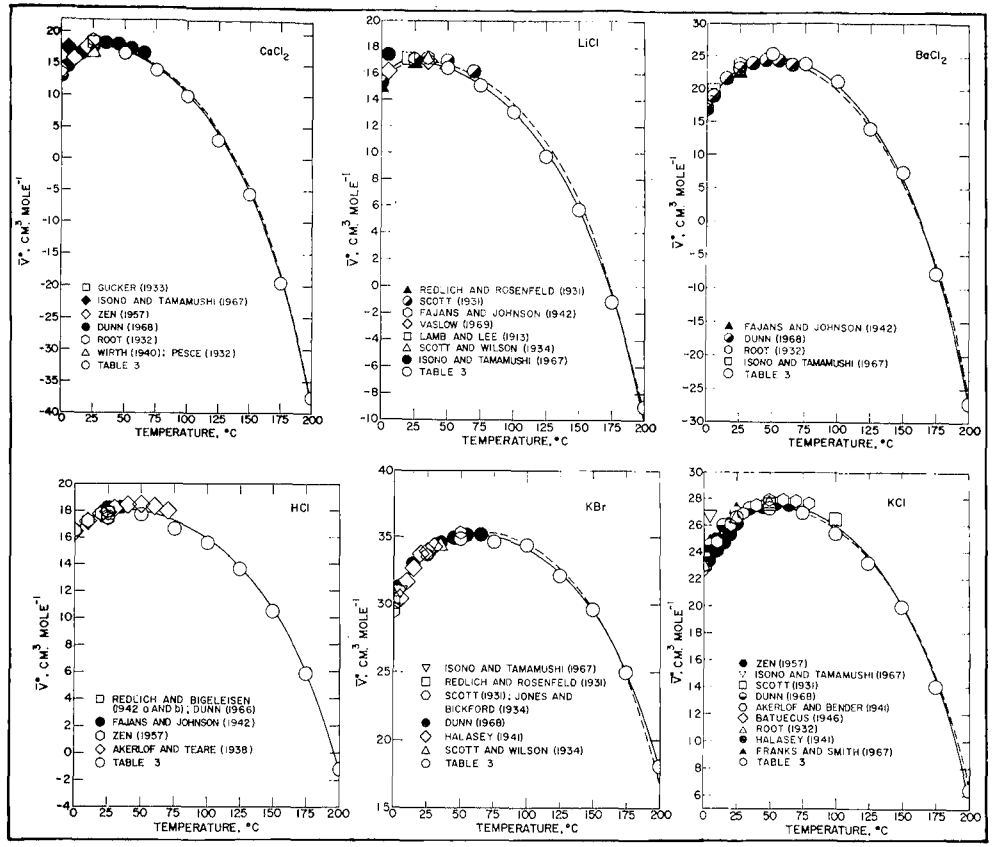

Fig. 17. Standard molal volumes ($\bar{V}^\circ$) of electrolytes (table 9) as a function of temperature at 20 bars. The symbols represent values given in table 3 for 20 bars or reported in the literature for 1 atm. The curves were generated by regression of the data with equation (40)—see text and tables 5, 6, 8, and 9.

in figures 18 and 19 and the fit coefficients in table 5 for these electrolytes are not valid at temperatures below 25°C. In the case of KF and NH_4ClO_4, values of $\bar{V}°$ at low temperatures were computed from additivity relations ($\bar{V}°_{KF} = \bar{V}°_{NaF} + \bar{V}°_{KCl} - \bar{V}°_{NaCl}$ and $\bar{V}°_{NH_4ClO_4} = \bar{V}°_{NaClO_4} + \bar{V}°_{NH_4Cl} - \bar{V}°_{NaCl} = \bar{V}°_{KClO_4} + \bar{V}°_{NH_4Cl} - \bar{V}°_{KCl}$) to supplement the few data available for these electrolytes at low temperatures. The additivity calculations were carried out by combining experimental values of $\bar{V}°$ reported by Robertson and others (1966) for NaF at 5°, 10°, and 20°C, Millero (1967), Couture and Laidler (1957), and Desnoyers and others (1969) for NaF at 25°C, Wirth and Collier (1950) and Kohner (1928) for $NaClO_4$ at 25°C, and Fajans and Johnson (1942) for $KClO_4$ at 25°C with values of $\bar{V}°_{NaCl}$, $\bar{V}°_{KCl}$, and $\bar{V}°_{NH_4Cl}$ computed from equation (40) and

TABLE 6

Standard partial molal volumes of aqueous electrolytes in cm^3 $mole^{-1}$ at 20 bars and temperatures from 25° to 200°C computed from equation (40), coefficients in table 5, and values of Q in table 4[a]

Electrolyte	Temperature, °C							
	25	50	75	100	125	150	175	200
HCl	17.9	17.9	17.2	15.9	13.8	10.6	5.9	-1.4
LiCl	17.0	16.4	15.1	13.1	10.2	6.0	-0.2	-9.8
NaCl	16.6	17.7	17.6	16.5	14.5	11.1	5.9	-2.3
KCl	26.7	27.6	27.3	26.0	23.8	20.2	14.6	5.8
CsCl	39.2	40.2	40.0	38.9	37.1	34.0	29.4	22.1
NH_4Cl	35.9	36.3	35.7	34.5	32.5	29.4	24.9	17.8
KBr	33.7	35.0	35.0	34.1	32.4	29.5	25.1	18.0
KF	7.5	7.2	6.1	4.3	1.6	-2.3	-8.1	-17.0
KI	45.3	47.2	47.8	47.4	46.2	44.0	40.3	34.4
$NaHCO_3$	23.0	25.4	25.4	24.3	22.3	19.2	14.4	7.0
KNO_3	37.9	40.1	40.9	40.7	39.8	37.9	34.8	29.6
NaHS	18.9	20.8	20.7	19.6	17.4	13.9	8.5	0.1
NH_4ClO_4	62.0	64.4	65.9	66.6	66.6	65.7	63.5	59.3
$MgCl_2$	14.9	13.7	10.9	6.4	-0.2	-9.8	-24.1	-46.2
$CaCl_2$	17.9	17.1	14.5	10.4	4.2	-4.8	-18.3	-39.0
$SrCl_2$	18.3	18.0	15.7	11.7	5.7	-3.2	-16.3	-36.7
$BaCl_2$	23.4	24.8	23.7	20.4	14.9	6.3	-6.9	-27.5
Na_2SO_4	11.5	13.4	12.7	9.9	5.1	-2.6	-14.3	-32.7
K_2SO_4	32.1	33.4	32.1	29.0	23.8	16.0	4.1	-14.3

[a]The values given in this table are represented by the solid curves in figures 17 through 19.

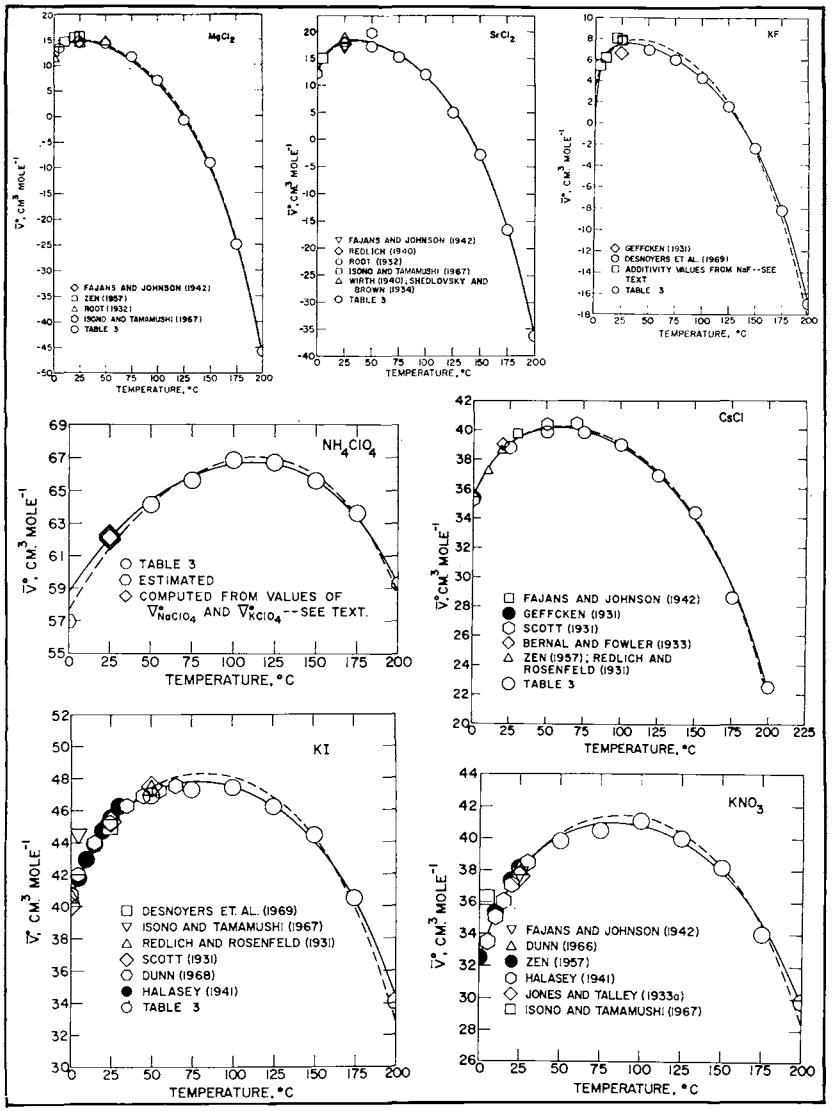

Fig. 18. Standard partial molal volumes ($\bar{V}^\circ$) of electrolytes (table 9) as a function of temperature at 20 bars. The symbols represent values given in table 3 for 20 bars or reported in the literature for 1 atm. The curves were generated by regression of the data with equation (40) — see text and tables 5, 6, 8, and 9.

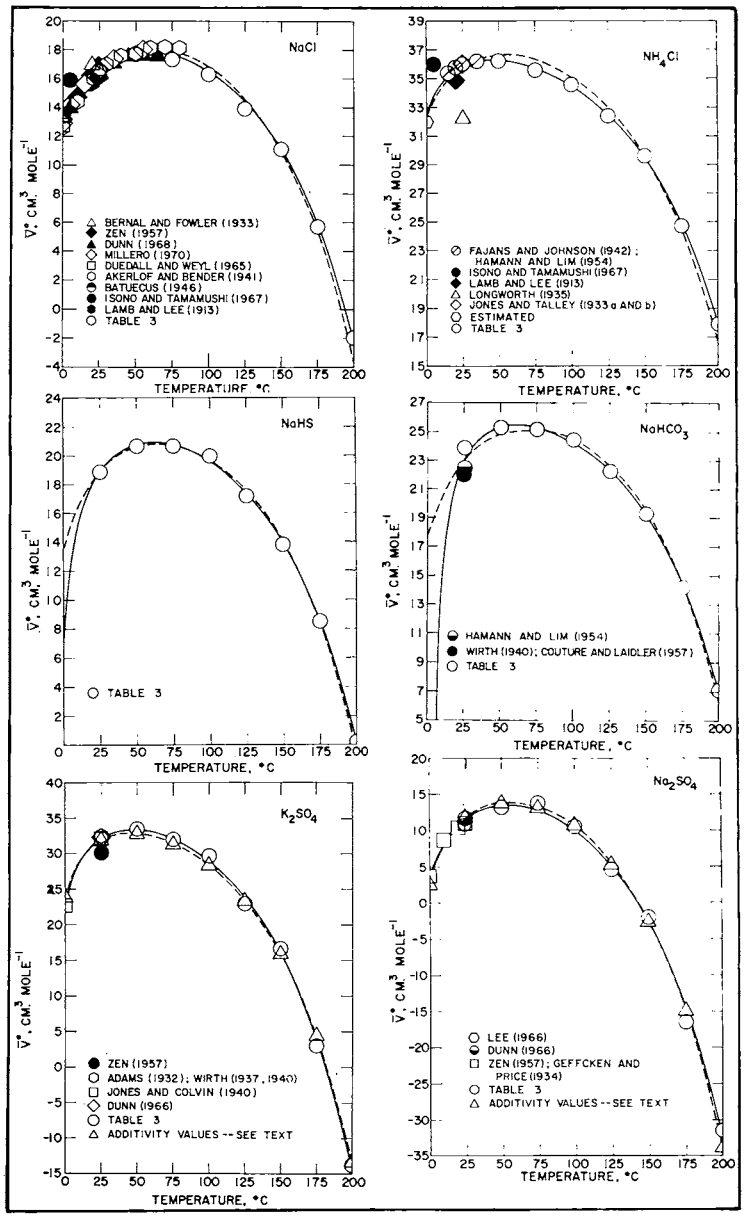

Fig. 19. Standard partial molal volumes ($\bar{V}^\circ$) of electrolytes (table 9) as a function of temperature at 20 bars. The symbols represent values given in table 3 for 20 bars or reported in the literature for 1 atm. The curves were generated by regression of the data with equation (40) — see text and tables 5, 6, 8, and 9.

appropriate coefficients in table 5. This procedure minimized the effect of experimental uncertainties on the results of the calculations. The estimated values of $\bar{V}^\circ_{NH_4Cl}$ and $\bar{V}^\circ_{NH_4ClO_4}$ at 0°C shown in figures 18 and 19 (see below) were not included in the regression calculations.

The close agrement of the regression curves generated by the four-parameter fits of equation (40) to the experimental data in figures 17 through 19 affords a basis for calculating values of the effective electrostatic radii of ions in aqueous solution. A predictive equation for these radii can be derived from regression values of ω for a series of electrolytes with a common anion.

Ionic radii and the Born coefficient (ω).—Early consideration of the energetic consequences of ion hydration by Voet (1936), Latimer, Pitzer, and Slansky (1939), and others has led to a myriad of models and algorithms for predicting the effective electrostatic radii and thermodynamic properties of ions in aqueous solution (for example, see Powell and Latimer, 1951; Booth, 1957; Kapustinskii, Drakin, and Yakushevskii, 1953; Latimer, 1955; Laidler, 1956; Couture and Laidler, 1956; Laidler and

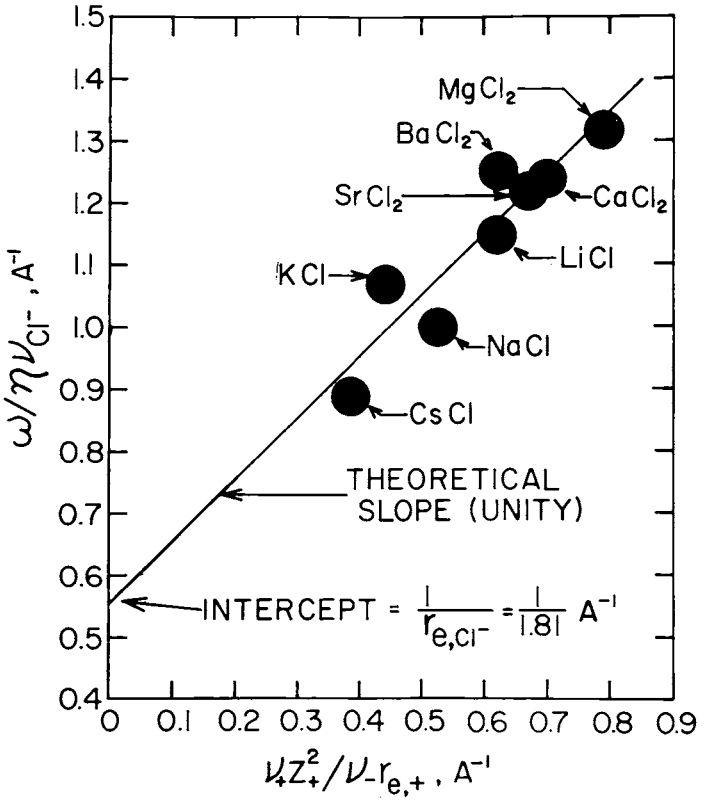

Fig. 20. Graphic representation of equation (61A) for alkali and alkaline earth chlorides.

Pegis, 1957; Hepler, 1957; Drakin and Mikhailov, 1959; Mikhailov and Drakin, 1960; Mukerjee, 1961, 1966; Stokes, 1964; Glueckauf, 1964, 1965). Many of these are strictly empirical, but others are based in part on theoretical concepts, some of which contravene electrostatic theory. Although Latimer, Pitzer, and Slansky (1939) demonstrated that the standard partial molal entropies of hydration of univalent ions could be correlated with their crystallographic radii (r_x) by adding 0.85A to r_x for cations and 0.1A to r_x for anions, little agreement has been reached on the significance of such additivity constants, or even whether Pauling (1948), Gourary and Adrain (1960), or other sets of crystallographic radii should be used for this purpose. Various values of additivity constants for aqueous radii have been suggested to account for one or another observation, but none has yet proved generally applicable. Glueckauf (1964, 1965, 1966) concluded from empirical and theoretical consideration of the effects of the dielectric constant and structure of the solvent in the immediate vicinity of aqueous ions on their standard partial molal enthalpies, entropies, and volumes that the effective electrostatic radius of an ion (r_e) differs from its intrinsic solvated counterpart (r_i) by 0.83A. According to Glueckauf, $r_e = r_x + 1.38$ and $r_i = r_x + 0.55$, which are in qualitative but not quantitative agreement with conclusions reached below.

Regression values of ω are given in table 5 for eight alkali and alkaline earth chlorides. Fits of equation (19) to these values with alternate functions of r_x to represent the effective electrostatic radii of ions indicate that the regression values of ω are closely consistent with

$$r_{e,j} = r_{x,j} + |Z_j|\Gamma_{Z,j} \tag{61}$$

where $r_{e,j}$ stands for the electrostatic radius of the jth ion, $r_{x,j}$ refers to its crystallographic counterpart, Z_j denotes the charge on the ion, and $\Gamma_{Z,j}$ represents a parameter characteristic of cations (Γ_+) or anions (Γ_-). Combining equations (19) and (61) leads to

$$\frac{\omega}{\eta\nu_-} = \frac{\nu_+ Z_+^{\,2}}{\nu_-(r_{x,+} + Z_+\Gamma_+)} + \frac{Z_-^{\,2}}{r_{x,-} - Z_-\Gamma_-} \tag{61A}$$

which describes $\omega/\eta\nu_-$ for electrolytes with a common anion as a linear function of $\nu_+Z_+^{\,2}/(\nu_-(r_{x,+} + Z_+\Gamma_+))$ with unit slope and an intercept equal to $Z_-^{\,2}/(r_{x,-} - Z_-\Gamma_-)$. Fits of equation (61A) to the regression values of ω for the alkali and alkaline earth chlorides in table 5 using values of r_x (table 7) taken from Sienko and Plane (1963) generated 0.94 A and 0.02 A for Γ_+ and Γ_-, respectively. Because the latter value is so close to zero, the regression calculations were repeated with Γ_- set to zero, which also resulted in 0.94 A for Γ_+. It can be seen in figure 20 that the curve generated by equation (61A) with $\Gamma_+ = 0.94$ and $\Gamma_- = 0$ closely represents the regression values of ω for the electrolytes. It thus appears that the effective electrostatic radii of aqueous anions can be taken to be equal to their crystallographic counterparts, but that those for aqueous cations differ from their crystallographic radii by 0.94 Z. This value is close to that (0.85A) obtained by Latimer, Pitzer, and

TABLE 7

Summary of ionic radii, absolute values of ω, and conventional standard

Ion	$r_{x,j}^{s}$	$r_{e,j}^{s}$	ω_j^{abs} $\times 10^{-5}$	$\bar{S}^{\circ}_{j}$	$\Delta\bar{S}^{\circ}_{s,j}$	$\left(\Delta\bar{S}^{\circ}_{n,j} - Z_j \bar{S}^{\circ}_{H^+}\right)^{abs}$
H^+	2.14[a]	3.08[g]	0.5387[b]	0	-3.13	3.13
Li^+	0.68[h]	1.62[f]	1.0249[i]	2.7[k]	-5.95	8.7
Na^+	0.97[h]	1.91[f]	0.8692[i]	14.0[k]	-5.04	19.0
K^+	1.33[h]	2.27[f]	0.7314[i]	24.2[k]	-4.24	28.4
Rb^+	1.47[h]	2.41[f]	0.6889[i]	28.8[k]	-4.00	32.8
Cs^+	1.67[h]	2.61[f]	0.6361[i]	31.8[k]	-3.69	35.5
Tl^+	1.47[h]	2.41[f]	0.6889[i]	30.0[ℓ]	-4.00	34.0
NH_4^+	1.37[a]	2.31[c]	0.7178[i]	26.6[k]	-4.16	30.8
Ag^+	1.26[h]	2.20[f]	0.7547[i]	17.5[k]	-4.38	21.9
Cu^+	0.96[h]	1.90[f]	0.8738[i]	9.7[ℓ]	-5.07	14.8
Mg^{++}	0.66[h]	2.54[f]	2.6146[i]	-33.0[ℓ]	-15.17	-17.8
Ca^{++}	0.99[h]	2.87[f]	2.3140[i]	-12.7[ℓ]	-13.43	0.7
Sr^{++}	1.12[h]	3.00[f]	2.2137[i]	-7.8[ℓ]	-12.84	5.0
Ba^{++}	1.34[h]	3.22[f]	2.0625[i]	2.3[ℓ]	-11.97	14.3
Mn^{++}	0.80[h]	2.68[f]	2.4780[i]	-17.6[ℓ]	-14.38	-3.2
Fe^{++}	0.74[h]	2.62[f]	2.5348[i]	-32.9[ℓ]	-14.71	-18.2
Cu^{++}	0.72[h]	2.60[f]	2.5543[i]	-23.8[ℓ]	-14.82	-9.0
Zn^{++}	0.74[h]	2.62[f]	2.5348[i]	-26.0[v]	-14.71	-11.3
Cd^{++}	0.97[h]	2.85[f]	2.3302[i]	-17.5[ℓ]	-13.52	-4.0
Pb^{++}	1.20[h]	3.08[f]	2.1562[i]	2.5[ℓ]	-12.51	15.0
Al^{+++}	0.51[h]	3.33[f]	4.4872[i]	-76.9[ℓ]	-26.04	-50.9
Fe^{+++}	0.64[h]	3.46[f]	4.3186[i]	-75.5[ℓ]	-25.06	-50.4
La^{+++}	1.14[h]	3.96[f]	3.7733[i]	-52.0[w]	-21.89	-30.1
Ga^{+++}	0.62[h]	3.44[f]	4.3437[i]	-79.0[ℓ]	-25.20	-53.8
Gd^{+++}	0.97[h]	3.79[f]	3.9426[i]	-49.2[w]	-22.88	-26.3
In^{+++}	0.81[h]	3.63[f]	4.1164[i]	-63.0[ℓ,m]	-23.88	-39.1
Tl^{+++}	0.95[h]	3.77[f]	3.9635[i]	-46.0[ℓ]	-23.00	-23.0
F^-	1.33[h]	1.33[f]	1.2483[i]	-3.3[ℓ]	-7.24	3.9
Cl^-	1.81[h]	1.81[f]	0.9173[i]	13.6[k]	-5.32	18.9

partial molal entropies of aqueous species at 25°C and 1 bar

Ion	$\underline{r}_{x,j}$	$\underline{r}_{e,j}$	$\underline{\omega}_j^{abs} \times 10^{-5}$	$\bar{S}°_j$	$\Delta\bar{S}°_{s,j}^{abs}$	$\left(\Delta\bar{S}°_{n,j}^{abs} - z_j \bar{S}°_{H^+}^{abs}\right)^{p,r}$
Br^-	1.96[h]	1.96[f]	0.8471[i]	19.8[k]	-4.91	24.7
I^-	2.20[h]	2.20[f]	0.7547[i]	25.5[k]	-4.38	29.9
OH^-	1.40[d]	1.40[f]	1.1859[i]	-2.6[k]	-6.88	4.3
HS^-	1.84[e]	1.84[f]	0.9023[i]	15.0[ℓ]	-5.24	20.2
NO_3^-	2.81[a]	2.81[c,u]	0.5908[i]	35.1[k]	-3.43	38.5
HCO_3^-	2.10[a]	2.10[c]	0.7906[i]	21.8[ℓ]	-4.59	26.4
HSO_4^-	2.37[a]	2.37[c]	0.7005[i]	27.7[t]	-4.06	31.8
ClO_4^-	3.59[a]	3.59[c,u]	0.4625[i]	43.5[ℓ]	-2.68	46.2
SO_4^{--}	3.15[a]	3.15[c,u]	2.1083[i]	4.8[ℓ]	-12.23	17.0
ReO_4^-	4.23[a]	4.23[c,u]	0.3925[i]	48.1[ℓ]	-2.28	50.4
CO_3^{--}	2.81[a]	2.81[c]	2.3634[i]	-13.6[ℓ]	-13.71	0.1

[a] Hypothetical $\underline{r}_{x,j}$ computed from $\underline{r}_{e,j}$ and equation (61). [b] Computed from equation (19), the regression value of ω for HCl in table 5, and the value of $\omega_{Cl^-}^{abs}$ given above. [c] Computed from equation (74) and values of $\bar{S}°_j$ given above with $\eta = 1.66027 \times 10^5$ A cal mole^{-1} and $Y = 5.8021 \times 10^{-5}$ (°K)$^{-1}$ (Helgeson and Kirkham, 1974a). [d] Computed from equation (61) assuming $\underline{r}_{x,OH^-_f} = \underline{r}_{x,O^{--}}$. [e] Computed from equation (61) assuming $\underline{r}_{x,HS^-} = \underline{r}_{x,S^{--}}$. [f] Computed from equation (61) and values of $\underline{r}_{x,j}$ given above. [g] Computed from equation (15) and the value of $\omega_{H^+}^{abs}$ given above. [h] Sienko and Plane (1963). [i] Computed from equation (15) and the values of $\underline{r}_{e,j}$ given above. [k] CODATA (1975). [ℓ] Wagman and others (1968, 1969, 1971). [m] Corrected typographical error in Wagman and others (1968). [n] Computed from equation (63) and the values of ω_j^{abs} given above with $Y = 5.8021 \times 10^{-5}$ (°K)$^{-1}$ (Helgeson and Kirkham, 1974a). [p] Computed from equation (67) and the values of $\bar{S}°_j$ and $\Delta\bar{S}°_{s,j}^{abs}$ shown above. [q] cal mole^{-1}. [r] cal mole^{-1} (°K)$^{-1}$. [s] Angstroms. [t] Computed from data given by Readnour and Cobble (1969). [u] Uncertain -- see text. [v] Wulff (1967). [w] Schumm and others (1973).

Slansky (1939) from analysis of entropy data. In contrast, it differs substantially from the value of 1.38A proposed by Glueckauf (1965), which corresponds to the radius of an H_2O molecule. Although $\Gamma_- = 0$ is significantly different from the value proposed by Latimer, Pitzer, and Slansky (1939) for 1:1 electrolytes (0.1A), it is essentially equal to that obtained by Gardner, Mitchell, and Cobble (1969) and Murray, Sen, and Cobble (in preparation) for Cl^-.

The value of Γ_+ computed above is almost equivalent to the hydrogen-oxygen distance in the H_2O molecule (0.95A), but the significance of this observation is highly speculative. Despite repeated attempts in the literature to rationalize experimental observations by regarding $r_{e,j}$ as an ion radius, the electrostatic radius parameter should not be confused with the physical radius of an aqueous ion. The effective electrostatic radius of an ion is related to an idealized spherical representation of the charge distribution about the ion, which is a vector quantity. From a conceptual point of view, $r_{e,j}$ represents the spatial consequences of the solvation contribution to the electrostriction process. Nevertheless, $r_{e,j}$ is not readily identifiable with a physical distance of separation. This can be demonstrated by first designating the distance from the center of the jth ion to the outer limit of its influence on the orientational polarizability of the H_2O dipoles in its solvation shell as $r_{o,j}$. If we then let $r_{d,j}$ represent the Born radius of the jth ion in the aqueous disordered state, it follows that

$$r_{e,j} = \frac{r_{o,j}\, r_{d,j}}{r_{d,j} - r_{o,j}} \tag{62}$$

The relation of $r_{d,j}$ to its crystalline counterpart ($r_{x,j}$) is a function of the difference in confining pressure between the aqueous and crystalline states. As a first approximation of this relation we can write

$$r_{d,j} = \hat{a}_j r_{x,j} \tag{62A}$$

where $\hat{a}_j$ stands for a proportionality constant for the jth ion. Combining equations (61), (62), and (62A) and recalling that $\Gamma_- = 0$ then leads to

$$r_{o,j} = \frac{\hat{a}_j r_{x,j}(r_{x,j} + Z_j \Gamma_{Z,j})}{\hat{a}_j r_{x,j} + r_{x,j} + Z_j \Gamma_{Z,j}} \tag{62B}$$

Because H_2O is more compressible than crystalline solids, $\hat{a}_j$ is almost certainly greater than 1. However, if Benson and Copeland's (1963) interpretation of the magnitude of the enthalpies of solution of ionic crystals is correct (Guggenheim and Stokes, 1969), $\hat{a}_j$ is probably not much greater than $\backsim 2$. The order of magnitude of $r_{o,j}$ can be assessed from equation (62B) by assuming a reasonable value for $\hat{a}_j$. For example, if $\hat{a}_j = 2$ for Na^+, Li^+, K^+, and Cl^-, $r_{o,j}$ for these ions would be 0.96, 0.74, 1.22, and 1.21A, respectively. The differences between these values and the corresponding values of $r_{d,j}$ (1.94, 1.32, 2.66, and 3.62A) result from electrostriction of the ions during assembly and orientation of H_2O dipoles to form

solvation shells about the ions. Note that these differences are not equal to $r_{e,j}$.

Despite the fact that the calculations of $r_{o,j}$ summarized above are based on a hypothetical value of $\hat{a}_j$, they serve to illustrate the importance of regarding $r_{e,j}$ as an electrostatic parameter rather than a physical radius comparable to $r_{o,j}$, $r_{d,j}$, $r_{i,j}$, or $r_{x,j}$. The computed values of $r_{o,j}$ for Na^+ Li^+, and K^+ assuming $\hat{a}_j = 2$ are not greatly different from their crystallographic counterparts, but the calculated value of $r_{o,j}$ for Cl^- is substantially smaller than its crystal radius. Because $\Gamma_{Z,j} = 0$ for anions, equation (62B) can be written for negatively charged species as

$$r_{o,j} = \frac{\hat{a}_j r_{x,j}}{\hat{a}_j + 1} \tag{62C}$$

It can be seen that $r_{o,j} \rightarrow r_{x,j}$ only in the limit as $\hat{a}_j \rightarrow \infty$. If $\hat{a}_j = 2$, $r_{o,j}$ for anions equals $2/3\ r_{x,j}$.

The close correspondence of the curve and symbols in figure 20 (as well as other observations and calculations presented below) strongly supports the general validity of equation (61), which was used together with $\Gamma_+ = 0.94$A and $\Gamma_- = 0$ to calculate the values or $r_{e,j}$ and ω_j^{abs} for the nonoxygenated ions (except H^+) listed in table 7. The value of $\omega_{H^+}{}^{abs}$ in table 7 was calculated by subtracting the computed value of $\omega_{Cl^-}{}^{abs}$ from the regression value of ω_{HCl} in table 5, which permits calculation of r_{e,H^-} and a hypothetical value of r_{x,H^+} from equations (15) and (61). The values of r_{x,HS^-} and r_{x,OH^-} used to compute $\omega_{HS^-}{}^{abs}$ and $\omega_{OH^-}{}^{abs}$ were taken to be those of S^{--} and O^{--}, respectively, but in other cases where crystallographic radii are not available (such as NO_3^-, HCO_3^-, SO_4^{--}, et cetera) values of $r_{e,j}$ and ω_j^{abs} were computed from entropy correlations (discussed below).

The values of $r_{e,j}$ for Ba^{++}, Gd^{+++}, and H^+ in table 7 differ considerably from those obtained by Murray, Sen, and Cobble (in preparation) from regression of standard partial molal heat capacities, entropies, and Gibbs free energies of ion hydration as a function of temperature. Nevertheless, the values in table 7 are consistent with entropy data, and it will be shown in a later communication (Helgeson and Kirkham, in preparation) that they are also consistent with activity coefficient and standard partial molal heat capacity data. Although Murray, Sen, and Cobble based their values of $r_{e,j}$ on $r_{e,Na^+} = 1.779$A (Gardner, Mitchell, and Cobble, 1969), the large discrepancies between their values of $r_{e,j}$ for Ba^{++}, Gd^{+++}, and H^+ (2.334, 1.804, and 0.648A, respectively) and the corresponding values in table 7 (3.22, 3.79, and 3.08A) cannot be attributed to the different conventions used in the calculations. It can be shown that the discrepancies are a likely consequence of the temperature independence assumed for the nonelectrostatic entropy in Murray, Sen, and Cobble's model, which introduces inconsistencies in their regression results for various electrolytes. The assumption of a temperature-independent nonelectrostatic entropy of hydration is also inconsistent with the observed behavior of the standard partial molal heat capacities of aqueous electrolytes as a function of temperature.

Entropy considerations.—The entropy analog of equation (16) can be written as

$$-\left(\frac{\partial \Delta \bar{G}^{\circ}_{s,j}{}^{abs}}{\partial T}\right)_P = \Delta \bar{S}^{\circ}_{s,j}{}^{abs} = \omega_j{}^{abs}\, Y \tag{63}$$

where $\Delta \bar{S}^{\circ}_{s,j}{}^{abs}$ stands for the absolute standard partial molal entropy of solvation for the jth aqueous ion and

$$Y = \frac{1}{\varepsilon}\left(\frac{\partial \ln \varepsilon}{\partial T}\right)_P \tag{64}$$

for the solvent. $\Delta \bar{S}^{\circ}_{s,j}{}^{abs}$ is related to its conventional counterpart ($\Delta S^{\circ}_{s,j}$) by

$$\Delta \bar{S}^{\circ}_{s,j} = \Delta \bar{S}^{\circ}_{s,j}{}^{abs} - Z_j \Delta \bar{S}^{\circ}_{s,H^+}{}^{abs} \tag{65}$$

which can be combined with

$$\bar{S}^{\circ}_j = \bar{S}^{\circ}_j{}^{abs} - Z_j \bar{S}^{\circ}_{H^+}{}^{abs} = \Delta \bar{S}^{\circ}_{n,j} + \Delta \bar{S}^{\circ}_{s,j} \tag{66}$$

and equation (63) to give

$$\Delta \bar{S}^{\circ}_{n,j} - Z_j \bar{S}^{\circ}_{H^+}{}^{abs} = \bar{S}^{\circ}_j - \Delta \bar{S}^{\circ}_{s,j}{}^{abs} = \bar{S}^{\circ}_j - \omega_j{}^{abs}\, Y \tag{67}$$

where $\bar{S}^{\circ}_j$ and $\bar{S}^{\circ}_j{}^{abs}$ are the conventional and absolute standard partial molal entropies of the jth ion, respectively, and

$$\Delta \bar{S}^{\circ}_{n,j} = \Delta \bar{S}^{\circ}_{n,j}{}^{abs} - Z_j \Delta \bar{S}^{\circ}_{n,H^+}{}^{abs} = \bar{S}^{\circ}_{i,j} + \Delta \bar{S}^{\circ}_{c,j}\,, \tag{68}$$

where

$$\Delta \bar{S}^{\circ}_{n,j}{}^{abs} = \bar{S}^{\circ}_{i,j}{}^{abs} + \Delta \bar{S}^{\circ}_{c,j}{}^{abs} \tag{69}$$

where $\bar{S}^{\circ}_{i,j}$ stands for the conventional standard intrinsic partial molal entropy of the jth ion, $\Delta \bar{S}^{\circ}_{c,j}$ denotes its conventional standard partial molal entropy of solvent collapse, and $\bar{S}^{\circ}_{i,j}{}^{abs}$ and $\Delta \bar{S}^{\circ}_{c,j}{}^{abs}$ represent the absolute counterparts of $\bar{S}^{\circ}_{i,j}$ and $\Delta \bar{S}^{\circ}_{c,j}$, respectively.

Values of $\Delta \bar{S}^{\circ}_{s,j}{}^{abs}$ at 25°C and 1 bar computed from the values of $\omega_j{}^{abs}$ in table 7 and equation (63) with $Y = -5.802 \times 10^{-5}$ $(°K)^{-1}$ (Helgeson and Kirkham, 1974a) are given in table 7 together with conventional standard partial molal entropies of aqueous ions ($\bar{S}^{\circ}_j$) taken from the literature and values of $\Delta \bar{S}^{\circ}_{n,j} - Z_j \bar{S}^{\circ}_{H^+}{}^{abs}$ computed from equation (67). It can be seen in figure 21 that the latter variable for ions with the same absolute charge exhibits a striking correlation with the reciprocal of the $r_{e,j}$ values computed above. A similar correlation of the conventional standard partial molal entropies of hydration from a gas phase for aqueous ions ($\Delta \bar{S}^{\circ}_{h,j}$) at 25°C and 1 bar with $r_{e,j}{}^{-1}$ is apparent in figure 22. $\Delta \bar{S}^{\circ}_{h,j}$ is related to $\bar{S}^{\circ}_j$ by

$$\Delta \bar{S}^{\circ}_{h,j} = \bar{S}^{\circ}_j - \bar{S}^{\circ}_{j,gas} \tag{70}$$

where $\bar{S}^{\circ}_{j,gas}$ stands for the standard partial molal entropy of the jth ion

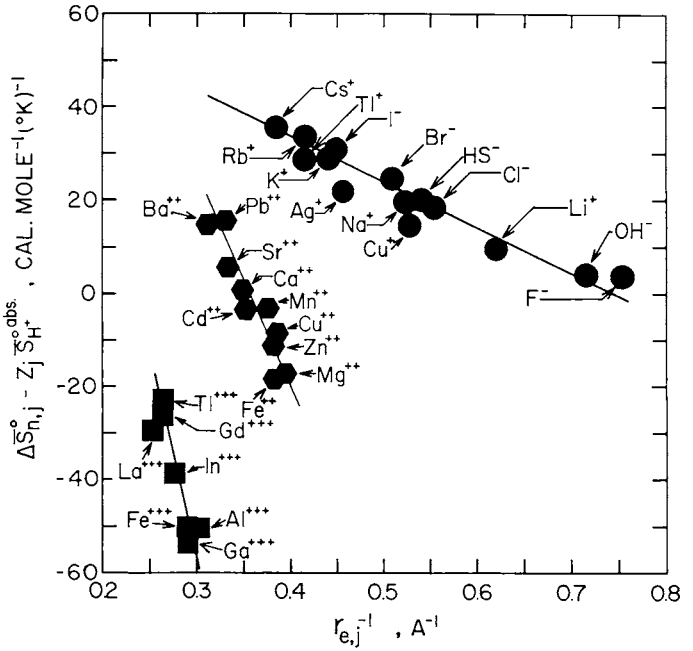

Fig. 21. Correlation of $\Delta\bar{S}^\circ_{n,j} - Z_j\bar{S}^\circ_{H^+}{}^{abs}$ (eq 67) with $r_{e,j}$ (eq 61) at 25°C and 1 bar (table 7).

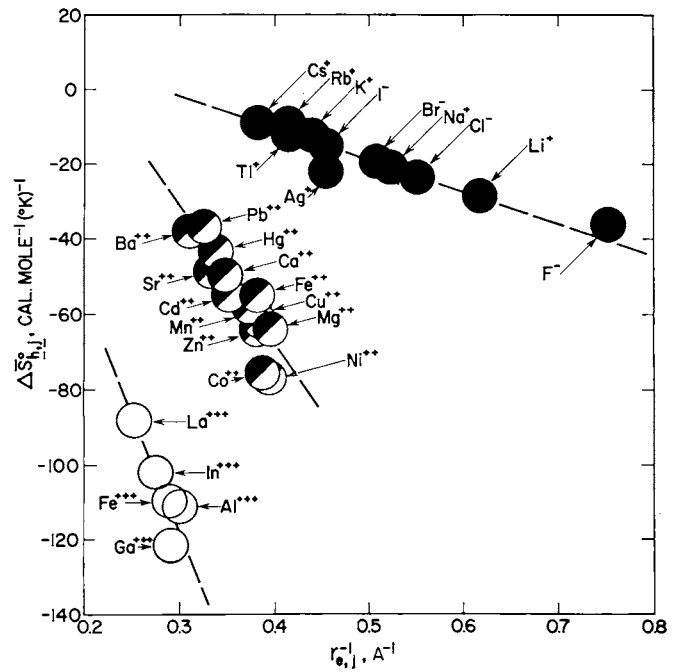

Fig. 22. Correlation of the conventional standard partial molal entropies of hydration from a gas phase of aqueous ions ($\Delta\bar{S}^\circ_{h,j}$) at 25°C and 1 bar taken from Hunt (1965) with $r_{e,j}$ (eq 61 and table 7).

in the gas state. $\bar{S}^\circ_{j,gas}$ is commonly computed from the Sakur-Tetrode equation for monatomic gases; that is,

$$\bar{S}^\circ_{j,gas} = R\left(\frac{3 \ln \mathbf{M}_j}{2} + \frac{5 \ln T}{2} - \ln P + \ln Q_{e,j} - 0.5055\right) \quad (71)$$

where R represents the gas constant, $\mathbf{M}_j$ stands for the atomic mass of the jth ion, and $Q_{e,j}$ is the electronic multiplicity of its ground state. At constant temperature, pressure, and electronic multiplicity, the Sakur-Tetrode equation is a linear function of the logarithm of atomic mass ($\ln \mathbf{M}_j$), which is the theoretical basis for such terms in empirical correlation equations for the standard partial molal entropies of aqueous ions such as those proposed by Latimer (1955), Laidler and Pegis (1957), and others.

The linear relations shown in figures 21 and 22 require a linear dependence of $r_{e,j}^{-1}$ on $\ln \mathbf{M}_j$, but it is obvious from comparison of figures 21 and 23 that the correlation of $\Delta\bar{S}^\circ_{n,j} - Z_j\bar{S}^\circ_{H^+}{}^{abs}$ with $r_{e,j}^{-1}$ is much better than that with $\ln \mathbf{M}_j$. Although linear curves have been drawn through the symbols in figure 21, there is little other than empirical justification for doing so. From a theoretical standpoint, the standard partial molal entropy change accompanying collapse of the solvent molecules might be expected to correlate with ionic potential, but not necessarily in a linear fashion. Such a correlation is evident in figure 24, where it can be seen that $\Delta\bar{S}^\circ_{n,j} - Z_j\bar{S}^\circ_{H^+}{}^{abs}$ is a nonlinear monotonic function of $Z_j/r_{e,j}$. Nevertheless, the linear approximations in figure 21 are useful for predicting values of $r_{e,j}$ within the range of the data represented by the symbols.

The linear curves in figures 21 and 22 can be represented by

$$\Delta\bar{S}^\circ_{n,j} - Z_j\bar{S}^\circ_{H^+}{}^{abs} = a_1^* + a_2^* r_{e,j}^{-1} \quad (72)$$

and

$$\Delta\bar{S}^\circ_{n,j} = b_1^* + b_2^* r_{e,j}^{-1} \quad (73)$$

where a_1^*, a_2^*, b_1^*, and b_2^* stand for coefficients for univalent ($a_1^* = 74$; $a_2^* = -100$; $b_1^* = 24$; $b_2^* = -85$), divalent ($a_1^* = 160$; $a_2^* = -450$; $b_1^* = 80$; $b_2^* = -370$) and trivalent ($a_1^* = 214$; $a_2^* = -900$; $b_1^* = 71$; $b_2^* = -630$) ions at 25°C and 1 bar. Combining equations (15), (67), and (72) leads to

$$r_{e,j} = \frac{\eta Z_j^2 Y + a_2^*}{\bar{S}^\circ_j - a_1^*} \quad (74)$$

which can be used to compute values of $r_{e,j}$ for ions from their standard partial molal entropies. The values of $r_{e,j}$ shown for NH_4^+, NO_3^-, HCO_3^-, HSO_4^-, SO_4^{--}, ClO_4^-, and ReO_4^- in table 7 were calculated in this manner from the values of $\bar{S}^\circ_j$ for the ions in table 7 and equation (74) with $\eta = 1.66027 \times 10^5$ A cal mole^{-1}, $Y = -5.802 \times 10^{-5}$ (°K)$^{-1}$, $a_1^* = 74$ cal mole^{-1} (°K)$^{-1}$, and $a_2^* = -100$ A cal mole^{-1} (°K)$^{-1}$ for the univalent ions, and $a_1^* = 160$ and $a_2^* = -450$ for SO_4^{--} and

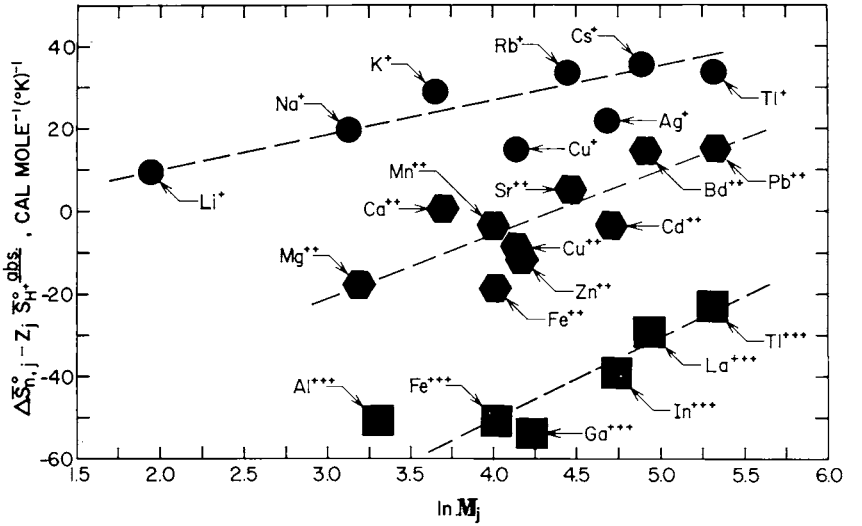

Fig. 23. Correlation of $\Delta\bar{S}^\circ_{n,j} - Z_j\bar{S}^\circ_{H^+}{}^{abs}$ (eq 67) at 25°C and 1 bar (table 7) with the logarithm of atomic mass ($\mathbf{M}_j$).

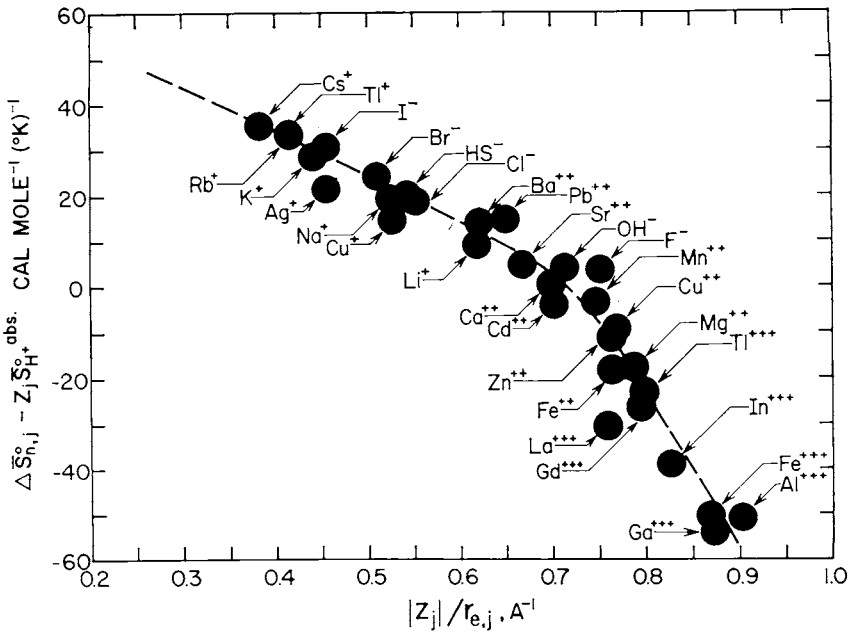

Fig. 24. Correlation of $\Delta\bar{S}^\circ_{n,j} - Z_j\bar{S}^\circ_{H^+}{}^{abs}$ (eq 67) at 25°C and 1 bar (table 7) with the product of $|Z_j|$ and $r_{e,j}^{-1}$ (eq 61 and table 7).

CO_3^{--}. The effective electrostatic radii were then used to compute hypothetical crystallographic radii for the ions from equation (61) and values of ω_j^{abs} from equation (15), which are also shown in table 7. Although $\Delta\bar{S}^\circ_{n,j} - Z_j\bar{S}^\circ_{H^+}{}^{abs}$ for NO_3^-, ClO_4^-, and ReO_4^- do not plot within the range of the symbols for the univalent ions in figure 21, consideration of figure 24 suggests that little error should result from using equation (74) to compute values of $r_{e,j}$ for these ions.

Taking account of the dependence of $\Delta\bar{S}^\circ_{n,j}$ on $Z_j/r_{c,j}$ and $\Delta\bar{S}^\circ_{s,j}$ on $Z_j^2/r_{e,j}$, it is not surprising that the sum of these entropy contributions ($\bar{S}^\circ_j$) exhibits a wide range of simple quasi-linear correlations with $Z_j^a/r_{e,j}^b$, where a and b represent various positive or negative integers (for example, see Powell and Latimer, 1951). However, the theoretical significance of these observations (such as Latimer's (1955) conclusion that $r_{e,j}$ should be treated as a temperature-dependent variable) is highly questionable. The same criticism can be leveled at similar empirical correlations of $\bar{V}^\circ$ with charge and radius (for example, Couture and Laidler, 1956).

The relations depicted in figures 20 through 24 strongly reinforce the validity of equation (61)as a general equation for the effective electrostatic radii of ionic species in aqueous solution. The equation is further substantiated by figure 25, where values of ω for electrolytes (table 8) computed (eq 19) from the values of ω_j^{abs} in table 7 are plotted against their regression counterparts (table 5). It can be seen that the values predicted from the correlation algorithms are in close agreement with those obtained by regression of the standard partial molal volume data with equation (40). The agreement is particularly impressive in view of the fact that the pre-

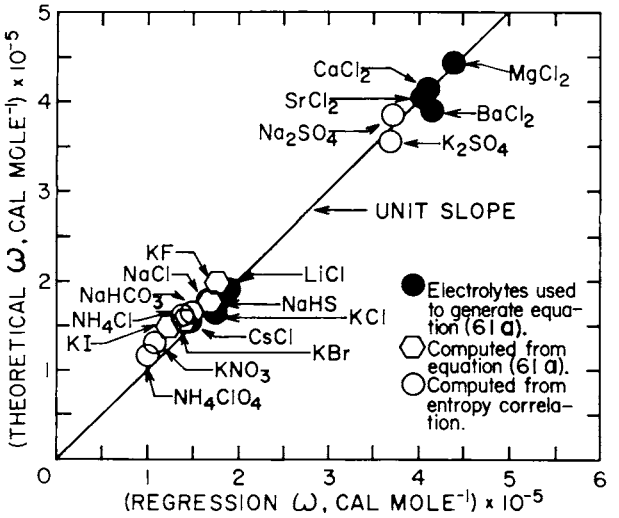

Fig. 25. Correlation of theoretical Born coefficients (ω) for electrolytes computed from equations (19) and (61) with their regression counterparts.

dicted values of ω for many of the electrolytes were derived solely from correlation of entropies with $r_{e,j}$. Because the effective electrostatic radii of aqueous ions in table 7 are consistent with both standard partial molal volume and entropy data, the predicted values of ω in table 8 were accepted in preference to their regression counterparts (table 5). Accordingly, the values of ω in table 8 were specified in equation (40), which was then used to refit the standard partial molal volume data to obtain revised values of σ, ξ, and θ for the electrolytes. This procedure amounts to fitting equation (30) to values of $\Delta\bar{V}^\circ_n$, which corresponds to the sum of the standard intrinsic partial molal volume ($\bar{V}^\circ_i$) and the standard partial molal volume of electrostriction collapse ($\Delta\bar{V}^\circ_c$).

Intrinsic Volume and Electrostriction Collapse

Regression of the values of $\bar{V}^\circ$ in table 3 and those at low temperatures taken from the literature (Millero, 1972b) using Q for 20 bars (table 4) and equation (40) with ω set to its theoretical value (table 8) generated the dashed curves in figures 17 through 19 and the fit coefficients in table 8. The dashed curves thus correspond to the results of regressing values of $\Delta\bar{V}^\circ_n$ computed from experimental values of $\bar{V}^\circ$ and theoretical values of $\Delta\bar{V}^\circ_s$. Standard partial molal volumes computed from equation (40) and the coefficients in table 8 are listed in table 9.

As in the case of the four-parameter regression calculations described above, additivity values of $\bar{V}^\circ$ for KF and NH_4ClO_4 at 5°, 10°, 20°, and/or 25°C were included in the data arrays for these electrolytes to afford better control of the three-parameter fits. The same experimental data cited in the discussion of the four-parameter fits were used in the calculations, but to insure internal consistency the requisite values of $\bar{V}^\circ_{KCl}$, $\bar{V}^\circ_{NaCl}$, and $\bar{V}^\circ_{NH_4Cl}$ were computed from equation (40) and appropriate coefficients in table 8. Estimates of $\bar{V}^\circ$ at 0°C were also included in the data arrays for NH_4Cl and NH_4ClO_4 (figs. 18 and 19) to obtain convergence in the three-parameter regression calculations for these electrolytes. The estimates are based on the results of the corresponding four-parameter fits (which involved only experimental values of $\bar{V}^\circ$) and alternate regression of the data with different trial estimates to obtain the best fit. In certain instances one or more of the data points were weighted to minimize errors in the fit coefficients which might be caused by an uneven distribution of data.

To insure internal consistency in the equation of state coefficients for Na_2SO_4 and K_2SO_4, additivity values of $\bar{V}^\circ_{MgSO_4}$ were calculated from experimental standard partial molal volumes of these electrolytes (table 3 and fig. 19) by taking account of

$$\begin{aligned}\bar{V}^\circ_{MgSO_4} &= \bar{V}^\circ_{MgCl_2} + 2\bar{V}^\circ_{Na_2SO_4} - 2\bar{V}_{NaCl} \\ &= \bar{V}_{MgCl_2} + 2\bar{V}^\circ_{K_2SO_4} - 2\bar{V}^\circ_{KCl}\end{aligned} \tag{75}$$

Values of $\bar{V}^\circ_{MgCl_2}$, $\bar{V}^\circ_{NaCl}$, and $\bar{V}^\circ_{KCl}$ computed from equation (40) and appropriate coefficients in table 8 were used in these calculations to minimize accumulation of experimental uncertainties. The additivity values

TABLE 8

Summary of fit coefficients generated by three-parameter regression of standard partial molal volume data for aqueous electrolytes as a function of temperature at 20 bars (table 3 and figures 17 through 19, 26, and 27) with equation (40), values of Q in table 4, and Born coefficients (ω) computed from equation (19) and the values of ω_j^{abs} in table 7[a]

Electrolyte	σ[b]	ξ[b] × 10^2	θ[c]	ω[d,e] × 10^{-5}
HCl	0.5747	-1.0491	246.02	1.4560
LiCl	0.5798	-1.0827	246.49	1.9421
NaCl	0.7532	-5.7947	228.58	1.7865
KCl	0.8841	-2.8777	240.20	1.6487
CsCl	1.234	-4.6499	231.08	1.5534
NH_4Cl	1.1258	-3.6962	234.68	1.6351
LiBr	0.8928[f]	-6.3724[f]	209.09[f]	1.8719
NaBr	1.0801[f]	-12.0208[f]	211.21[f]	1.7163
KBr	1.1920	-7.7758	219.27	1.5785
NaF	0.2221[f]	-2.6240[f]	248.38[f]	2.1176
KF	0.3737	-0.9590	259.66	1.9797
KI	1.6626	-15.6023	204.46	1.4861
CsI	2.0408[f]	-19.4275[f]	198.67[f]	1.3908
$NaHCO_3$	0.9695	-7.6654	226.95	1.6599
HNO_3	1.2373[f]	-18.0627[f]	185.29[f]	1.1295
$NaNO_3$	1.4073[f]	-21.9819[f]	198.33[f]	1.4601
KNO_3	1.5070	-16.7989	203.02	1.3222
NaOH	0.2023[g]	-4.0897[f]	242.89	2.0552
NaHS	0.8168	-5.3073	237.21	1.7716
NH_4ClO_4	4.8235	-249.9635	71.37	1.1803
$MgCl_2$	0.7338	-2.0342	247.32	4.4492
$CaCl_2$	0.7894	-1.9642	252.00	4.1485
$SrCl_2$	0.7970	-1.7292	256.90	4.0483
$BaCl_2$	1.0408	-4.3526	245.52	3.8970
H_2SO_4	0.5834[f]	-0.6359[f]	263.03[f]	3.1857
Na_2SO_4	0.9005[f]	-7.7870[f]	239.39[f]	3.8468
K_2SO_4	1.1863[f]	-3.4200[f]	250.97[f]	3.5711
$MgSO_4$	0.1691	-0.6357	263.32	4.7229

[a]Values of $\bar{V}^\circ$ computed from the coefficients listed above are given in table 9 and shown as dashed curves in figures 17 through 19, 26, and 27. [b]cal mole^{-1} bar^{-1}. [c]°K. [d]cal mole^{-1}. [e]Computed from equation (19) and values of ω_j^{abs} in table 7. [f]Generated by regression of additivity values of $\bar{V}^\circ$ calculated (eqs 75 and 81 through 87) from standard partial molal volumes of other electrolytes computed from equation (40), coefficients given above, and values of Q in table 4--see text. [g]Calculated from equations (28) and (29) using the values of $a_{2,NaOH}$ and $a_{4,NaOH}$ in table 11.

TABLE 9

Standard partial molal volumes of electrolytes in cm^3 $mole^{-1}$ at 20 bars and temperatures from 0° to 200°C computed from equation (40), coefficients in table 8, and values of Q in table 4[a]

Electrolyte	Temperature, °C								
	0	25	50	75	100	125	150	175	200
HCl	16.4	17.9	17.9	17.2	15.9	13.8	10.6	5.9	-1.4
LiCl	15.3	16.8	16.7	15.6	13.7	10.9	6.7	0.3	-9.4
NaCl	12.6	16.7	18.0	17.9	16.8	14.6	11.0	5.5	-3.3
KCl	23.3	26.7	27.4	27.1	25.8	23.6	20.2	14.9	6.8
CsCl	35.5	39.1	40.2	40.2	39.2	37.2	34.1	29.3	21.7
NH_4Cl	32.5	35.8	36.7	36.4	35.2	33.1	29.7	24.6	16.5
LiBr	21.8	23.8	24.3	23.8	22.4	20.0	16.2	10.3	1.0
NaBr	19.2	23.7	25.6	26.1	25.5	23.7	20.5	15.4	7.2
KBr	29.8	33.7	35.1	35.3	34.5	32.7	29.7	24.9	17.2
NaF	-7.6	-2.5	-1.7	-2.3	-4.0	-6.9	-11.4	-18.1	-28.7
KF	3.1	7.6	7.8	6.8	4.9	2.1	-2.2	-8.7	-18.6
KI	40.3	45.1	47.4	48.3	48.1	46.8	44.3	40.0	33.0
CsI	52.5	57.6	60.2	61.4	61.4	60.4	58.2	54.4	47.9
$NaHCO_3$	17.9	23.0	24.9	25.3	24.5	22.7	19.5	14.5	6.4
HNO_3	25.7	29.0	30.7	31.5	31.4	30.5	28.7	25.6	20.3
$NaNO_3$	22.0	27.8	30.8	32.2	32.3	31.4	29.1	25.2	18.4
KNO_3	32.7	37.8	40.3	41.3	41.4	40.4	38.3	34.6	28.5
NaOH	-11.6	-5.8	-4.4	-4.7	-6.2	-8.8	-13.0	-19.5	-29.7
NaHS	13.3	18.9	20.6	20.7	19.7	17.6	14.0	8.6	-0.1
NH_4ClO_4	57.6	61.4	64.1	65.9	66.9	67.0	66.0	63.5	58.8
$MgCl_2$	11.7	14.7	14.0	11.5	7.1	0.5	-9.2	-23.7	-46.0
$CaCl_2$	13.1	17.5	17.1	14.9	10.8	4.7	-4.3	-17.8	-38.6
$SrCl_2$	12.1	18.1	18.0	15.8	11.8	5.9	-2.9	-16.1	-36.4
$BaCl_2$	16.8	23.6	24.5	23.1	19.8	14.3	6.1	-6.5	-25.9
H_2SO_4	10.1	14.3	13.6	11.7	8.4	3.6	-3.4	-13.8	-29.9
Na_2SO_4	2.7	11.6	13.8	13.1	10.4	5.3	-2.5	-14.7	-33.7
K_2SO_4	24.0	31.8	32.8	31.4	28.3	23.3	15.7	4.3	-13.6
$MgSO_4$	-10.9	-6.9	-8.2	-11.3	-16.2	-23.4	-33.8	-49.3	-73.1

[a]The values given in this table are represented by the dashed curves in figures 17 through 19, 26, and 27.

of $\bar{V}^\circ_{MgSO_4}$ were combined with experimental standard partial molal volumes of the electrolyte at low temperatures (fig. 26) and regressed with the equation of state to generate the fit coefficients and values of $\bar{V}^\circ_{MgSO_4}$ in tables 8 and 9. The latter values, which are represented by the curve for $MgSO_4$ in figure 26, were then used together with $\bar{V}^\circ_{MgCl_2}$, $\bar{V}^\circ_{NaCl}$, and $\bar{V}^\circ_{KCl}$ computed from equation (40) and appropriate coefficients in table 8 to solve equation (75) for $\bar{V}^\circ_{Na_2SO_4}$ and $\bar{V}^\circ_{K_2SO_4}$ at a series of temperatures from 0° to 200°C. The results of these calculations at 25° intervals are plotted in figure 19, where it can be seen that a number of the additivity values differ significantly from their experimental counterparts. The discrepancies arise from inconsistencies in the experimental data for the two electrolytes, which are also manifest in the additivity values of $\bar{V}^\circ_{MgSO_4}$ in figure 26. The regression curve for $MgSO_4$ in figure 26 and the dashed curves for Na_2SO_4 and K_2SO_4 in figure 19 depreciate these inconsistencies. The curves were computed from equation (40) and the coefficients for $MgSO_4$, Na_2SO_4, and K_2SO_4 in table 8, which afford an internally consistent set of standard partial molal volumes for these electrolytes (table 9).[6] The values of σ, ξ, and θ for Na_2SO_4 and K_2SO_4 in table 8 were obtained by regressing the additivity values of $\bar{V}^\circ$ with equation (40) after setting ω for each electrolyte to its theoretical value (table 8). This procedure was invoked instead of computing the coefficients from additivity relations (described below) to insure agreement between standard partial molal volumes of Na_2SO_4 and K_2SO_4 computed from equation (40) and those derived by addition and subtraction of corresponding values of $\bar{V}^\circ$ for other electrolytes.

In principle, σ, ξ, and θ for Na_2SO_4 and K_2SO_4 can be computed directly from regression coefficients for other electrolytes in table 8 by taking account of equations (40) and (75), which permit us to write

$$\sigma_{Na_2SO_4} = \sigma_{MgSO_4} + 2\sigma_{NaCl} - \sigma_{MgCl_2} \tag{76}$$

and

$$\frac{\xi_{Na_2SO_4}}{T - \theta_{Na_2SO_4}} = \frac{\xi_{MgSO_4}}{T - \theta_{MgSO_4}} + \frac{2\xi_{NaCl}}{T - \theta_{NaCl}} - \frac{\xi_{MgCl_2}}{T - \theta_{MgCl_2}} \tag{77}$$

Alternately setting $T = \infty$ and $T = 0$ in equation (77) leads to

$$\xi_{Na_2SO_4} = \xi_{MgSO_4} + 2\xi_{NaCl} - \xi_{MgCl_2} \tag{78}$$

and

$$\frac{\xi_{Na_2SO_4}}{\theta_{Na_2SO_4}} = \frac{\xi_{MgSO_4}}{\theta_{MgSO_4}} + \frac{2\xi_{NaCl}}{\theta_{NaCl}} - \frac{\xi_{MgCl_2}}{\theta_{MgCl_2}} \tag{79}$$

---

[6] Despite the fact that $MgSO_4$, Na_2SO_4, and K_2SO_4 solutions are not completely dissociated, the additivity calculations of $\bar{V}^\circ$ in this study apply to the dissociated solute for these electrolytes. Owing to the procedure used in extrapolating ϕ_V to infinite dilution (see above), contributions of ion association to ϕ_V are not manifested in the extrapolated values of $\bar{V}^\circ$.

or

$$\theta_{Na_2SO_4} = \frac{\xi_{Na_2SO_4}\theta_{MgSO_4}\theta_{NaCl}\theta_{MgCl_2}}{\xi_{MgSO_4}\theta_{NaCl}\theta_{MgCl_2} + 2\xi_{NaCl}\theta_{MgSO_4}\theta_{MgCl_2} - \xi_{MgCl_2}\theta_{MgSO_4}\theta_{NaCl}} \quad (80)$$

Evaluation of equations (76), (78), and (80) as well as analogous expressions for K_2SO_4 using the fit coefficients for NaCl, KCl, and $MgCl_2$ in table 8 yields values of σ, ξ, θ, and $\bar{V}^\circ$ which differ somewhat from those generated by regression of the standard partial molal volumes of Na_2SO_4 and K_2SO_4 computed from equation (75) and the values of $\bar{V}^\circ_{MgSO_4}$, $\bar{V}^\circ_{NaCl}$, $\bar{V}^\circ_{KCl}$, and $\bar{V}^\circ_{MgCl_2}$ in table 9. The discrepancies are caused by inconsistencies in the relative extent to which $\Delta\bar{V}^\circ_n$ is distributed among $\bar{V}^\circ_i$ and $\Delta\bar{V}^\circ_c$ in the fits of equation (40) to $\bar{V}^\circ$, together with the fact that slight inconsistencies in the regression results for different electrolytes are magnified by subtraction or addition of the curves, all of which exhibit extrema. Because the regression equation is a nonlinear function of ξ and θ, the distribution of $\Delta\bar{V}^\circ_n$ among $\bar{V}^\circ_i$ and $\Delta\bar{V}^\circ_c$ is sensitive to the number and distribution of experimental data points in the fit array. Different data arrays for different electrolytes may thus lead to values of σ, ξ, and θ which are slightly inconsistent with equations (76), (78), and (80), despite an acceptable sum of squares reduction in each of the independent fits. It follows that the values of σ, ξ, and θ generated by the fits may lead to inaccurate values of $\bar{V}^\circ_i$ and $\Delta\bar{V}^\circ_c$. However, owing to regression compensation among the terms in equation (40), different values of σ, ξ, and θ generated by regression of $\bar{V}^\circ$ for a given electrolyte before and after minor perturbation of the data array do not cause corresponding differences in the fit residuals or computed values of $\Delta\bar{V}^\circ_n$ and $\bar{V}^\circ$. Consequently, errors in the absolute magnitudes of σ, ξ, and θ caused by nonrandom scatter in the distribution of experimental data for different electrolytes are not transmitted to additivity values of $\bar{V}^\circ$. In contrast, accumulation of these errors in computing coefficients for other electrolytes from expressions like equations (76), (78), and (80) invariably leads to erroneous values of $\bar{V}^\circ$ and $\Delta\bar{V}^\circ_n$, as well as $\bar{V}^\circ_i$ and $\Delta\bar{V}_c$.

The numerical values of the fit coefficients in the asymptotic term of the regression equation are determined primarily by the distribution of experimental data at low temperatures, where $\Delta\bar{V}^\circ_c$ is a relatively large negative number. In cases where these data are sparse and/or scattered, the regression calculations yield only approximate values of $\bar{V}^\circ_i$ and $\Delta\bar{V}^\circ_c$ which may or may not combine to give accurate values of $\Delta\bar{V}^\circ_n$. Because additivity values of $\Delta\bar{V}^\circ_n$ are obtained from the sums and differences of asymptotic functions, significant residuals may result from fits of additivity values of $\bar{V}^\circ$ derived from corresponding values for electrolytes computed from equation (40) and the fit coefficients in tables 5 or 8. In the case of the additivity values of $\bar{V}^\circ$ for K_2SO_4 and Na_2SO_4, the regression calculations resulted in maximum residuals of 0.09 and 0.24 $cm^3\ mole^{-1}$, respectively.

It can be seen in figures 17 through 19 that the dashed curves represent the experimental data for most of the electrolytes as well as or better than the solid curves, which were generated without forcing theoretical

values of ω or (in the case of Na_2SO_4 and K_2SO_4) insuring internal consistency and agreement with additivity values of $\bar{V}°$. In certain cases (for example, NH_4Cl, $NaHCO_3$, NH_4ClO_4, and KF) where few reliable low temperature data are available to control the fits of $\bar{V}°$ below 25°C, the dashed curves depart from their solid counterparts by up to $\backsim$ 0.5 cm^3 $mole^{-1}$. Nevertheless, the dashed curves closely represent the experimental data for these electrolytes, which may be in error by more than the discrepancy between the curves. Because the theoretical values of ω satisfy both entropy and volume data, the regression calculations represented by the dashed curves afford a more reliable representation of $\bar{V}°$. For this reason, the values of σ, ξ, and θ generated by the fits of $\Delta\bar{V}°_n$ and the Born coefficients summarized in table 8 were adopted in the equation of state calculations described in subsequent pages. Standard partial molal volumes of 28 electrolytes computed from these coefficients and equation (40) for 20 bars and 0° to 200°C are given in table 9. The values shown for 25°C in table 9 are in close agreement with corresponding values of $\bar{V}°$ obtained by extrapolating to infinite dilution apparent molal volumes reported by Allam (ms) and Fortier, Leduc, and Desnoyers (1974) with the aid of equation (57A) using theoretical values of å (Helgeson and Kirkham, 1976).

Values of σ, ξ, θ, ω, and $\bar{V}°$ are given in tables 8 and 9 for NaOH and seven other electrolytes (in addition to $MgSO_4$) which are not listed in tables 3, 5, and 6. The Born coefficients for these electrolytes were calculated (eq 19) from appropriate values of ω_j^{abs} in table 7, but the remainder of the coefficients were generated by regression of standard partial molal volumes computed from

$$\bar{V}°_{NaNO_3} = \bar{V}°_{KNO_3} + \bar{V}°_{NaCl} - \bar{V}°_{KCl} \tag{81}$$

$$\bar{V}°_{HNO_3} = \bar{V}°_{KNO_3} + \bar{V}°_{HCl} - \bar{V}°_{KCl} \tag{82}$$

$$\bar{V}°_{NaBr} = \bar{V}°_{KBr} + \bar{V}°_{NaCl} - \bar{V}°_{KCl} \tag{83}$$

$$\bar{V}°_{NaF} = \bar{V}°_{KF} + \bar{V}°_{NaCl} - \bar{V}°_{KCl} \tag{84}$$

$$\bar{V}°_{H_2SO_4} = \bar{V}°_{MgSO_4} + 2\bar{V}°_{HCl} - \bar{V}°_{MgCl_2} \tag{85}$$

$$\bar{V}°_{LiBr} = \bar{V}°_{LiCl} + \bar{V}°_{KBr} - \bar{V}°_{KCl} \tag{86}$$

and

$$\bar{V}°_{CsI} = \bar{V}°_{CsCl} + \bar{V}°_{KI} - \bar{V}°_{KCl} \tag{87}$$

using values of $\bar{V}°$ for KNO_3, NaCl, KCl, HCl, KBr, KF, $MgSO_4$, $MgCl_2$, LiCl, KI, and CsCl computed from equation (40) and appropriate coefficients in table 8. As in the case of Na_2SO_4 and K_2SO_4 above, the additivity values of $\bar{V}°$ calculated from equations (81) through (87) were regressed with equation (40) using values of Q for 20 bars (table 4) and theoretical Born coefficients (table 8) to avoid introducing errors in the equation of state coefficients by computing them from expressions analogous to equations (76), (78), and (80). The additivity values of $\bar{V}°$ are shown in figures

26 and 27 together with curves representing the standard partial molal volumes of $NaNO_3$, HNO_3, NaBr, NaF, H_2SO_4, LiBr, and CsI (table 9) computed from the regression coefficients (table 8) and equation (40). Although the additivity ambiguities discussed above led to slight residuals in the regression calculations ($\leq$ 0.01 cm^3 $mole^{-1}$ for all the electrolytes except NaF, for which the maximum residual is $\leq$ 0.2 cm^3 $mole^{-1}$), it can be seen that in every case both the additivity values and the regression curves are closely consistent with the experimental data reported in the literature.

The regression curve for NaOH in figure 27 is based solely on low temperature data at 1 atm. Accordingly, values of Q for H_2O vapor-saturation pressures (table 4) were used together with equation (40) and the theoretical Born coefficient for NaOH in table 8 to regress the experimental data for this electrolyte at temperatures from 0° to 100°C. Over this temperature range, Q at 1 bar is essentially equal to Q at vapor-saturation pressures. The 1 bar values of σ and ξ generated by the fit were then used to calculate (eq 28 and 29) corresponding values at 20 bars (table 8) from compressibility parameters for NaOH, which are computed in the following pages. The values of σ, ξ, θ, and ω for NaOH in table 8 were used together with equation (40) to generate the standard partial molal volumes of sodium hydroxide in table 9 and the corresponding curve in figure 27.

It can be seen in figure 27 that considerable discrepancy exists between the regression curve for NaOH and the high temperature values of $\bar{V}°_{NaOH}$ reported by Dibrov, Mashovets, and Mateeva (1964). The latter values were obtained by extrapolation of apparent molal volume data to infinite dilution without taking account of ion association or constraints imposed by the theoretical Debye-Hückel limiting law. Consideration of these data, together with appropriate values of A_V (Helgeson and Kirkham, 1974b) indicates that the extrapolation procedure used by Dibrov, Mashovets, and Mateeva introduced large errors in the reported values of $\bar{V}°$ above 100°C. Efforts to rectify these errors in the present study were unsuccessful, owing to insufficient accuracy in the high-temperature density data.

Discussion.—The agreement between the curves and symbols plotted in figures 17 through 19, 26, and 27 is remarkably close for all 28 electrolytes. It can be seen that in every instance the curves exhibit an extremum between $\backsim$ 25° and 125°C. At both higher and lower temperatures, $\bar{V}°$ decreases to an increasing degree as temperature increases or decreases, respectively. $\bar{V}°$ for all of the electrolytes becomes negative at high temperatures, but in certain cases (NaOH, NaF, and $MgSO_4$) $\bar{V}°$ is negative at all temperatures. The effect of increasing temperature on the standard partial molal volumes of 1:2 and 2:1 electrolytes is particularly dramatic. It can be seen that $\bar{V}°$ for 1:1 electrolytes decreases by $\backsim$ 100 percent of its value at the extremum as temperature increases to 200°C from the temperature coresponding to the extremum. In contrast, $\bar{V}°$ for 1:2 and 2:1 electrolytes decreases of the order of 200 to 300 percent for

the same temperature increase. As shown below, increasing temperature above 200°C causes the standard partial molal volumes of all electrolytes to become large negative numbers and approach negative infinity at the critical point for H_2O.

The change in the relative contributions of $\Delta\bar{V}^\circ_c$ and $\Delta\bar{V}^\circ_s$ to the standard partial molal volume of an electrolyte with increasing temperature at low pressures is manifested by the extrema in the curves shown in figures 17 through 19, 26, and 27. At low temperatures, where water is a highly structured liquid, $\Delta\bar{V}^\circ_c$ in equation (10) is relatively large and negative, but as temperature increases at low pressures and the structure of the solvent becomes increasingly disrupted, $\Delta\bar{V}^\circ_c$ becomes increasingly less negative and (as predicted by Ellis, 1966) approaches a value close to

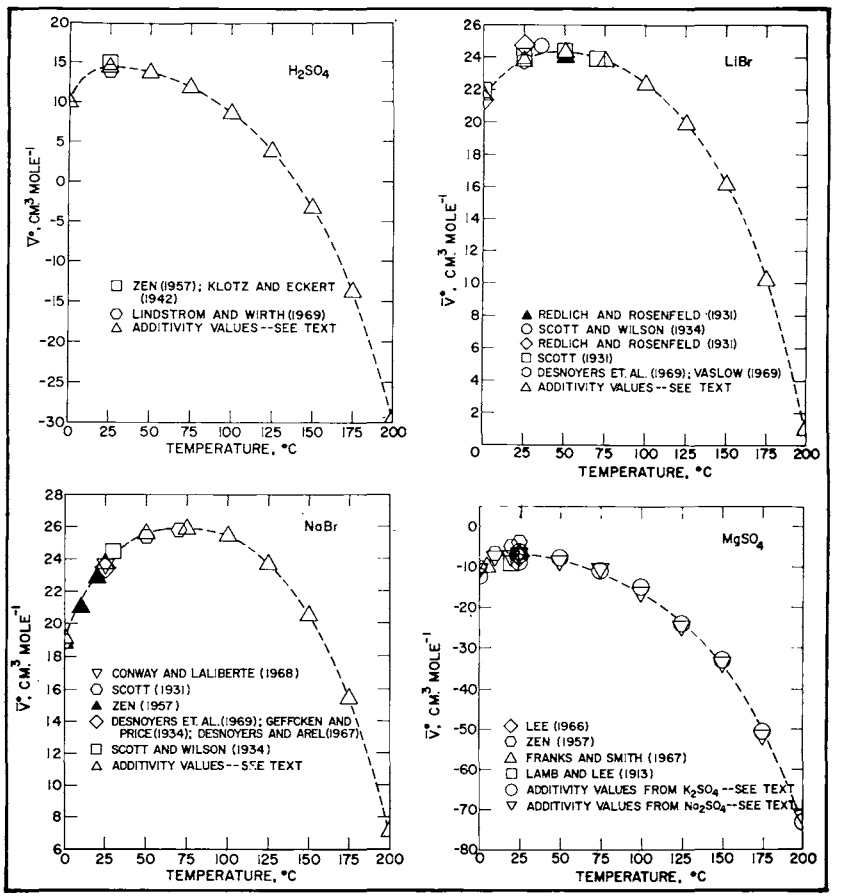

Fig. 26. Standard partial molal volumes of electrolytes as a function of temperature at 20 bars. The symbols represent values for 20 bars computed from additivity relations or reported in the literature for 1 atm. The curves were generated by regression of the data with equation (40) — see text and tables 8 and 9.

zero. At high temperatures and low pressures, $\Delta\bar{V}^\circ_c \approx a_3$, which is of the order of -1 to -10 cm^3 mole^{-1}. This behavior is apparent in figures 28A and B, where values of $\Delta\bar{V}^\circ_n$ for KBr and Na_2SO_4 at 20 bars are plotted against temperature. At high temperatures, $\Delta\bar{V}^\circ_n$ approaches $a_1 + a_3$.

In contrast to $\Delta\bar{V}^\circ_c$, $\Delta\bar{V}^\circ_s$ in equation (10) is a relatively small negative number at low temperatures and pressures. Also, where $(\partial\Delta\bar{V}^\circ_c/\partial T)_P$ is positive, $(\partial\Delta\bar{V}^\circ_s/\partial T)_P$ is negative. Because the dielectric constant of H_2O decreases to an increasing degree with increasing temperature, $\Delta\bar{V}_s$ becomes increasingly more negative as temperature increases (figs. 28C and D). As a consequence, addition of $\Delta\bar{V}^\circ_n$ and $\Delta\bar{V}^\circ_s$ leads to an ex-

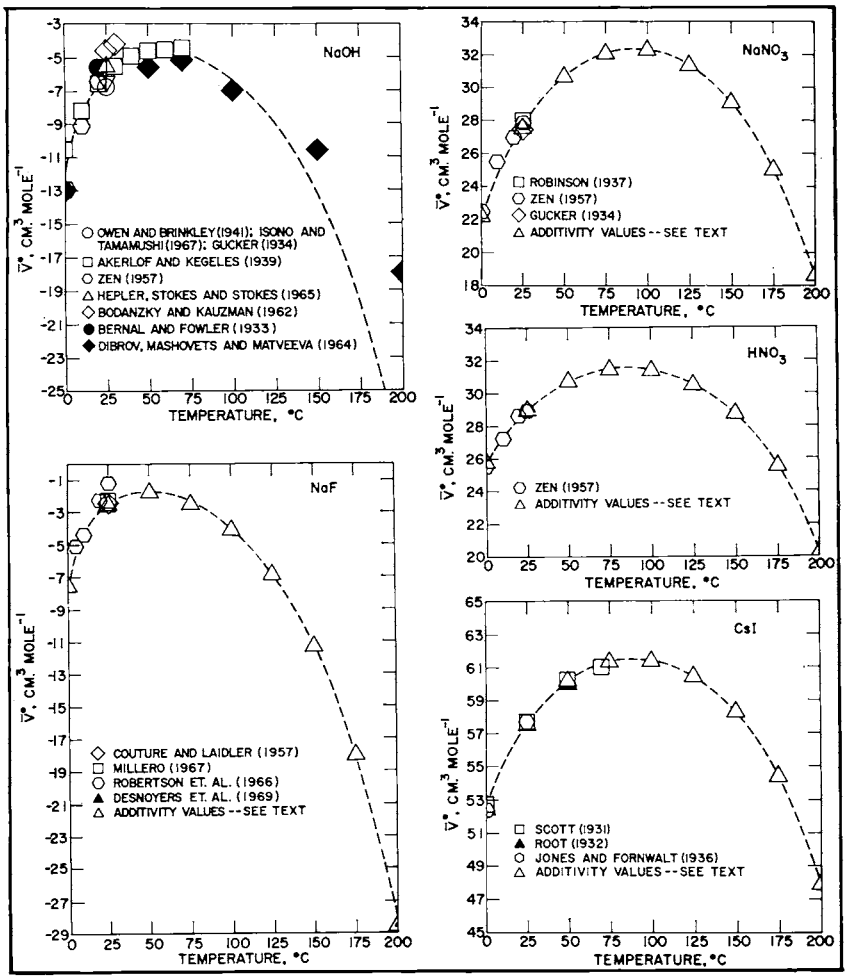

Fig. 27. Standard partial molal volumes of electrolytes as a function of temperature at 20 bars. The symbols represent values for 20 bars computed from additivity relations or reported in the literature for 1 atm. The curves were generated by regression of the data with equation (40) — see text and tables 8 and 9.

tremum in $\bar{V}^\circ$ as a function of temperature at low (constant) pressures. At low temperatures, $\Delta\bar{V}^\circ_n$ is primarily responsible for the magnitude of $\bar{V}^\circ$ and its dependence on temperature, but at high temperatures and low pressures, $\Delta\bar{V}^\circ_s$ dominates $\bar{V}^\circ$ and largely controls its behavior as a function of temperature and pressure (see below).

The relative contributions of $\Delta\bar{V}^\circ_n$ and $\Delta\bar{V}^\circ_s$ to $\bar{V}^\circ$ at 20 bars and temperatures from 0° to 200°C can be assessed in figure 29, where $\Delta\bar{V}^\circ_s$ is plotted against $\Delta\bar{V}^\circ_n$ for KBr. It can be seen that $\Delta\bar{V}^\circ_s$ is only -3 cm^3 mole^{-1} at 0°C and decreases less than 1 cm^3 mole as temperature increases to 50°C. In contrast, $\Delta\bar{V}^\circ_n$, which is $\sim$ 33 cm^3 mole^{-1} at 0°C, increases to $\sim$ 39 cm^3 mole^{-1} at 50°C. Between $\sim$ 50° and 100°C, both $\Delta\bar{V}^\circ_n$ and $\Delta\bar{V}^\circ_s$ contribute comparably to $\bar{V}^\circ$, but above 100°C the low-temperature roles of $\Delta\bar{V}^\circ_n$ and $\Delta\bar{V}^\circ_s$ are reversed; that is, $\Delta\bar{V}^\circ_n$ increases only slightly with increasing temperature compared to a dramatic decrease in $\Delta\bar{V}^\circ_s$. As shown below, increasing temperature above 200°C along the H_2O saturation curve causes the absolute value of $\Delta\bar{V}^\circ_s$ to become much larger than $\Delta\bar{V}^\circ_n$, which forces $\bar{V}^\circ$ to become a large negative number.

Standard partial molal expansibility.—Standard partial molal expansibilities ($\bar{E}^\circ_J$) computed from equation (41) and values of U, σ, ξ, θ,

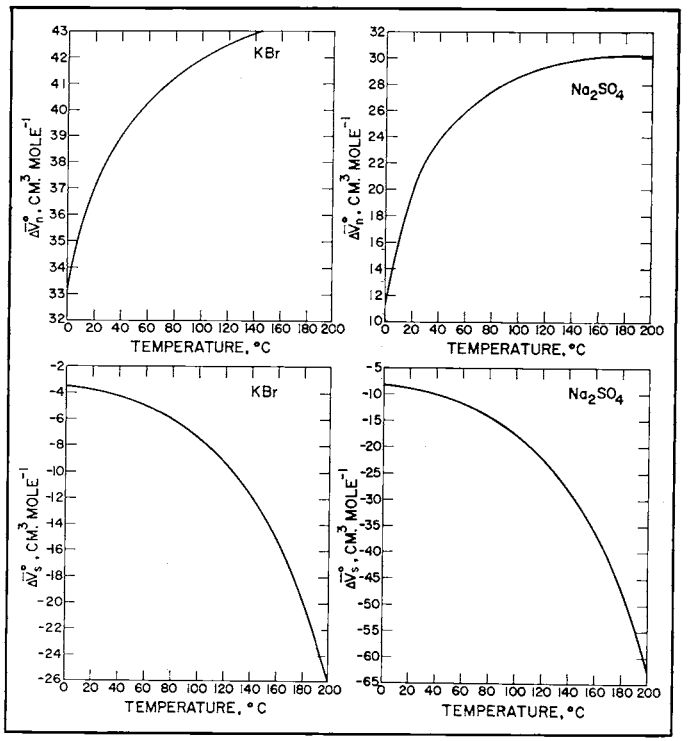

Fig. 28. $\Delta\bar{V}^\circ_s$ and $\Delta\bar{V}^\circ_n$ for KBr and Na_2SO_4 as a function of temperature at 20 bars computed from equations (18) and (26) and values of σ, ξ, θ, ω, and Q in tables 4 and 8.

and ω (tables 4 and 8) are given in table 10 for 28 electrolytes at 20 bars and 0° to 200°C. It can be seen in figure 30 that the predicted values of $\bar{E}^\circ_x$ are in close agreement with standard partial molal expansibilities reported in the literature for 1 atm, as well as with finite difference derivatives $(\Delta\bar{V}^\circ/\Delta T)_P$ of the experimental and/or additivity values of $\bar{V}^\circ$. Similar agreement can be demonstrated for the other electrolytes shown in table 10. The striking correspondence of the symbols and curves in figure 30 strongly supports the validity of the theoretical values of ω in table 8 as well as the equation of state itself. Note that the dependence of $\bar{E}^\circ_x$ on temperature is similar to that exhibited by b'_V in figures 14 and 15. Despite the fact that both variables are sensitive functions of ion-solvent interaction, the qualitative correspondence in the graphic configurations of the two functions is not necessarily a manifestation of a simple underlying relation between them.

It can be seen in figure 30 that $\bar{E}^\circ_x$ exhibits a sigmoid dependence on temperature at 20 bars, changing from values of the order of 0.1 to 1.0 $cm^3\ mole^{-1}\ (°K)^{-1}$ at 0°C to values ranging from −0.3 to −1.3 at 200°C, depending on the electrolyte. The 2:1 and 1:2 electrolytes exhibit the largest change in $\bar{E}^\circ_x$ with increasing temperature.

The cause of the sigmoid dependence of $\bar{E}^\circ_x$ on temperature at low pressures is apparent in figure 31, where $\Delta\bar{E}^\circ_{x,c}$ (which is equal to $\Delta\bar{E}^\circ_{x,n}$) and $\Delta\bar{E}^\circ_{x,s}$ (which is equal to $\Delta\bar{E}^\circ_{x,c}$) for KBr and Na_2SO_4 are plotted as functions of temperature at 20 bars. At low temperatures, $\Delta\bar{E}^\circ_{x,c}$ is a large

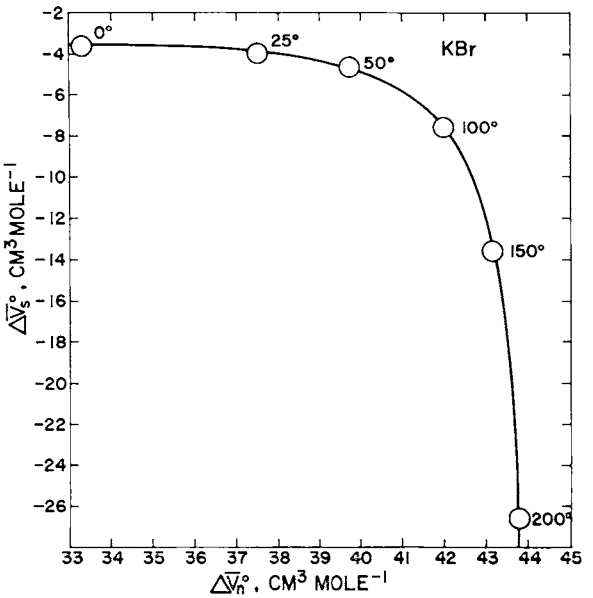

Fig. 29. Correlation of $\Delta\bar{V}^\circ_s$ and $\Delta\bar{V}^\circ_n$ for KBr as a function of temperature at 20 bars computed from equations (18) and (26) and values of σ, ξ, θ, ω, and Q in tables 4 and 8.

TABLE 10

Standard partial molal expansibilities of electrolytes ($\bar{E}°_x$) in cm^3 $mole^{-1}$ $(°K)^{-1}$ at 20 bars and temperatures from 0° to 200°C computed from equation (41), coefficients in table 8, and values of U in table 4

Electrolyte	Temperature, °C								
	0	25	50	75	100	125	150	175	200
HCl	0.14	0.02	-0.02	-0.04	-0.07	-0.10	-0.15	-0.23	-0.37
LiCl	0.14	0.02	-0.03	-0.06	-0.09	-0.14	-0.20	-0.31	-0.49
NaCl	0.26	0.09	0.02	-0.02	-0.07	-0.11	-0.18	-0.28	-0.44
KCl	0.25	0.06	0.00	-0.03	-0.07	-0.11	-0.17	-0.26	-0.41
CsCl	0.24	0.08	0.02	-0.02	-0.06	-0.10	-0.15	-0.24	-0.38
NH_4Cl	0.23	0.07	0.01	-0.03	-0.07	-0.11	-0.16	-0.25	-0.41
LiBr	0.12	0.05	0.00	-0.04	-0.08	-0.12	-0.19	-0.29	-0.46
NaBr	0.26	0.12	0.04	0.00	-0.05	-0.10	-0.16	-0.26	-0.42
KBr	0.23	0.09	0.03	-0.01	-0.05	-0.09	-0.15	-0.24	-0.39
NaF	0.43	0.08	0.00	-0.05	-0.09	-0.14	-0.22	-0.33	-0.53
KF	0.56	0.04	0.02	-0.06	-0.09	-0.14	-0.20	-0.31	-0.50
KI	0.27	0.13	0.06	0.01	-0.03	-0.07	-0.13	-0.22	-0.36
CsI	0.28	0.14	0.07	0.02	-0.02	-0.06	-0.12	-0.20	-0.33
$NaHCO_3$	0.32	0.12	0.04	-0.01	-0.05	-0.10	-0.16	-0.25	-0.41
HNO_3	0.17	0.10	0.05	0.01	-0.02	-0.05	-0.10	-0.16	-0.27
$NaNO_3$	0.31	0.16	0.08	0.03	-0.02	-0.06	-0.12	-0.21	-0.34
KNO_3	0.28	0.14	0.07	0.02	-0.02	-0.06	-0.11	-0.19	-0.31
NaOH	0.44	0.11	0.02	-0.04	-0.08	-0.13	-0.21	-0.32	-0.51
NaHS	0.39	0.12	0.03	-0.02	-0.06	-0.11	-0.17	-0.27	-0.44
NH_4ClO_4	0.17	0.13	0.09	0.06	0.02	-0.02	-0.07	-0.14	-0.25
$MgCl_2$	0.28	0.02	-0.07	-0.14	-0.21	-0.32	-0.47	-0.71	-1.12
$CaCl_2$	0.43	0.42	-0.06	-0.12	-0.20	-0.30	-0.44	-0.66	-1.04
$SrCl_2$	0.67	0.06	-0.05	-0.12	-0.19	-0.29	-0.43	-0.64	-1.02
$BaCl_2$	0.56	0.11	-0.02	-0.10	-0.17	-0.27	-0.40	-0.61	-0.97
H_2SO_4	0.66	0.01	-0.01	-0.10	-0.16	-0.23	-0.34	-0.51	-0.80
Na_2SO_4	0.66	0.17	0.02	-0.07	-0.15	-0.25	-0.39	-0.60	-0.96
K_2SO_4	0.70	0.11	-0.02	-0.09	-0.16	-0.25	-0.37	-0.56	-0.89
$MgSO_4$	0.69	0.00	-0.09	-0.16	-0.24	-0.34	-0.50	-0.76	-1.19

positive number in contrast to $\Delta\bar{E}^\circ_{x,s}$, which is nearly zero. At high temperatures and low pressures where $\Delta\bar{E}^\circ_{x,c}$ approaches zero, $\Delta\bar{E}^\circ_{x,s}$ becomes a large negative number. The sum of these two asymptotic functions yields the sigmoid curves in figure 30. Although both $\Delta\bar{E}^\circ_{x,c}$ and $\Delta\bar{E}^\circ_{x,s}$ decrease with increasing temperature, their second partial derivatives with respect to temperature at constant pressure are of opposite sign. The relation of the first derivatives to the pressure dependence of the isobaric standard partial molal heat capacity ($\bar{C}^\circ_P$) of an electrolyte is given by equation (34). Owing to the sigmoid configuration of the curves in figure 30, $(\partial^2\bar{V}^\circ/\partial T^2)_P$, which is negative, maximizes as a function of temperature at 20 bars. It can be deduced from figure 31 that the contribution of $(\Delta\bar{E}^\circ_{x,c}/\partial T)_P$ to the pressure dependence of C°_P approaches zero asymptotically with increasing temperature at 20 bars. In contrast, $(\partial\Delta\bar{E}^\circ_{x,s}/\partial T)_P$ is a sigmoid function of temperature at low pressures, which decreases by several orders of magnitude as temperature increases from 0°C (where

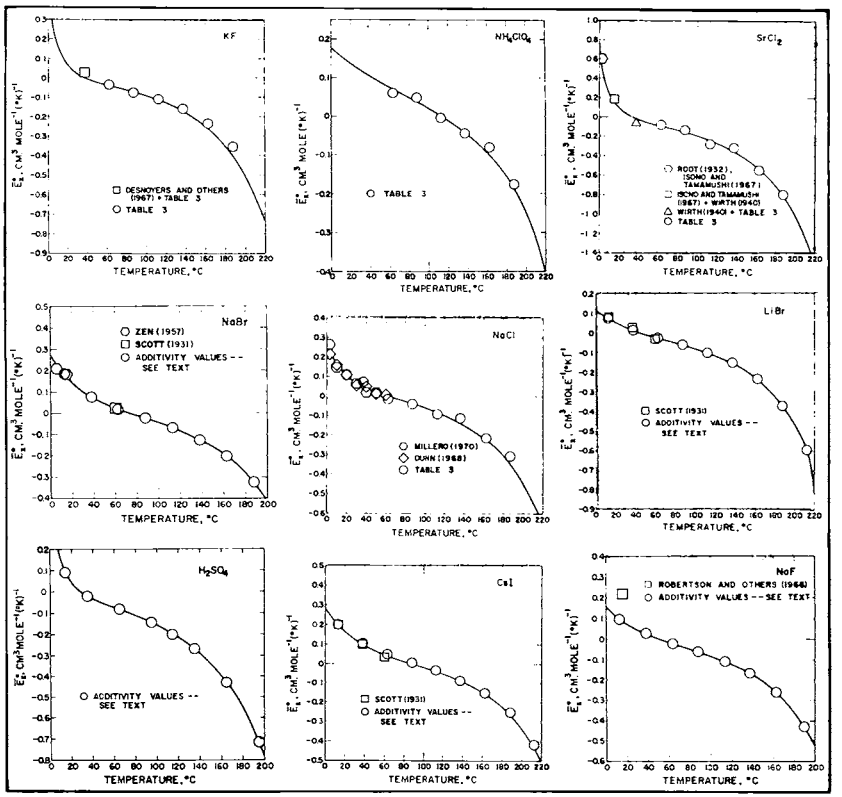

Fig. 30. Standard partial molal expansibilities ($\bar{E}^\circ_x$) of electrolytes (table 10) as a function of temperature at 20 bars computed from equation (41), coefficients in table 8, and values of U in table 4 (curves). The symbols represent finite difference derivatives of experimental standard partial molal volumes at 20 bars (table 3) or those reported in the literature for 1 atm.

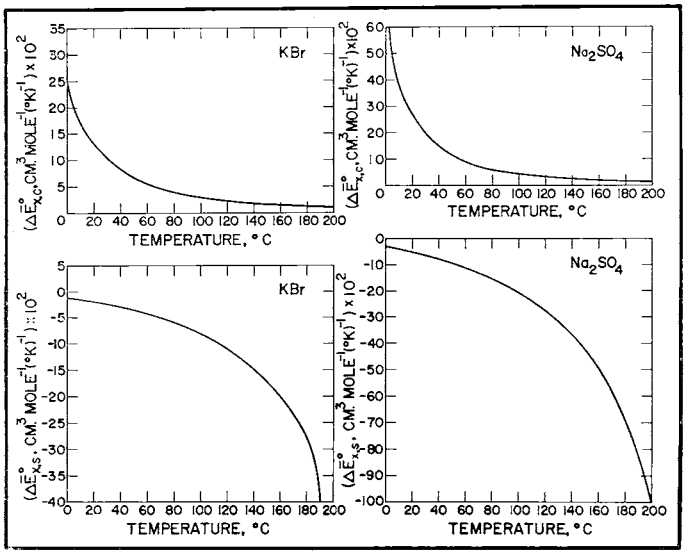

Fig. 31. $\Delta\bar{E}^{\circ}_{x,s}$ and $\Delta\bar{E}^{\circ}_{x,c}$ for KBr and Na_2SO_4 as a function of temperature at 20 bars computed from equations (20) and (33) and values of σ, ξ, θ, ω, and U in tables 4 and 8.

$(\partial\Delta\bar{E}^{\circ}_{x,s}/\partial T)_P$ is close to zero) to ~ 200°C. As a consequence, $(\partial\bar{C}^{\circ}_P/\partial P)_T$, which is positive at low pressures, maximizes with increasing temperature at 20 bars. As shown below, the increasingly dominant role played by the solvation contribution to the electrostriction volume loss with increasing temperature leads to large negative standard partial molal expansibilities of electrolytes at high temperatures and low pressures.

Standard partial molal compressibility.—Standard partial molal compressibility data for 1 atm (Millero, 1973; Millero, written commun., 1973; Lepple and Millero, 1971; Millero, Lepple, Hoff, and Ward, in preparation, 1974) are shown in figures 32 through 36, together with regression curves generated by fits of equation (43) to the data. Appropriate values of N, ω, and θ taken from tables 4 and 8 were specified in the regression equations, which (as a consequence) represented $-\Delta\bar{\kappa}^{\circ}_c$. The values of a_2, a_4, and $-\bar{\kappa}^{\circ}$ generated by the fits are given in tables 11 and 12. The other coefficients (ω and θ) employed in the calculations are also given in table 11 along with the values of a_1 and a_3 computed below. In contrast to the standard partial molal compressibilities represented by the curves in figures 32 through 36, which are for H_2O vapor saturation pressures, those in table 12 refer to 20 bars (see below).

Despite the fact that reliable compressibility data are available only in the temperature range 0° to 55°C, it can be seen in figures 32 through 36 that the curves represent the experimental values of $-\bar{\kappa}^{\circ}$ well within the uncertainty range defined by the various sets of data for each electrolyte. Note that different sets for a given electrolyte describe semiparallel trends with increasing temperature. The discrepancies arise from differ-

TABLE 11

Summary of equation of state coefficients generated by regression of standard partial molal compressibilities and volumes of aqueous electrolytes as functions of temperature at 1 and 20 bars (table 3 and figures 17 through 19, 26, 27, and 32 through 36) with equations (28), (29), (40), and (43) and values of Q, N, and ω in tables 4 and 8[a]

Electrolyte	a_1[b,g]	a_2[c] $\times 10^5$	a_3[b,g] $\times 10^2$	a_4[c] $\times 10^5$	θ[d]	ω[e,f] $\times 10^{-5}$
HCl	0.5761	-6.9590	-1.0698	1.0365	246.02	1.4560
NaCl	0.7555	-11.5626	-5.8839	4.4546	228.58	1.7865
KCl	0.8854	-6.2505	-2.9274	2.4848	240.20	1.6487
NaBr	1.0844	-21.4743[h]	-12.1786	7.8899[h]	211.21	1.7163
KBr	1.1950	-15.4202	-7.8827	5.3474	219.27	1.5785
NaF	0.2227	-2.9393	-2.6750	2.5484	248.38	2.1176
KF	0.3733	2.2836	-0.9797	1.0379	259.66	1.9797
$NaHCO_3$	0.9721	-12.9561	-7.7578	4.6192	226.95	1.6599
$NaNO_3$	1.4145	-35.9299[h]	-22.2521	13.5110[h]	198.33	1.4601
KNO_3	1.5129	-29.6084[h]	-17.0114	10.6254[h]	203.02	1.3222
HNO_3	1.2438	-32.0602	-18.2754	10.6342	185.29	1.1295
NaOH	0.2033	-4.8777	-4.1577	3.4000	242.89	2.0552
H_2SO_4	0.5825	4.4576[h]	-0.6501	0.7125[h]	263.03	3.1857
K_2SO_4	1.1850	6.4638[h]	-3.4828	3.1415[h]	250.97	3.5711
Na_2SO_4	0.9012	-3.4031	-7.9143	6.3643	239.39	3.8468
$MgSO_4$	0.1655	17.8302[h]	-0.6552	0.9764[h]	263.32	4.7229
$MgCl_2$	0.7343	-2.2157	-2.0919	2.8850	247.32	4.4492
$SrCl_2$	0.7969	0.7078	-1.7593	1.5043	256.90	4.0483
$CaCl_2$	0.7899	-2.4571	-2.0070	2.1399	252.00	4.1485

[a]The regression curves generated by the fits correspond to the dashed curves in figures 17 through 19, 26, 27, and 32 through 36. [b]cal mole^{-1} bar^{-1}. [c]cal mole^{-1} bar^{-2}. [d]°K (taken from table 8). [e]cal mole^{-1}. [f]Computed from equation (19) and values of ω_j^{abs} in table 7. [g]Calculated (eqs 28 and 29) from values of σ and ξ in table 8 and the a_2 and a_4 coefficients for NaOH given above. [h]Generated by regression of additivity values of $-\overline{K}^\circ$ calculated (eqs 88 through 91) from standard partial molal compressibilities of other electrolytes computed from equation (42), coefficients given above, and values of N in table 4--see text.

ent methods of measuring the compressibilities of electrolyte solutions and the procedures used to extrapolate the measurements to infinite dilution. Because the acoustic method affords the most reliable values of $\bar{K}^\circ$ (owing to the high accuracy achieved in dilute solutions), only sonic data were used in the regression calculations for most of the electrolytes. Nonacoustic data for these electrolytes are plotted in the diagrams for comparison. Where few or no acoustic values of $\bar{K}^\circ$ were available, all values given by Millero (1973; written commun., 1973), Lepple and Millero (1971), and Millero, Lepple, Hoff, and Ward (in preparation, 1974), some of which are estimates, were included in the regression analysis.

To insure internal consistency in the fits of equation (43) to the standard partial molal compressibilities of nitrates, sulfates, bromides, and chlorides, additivity values of $-\bar{K}^\circ$ for HNO_3 and KBr at 1 bar were first calculated from the experimental standard partial molal compressibilities of $NaNO_3$ and NaBr, which were used together with values of

TABLE 12

Standard partial molal compressibilities ($\bar{K}^\circ$) of aqueous electrolytes (expressed as $-\bar{K}^\circ$) in (cm^3 $mole^{-1}$ bar^{-1}) $\times$ 10^3 at 20 bars and temperatures from 0° to 200°C computed from equation (43), coefficients in table 11, and values of N in table 4

Electrolyte	Temperature, °C								
	0	25	50	75	100	125	150	175	200
HCl	2.3	0.9	0.5	0.8	1.6	3.3	6.4	12.1	23.2
NaCl	7.6	4.8	3.5	3.3	4.0	5.8	9.4	16.2	29.7
KCl	7.0	4.2	3.3	3.2	4.0	5.8	9.1	15.5	28.1
NaBr	6.6	3.9	2.5	2.0	2.5	4.0	7.3	13.8	26.7
KBr	5.8	3.4	2.3	2.0	2.5	4.0	7.2	13.6	25.1
NaF	11.7	7.1	5.7	5.7	6.7	9.0	13.4	21.6	37.7
KF	10.9	6.1	5.4	5.7	6.8	9.1	13.3	21.1	36.2
$NaHCO_3$	7.0	4.2	2.9	2.6	3.2	4.9	8.2	14.5	27.1
$NaNO_3$	6.4	3.2	1.2	0.3	0.3	1.3	3.9	9.2	20.0
KNO_3	5.7	2.8	1.0	0.3	0.3	1.3	3.7	8.5	18.3
HNO_3	1.1	-0.6	-1.7	-2.2	-2.1	-1.2	0.9	5.1	13.5
NaOH	12.0	7.5	6.0	5.8	6.6	8.8	13.0	20.9	36.5
H_2SO_4	11.7	7.3	7.0	7.9	10.0	13.9	20.7	33.3	57.7
K_2SO_4	20.9	14.3	12.6	12.8	14.7	18.7	26.2	40.1	67.4
Na_2SO_4	22.3	15.6	13.1	12.9	14.6	18.7	26.5	41.4	70.6
$MgSO_4$	21.5	15.3	14.9	16.3	19.4	25.1	35.3	54.0	90.2
$MgCl_2$	14.4	10.2	9.2	10.0	12.6	17.8	27.2	44.7	78.7
$SrCl_2$	13.2	8.5	7.9	8.8	11.4	16.2	24.9	40.8	71.8
$CaCl_2$	12.9	8.5	7.6	8.5	11.0	15.9	24.7	41.0	72.8

$-\bar{K}^\circ_{KCl}$, $-\bar{K}^\circ_{NaCl}$, and $-\bar{K}^\circ_{HCl}$ computed from equation (43) and values of N, a_2, a_4, θ, and ω in tables 4 and 11 to evaluate

$$\bar{K}^\circ_{HNO_3} = \bar{K}^\circ_{NaNO_3} + \bar{K}^\circ_{HCl} - \bar{K}^\circ_{NaCl} \tag{88}$$

and

$$\bar{K}^\circ_{KBr} = \bar{K}^\circ_{NaBr} + \bar{K}^\circ_{KCl} - \bar{K}^\circ_{NaCl} \tag{89}$$

The results of the calculations were then combined with corresponding experimental data for HNO_3 and KBr and regressed with equation (43) in the manner described above. The resulting fit coefficients are shown in table 11, together with the values of ω and θ specified in the regression equations. The additivity values of $-\bar{K}^\circ$ for these electrolytes are plotted in figure 34, as are the regression curves representing values of $-\bar{K}^\circ$ (table 12) computed from equation (43), values of N for H_2O at vapor-saturation pressures (table 4), and the coefficients for HNO_3 and KBr in table 11. It can be seen that both the additivity values of $-\bar{K}^\circ$ and the regression curves are in close agreement with the experimental data.

The curves and coefficients for HNO_3 and KBr in figure 34 and table 11 afford internally consistent values of $-\bar{K}^\circ$ for other electrolytes, which were generated from additivity relations using equation (43) and appropriate fit coefficients in table 11 to evaluate equations (88) and (89) for $\bar{K}^\circ_{NaNO_3}$, $\bar{K}^\circ_{KNO_3}$, and $\bar{K}^\circ_{NaBr}$. Similar calculations were carried out for KF, $MgSO_4$, K_2SO_4, and H_2SO_4 by taking account of

$$\bar{K}^\circ_{KF} = \bar{K}^\circ_{NaF} + \bar{K}^\circ_{KCl} - \bar{K}^\circ_{NaCl} \tag{90}$$

and

$$\begin{aligned} \bar{K}^\circ_{MgSO_4} &= \bar{K}^\circ_{Na_2SO_4} + \bar{K}^\circ_{MgCl_2} - 2\bar{K}^\circ_{NaCl} \\ &= \bar{K}^\circ_{K_2SO_4} + \bar{K}^\circ_{MgCl_2} - 2\bar{K}^\circ_{KCl} \\ &= \bar{K}^\circ_{H_2SO_4} + \bar{K}^\circ_{MgCl_2} - 2\bar{K}^\circ_{HCl} \end{aligned} \tag{91}$$

Additivity values of $\bar{K}^\circ_{MgSO_4}$ were accepted in preference to those reported in the literature because the latter values are inconsistent with the compressibilities reported for Na_2SO_4, $MgCl_2$, and NaCl. The extent of the discrepancies in the data can be deduced from figure 6.

Regression of the additivity values of $\bar{K}^\circ$ computed above (figs. 35 and 36) with equation (43) and appropriate values of N, ω, and θ taken from tables 4 and 8 resulted in the values of a_2 and a_4 in table 11 for $NaNO_3$, KNO_3, Mg_2SO_4, NaBr, KF, H_2SO_4, and K_2SO_4, and the corresponding regression curves in figures 35 and 36. This procedure precluded introducing errors in a_2 and a_4 by calculating these coefficients directly (see above) from additivity relations analogous to equation (76). It can be seen in figures 35 and 36 that both the additivity values of $\bar{K}^\circ$ and the regression curves are in close agreement with the experimental data for $NaNO_3$ and NaBr but not $MgSO_4$ at temperatures $\leq 10°$ and $\geq 30°$C. Agreement in the latter case is precluded by inconsistencies in the experimental data for Na_2SO_4 and $MgSO_4$ discussed in previous pages.

The close correspondence of the curves in figures 32 through 36 with the experimental and/or additivity values of $-\bar{K}^\circ$ further confirms the validity of the theoretical values of ω and the pressure independence of

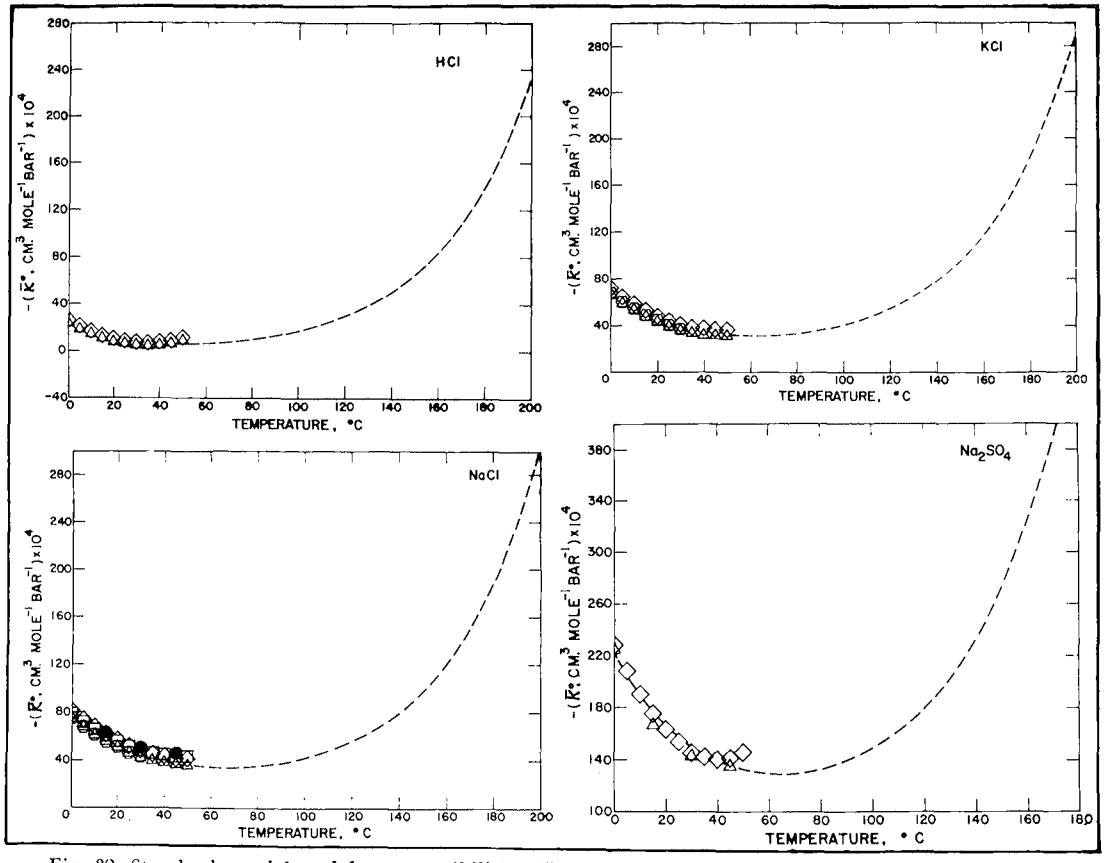

Fig. 32. Standard partial molal compressibilities ($\bar{K}^\circ$) of aqueous electrolytes (table 12) as a function of temperature at 1 bar (for temperatures < 100°C) and pressures corresponding to the vapor-saturation curve for H_2O (at temperatures > 100°C) computed from equation (43), coefficients in table 11, and values of N in table 4 (curves). The symbols represent values of $-\bar{K}^\circ$ reported by Millero (1973; written commun., 1973).

θ. It can be seen in these figures that regression of the low-temperature data with equation (43) predicts a minimum in $-\bar{\kappa}°$ as a function of temperature between ~40° and 80°C. Although calculations of $-\bar{\kappa}°$ at higher temperatures with the regression equation are tenuous owing to the relatively short temperature range for which experimental values of $\bar{\kappa}°$ are available (0° to 55°C), the close agreement between the regression curves and the data together with the similarity in the configurations of the curves for all of the electrolytes suggest that equation (43) and the coefficients in table 11 can be used to obtain close approximations of $\bar{\kappa}°$ at high temperatures. This conclusion is substantiated by theoretical considerations and additional calculations summarized below.

At 0°C and 20 bars, $\bar{\kappa}°$ for aqueous electrolytes is of the order of -10^3 to -2.5×10^{-2} cm^3 mole^{-1} bar^{-1}, depending on the electrolyte. As temperature increases from 0°C to the temperature corresponding to the maximum value of $\bar{\kappa}°$ (that is, the minimum value of $-\bar{\kappa}°$ in figs. 32 through 36), $\bar{\kappa}°$ increases by ~ 5×10^{-3} cm^3 mole^{-1} bar^{-1} for 1:1 electrolytes and ~ 1×10^{-2} cm^3 mole^{-1} bar^{-1} for 2:1 electrolytes. In certain cases (for example, HCl, KNO_3, $NaNO_3$), $\bar{\kappa}°$ approaches zero at the maximum and in one instance (HNO_3) becomes positive. With further increase

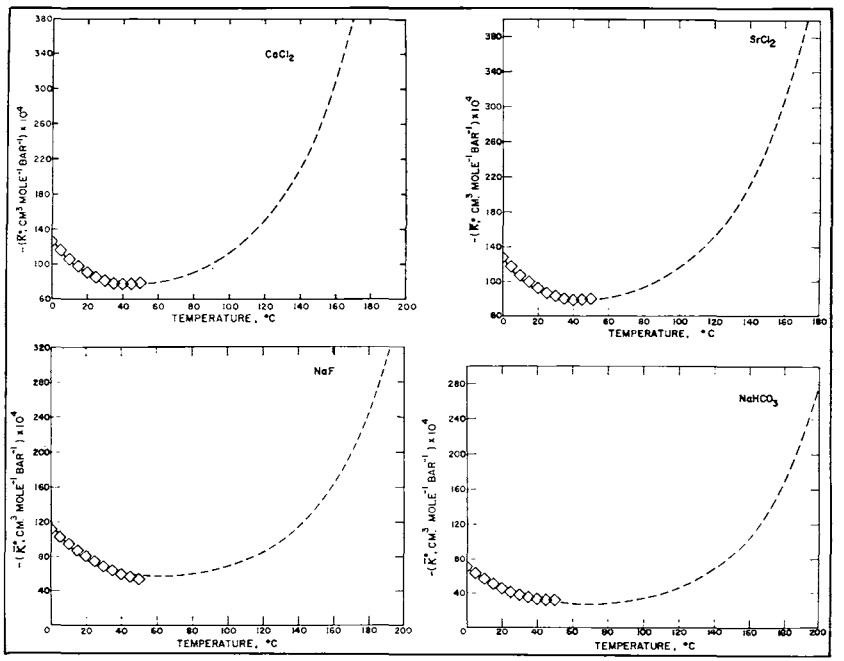

Fig. 33. Standard partial molal compressibilities ($\bar{\kappa}°$) of aqueous electrolytes (table 12) as a function of temperature at 1 bar (for temperatures < 100°C) and pressures corresponding to the vapor-saturation curve for H_2O (at temperatures > 100°C) computed from equation (43), coefficients in table 11, and values of N in table 4 (curves). The symbols represent values of $-\bar{\kappa}°$ reported by Millero (1973; written commun., 1973).

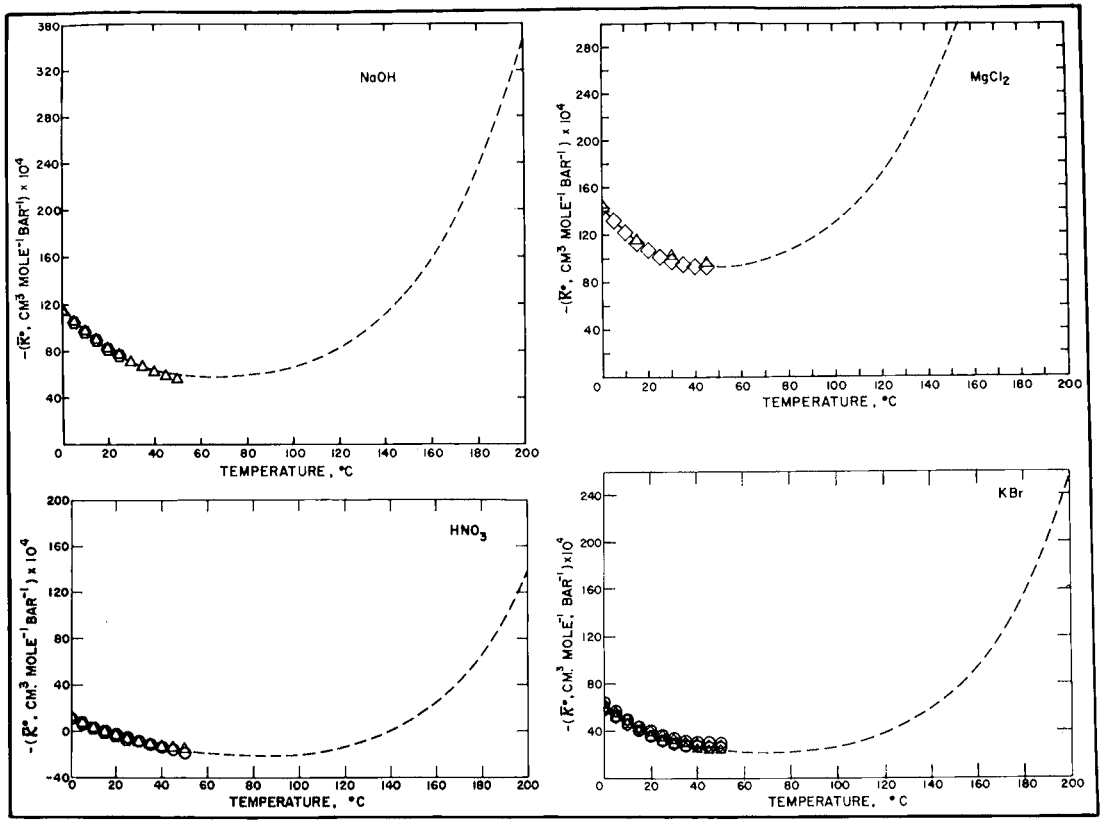

Fig. 34. Standard partial molal compressibilities ($\bar{K}^\circ$) of aqueous electrolytes (table 12) as a function of temperature at 1 bar (for temperatures < 100°C) and pressures corresponding to the vapor-saturation curve for H_2O (at temperatures > 100°C) computed from equation (43), coefficients in table 11, and values of N in table 4 (curves). Except for the open circles, the symbols represent values of $-\bar{K}^\circ$ reported by Millero (1973; written commun., 1973). The open circles designate additivity values of $-\bar{K}^\circ$ (see text).

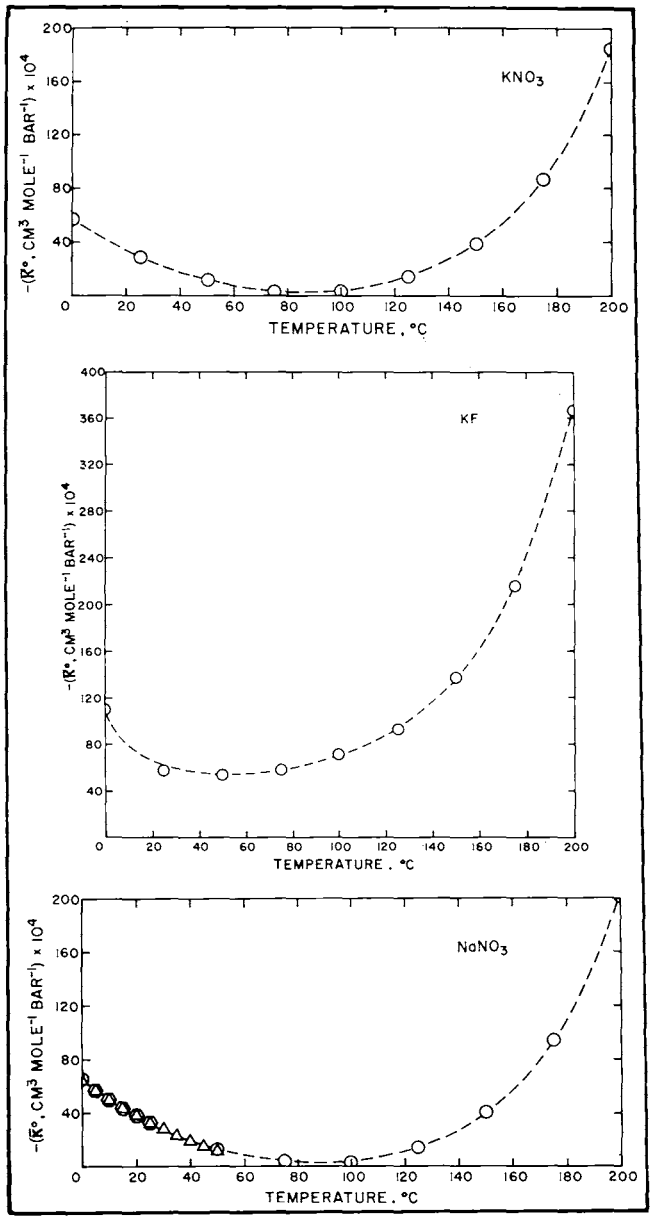

Fig. 35. Standard partial molal compressibilities ($\bar{K}^\circ$) of aqueous electrolytes (table 12) as a function of temperature at 1 bar (for temperatures < 100°C) and pressures corresponding to the vapor-saturation curve for H_2O (at temperatures > 100°C) computed from equation (43), coefficients in table 11, and values of N in table 4 (curves). Except for the open circles, the symbols represent values of $-\bar{K}^\circ$ reported by Millero (1973; written commun., 1973). The open circles designate additivity values of $-\bar{K}^\circ$ (see text).

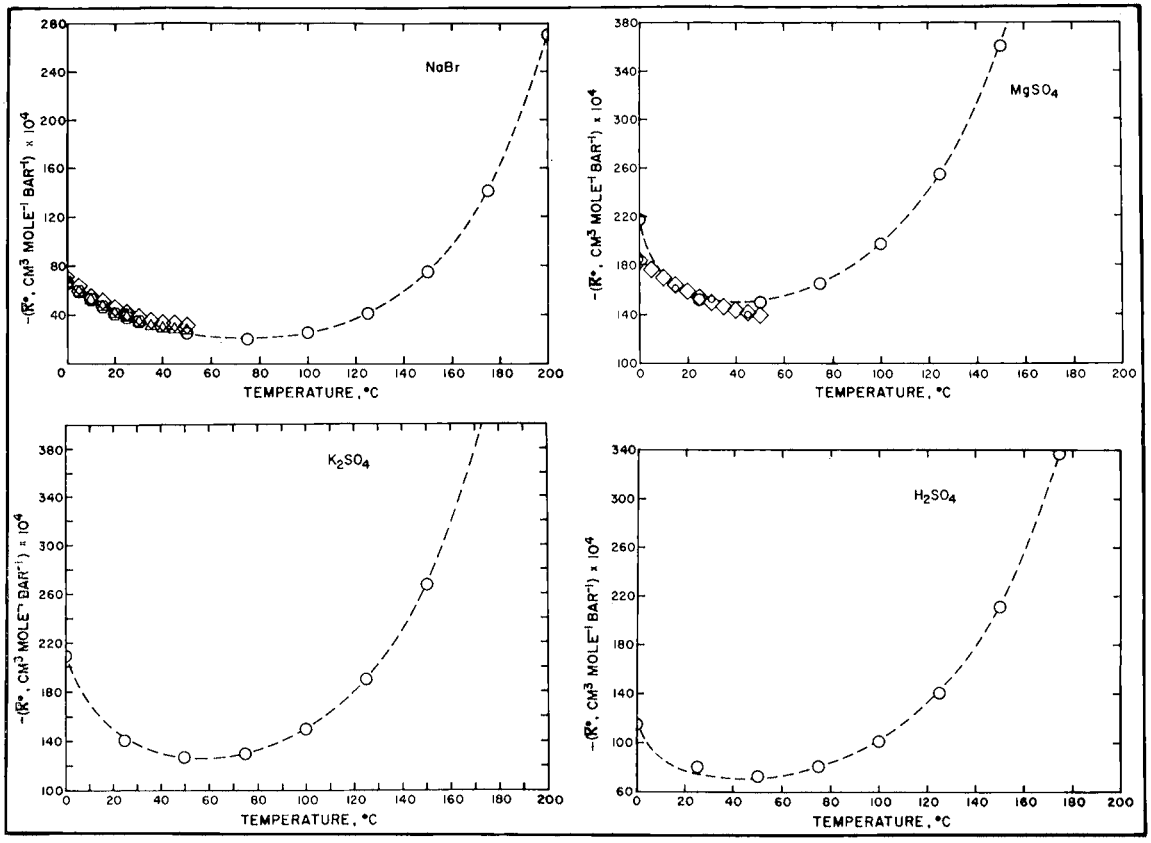

Fig. 36. Standard partial molal compressibilities ($\bar{\kappa}^\circ$) of aqueous electrolytes (table 12) as a function of temperature at 1 bar (for temperatures < 100°C) and pressures corresponding to the vapor-saturation curve for H_2O (at temperatures > 100°C) computed from equation (43), coefficients in table 11, and values of N in table 4 (curves). Except for the open circles, the symbols represent values of $-\bar{\kappa}^\circ$ reported by Millero (1973; written commun., 1973). The open circles designate additivity values of $-\bar{\kappa}^\circ$ (see text).

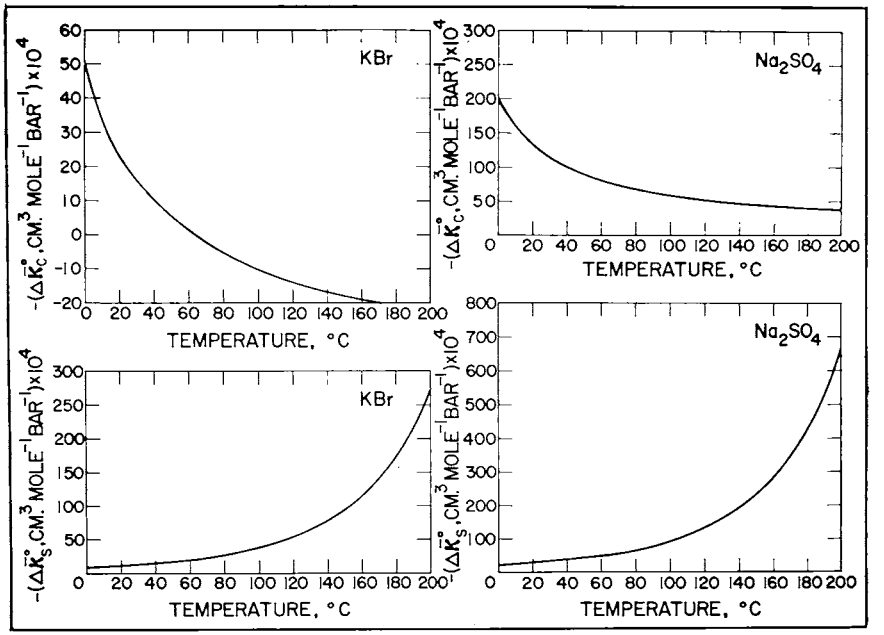

Fig. 37. $-\Delta\bar{K}^\circ_s$ and $-\Delta\bar{K}^\circ_c$ for KBr and Na_2SO_4 as a function of temperature at 20 bars computed from equations (24) and (37), coefficients in table 11, and values of N in table 4.

in temperature to 200°C, $\bar{K}^\circ$ decreases by several hundredths of a cm^3, $mole^{-1}$ bar^{-1} in the case of 1:1 electrolytes and of the order of 5×10^{-2} cm^3 $mole^{-1}$ bar^{-1} or more for 2:1 and 1:2 electrolytes. As expected, the dependence of $\bar{K}^\circ$ on temperature for the 1:2 and 2:1 electrolytes is more dramatic than that of the 1:1 electrolytes.

The maximum in $\bar{K}^\circ$ as an isobaric function of temperature at low pressures arises from the opposing contributions of $\Delta\bar{K}^\circ_c$, which increases asymptotically with increasing temperature, and $\Delta\bar{K}^\circ_s$, which decreases to an increasing degree with increasing temperature (fig. 37). At high temperatures, $\Delta\bar{K}^\circ_s$ dominates the behavior of $\bar{K}^\circ$, resulting in large positive values of $(\partial\bar{V}^\circ/\partial P)_T$. For a given electrolyte at constant pressure, $\bar{K}^\circ$ is only a quasilinear function of $\bar{V}^\circ$ (fig. 38), but it follows from equations (12), (35), and (38) that $\Delta\bar{K}^\circ_c$ is a linear function of either $\Delta\bar{V}^\circ_c$ or $\Delta\bar{V}^\circ_n$ with changing temperature at constant pressure. Four examples of this relation are shown in figure 39.

Summary of equation of state coefficients.—Pressure/temperature-independent coefficients for equations (39) and (41) through (43) are given in table 11 for 19 electrolytes. The values of a_1 and a_3 in the table were computed by combining a_2 and a_4 for each electrolyte with corresponding values of σ and ξ for 20 bars (table 8) and equations (28) and (29). The coefficients in table 11 permit predictions of the thermodynamic behavior

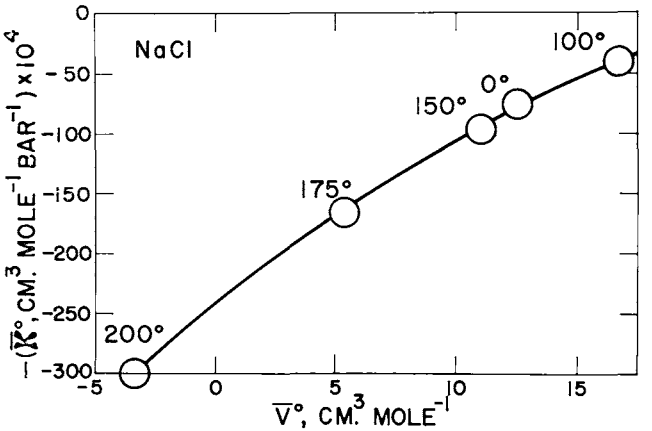

Fig. 38. Correlation of $-\bar{K}°$ with $\bar{V}°$ for NaCl as a function of temperature at 20 bars computed from equations (39) and (41), coefficients in table 11, and values of Q and N in table 4.

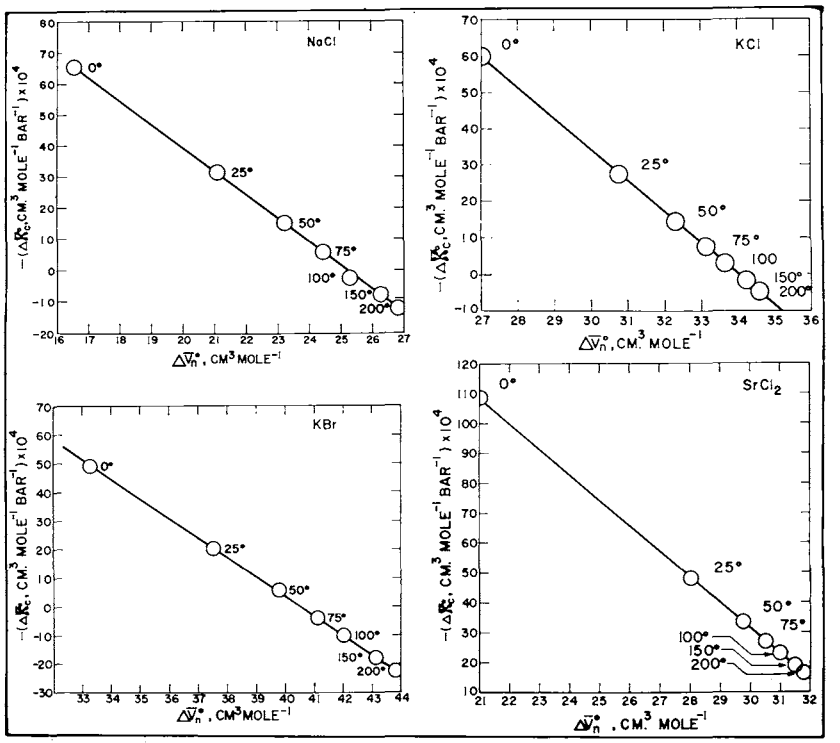

Fig. 39. Correlation of $-\Delta\bar{K}°_c$ with $\Delta\bar{V}°_n$ (eq 38) for NaCl, KCl, KBr, and $SrCl_2$ as a function of temperature at 20 bars computed from equations (30) and (37) and coefficients in table 11.

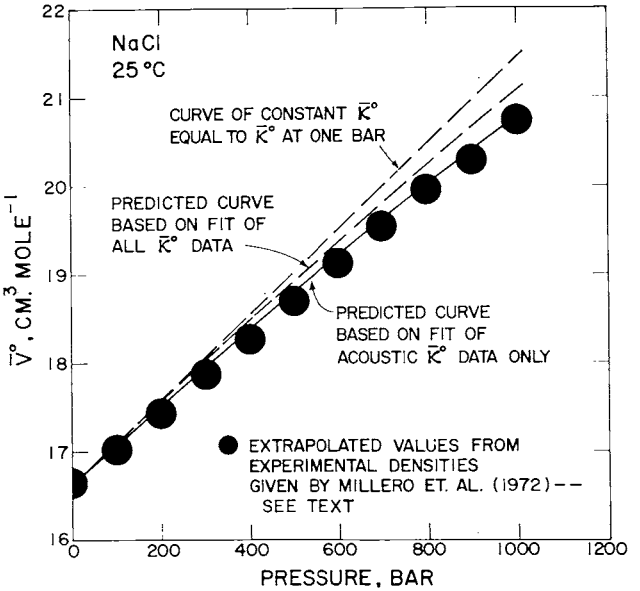

Fig. 40. Standard partial molal volume ($\bar{V}^\circ$) of NaCl as a function of pressure (table 13) at 25°C computed from equation (39), coefficients in table 11, and values of Q in table 13.

of aqueous electrolytes in the standard state at high pressures and temperatures.

COMPARISON OF HIGH PRESSURE/TEMPERATURE DATA WITH PREDICTIONS FROM THE EQUATION OF STATE

The paucity of reliable high-precision measurements of the densities of aqueous electrolyte solutions at high pressures and temperatures precludes comprehensive comparison of experimental values of $\bar{V}^\circ$ with those computed from the coefficients in table 11 to check the high pressure/temperature validity of the equation of state derived in the preceding pages. Owing to ambiguities, inaccuracies, insufficient precision, and/or uncontrolled extrapolation of apparent molal volumes to infinite dilution (that is, without provision for ion association or constraints imposed by the Debye-Hückel limiting law), the densities and apparent and partial molal volumes of KOH, NaCl, NaOH, K_2SO_4, LiCl, and KCl at high temperatures and pressures reported by Tham, Gubbins, and Walker (1967), Copeland, Silverman, and Benson (1953), Dibrov, Mashovets, and Matveeva (1964), Ravich and Borovaya (1971), and Ostapenko and Samoilovich (1971) are not suitable for this purpose. Most solubility studies are equally inadequate owing to uncertainties introduced by ion association and activity coefficients at high pressures and temperatures. Nevertheless, two limited (but convincing) demonstrations of the high pressure/temperature validity of the equation of state can be made by

comparing predicted values of $\bar{V}^\circ$ with corresponding values computed from experimental data.

$\bar{V}^\circ_{NaCl}$ as a function of pressure at 25°C.—Standard partial molal volumes of NaCl at 25°C and pressures from 1 to 1000 bars are shown in figure 40. The values of $\bar{V}^\circ$ represented by the symbols were calculated from the molal analog of the Redlich-Meyer equation (eq 53) using the Debye-Hückel limiting law coefficients given in table 13 and apparent molal volumes of NaCl computed from equation (45) and the high-precision density measurements reported by Millero, Knox, and Emmet (1972) for 0.7546 *m* and 1.0085 *m* NaCl solutions. Because only two concentrations are represented by the density measurements, the reliability of the values of b'_V employed in extrapolating the apparent molal volumes to infinite dilution is highly uncertain. It can be seen in figure 41 that the b'_V values computed from the data obtained by Millero, Knox,

TABLE 13

Debye-Hückel limiting law coefficient for the relative partial molal volumes of aqueous electrolytes (A_V), the b'_V parameter for NaCl in the molal analog of the Redlich-Meyer equation (eq 53), the Born function (Q) for equation (39), and experimental and predicted values of the standard partial molal volume ($\bar{V}^\circ$) of NaCl at 25°C and pressures from 1 to 1000 bars

Pressure[ℓ]	A_V [a,f]	$\hat{b}_{V,NaCl}$ [g]	Q [c,h] × 10^7	Exp. $\bar{V}^\circ_{NaCl}$ [d,k]	Calc. $\bar{V}^\circ_{NaCl}$ [e,k]
1	2.748	0.24[b]	5.952	16.60[m]	16.61[m]
100	2.652	0.25[b]	5.743	17.01	17.08
200	2.569	0.24[b]	5.559	17.43	17.53
300	2.494	0.22[b]	5.397	17.86	17.97
400	2.427	0.16[b]	5.251	18.26	18.40
500	2.367	0.09[b]	5.119	18.69	18.81
600	2.312	0.00[b]	4.999	19.13	19.21
700	2.261	-0.10[b]	4.889	19.53	19.61
800	2.214	-0.22[b]	4.788	19.95	20.00
900	2.170	-0.36[b]	4.692	20.28	20.39
1000	2.128	-0.54[b]	4.603	20.75	20.77

[a]Helgeson and Kirkham (1974b). [b]Smoothed values corresponding to the curve in figure 41. [c]Helgeson and Kirkham (1974a) [d]Generated by extrapolation (eq 53) of apparent molal volumes of NaCl computed (eq 45) from density data reported by Millero, Knox and Emmet (1972). [d]Computed from the equation of state (eq 39), coefficients in table 12, and the values of Q shown above. [f]$cm^3\ kg^{1/2}\ mole^{-3/2}$. [g]$cm^3\ kg\ mole^{-2}$. [h]$bar^{-1}$. [k]$cm^3\ mole^{-1}$. [ℓ]bar. [m]Experimental values of $\bar{V}^\circ_{NaCl}$ at 25°C and one bar compiled by Millero (1972b) range from 15.9 to 17.03 $cm^3\ mole^{-1}$, but the most substantiated value is 16.61 $cm^3\ mole^{-1}$.

and Emmet at low pressures are not consistent with other reported values at 1 bar. Nevertheless, owing to the relatively small magnitude of b'_V for NaCl at low pressures and temperatures, errors in $\bar{V}°$ arising from the uncertainties in b'_V implied by the scatter of low-pressure data points in figure 41 are slight. Discrepancies between the b'_V values computed above and those reported by Millero (1970) and Dunn (1968) for 25°C and 1 bar suggest the possibility of a systematic error in Millero, Knox, and Emmet's data or, alternatively, imply the existence of a pronounced low-pressure extremum in b'_V as an isothermal function of pressure. To minimize the consequence of the scatter in the computed values of b'_V on the extrapolation of ϕ_V and preserve the internal consistency of Millero, Knox, and Emmet's data, the values of b'_V defined by the smooth curve in figure 41 were used to calculate $\bar{V}°$ from the apparent molal volumes. These values of b'_V and the extrapolated values of $\bar{V}°$ are listed in table 13. Note that b'_V decreases to an increasing degree as pressure increases above $\sim$ 200 bars.

The solid curve in figure 41 was computed from the equation of state derived above (eq 39) together with the values of Q listed in table 13 and the fit coefficients for NaCl obtained from isobaric regression of $\bar{\kappa}°$ and $\bar{V}°$ data at low pressures and temperatures (table 11). It can be seen that the curve predicted by the equation of state represents almost exactly (within 0.14 cm^3 $mole^{-1}$ or less) the values of $\bar{V}°$ computed *independently* from the density measurements at 100 to 1000 bars. The predicted and experimental values can be compared numerically by inspection of table 13.

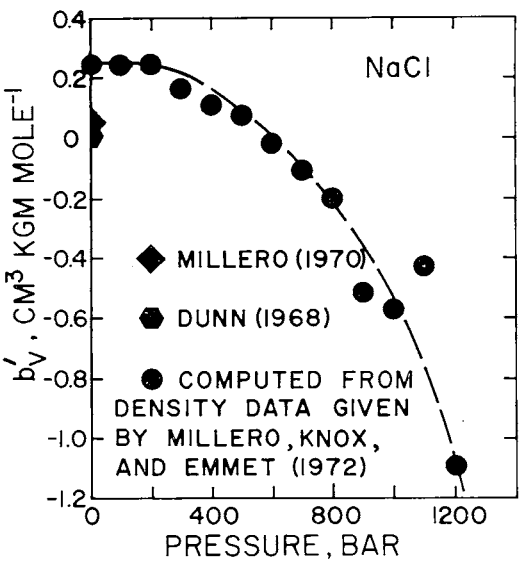

Fig. 41. Molal b'_V coefficient for NaCl (eq 53) as a function of pressure at 25°C derived from extrapolation plots of apparent molal volumes consistent with equation (53) using data reported by Millero, Knox, and Emmet (1972).

The upper dashed curve in figure 41 affords comparison of the consequences of assuming $\bar{\kappa}°$ to be independent of pressure (as advocated by Lown, Thirsk, and Lord Wynne-Jones, 1970) with the actual behavior of $\bar{V}°$ as an isothermal function of pressure. This assumption leads to considerable error at high pressures, especially (see below) at high temperatures. A smaller error may result if the equation of state is used with regression coefficients obtained from isobaric fits of $\bar{\kappa}°$ values at a series of temperatures which were derived by extrapolation to infinite dilution without regard for Debye-Hückel constraints. It can be seen in figure 41 that the curve generated by the equation of state and values of a_2 and a_4 obtained by regression of all the data points shown for NaCl in figure 32 differs significantly from that computed with regression coefficients derived solely from the more accurate acoustic values of $\bar{\kappa}°$. Nevertheless, this procedure affords a closer approximation of the experimental data than the curve computed assuming $\bar{\kappa}°$ to be independent of pressure.

Conductance data at high pressures and temperatures.—Dissociation constants for H_2O at high pressures and temperatures also afford an independent check of the general validity of the equation of state derived above. The standard partial molal volume of dissociation ($\Delta\bar{V}°$) for an unrestricted standard state with respect to both temperature and pressure is given by

$$\Delta\bar{V}° = -2.303\ RT\left(\frac{\partial \log K}{\partial P}\right)_T \tag{92}$$

where K is the dissociation constant for

$$H_2O \rightleftharpoons H^+ + OH^- \tag{93}$$

Equation (92) can be evaluated for the dissociation of H_2O at high pressures and temperatures by approximating the partial derivative on the right side of the expression with finite difference derivatives ($(\Delta \log K/\Delta P)_T$) computed from the values of log K reported by Quist (1970) and (in the case of the vapor saturation pressure for H_2O at 300°C) Fisher and Barnes (1972). The log K values employed in the calculations are plotted in figure 2. Having computed $\Delta\bar{V}°$, the sum of the standard partial molal volumes of H^+ and OH^- can be calculated from

$$\bar{V}°_{H^+} + \bar{V}°_{OH^-} = \Delta\bar{V}° + \bar{V}°_{H_2O} \tag{94}$$

where $\bar{V}°_{H_2O}$ represents the standard partial molal volume of H_2O at the temperature and pressure of interest. Values of $\bar{V}°_{H^+} + \bar{V}°_{OH^-}$ computed in this way using densities of H_2O taken from Helgeson and Kirkham (1974a) are plotted as symbols in figure 42. The curves in figure 42 were computed *independently* from the equation of state and the additivity relation

$$\bar{V}°_{H^+} + \bar{V}°_{OH^-} = \bar{V}°_{NaOH} + \bar{V}°_{HCl} - \bar{V}°_{NaCl} \tag{95}$$

using computed values of Q (Helgeson and Kirkham, 1974a) and the coefficients for NaOH, HCl, and NaCl in table 11.

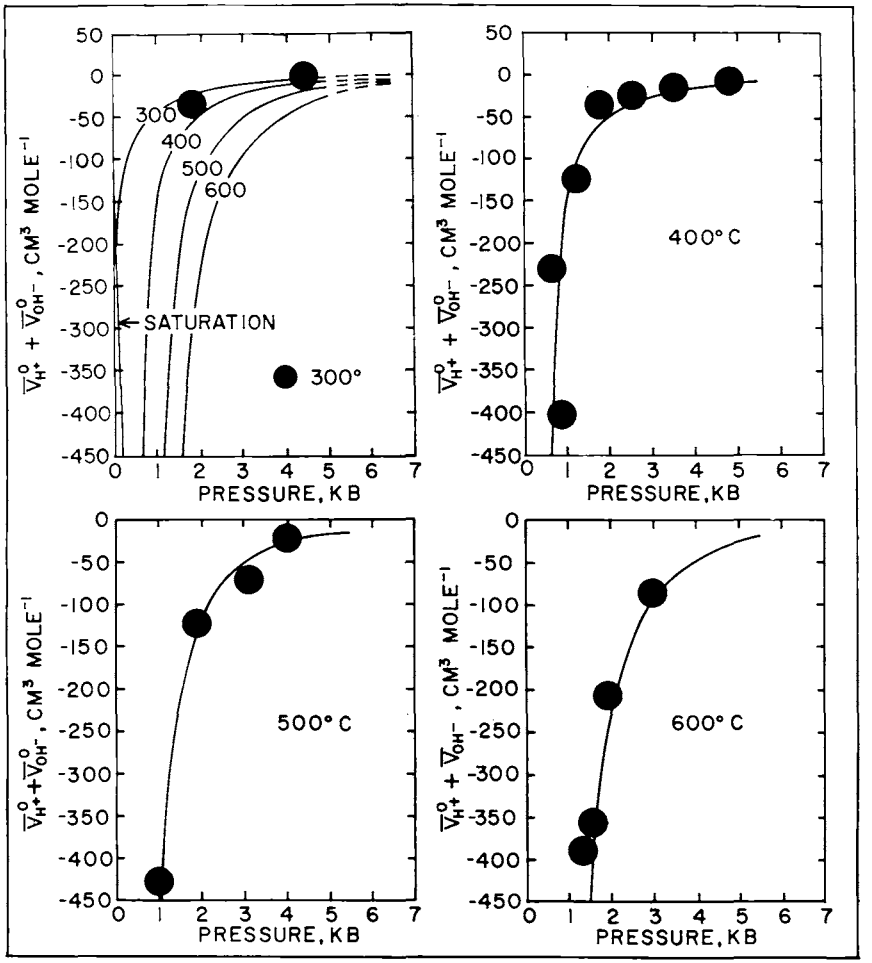

Fig. 42. Sum of the standard partial molal volumes of H^+ and OH^- as a function of pressure at constant temperature (labeled in kb). The curves were computed from equations (39) and (95), coefficients in table 11, and values of Q given by Helgeson and Kirkham (1974a). The symbols represent values computed from equations (93) and (94), densities of H_2O (Helgeson and Kirkham, 1974a) and finite difference partial derivatives of the values of log K_{NaCl} reported by Quist (1970) and Fisher and Barnes (1972) with respect to pressure at constant temperature ($(\Delta \log K/\Delta P)_T$).

It can be seen in figure 42 that the curves predicted from the equation of state are in striking agreement with the values derived from the conductance data at all pressures and temperatures to 5 kb and 600°C. The agreement is particularly impressive in view of the uncertainty in the log K values reported by Quist (1970) and the fact that the curves were generated from separate statements of the equation of state for three electrolytes in which all the coefficients other than ω (which was computed independently) were derived solely from regression of isobaric data at temperatures and pressures at or below 200°C and 20 bars. Quist (1970) reports the uncertainty in the experimental values of log K to be 0.3 to 0.5 log units, which is magnified considerably in values of $\Delta\bar{V}°$ derived from finite difference derivatives of the log K values. With the exception of a few obviously spurious values (which are not shown in fig. 42), the agreement between the curves in figure 42 and the values of $\Delta\bar{V}°$ computed from Quist's data suggest that his log K values are more accurate than the reported uncertainties imply.

The agreement of the curves and symbols in figure 42 is not in itself unique. Similar agreement may be obtained in part by using alternate approaches such as that advocated by Marshall (1968, 1969, 1970, 1972), which leads to equation (7). However, as emphasized above, equation (7) is empirical, inconsistent with electrostatic theory, and almost certainly a fortuitous consequence of the dependence of ε_{H_2O} on $\overline{\rho}°_{H_2O}$. In contrast, the equation of state derived in the preceding pages is general and based on a theoretical model which takes explicit account of the intrinsic properties of aqueous species as well as electrostriction collapse of the solvent structure and solvation of the ions in solution. Where the equation of state affords independent predictions of $\bar{V}°$, equation (7) requires experimental data at the temperatures of interest to establish appropriate values of k.

STANDARD PARTIAL MOLAL VOLUMES, EXPANSIBILITIES, AND COMPRESSIBILITIES OF ELECROLYTES AT HIGH PRESSURES AND TEMPERATURES

The relations portrayed in figures 40 and 42 leave little doubt that the equation of state derived above affords reliable prediction of the pressure dependence of the standard partial molal heat capacities, entropies, enthalpies, and Gibbs free energies of aqueous electrolytes at high pressures and temperatures. Standard partial molal volumes of NaCl and $SrCl_2$ computed from the equation of state, values of Q (Helgeson and Kirkham, 1974a), and appropriate coefficients in table 11 are depicted in figure 43 as functions of pressure and temperature from 1 to 5000 bars and 0° to 600°C. The configurations of the curves in figure 43 are typical of those for the other 17 electrolytes listed in table 11.

It can be seen in figure 43 that the extrema in the isobars for low pressures and the curves for H_2O vapor saturation pressures dampen with increasing pressure and disappear between 1 and 2 kb. At higher pressures, $\bar{V}°$ is a sigmoid function of temperature at constant pressure. As temperature increases from 25° to 600°C at 5 kb, $\bar{V}°_{NaCl}$ decreases by $\sim$ 50

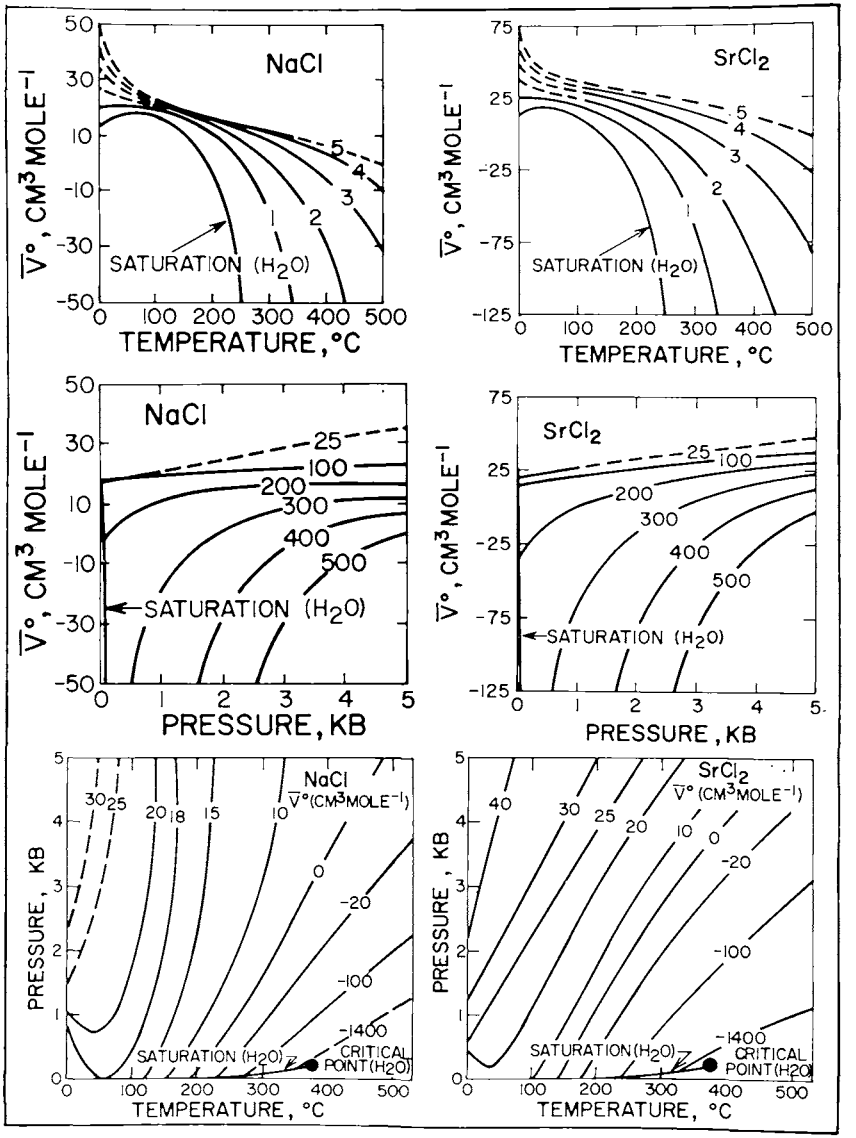

Fig. 43. Standard partial molal volumes ($\bar{V}°$) of NaCl and $SrCl_2$ as a function of temperature (in °C) and pressure (in kb) computed from equation (39), coefficients in table 11, and values of Q given by Helgeson and Kirkham (1974a).

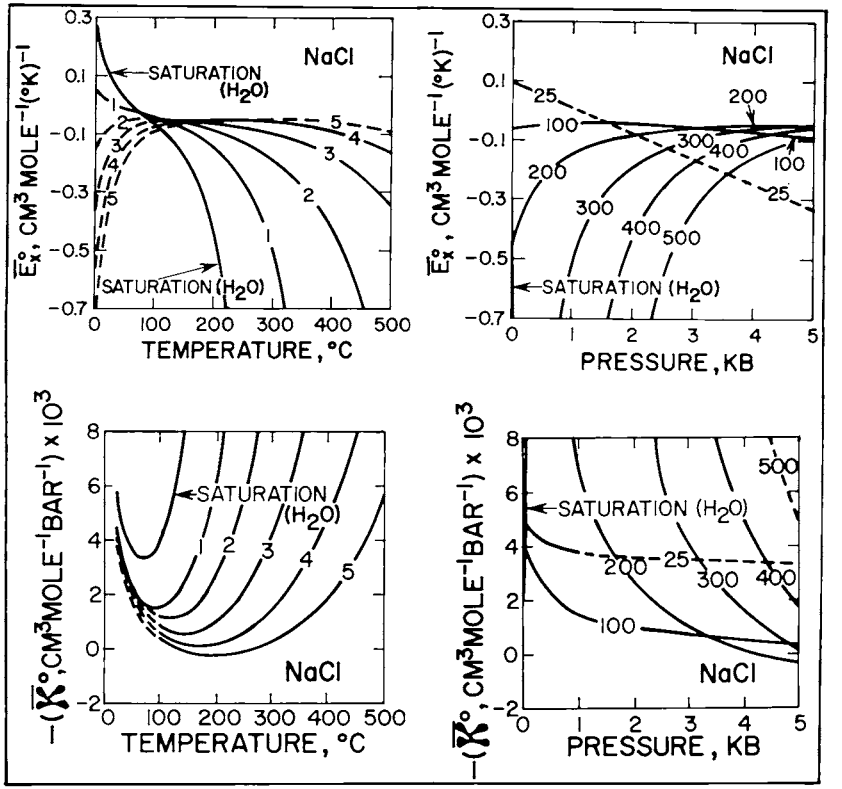

Fig. 44. Standard partial molal expansibility ($\bar{E}^\circ_x$) and compressibility ($\bar{\kappa}^\circ$) of NaCl as functions of temperature (in °C) and pressure (in kb) computed from equations (41) and (43), coefficients in table 11, and values of U and N given by Helgeson and Kirkham (1974a).

cm^3 $mole^{-1}$. In contrast, as temperature increases along the saturation curve for H_2O from $\sim$ 50°C to the critical temperature, $\bar{V}^\circ_{NaCl}$ decreases by orders of magnitude and approaches $-\infty$ at the critical point. The extrema in the low pressure isobars are manifested by minima in the low pressure-temperature isochores in figure 43. As pressure increases isothermally at successively lower temperatures, $\bar{V}^\circ_{NaCl}$ and $\bar{V}^\circ_{SrCl_2}$ increase to a decreasing degree.

Standard partial molal expansibilities and compressibilities of NaCl and $SrCl_2$ as functions of temperature and pressure are shown in figures 44 and 45. The curves are consistent with those in figure 43; that is, they were computed from equations (41) and (43) using coefficients in table 11 and values of U and N reported by Helgeson and Kirkham (1974a). It can be seen in figures 44 and 45 that $\bar{E}^\circ_{x,NaCl}$ and $\bar{E}^\circ_{x,SrCl_2}$ are sigmoid functions of temperature only at pressures $\leq$ 1300 and 1700 bars, respectively. Because $\bar{V}^\circ_{NaCl}$ and $\bar{V}^\circ_{SrCl_2}$ exhibit a sigmoid isobaric temperature configuration at higher pressures (fig. 43), the corresponding isobars

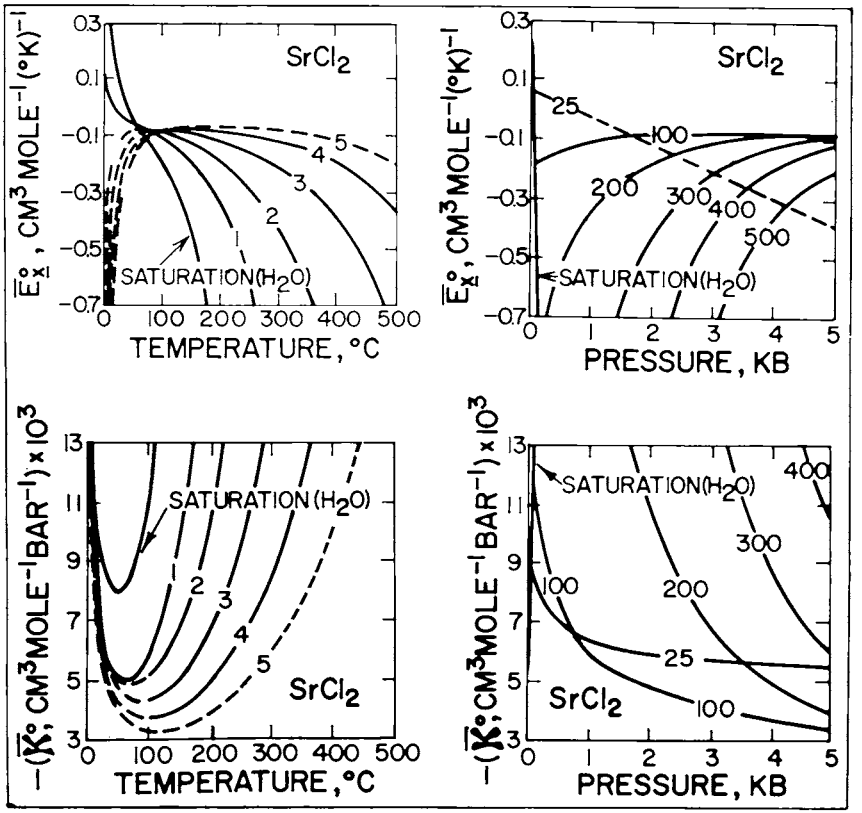

Fig. 45. Standard partial molal expansibility ($\bar{E}^\circ_x$) and compressibility ($\bar{\kappa}^\circ$) of $SrCl_2$ as functions of temperature (in °C) and pressure (in kb) computed from equations (41) and (43), coefficients in table 11, and values of U and N given by Helgeson and Kirkham (1974a).

for $\bar{E}^\circ_{x,NaCl}$ and $\bar{E}^\circ_{x,SrCl_2}$ in figures 44 and 45 pass through extrema with increasing temperature. At low temperatures where H_2O is a highly structured liquid and $\Delta\bar{E}^\circ_{x,c}$ contributes substantially to the standard partial molal expansibility of an electrolyte, $\bar{E}^\circ_x$ decreases almost linearly with increasing pressure at constant temperature. In contrast, the 100°C isotherms in figures 44 and 45 exhibit gentle extrema, and at still higher temperatures $\bar{E}^\circ_x$ increases monotonically with increasing pressure (to 5 kb) at constant temperature. Along the vapor saturation curve for H_2O, $\bar{E}^\circ_x$ decreases exponentially and approaches $-\infty$ at the critical point, where $(\partial\bar{V}^\circ_{H_2O}/\partial P)_T$, $-(\partial\bar{V}^\circ_{H_2O}/\partial T)_P$, $-\bar{C}^\circ_{P,H_2O}$, $(\partial \ln \varepsilon_{H_2O}/\partial T)_P$, $-(\partial \ln \varepsilon_{H_2O}/\partial P)_T$, and their isobaric and isothermal partial derivatives with respect to temperature and pressure also approach $-\infty$.

The standard partial molal compressibilities of electrolytes ($\bar{\kappa}^\circ$) decrease dramatically as temperature increases isobarically or pressure decreases isothermally at high temperatures. It can be seen in figures 44 and

45 that the minima in the isobars become progressively broader as pressure increases, which causes $(\partial\bar{V}^\circ/\partial P)_T$ for NaCl to become negative between ~100° and 330°C at 5 kb. At the critical point, $\bar{\kappa}^\circ = -\infty$.

The complicated surfaces delineated by the isobars, isotherms, and isochores in figures 43 through 45 are a consequence of changes in the competing effects of solvent collapse and ion solvation on the electrostriction volume loss with increasing temperature and/or pressure. The relative extent of these changes and their consequences with respect to the thermodynamic behavior of aqueous electrolytes in the standard state can be assessed with the aid of the coefficients in table 11 and equations (18), (20), (21), (24), (30), (33), (34), and (37).

Contributions of solvent collapse and ion solvation.—The relative contribution of $\Delta\bar{V}^\circ_s$ and $\Delta\bar{V}^\circ_n$ to the standard partial molal volume of NaCl is depicted in figure 46 in terms of the absolute percent (p_n) of $\bar{V}^\circ$ attributable to $\Delta\bar{V}^\circ_n$; that is,

$$p_n = \frac{100\Delta\bar{V}^\circ_n}{\Delta\bar{V}^\circ_n + |\Delta\bar{V}^\circ_s|} \tag{95}$$

It can be seen in these figures that $\Delta\bar{V}^\circ_n$ accounts for > 80 percent of $\bar{V}^\circ$ at low temperatures but only a few percent at high temperatures and low pressures where the dielectric constant of H_2O is small. As pressure increases and/or temperature decreases, the contribution of $\Delta\bar{V}^\circ_n$ to $\bar{V}^\circ$ becomes increasingly more important. The percentages and configurations of the curves shown in figure 46 are typical of electrolytes in general. Comparison of the behavior of $\Delta\bar{V}^\circ_n$ for electrolytes with the same cation or anion suggests that both species contribute significantly to the collapse of the solvent structure. Despite repeated suggestions to the contrary in the chemical literature, the present analysis also suggests that both cations and anions solvate to a significant degree.

The behavior of $\Delta\bar{V}^\circ_s$ and $\Delta\bar{V}^\circ_n$ with increasing pressure and/or temperature is depicted for NaCl and $SrCl_2$ in figures 47 and 48. It can be seen that $\Delta\bar{V}^\circ_s$ is small and negative at low temperatures, but that it

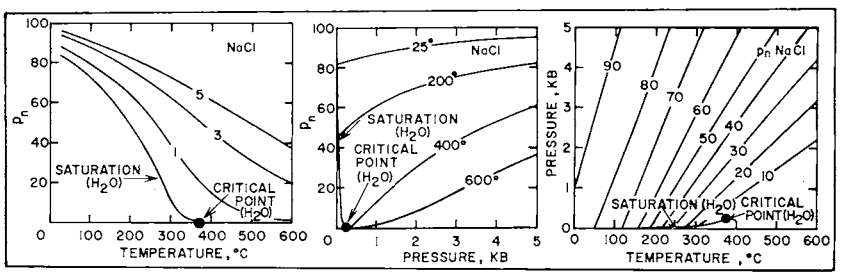

Fig. 46. Absolute percentage (p_n) of $\bar{V}^\circ_{NaCl}$ attributable to $\Delta\bar{V}^\circ_n$ as a function of temperature (in °C) and pressure (in kb) computed from equations (18), (30), (39), and (95), coefficients in table 11, and values of Q given by Helgeson and Kirkham (1974a).

becomes increasingly more negative as the dielectric constant of H_2O decreases with increasing temperature at constant pressure or decreasing pressure at constant temperature. Note in figures 49 and 50 that $\Delta\bar{E}^\circ_{x,s}$ and $\Delta\bar{\kappa}^\circ_s$ exhibit the same behavior. In contrast to the contribution of ion solvation to $\bar{V}^\circ$, $\Delta\bar{V}^\circ_n$ is positive and becomes more positive as pressure increases at constant temperature, but in the case of NaCl, only at temperatures $\leq$ 100°C. At higher temperatures, $\Delta\bar{\kappa}^\circ_{c,\mathrm{NaCl}}$ is negative (fig. 50), and $\Delta\bar{V}^\circ_{n,\mathrm{NaCl}}$ decreases with increasing pressure at constant temperature (fig. 47).

The configuration of the asymptotic surface corresponding to $\Delta\bar{V}^\circ_{n,\mathrm{NaCl}}$ as a function of pressure and temperature in figure 47 arises from the changing contribution of electrostriction collapse to $\Delta\bar{V}^\circ_n$ with increasing pressure and/or temperature. As pressure increases at low temperature and the relatively open tetrahedral solvent structure is compressed, the absolute volume change attending solvent collapse decreases; that is, $\Delta\bar{V}^\circ_c$ becomes less negative and $\Delta\bar{V}^\circ_n$ increases, as does the relative contribution of the intrinsic volume of the electrolyte ($\bar{V}^\circ_i$) to $\Delta\bar{V}^\circ_n$. Conversely, as temperature increases at high pressures, the expansion of the solvent structure results in a more negative $\Delta\bar{V}_c$, which causes $\Delta\bar{V}^\circ_n$ to decrease. However, as pressure decreases, the tendency for $\Delta\bar{V}^\circ_c$ to become more negative with increasing temperature is opposed to an increasing degree by the thermal disruption of the solvent structure, which accompanies increasing temperature at low pressures. As the distribution of the solvent molecules becomes more disorganized, the effectiveness of the electrolyte in collapsing the solvent structure diminishes, causing $\Delta\bar{V}^\circ_c$ to become less negative with increasing temperature at low pressures. As a consequence, $\Delta\bar{V}^\circ_{n,\mathrm{NaCl}}$ increases asymptotically with increasing temperature and approaches $\bar{V}^\circ_i$. At ~1300 bars, the opposing consequences of thermal expansion and structural disruption of the solvent on $\Delta\bar{V}^\circ_{c,\mathrm{NaCl}}$ are balanced, and $\Delta\bar{V}^\circ_n$ exhibits no temperature dependence.

At high temperatures, the effect of increasing pressure on $\Delta\bar{V}^\circ_{c,\mathrm{NaCl}}$ is opposite to that at low temperatures. The increasing structural order of solvent molecules opposes the effects of solvent compression and causes $\Delta\bar{V}^\circ_{c,\mathrm{NaCl}}$ to become more negative. Accordingly, $\Delta\bar{V}^\circ_{n,\mathrm{NaCl}}$ decreases with increasing pressure at high temperatures. At ~100°C, these two effects are balanced, and $\Delta\bar{V}^\circ_n$ exhibits no pressure dependence.

It can be seen in figures 47 and 48 that the behavior of $\Delta\bar{V}^\circ_n$ as a function of pressure and temperature is not the same for all electrolytes. Although the curves for other electrolytes representing $\Delta\bar{V}^\circ_n$ as an isobaric function of temperature have configurations similar to those of the curves for NaCl in figure 47, in certain instances the curves do not cross each other, and the pressure at which $(\partial^2\Delta\bar{V}^\circ_n/\partial T^2)_P$ changes sign is different (as, for example, in the case of $SrCl_2$ in fig. 48). Whether or not $\Delta\bar{V}^\circ_n$ decreases with increasing pressure at high temperatures depends on the sign of the a_2 coefficient in the equation of state. If this parameter is negative (as is the case for nearly all the 1:1 electrolytes—see table 11), $\Delta\bar{\kappa}^\circ_c$ becomes positive at higher temperatures (as it does for NaCl in

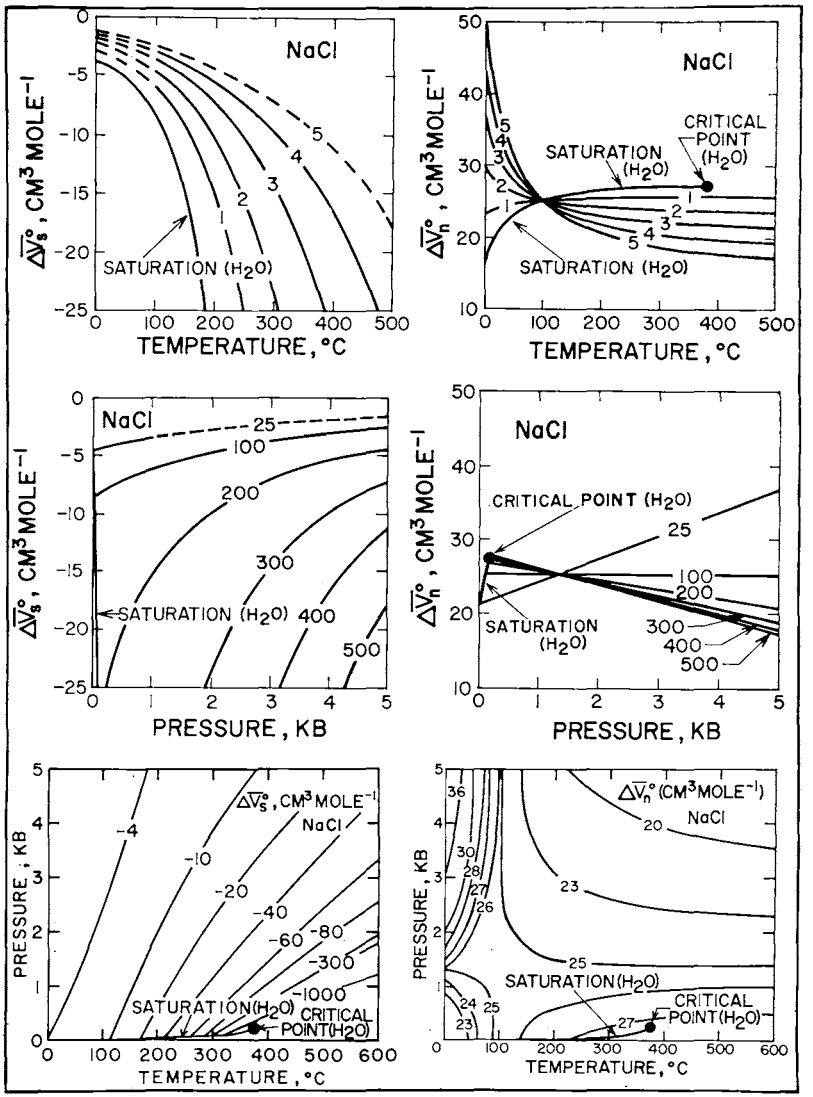

Fig. 47. $\Delta\bar{V}^\circ_s$ and $\Delta\bar{V}^\circ_n$ of NaCl as functions of temperature (in °C) and pressure (in kb) computed from equations (18) and (30), coefficients in table 11, and values of Q given by Helgeson and Kirkham (1974a).

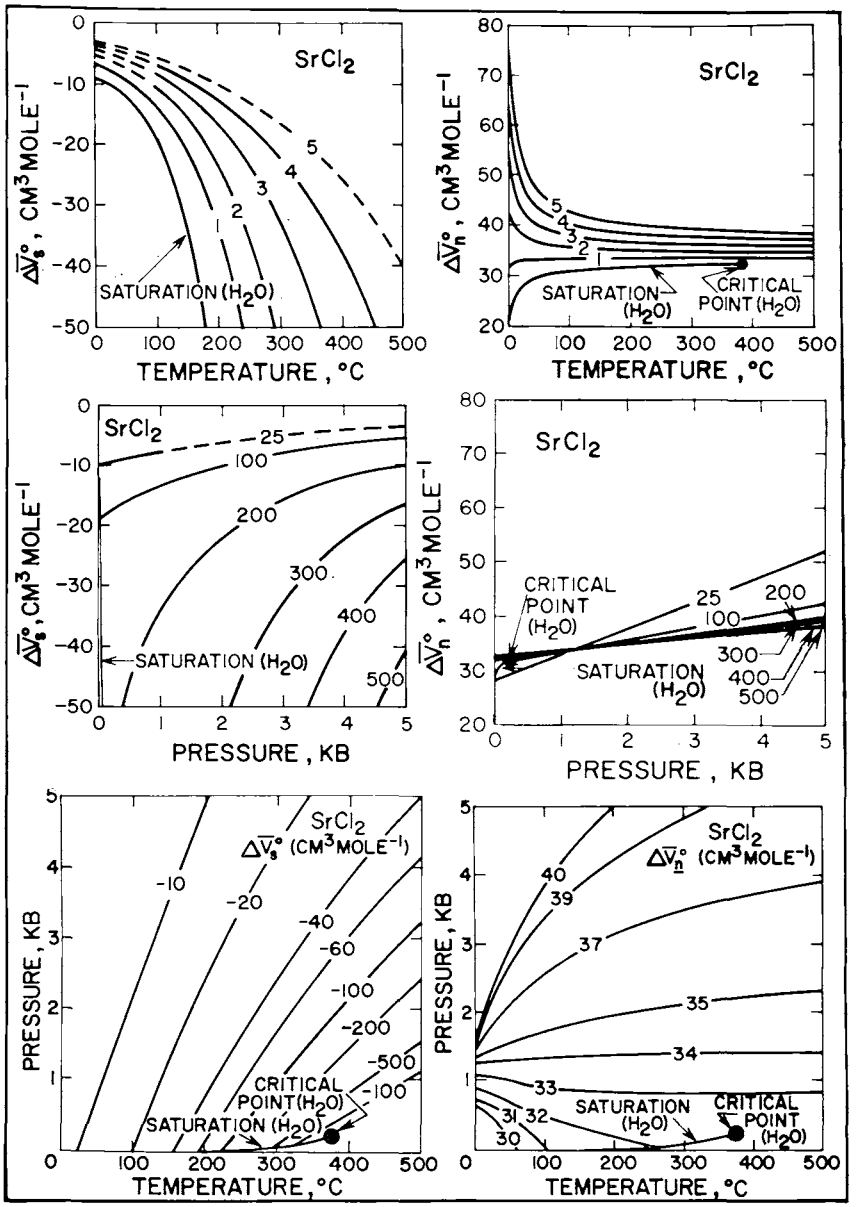

Fig. 48. $\Delta\bar{V}^\circ_s$ and $\Delta\bar{V}^\circ_n$ of $SrCl_2$ as functions of temperature in (°C) and pressure (in kb) computed from equations (18) and (30), coefficients in table 11, and values of Q given by Helgeson and Kirkham (1974a).

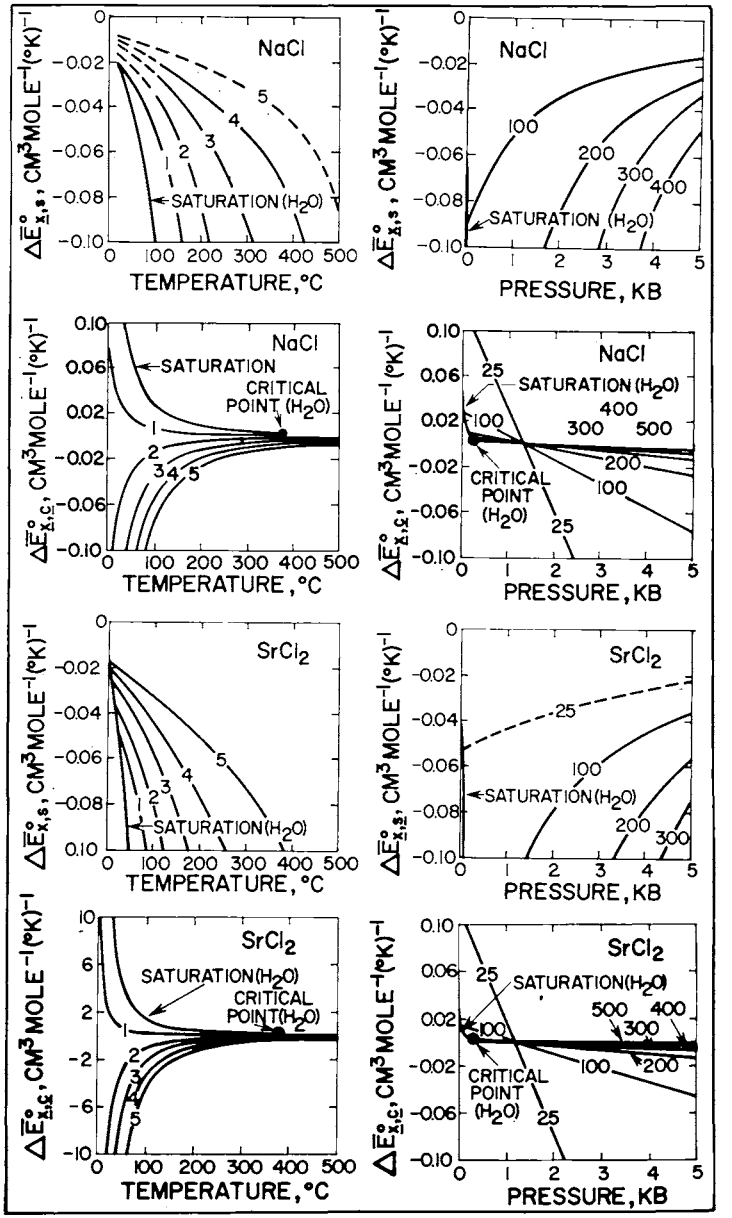

Fig. 49. $\Delta\bar{E}^{\circ}_{x,s}$ and $\Delta\bar{E}^{\circ}_{x,c}$ of NaCl and $SrCl_2$ as functions of temperature (in °C) and pressure (in kb) computed from equations (20) and (33), coefficients in table 11, and values of U given by Helgeson and Kirkham (1974a).

fig. 50), and $\Delta\bar{V}^\circ_n$ exhibits behavior similar to that shown in figure 47. However, the temperature at which $\Delta\bar{V}^\circ_n$ exhibits no pressure dependence may be different, depending on the relative magnitudes of the a_2 and a_4 coefficients in the equation of state. At high temperatures where $T/(T-\theta)$ is small, the a_2P term controls the behavior of $\Delta\bar{V}^\circ_n$ as a function of pressure. At low temperatures, the term $a_4PT/(T-\theta)$, which is positive for all the electrolytes considered in this study, causes $\Delta\bar{V}^\circ_n$ to increase with increasing pressure. The temperature at which the two terms are equal thus varies according to the relative magnitude of a_2 and a_4. If a_2 is positive, which is the case for $SrCl_2$, $MgSO_4$, K_2SO_4, H_2SO_4, and KF (table 11), $\Delta\bar{V}^\circ_n$ increases with increasing pressure at all temperatures, and the curves representing the isothermal dependence of $\Delta\bar{V}^\circ_n$ on temperature do not cross each other. The pressure at which $(\partial^2\Delta\bar{V}^\circ_n/\partial T^2)_P$ changes sign depends on the relative magnitude of the a_3 and a_4 coefficients, which are of opposite sign.

The behavior of $\Delta\bar{V}^\circ_n$ for $SrCl_2$ depicted in figure 48 is typical of electrolytes with positive a_2 coefficients. These electrolytes commonly involve a divalent cation and/or anion. Although a_2 is negative for $MgCl_2$ and $CaCl_2$, it can be seen in table 11 that the absolute values of a_2 for these electrolytes are smaller than any of the others in the table. Divalent ions would be expected to be more effective in collapsing the solvent structure than monovalent ions, owing to the higher charge density of the divalent species. As a consequence, $\Delta\bar{V}^\circ_c$ for electrolytes involving divalent ions should increase to a lesser extent with increasing temperature at low pressures than $\Delta\bar{V}^\circ_c$ for electrolytes consisting of monovalent ions. It can be seen in figure 50 that $\Delta\bar{\kappa}^\circ_{c,SrCl_2}$ remains negative at high temperatures where $\Delta\bar{\kappa}^\circ_{c,NaCl}$ is positive. $\Delta\bar{V}^\circ_c$ and $\Delta\bar{V}^\circ_n$ for $SrCl_2$ accordingly increase with increasing pressure at all temperatures, unlike $\Delta\bar{V}^\circ_{c,NaCl}$ and $\Delta\bar{V}^\circ_{n,NaCl}$. The contribution of $\Delta\bar{V}^\circ_n$ to $\bar{V}^\circ$ with increasing pressure at high temperatures thus reinforces $\Delta\bar{V}^\circ_s$ in the case of $SrCl_2$ but opposes $\Delta\bar{V}^\circ_s$ for NaCl and most other 1:1 electrolytes. Because $\Delta\bar{V}^\circ_s$ is the dominant contribution to $\bar{V}^\circ$ for all electrolytes at high temperatures, the consequences of these reinforcing or opposing contributions are not readily apparent in the behavior of $\bar{V}^\circ$ as a function of pressure and temperature.

CONVENTIONAL STANDARD PARTIAL MOLAL VOLUMES, COMPRESSIBILITIES, AND EXPANSIBILITIES OF IONIC SPECIES

The conventional standard partial molal volume of the jth aqueous species ($\bar{V}^\circ_j$) is related to its absolute counterpart ($\bar{V}^\circ_j{}^{abs}$) by

$$\bar{V}^\circ_j = \bar{V}^\circ_j{}^{abs} - Z_j\,\bar{V}^\circ_{H^+}{}^{abs} \tag{96}$$

Taking account of equations (10) through (12) we can also write

$$\bar{V}^\circ_{i,j} = \bar{V}^\circ_{i,j}{}^{abs} - Z_j\,\bar{V}^\circ_{i,H^+}{}^{abs} \tag{97}$$

$$\Delta\bar{V}^\circ_{n,j} = \Delta\bar{V}^\circ_{n,j}{}^{abs} - Z_j\,\Delta\bar{V}^\circ_{n,H^+}{}^{abs} \tag{98}$$

$$\Delta\bar{V}^\circ_{c,j} = \Delta\bar{V}^\circ_{c,j}{}^{abs} - Z_j\,\Delta\bar{V}^\circ_{c,H^+}{}^{abs} \tag{99}$$

$$\Delta\bar{V}^\circ_{s,j} = \Delta\bar{V}^\circ_{s,j}{}^{abs} - Z_j\,\Delta\bar{V}^\circ_{s,H^+}{}^{abs} \tag{100}$$

and

$$\Delta\bar{V}^\circ_{c,j} = \Delta\bar{V}^\circ_{e,j}{}^{abs} - Z_j\,\Delta\bar{V}^\circ_{e,H^+}{}^{abs} \tag{101}$$

which are consistent with

$$\bar{V}^\circ_j = \bar{V}^\circ_{i,j} + \Delta\bar{V}^\circ_{e,j} = \bar{V}^\circ_{i,j} + \Delta\bar{V}^\circ_{c,j} + \Delta\bar{V}^\circ_{s,j} = \Delta\bar{V}^\circ_{n,j} + \Delta\bar{V}^\circ_{s,j} \tag{102}$$

and

$$\begin{aligned}\bar{V}^\circ_j{}^{abs} = \bar{V}^\circ_{i,j}{}^{abs} + \Delta\bar{V}^\circ_{e,j}{}^{abs} &= \bar{V}^\circ_{i,j}{}^{abs} + \Delta\bar{V}^\circ_{c,j}{}^{abs} + \Delta\bar{V}^\circ_{s,j}{}^{abs} \\ &= \Delta\bar{V}^\circ_{n,j}{}^{abs} + \Delta\bar{V}^\circ_{s,j}{}^{abs}\end{aligned} \tag{103}$$

where

$$\Delta\bar{V}^\circ_{e,j} = \Delta\bar{V}^\circ_{c,j} + \Delta\bar{V}^\circ_{s,j} \tag{104}$$

$$\Delta\bar{V}^\circ_{e,j}{}^{abs} = \Delta\bar{V}^\circ_{c,j}{}^{abs} + \Delta\bar{V}^\circ_{s,j}{}^{abs} \tag{105}$$

$$\Delta\bar{V}^\circ_{n,j} = \bar{V}^\circ_{i,j} + \Delta\bar{V}^\circ_{c,j} \tag{106}$$

and

$$\Delta\bar{V}^\circ_{n,j} = \bar{V}^\circ_{i,j}{}^{abs} + \Delta\bar{V}^\circ_{c,j}{}^{abs} \tag{107}$$

As a consequence of equations (96) through (101), we can write the following identity:

$$\bar{V}^\circ_{H^+} = \bar{V}^\circ_{i,H^+} = \Delta\bar{V}^\circ_{n,H^+} = \Delta\bar{V}^\circ_{c,H^+} = \Delta\bar{V}^\circ_{s,H^+} = \Delta\bar{V}^\circ_{e,H^+} = 0 \tag{108}$$

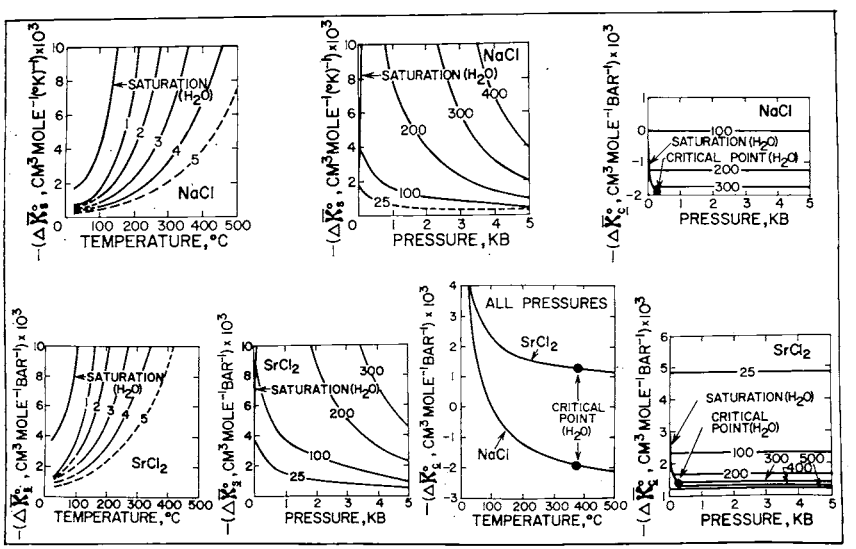

Fig. 50. $-\Delta\bar{K}^\circ_s$ and $-\Delta\bar{K}^\circ_c$ of NaCl and $SrCl_2$ as functions of temperature (in °C) and pressure (in kb) computed from equations (24) and (37), coefficients in table 11, and values of N given by Helgeson and Kirkham (1974a).

TABLE 14

Conventional standard partial molal volumes of aqueous ions in cm^3 $mole^{-1}$ at 20 bars and temperatures from 0° to 200°C computed from equation (40), the coefficients in table 17, and values of Q in table 4

Species	Temperature, °C								
	0	25	50	75	100	125	150	175	200
H^+	0	0	0	0	0	0	0	0	0
Li^+	-1.1	-1.1	-1.3	-1.6	-2.1	-2.9	-4.0	-5.6	-8.0
Na^+	-3.7	-1.2	0.05	0.7	0.9	0.8	0.4	0.4	-1.9
K^+	6.9	8.8	9.5	9.9	9.9	9.8	9.6	9.1	8.2
Cs^+	19.1	21.2	22.3	22.9	23.3	23.5	23.5	23.4	23.1
NH_4^+	16.0	17.9	18.7	19.2	19.3	19.3	19.1	18.7	17.9
Mg^{++}	-21.0	-21.2	-21.8	-23.0	-24.6	-27.0	-30.4	-35.5	-43.2
Ca^{++}	-19.6	-18.4	-18.8	-19.6	-20.9	-22.8	-25.5	-29.6	-35.8
Sr^{++}	-20.6	-17.7	-18.0	-18.7	-19.9	-21.6	-24.1	-27.9	-33.6
Ba^{++}	-15.9	-12.3	-11.3	-11.3	-12.0	-13.2	-15.2	-18.3	-23.1
F^-	-3.9	-1.1	-1.8	-3.1	-5.0	-7.8	-11.8	-17.7	-26.7
Cl^-	16.4	17.9	17.9	17.2	15.9	13.8	10.6	5.9	-1.4
Br^-	22.9	24.9	25.6	25.4	24.5	22.9	20.1	15.8	9.0
I^-	33.3	36.4	37.9	38.4	38.1	36.9	34.7	31.0	24.9
HS^-	17.0	20.2	20.6	20.0	18.7	16.7	13.6	9.0	1.8
NO_3^-	25.7	29.0	30.7	31.5	31.4	30.5	28.7	25.6	20.3
OH^-	-7.9	-4.5	-4.5	-5.5	-7.1	-9.7	-13.4	-19.1	-27.7
ClO_4^-	41.0	44.0	46.0	47.0	48.0	48.0	47.0	45.0	41.0
HCO_3^-	21.6	24.2	24.9	24.6	23.6	21.8	19.1	14.9	8.3
SO_4^{--}	10.1	14.3	13.6	11.7	8.4	3.6	-3.4	-13.8	-29.9

TABLE 15

Conventional standard partial molal expansibilities of aqueous ions in cm^3 $mole^{-1}$ $(°K)^{-1}$ at 20 bars and temperatures from 0° to 200°C computed from equation (41), the coefficients in table 17, and values of U in table 4

Species	Temperature, °C								
	0	25	50	75	100	125	150	175	200
H^+	0	0	0	0	0	0	0	0	0
Li^+	0.00	0.00	-0.01	-0.02	-0.03	-0.03	-0.05	-0.08	-0.12
Na^+	0.15	0.07	0.04	0.02	0.00	-0.01	-0.02	-0.04	-0.08
K^+	0.12	0.04	0.02	0.01	0.00	-0.01	-0.02	-0.03	-0.05
Cs^+	0.12	0.06	0.03	0.02	0.01	-0.01	0.00	-0.01	-0.02
NH_4^+	0.12	0.05	0.02	0.01	0.00	0.00	-0.01	-0.02	-0.04
Mg^{++}	0.07	-0.02	-0.04	-0.05	-0.08	-0.11	-0.16	-0.03	-0.39
Ca^{++}	0.27	0.00	-0.03	-0.04	-0.06	-0.09	-0.14	-0.20	-0.31
Sr^{++}	0.87	0.03	-0.02	-0.04	-0.06	-0.08	-0.12	-0.18	-0.29
Ba^{++}	0.28	0.07	0.02	-0.01	-0.04	-0.06	-0.10	-0.15	-0.24
F^-	4.49	-0.02	-0.04	-0.06	-0.09	-0.13	-0.19	-0.29	-0.45
Cl^-	0.14	0.02	-0.02	-0.04	-0.07	-0.10	-0.15	-0.23	-0.37
Br^-	0.12	0.05	0.01	-0.02	-0.05	-0.09	-0.14	-0.21	-0.34
I^-	0.16	0.09	0.04	0.00	-0.03	-0.07	-0.12	-0.19	-0.31
HS^-	0.29	0.04	-0.01	-0.04	-0.07	-0.10	-0.15	-0.23	-0.36
NO_3^-	0.17	0.09	0.05	0.01	-0.02	-0.05	-0.10	-0.16	-0.27
OH^-	0.41	0.03	-0.02	-0.05	-0.08	-0.12	-0.18	-0.28	-0.43
ClO_4	0.12	0.09	0.07	0.04	0.01	-0.16	-0.06	-0.12	-0.21
HCO_3^-	0.19	0.05	0.00	-0.03	-0.05	-0.09	-0.14	-0.21	-0.33
SO_4^{--}	0.66	0.01	-0.06	-0.10	-0.16	-0.23	-0.34	-0.51	-0.80

Hence,

$$\bar{V}^\circ_{Cl^-} = \bar{V}^\circ_{HCl} \tag{109}$$

$$\bar{V}^\circ_{i,Cl^-} = \bar{V}^\circ_{i,HCl} \tag{110}$$

$$\Delta\bar{V}^\circ_{n,Cl^-} = \Delta\bar{V}^\circ_{n,HCl} \tag{111}$$

$$\Delta\bar{V}^\circ_{c,Cl^-} = \Delta\bar{V}^\circ_{c,HCl} \tag{112}$$

$$\Delta\bar{V}^\circ_{s,Cl^-} = \Delta\bar{V}^\circ_{s,HCl} \tag{113}$$

and

$$\Delta\bar{V}^\circ_{e,Cl^-} = \Delta\bar{V}^\circ_{e,HCl} \tag{114}$$

which permits calculation of $\bar{V}^\circ$ as well as $\bar{V}^\circ_{i,j}$, $\Delta\bar{V}^\circ_{n,j}$, $\Delta\bar{V}^\circ_{c,j}$, $\Delta\bar{V}^\circ_{s,j}$, and $\Delta\bar{V}^\circ_{e,j}$ for all aqueous species from corresponding standard partial molal volume data for electrolytes. Analogous relations hold for the partial derivatives of the standard partial molal volume and its various additive components, which permits similar calculation of the conventional ionic counterparts of all other standard partial molal properties of electrolytes.

Values of $\bar{V}^\circ_j$, $\bar{E}^\circ_{x,j}$, and $-\bar{\kappa}^\circ_j$ are given in tables 14, 15, and 16 for 20 ionic species at 20 bars and temperatures from 0° to 200°C. The values were computed from subscripted statements of equations (40), (41), and (43) using appropriate values of Q, U, and N (table 4) together with co-

TABLE 16

Conventional standard partial molal compressibilities ($\bar{\kappa}^\circ$) of aqueous ions (expressed as $-\bar{\kappa}^\circ$) in (cm^3 mole^{-1} bar^{-1}) $\times$ 10^3 at 20 bars and temperatures from 0° to 200°C computed from equation (43), the coefficients in table 18, and values of N in table 4

Species	Temperature, °C								
	0	25	50	75	100	125	150	175	200
H^+	0	0	0	0	0	0	0	0	0
Na^+	5.4	3.8	2.9	2.5	2.3	2.5	3.0	4.1	6.5
K^+	4.7	3.2	2.7	4.6	2.4	2.5	2.8	3.4	4.9
Mg^{++}	9.9	7.6	7.8	8.3	9.4	11.3	14.7	20.8	32.6
Ca^{++}	8.4	6.6	6.6	7.0	7.8	9.3	12.0	16.9	26.4
Sr^{++}	8.6	6.9	7.0	7.4	8.1	9.5	12.0	16.5	25.3
F^-	6.4	2.3	2.5	3.2	4.5	6.7	10.6	17.7	31.5
Cl^-	2.3	0.9	0.5	0.8	1.6	3.3	6.4	12.1	23.2
Br^-	1.2	0.1	-0.5	-0.5	0.1	1.6	4.4	9.7	20.2
NO_3^-	1.1	-0.6	-1.7	-2.2	-2.1	-1.2	0.9	5.1	13.5
OH^-	6.7	3.4	2.9	3.3	4.3	6.4	10.0	16.8	30.0
HCO_3^-	1.6	0.4	0.0	0.2	0.9	2.4	5.2	10.4	20.5
SO_4^{--}	11.7	7.3	7.0	7.9	10.0	13.9	20.7	33.3	57.7

TABLE 17

Summary of fit coefficients generated by regression of conventional standard partial molal volumes of aqueous ions as a function of temperature at 20 bars[a] with equation (40), values of Q in table 4, and Born coefficients (ω_j) computed (eq 115) from values of ω_j^{abs} in table 7

Species	o[b]	$\xi \times 10^2$[b]	θ[c]	$\omega \times 10^{-5}$[d]
H^+	0	0	0	0
Li^+	0.0052	-0.0379	253.94	0.4862
Na^+	0.1905	-5.5551	215.17	0.3306
K^+	0.3109	-1.9170	234.19	0.1927
Cs^+	0.6687	-4.2301	217.04	0.0974
NH_4^+	0.5540	-2.8468	225.29	0.1791
Mg^{++}	-0.4142	-0.0049	270.56	1.5372
Ca^{++}	-0.3550	-0.1217	266.14	1.2366
Sr^{++}	-0.3421	-0.1373	268.97	1.1363
Ba^{++}	-0.1086	-2.2555	245.02	0.9851
F^-	0.0823	-0.0212	272.42	1.7870
Cl^-	0.5747	-1.0491	246.02	1.4560
Br^-	0.8908	-6.5546	206.75	1.3858
I^-	1.3904	-16.6538	186.51	1.2933
HS^-	0.6501	-1.2713	252.19	1.4410
NO_3^-	1.2373	-18.0627	185.29	1.1295
OH^-	0.0471	-0.6938	259.90	1.7246
ClO_4	36.1422	-3.431	6.19	1.0012
HCO_3^-	0.7869	-2.6499	236.87	1.3293
SO_4^{--}	0.5834	-0.6359	263.03	3.1857

[a] The conventional standard partial molal volumes of the ions employed in the regression analysis were calculated from additivity relations analogous to equation (116) using values of $\bar{V}°$ (table 9) computed from equation (40) and coefficients in table 8. [b] cal mole^{-1} bar^{-1}. [c] °K. [d] cal mole^{-1} -- computed from equation (115) and values of ω_j^{abs} in table 7.

efficients in tables 17 and 18. The values of ω_j in these tables were computed from ω_j^{abs} (table 7) and

$$\omega_j = \omega_j^{abs} - Z_j \, \omega_{H^+}^{abs} \tag{115}$$

However, the other coefficients were generated by fitting equations (40) and (43) to additivity values of $\bar{V}^\circ_j$ and $-\bar{\kappa}^\circ_j$ derived from expressions such as

$$\bar{V}^\circ_{Mg^{++}} = \bar{V}^\circ_{MgCl_2} - 2\bar{V}^\circ_{Cl^-} \tag{116}$$

and

$$\bar{\kappa}^\circ_{Mg^{++}} = \bar{\kappa}^\circ_{MgCl_2} - 2\bar{\kappa}^\circ_{Cl^-} \tag{117}$$

where $\bar{V}^\circ_{Cl^-}$ is given by equation (109) and

$$\bar{\kappa}^\circ_{Cl^-} = \bar{\kappa}^\circ_{HCl} \tag{118}$$

The regression procedure (which reproduces the additivity values of $\bar{V}^\circ_j$ and $\bar{\kappa}^\circ_j$ to within 0.1 cm^3 mole^{-1} and 1×10^{-3} cm^3 mole^{-1} bar^{-1}, respectively, at temperatures and pressures $\leq$ 200°C and 20 bars) was in-

TABLE 18

Summary of equation of state coefficients generated by regression of conventional standard partial molal compressibilities and volumes of aqueous ions as a function of temperature at 1 and 20 bars (see text) with equations (28), (29), (40), and (42), and values of Q, N, and ω in tables 4 and 17[a]

Species	a_1[b]	$a_2 \times 10^5$[c]	$a_3 \times 10^2$[b]	$a_4 \times 10^5$[c]	θ[d]	$\omega \times 10^{-5}$[e]
H^+	0	0	0	0	0	0
Na^+	0.1914	-4.7852	-5.6282	3.6560	215.17	0.3306
K^+	0.3107	0.7452	-1.9460	1.4504	234.19	0.1927
Mg^{++}	-0.4170	14.0877	-0.0063	0.0704	270.56	1.5372
Ca^{++}	-0.3573	11.4034	-0.1252	0.1768	266.14	1.2366
Sr^{++}	-0.3447	13.0761	-0.1391	0.0903	268.97	1.1363
F^-	0.0821	1.1184	-0.0219	0.0313	272.42	1.7870
Cl^-	0.5761	-6.9590	-1.0698	1.0365	246.02	1.4560
Br^-	0.8941	-16.7628	-6.6404	4.2899	206.75	1.3858
NO_3^-	1.2438	-32.0602	-18.2754	10.6342	185.29	1.1295
OH^-	0.0471	-1.2610	-0.7082	0.7222	259.90	1.7246
HCO_3^-	0.7887	-8.9225	-2.6787	1.4350	236.87	1.3293
SO_4^{--}	0.5825	4.4576	-0.6501	0.7125	263.03	3.1857

[a] Values of $\bar{V}^\circ_j$, $\bar{E}^\circ_{x,j}$, and $-\bar{\kappa}^\circ_j$ computed from these coefficients and equations (39), (41), and (43) are shown in tables 16 and 19 through 30 (see text). [b] cal mole^{-1} bar^{-1}. [c] cal mole^{-1} bar^{-2}. [d] °K. [e] cal mole^{-1}--computed from equation (115) and values of ω_j^{abs} in table 7.

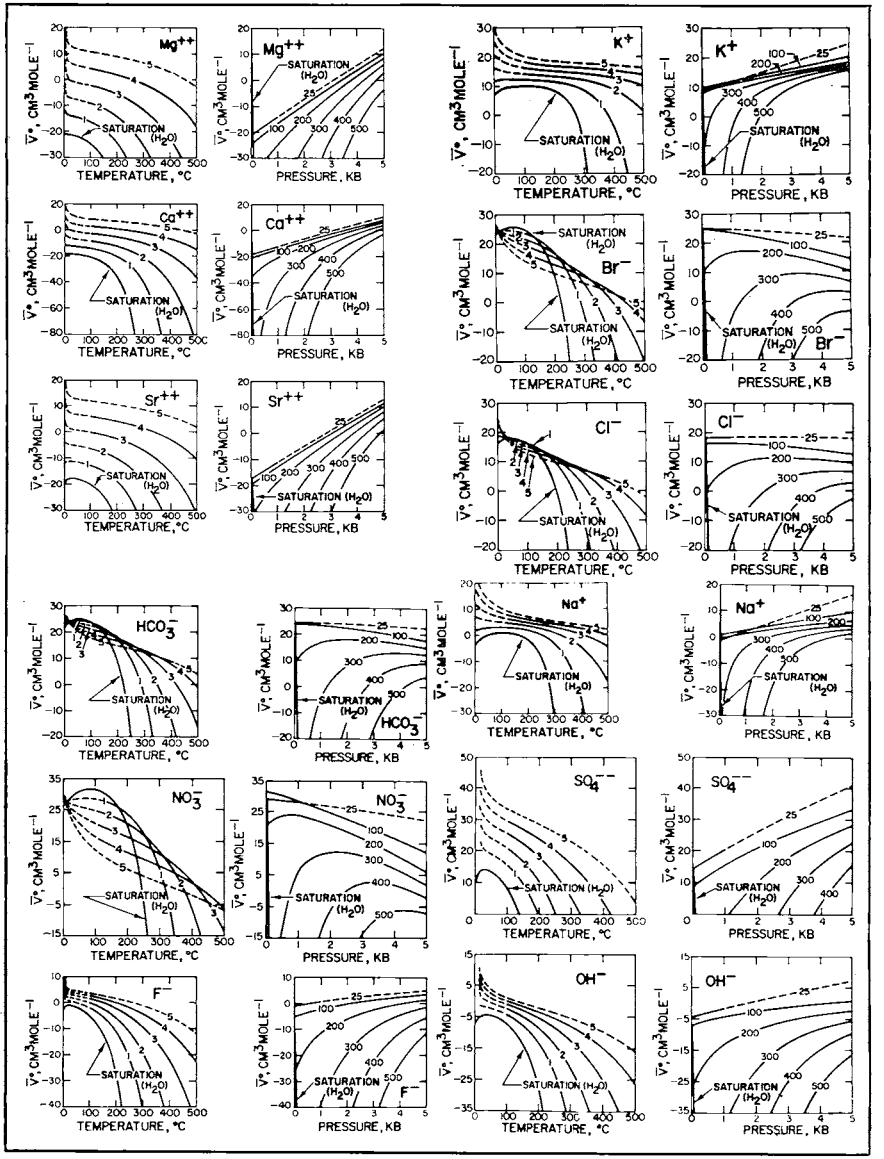

Fig. 51. Conventional standard partial molal volumes ($\bar{V}°$) of aqueous ions as a function of temperature (in °C) and pressure (in kb) computed from equation (39), coefficients in table 18, and values of Q given by Helgeson and Kirkham (1974a).

TABLE 19

Conventional standard partial molal volume ($\bar{V}°$) of Ca^{++} in cm^3 $mole^{-1}$ computed from equation (39), coefficients in table 18, and values of Q reported by Helgeson and Kirkham (1974a)

t	PRESSURE, KB									
(°C)	SAT	0.5	1	2	2.5	3	3.5	4	4.5	5
25	-18.9	-15.4	-12.4	(-6.4)	(-3.5)	(-.6)	(2.3)	(5.1)	(8.0)	(10.8)
50	-18.6	-15.8	-12.9	(-7.1)	(-4.3)	(-1.5)	(1.3)	(4.0)	(6.8)	(9.5)
75	-19.7	-16.5	-13.5	(-7.7)	(-4.8)	(-2.1)	(0.7)	(3.4)	(6.1)	(8.8)
100	-21.0	-17.5	-14.3	-8.3	-5.4	-2.6	0.2	2.9	5.6	(8.3)
125	-23.9	-18.8	-15.3	-9.0	-6.0	-3.1	-0.3	2.4	5.2	(7.9)
150	-25.7	-20.7	-16.7	-9.9	-6.8	-3.8	-0.9	2.0	4.7	(7.4)
175	-29.8	-23.2	-18.4	-11.1	-7.7	-4.5	-1.5	1.4	4.2	(7.0)
200	-35.9	-26.7	-20.7	-12.4	-8.7	-5.3	-2.2	0.8	3.7	(6.6)
225	-45.7	-31.7	-23.6	-14.1	-10.0	-6.3	-3.0	0.2	3.2	(6.1)
250	-62.3	-38.9	-27.7	-16.2	-11.5	-7.5	-3.9	-0.5	2.6	(5.6)
275	-93.1	-49.9	-33.1	-18.6	-13.3	-8.8	-4.9	-1.3	1.9	(5.0)
300	-158.3	-67.4	-40.7	-21.6	-15.4	-10.3	-6.0	-2.2	1.2	(4.5)
325	-332.6	-96.7	-51.4	-25.2	-17.8	-12.1	-7.3	-3.2	0.5	(3.9)
350	-1119.5	-149.3	-66.7	-29.5	-20.7	-14.1	-8.8	-4.3	-0.4	(3.2)
375		-253.2	-89.0	-34.9	-24.2	-16.4	-10.4	-5.5	-1.3	(2.5)
400		-488.3	-121.1	-41.6	-28.4	-19.2	-12.4	-6.9	-2.4	(1.6)
425		(-1100.4)	-167.7	-50.0	-33.4	-22.5	-14.6	-8.6	-3.6	(0.7)
450		(-2443.8)	-234.5	-60.7	-39.5	-26.4	-17.3	-10.5	-5.0	(-0.3)
475		(-3645.2)	-329.5	-74.2	-47.0	-31.1	-20.4	-12.7	-6.6	(-1.6)
500		(-4074.8)	-459.6	-91.0	-56.1	-36.6	-24.1	-15.3	-8.5	(-3.0)
525			(-624.9)	(-108.2)	(-64.0)	(-43.4)	(-30.0)	(-19.3)	(-11.0)	(-4.6)
550			(-810.7)	(-130.5)	(-75.9)	(-50.6)	(-34.7)	(-22.6)	(-13.3)	(-6.3)
575			(-987.0)	(-153.8)	(-88.6)	(-58.1)	(-39.5)	(-26.0)	(-15.7)	(-8.1)
600			(-1116.2)	(-175.3)	(-100.3)	(-65.0)	(-44.0)	(-29.0)	(-17.9)	(-9.8)

TABLE 20

Conventional standard partial molal volume ($\bar{V}°$) of Na^{+} in cm^3 $mole^{-1}$ computed from equation (39), coefficients in table 18, and values of Q reported by Helgeson and Kirkham (1974a)

t	PRESSURE, KB									
(°C)	SAT	0.5	1	2	2.5	3	3.5	4	4.5	5
25	-1.3	0.6	2.4	(6.0)	(7.8)	(9.6)	(11.4)	(13.2)	(15.0)	(16.7)
50	0.0	1.4	2.8	(5.5)	(6.9)	(8.2)	(9.5)	(10.9)	(12.2)	(13.5)
75	0.6	1.8	2.9	(5.1)	(6.2)	(7.3)	(8.3)	(9.4)	(10.4)	(11.5)
100	0.9	2.0	2.9	4.8	5.7	6.6	7.5	8.3	9.2	(10.0)
125	0.8	1.9	2.8	4.5	5.3	6.1	6.8	7.5	8.3	(9.0)
150	0.4	1.6	2.6	4.2	4.9	5.6	6.3	6.9	7.5	(8.2)
175	-0.5	1.1	2.2	3.8	4.5	5.2	5.8	6.4	6.9	(7.5)
200	-1.9	0.3	1.7	3.4	4.1	4.7	5.3	5.9	6.4	(6.9)
225	-4.4	-0.9	0.9	2.9	3.6	4.3	4.9	5.4	5.9	(6.4)
250	-8.7	-2.7	-0.1	2.3	3.2	3.9	4.5	5.0	5.5	(5.9)
275	-16.8	-5.6	-1.5	1.6	2.6	3.4	4.1	4.6	5.1	(5.5)
300	-34.1	-10.2	-3.5	0.8	2.0	2.9	3.6	4.2	4.7	(5.1)
325	-80.7	-17.9	-6.3	-0.2	1.3	2.4	3.2	3.8	4.3	(4.8)
350	-291.0	-32.0	-10.4	-1.4	0.4	1.7	2.7	3.4	3.9	(4.4)
375		-59.7	-16.3	-2.9	-0.5	1.0	2.1	2.9	3.6	(4.1)
400		-122.5	-24.9	-4.7	-1.7	0.2	1.5	2.5	3.2	(3.7)
425		(-286.1)	-37.3	-6.9	-3.0	-0.7	0.9	1.9	2.7	(3.3)
450		(-645.2)	-55.2	-9.8	-4.7	-1.8	0.1	1.4	2.2	(2.9)
475		(-966.3)	-80.5	-13.4	-6.8	-3.1	-0.8	0.7	1.7	(2.5)
500		(-1081.1)	-115.3	-17.9	-9.2	-4.6	-1.8	-0.1	1.1	(2.0)
525			(-159.4)	(-22.6)	(-11.3)	(-6.4)	(-3.5)	(-1.2)	(0.4)	(1.5)
550			(-209.1)	(-28.5)	(-14.5)	(-8.4)	(-4.8)	(-2.1)	(-0.3)	(1.0)
575			(-256.2)	(-34.8)	(-17.9)	(-10.4)	(-6.1)	(-3.1)	(-1.0)	(0.4)
600			(-290.7)	(-40.5)	(-21.1)	(-12.3)	(-7.3)	(-4.0)	(-1.6)	(-0.1)

TABLE 21

Conventional standard partial molal volume ($\bar{V}°$) of Cl^- in cm^3 $mole^{-1}$ computed from equation (39), coefficients in table 18, and values of Q reported by Helgeson and Kirkham (1974a)

t	PRESSURE, KB									
(°C)	SAT	0.5	1	2	2.5	3	3.5	4	4.5	5
25	17.9	18.2	18.3	(18.5)	(18.5)	(18.5)	(18.4)	(18.3)	(18.3)	(18.2)
50	17.9	18.0	17.8	(17.4)	(17.1)	(16.8)	(16.5)	(16.1)	(15.7)	(15.3)
75	17.2	17.3	17.1	(16.6)	(16.2)	(15.8)	(15.3)	(14.8)	(14.3)	(13.7)
100	15.8	16.3	16.2	15.7	15.4	14.9	14.4	13.8	13.2	(12.6)
125	13.7	14.7	15.0	14.8	14.5	14.1	13.6	13.0	12.4	(11.7)
150	10.5	12.6	13.5	13.7	13.5	13.2	12.7	12.2	11.6	(10.9)
175	5.8	9.7	11.4	12.3	12.4	12.2	11.9	11.4	10.8	(10.2)
200	-1.5	5.6	8.8	10.6	11.1	11.1	11.0	10.6	10.1	(9.5)
225	-13.1	-0.3	5.3	8.6	9.5	9.9	9.9	9.7	9.3	(8.8)
250	-32.7	-8.8	0.5	6.2	7.7	8.5	8.8	8.8	8.5	(8.1)
275	-69.1	-21.7	-5.9	3.3	5.6	6.9	7.6	7.8	7.7	(7.4)
300	-146.0	-42.3	-14.8	-0.2	3.1	5.1	6.2	6.7	6.8	(6.6)
325	-351.5	-76.7	-27.4	-4.5	0.2	3.0	4.6	5.5	5.8	(5.9)
350	-1278.4	-318.6	-45.5	-9.6	-3.3	0.6	2.9	4.2	4.8	(5.0)
375		-261.0	-71.6	-16.0	-7.4	-2.2	0.9	2.7	3.6	(4.1)
400		-537.8	-109.5	-23.9	-12.3	-5.5	-1.4	1.0	2.3	(3.1)
425		(-1258.5)	-164.3	-33.8	-18.2	-9.4	-4.1	-1.0	0.9	(2.0)
450		(-2840.3)	-243.0	-46.4	-25.4	-14.0	-7.3	-3.3	-0.8	(0.7)
475		(-4254.9)	-354.9	-62.2	-34.3	-19.5	-11.0	-5.9	-2.7	(-0.8)
500		(-4760.7)	-508.0	-82.1	-45.0	-26.0	-15.3	-8.9	-5.0	(-2.5)
525			(-702.6)	(-102.4)	(-54.2)	(-34.1)	(-22.2)	(-13.7)	(-7.9)	(-4.4)
550			(-921.4)	(-128.5)	(-68.3)	(-42.6)	(-27.8)	(-17.6)	(-10.7)	(-6.5)
575			(-1129.1)	(-156.0)	(-83.2)	(-51.4)	(-33.6)	(-21.6)	(-13.6)	(-8.6)
600			(-1281.1)	(-181.4)	(-97.1)	(-59.5)	(-38.8)	(-25.2)	(-16.2)	(-10.6)

TABLE 22

Conventional standard partial molal volume ($\bar{V}°$) of HCO_3^- in cm^3 $mole^{-1}$ computed from equation (39), coefficients in table 18, and values of Q reported by Helgeson and Kirkham (1974a)

t	PRESSURE, KB									
(°C)	SAT	0.5	1	2	2.5	3	3.5	4	4.5	5
25	24.2	24.3	24.2	(23.9)	(23.7)	(23.5)	(23.2)	(23.0)	(22.7)	(22.4)
50	24.9	24.7	24.3	(23.4)	(22.9)	(22.4)	(21.8)	(21.3)	(20.7)	(20.1)
75	24.6	24.4	24.0	(22.9)	(22.3)	(21.6)	(20.9)	(20.2)	(19.4)	(18.7)
100	23.6	23.7	23.3	22.3	21.7	20.9	20.2	19.4	18.5	(17.7)
125	21.8	22.4	22.4	21.5	20.9	20.2	19.5	18.6	17.7	(16.8)
150	19.0	20.6	21.1	20.6	20.1	19.5	18.8	17.9	17.0	(16.1)
175	14.8	18.0	19.3	19.4	19.1	18.7	18.0	17.2	16.4	(15.4)
200	8.2	14.3	16.9	17.9	18.0	17.7	17.2	16.5	15.7	(14.8)
225	-2.3	9.1	13.7	16.1	16.6	16.6	16.2	15.7	15.0	(14.2)
250	-20.2	1.3	9.5	13.9	14.9	15.3	15.2	14.8	14.2	(13.5)
275	-53.4	-10.4	3.7	11.3	13.0	13.9	14.1	13.9	13.5	(12.8)
300	-123.6	-29.2	-4.5	8.1	10.7	12.2	12.8	12.9	12.6	(12.1)
325	-311.2	-60.6	-15.9	4.2	8.1	10.3	11.4	11.8	11.8	(11.4)
350	-1157.4	-117.1	-32.4	-0.4	5.0	8.1	9.8	10.6	10.8	(10.6)
375		-228.8	-56.3	-6.2	1.3	5.6	8.0	9.2	9.8	(9.8)
400		-481.5	-90.9	-13.4	-3.2	2.6	5.9	7.7	8.6	(8.9)
425		(-1139.4)	-140.8	-22.5	-8.6	-1.0	3.4	5.9	7.2	(7.8)
450		(-2583.6)	-212.7	-34.0	-15.2	-5.2	0.6	3.8	5.7	(6.7)
475		(-3875.1)	-314.8	-48.4	-23.3	-10.2	-2.6	1.4	3.9	(5.3)
500		(-4336.9)	-454.6	-66.5	-33.1	-16.2	-6.8	-1.3	1.9	(3.7)
525			(-632.3)	(-85.1)	(-41.5)	(-23.5)	(-13.1)	(-5.7)	(-0.8)	(2.0)
550			(-832.0)	(-108.9)	(-54.4)	(-31.2)	(-18.2)	(-9.3)	(-3.4)	(0.1)
575			(-1021.6)	(-134.1)	(-68.0)	(-39.3)	(-23.4)	(-12.9)	(-6.0)	(-1.9)
600			(-1160.4)	(-157.2)	(-80.6)	(-46.7)	(-28.2)	(-16.2)	(-8.3)	(-3.6)

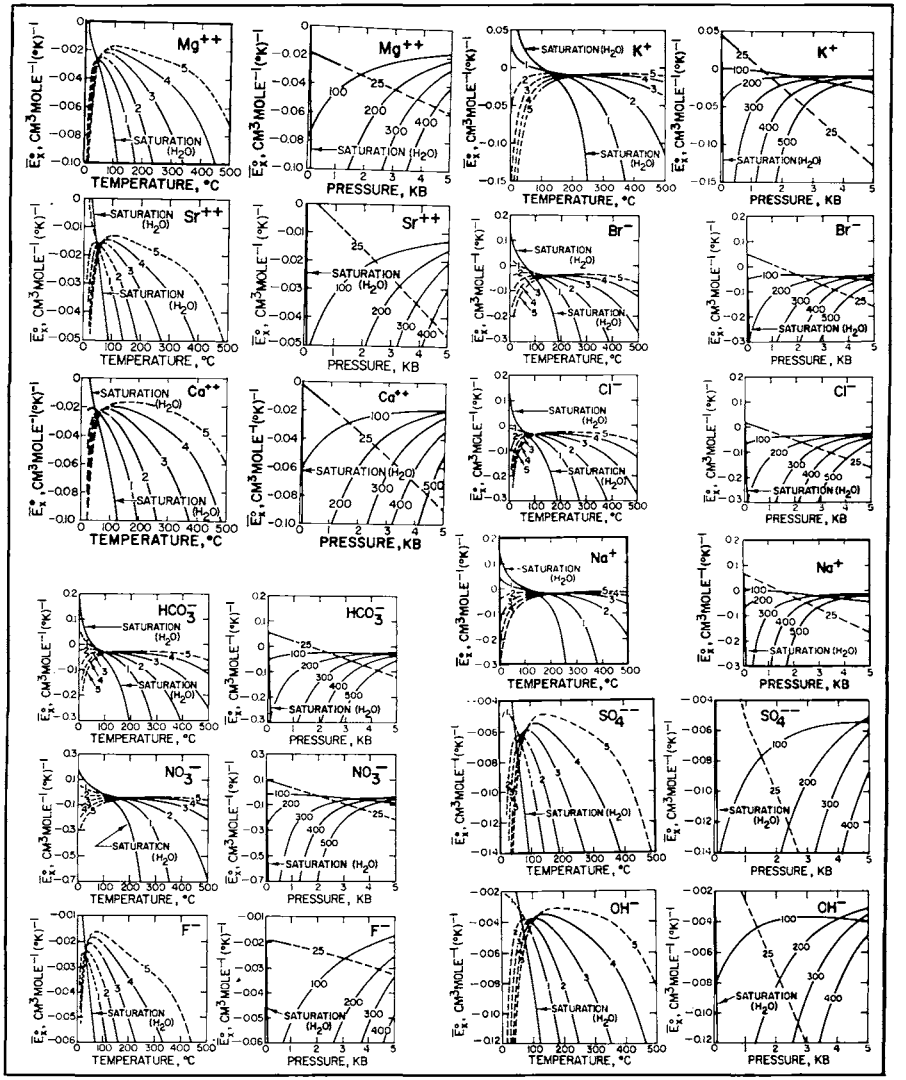

Fig. 52. Conventional standard partial molal expansibilities ($\bar{E}^{\circ}_{x}$) of aqueous ions as a function of temperature (in °C) and pressure (in kb) computed from equation (41), coefficients in table 18, and values of U given by Helgeson and Kirkham (1974a).

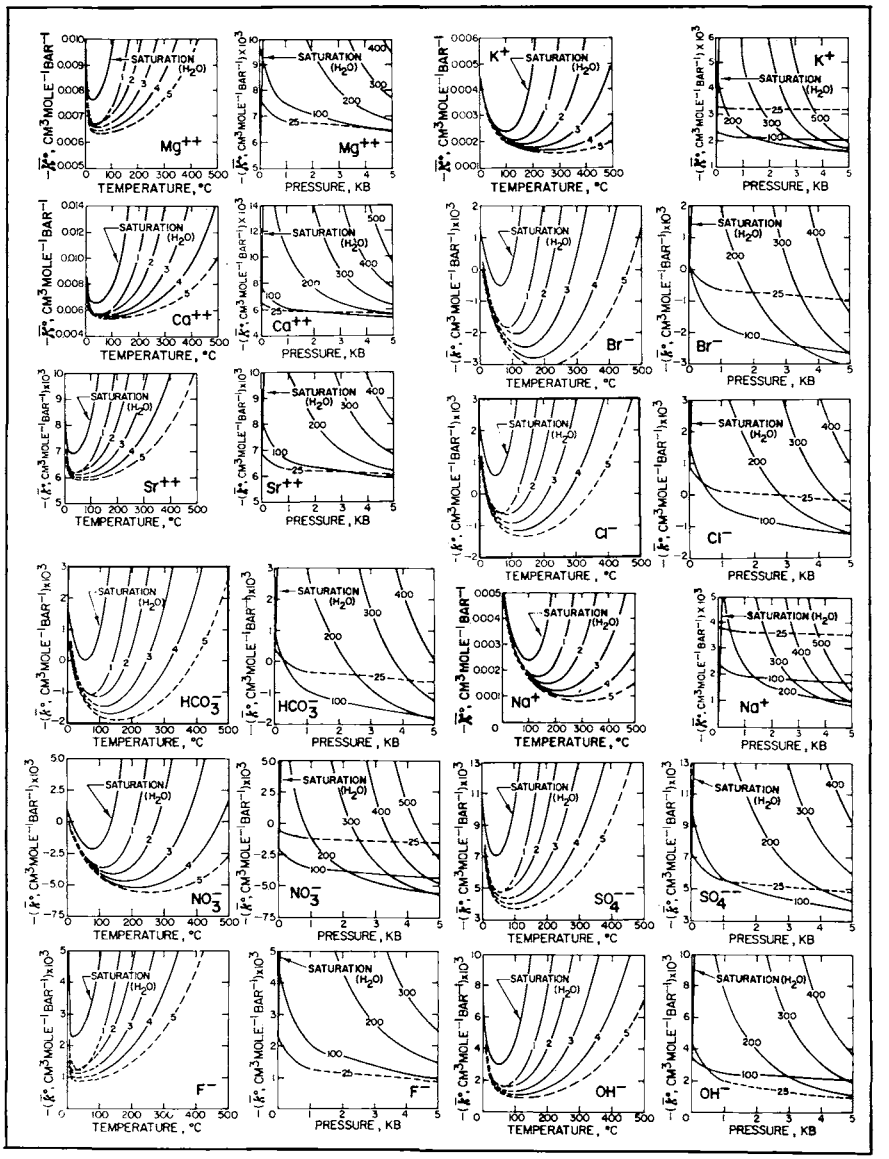

Fig. 53. Conventional standard partial molal compressibilities ($\bar{\kappa}°$) of aqueous ions as a function of temperature (in °C) and pressure (in kb) computed from equation (43), coefficients in table 18, and values of N given by Helgeson and Kirkham (1974a).

voked to avoid distributing possible errors in the coefficients for electrolytes among their ionic counterparts by employing relations analogous to equations (76) through (80). As indicated above, regression errors may accumulate in computing coefficients for a given electrolyte or ion directly from those of other electrolytes.

The coefficients in table 18 were used to compute values of $\bar{V}^\circ_j$, $\bar{E}^\circ_{x,j}$, and $-\bar{\kappa}^\circ_j$ for the various ionic species at pressures and temperatures to 5 kb and 600°C. The results of these calculations are plotted in figures 51 through 53, and numerical values for four of the ions (Ca^{++}, Na^+, Cl^-, and HCO_3^-) are given in tables 19 through 30. Corresponding values for the other ions shown in the figures can be computed from equations (39), (41), and (43) using the appropriate coefficients in table 18 and the values of Q, U, and N tabulated by Helgeson and Kirkham (1974a). The more uncertain values of $\bar{V}^\circ_j$, $\bar{E}^\circ_{x,j}$, and $-\bar{\kappa}^\circ_j$ computed in this study are shown in parentheses in the tables and plotted as dashed lines in the figures. The parenthetical values and dashed lines are for pressures and temperatures at the edges or beyond the region of pressure-temperature space where reliable values of Q, N, and U can be computed with confidence (temperatures $\leq$ 100°C at pressures $\geq$ 1 kb, temperatures $\geq$ 550°C, and pressures $\geq$ 5 kb — Helgeson and Kirkham, 1974a).

The curves in figures 51 through 53 are similar in configuration to the corresponding curves for electrolytes, but the effect of increasing temperature and/or decreasing pressure on $\bar{V}^\circ_j$, $\bar{E}^\circ_{x,j}$, and $-\bar{\kappa}^\circ_j$ is less pronounced at low temperatures than it is on $\bar{V}^\circ$, $\bar{E}^\circ_x$, and $-\bar{\kappa}^\circ$ for electrolytes. As a consequence, the extrema in the curves for the ions tend to be broader than the corresponding extrema for electrolytes. It can be seen in figures 51 through 53 that the isobars representing $\bar{V}^\circ_j$ as a function of temperature for the cations and F^-, OH^-, and SO_4^{--} are somewhat different in configuration than those for Br^-, Cl^-, HCO_3^-, and NO_3^-; that is, in the latter cases the curves cross each other and describe a spiral surface in pressure-temperature-$\bar{V}^\circ_j$ space. Also, in contrast to the isothermal dependence of $\bar{V}^\circ_j$ on pressure exhibited by the cations and F^-, OH^-, and SO_4^{--}, that for Br^-, Cl^-, HCO_3^-, and NO_3^- is negative at high pressures (fig. 53). Note that the extrema in $\bar{V}^\circ_j$ as a function of temperature at low pressures gradually change to sigmoid configurations above 1 to 2 kb. As a consequence, $\bar{E}^\circ_{x,j}$ exhibits the opposite behavior; that is, a sigmoid dependence on temperature at low pressures, but extrema at high pressures (fig. 52). It can be seen in figure 52 that these extrema occur over a broad temperature range for all the monovalent ions. In the case of the divalent ions, the extrema in $\bar{E}^\circ_{x,j}$ as a function of temperature occur below 100° to 200°C. Similar behavior is exhibited by $\bar{\kappa}^\circ_j$ for the ions depicted in figure 53. Both $\bar{E}^\circ_{x,j}$ and $\bar{\kappa}^\circ_j$ for the ions shown in figures 52 and 53 decrease dramatically with increasing pressure at constant (high) temperature.

Owing to round-off in the coefficients and the effect of ambiguities introduced by slight inconsistencies in the fit results for different electrolytes on values of $\bar{V}^\circ_j$ derived directly from $\bar{V}^\circ$ (see above), the regression

TABLE 23

Conventional standard partial molal expansibility ($\bar{E}°_x$) of Ca^{++} in cm^3 $mole^{-1}$ $(°K)^{-1}$ computed from equation (41), coefficients in table 18, and values of U given by Helgeson and Kirkham (1974a)

t	PRESSURE, KB									
(°C)	SAT	0.5	1	2	2.5	3	3.5	4	4.5	5
25	0.00	-0.01	(-0.02)	(-0.04)	(-0.05)	(-0.05)	(-0.06)	(-0.07)	(-0.08)	(-0.09)
50	-0.03	-0.02	(-0.02)	(-0.02)	(-0.02)	(-0.03)	(-0.03)	(-0.03)	(-0.03)	(-0.03)
75	-0.04	-0.03	(-0.03)	(-0.02)	(-0.02)	(-0.02)	(-0.02)	(-0.02)	(-0.02)	(-0.02)
100	-0.06	-0.05	-0.04	-0.03	-0.02	-0.02	-0.02	-0.02	-0.02	(-0.02)
125	-0.09	-0.06	-0.05	-0.03	-0.03	-0.02	-0.02	-0.02	-0.02	(-0.02)
150	-0.14	-0.09	-0.06	-0.04	-0.03	-0.03	-0.02	-0.02	-0.02	(-0.02)
175	-0.20	-0.12	-0.08	-0.05	-0.04	-0.03	-0.03	-0.02	-0.02	(-0.02)
200	-0.32	-0.17	-0.10	-0.06	-0.05	-0.04	-0.03	-0.03	-0.02	(-0.02)
225	-0.52	-0.24	-0.14	-0.07	-0.05	-0.04	-0.03	-0.03	-0.02	(-0.02)
250	-0.94	-0.35	-0.19	-0.09	-0.06	-0.05	-0.04	-0.03	-0.03	(-0.02)
275	-1.89	-0.55	-0.26	-0.11	-0.08	-0.06	-0.04	-0.03	-0.03	(-0.02)
300	-4.62	-0.89	-0.36	-0.13	-0.09	-0.06	-0.05	-0.04	-0.03	(-0.02)
325	-15.91	-1.53	-0.51	-0.16	-0.11	-0.07	-0.05	-0.04	-0.03	(-0.03)
350	-129.32	-2.85	-0.73	-0.20	-0.13	-0.09	-0.06	-0.05	-0.03	(-0.03)
375		(-5.93)	-1.06	-0.24	-0.15	-0.10	-0.07	-0.05	-0.04	(-0.03)
400		(-14.36)	-1.54	-0.30	-0.18	-0.12	-0.08	-0.06	-0.04	(-0.03)
425			-2.22	-0.37	-0.22	-0.14	-0.10	-0.07	-0.05	(-0.04)
450			-3.18	-0.47	-0.27	-0.17	-0.11	-0.08	-0.06	(-0.04)
475			(-4.47)	(-0.59)	(-0.33)	(-0.20)	(-0.13)	(-0.09)	(-0.07)	(-0.05)
500			(-5.95)	(-0.74)	(-0.39)	(-0.24)	(-0.15)	(-0.11)	(-0.08)	(-0.06)

TABLE 24

Conventional standard partial molal expansibility ($\bar{E}°_x$) of Na^+ in cm^3 $mole^{-1}$ $(°K)^{-1}$ computed from equation (41), coefficients in table 18, and values of U given by Helgeson and Kirkham (1974a)

t	PRESSURE, KB									
(°C)	SAT	0.5	1	2	2.5	3	3.5	4	4.5	5
25	0.07	0.05	(0.02)	(-0.03)	(-0.05)	(-0.07)	(-0.10)	(-0.12)	(-0.14)	(-0.17)
50	0.04	0.02	(0.01)	(-0.02)	(-0.03)	(-0.04)	(-0.06)	(-0.07)	(-0.09)	(-0.10)
75	0.02	0.01	(0.00)	(-0.01)	(-0.02)	(-0.03)	(-0.04)	(-0.05)	(-0.06)	(-0.07)
100	0.00	0.00	0.00	-0.01	-0.02	-0.02	-0.03	-0.04	-0.04	(-0.05)
125	-0.01	-0.01	-0.01	-0.01	-0.02	-0.02	-0.02	-0.03	-0.03	(-0.04)
150	-0.02	-0.02	-0.01	-0.01	-0.02	-0.02	-0.02	-0.02	-0.03	(-0.03)
175	-0.05	-0.03	-0.02	-0.02	-0.02	-0.02	-0.02	-0.02	-0.02	(-0.03)
200	-0.08	-0.04	-0.02	-0.02	-0.02	-0.02	-0.02	-0.02	-0.02	(-0.02)
225	-0.13	-0.06	-0.03	-0.02	-0.02	-0.02	-0.02	-0.02	-0.02	(-0.02)
250	-0.25	-0.09	-0.05	-0.03	-0.02	-0.02	-0.02	-0.02	-0.02	(-0.02)
275	-0.50	-0.14	-0.07	-0.03	-0.02	-0.02	-0.02	-0.02	-0.02	(-0.02)
300	-1.23	-0.23	-0.09	-0.04	-0.03	-0.02	-0.02	-0.02	-0.02	(-0.02)
325	-4.25	-0.41	-0.13	-0.04	-0.03	-0.02	-0.02	-0.02	-0.01	(-0.01)
350	-34.57	-0.76	-0.20	-0.05	-0.04	-0.03	-0.02	-0.02	-0.02	(-0.01)
375		(-1.58)	-0.28	-0.06	-0.04	-0.03	-0.02	-0.02	-0.02	(-0.01)
400		(-3.84)	-0.41	-0.08	-0.05	-0.03	-0.02	-0.02	-0.02	(-0.01)
425			-0.59	-0.10	-0.06	-0.04	-0.03	-0.02	-0.02	(-0.01)
450			-0.85	-0.13	-0.07	-0.05	-0.03	-0.02	-0.02	(-0.02)
475			(-1.19)	(-0.16)	(-0.09)	(-0.06)	(-0.04)	(-0.03)	(-0.02)	(-0.02)
500			(-1.59)	(-0.20)	(-0.11)	(-0.06)	(-0.04)	(-0.03)	(-0.02)	(-0.02)

TABLE 25

Conventional standard partial molal expansibility ($\bar{E}°_x$) of Cl^- in cm^3 $mole^{-1}$ $(°K)^{-1}$ computed from equation (41), coefficients in table 18, and values of U given by Helgeson and Kirkham (1974a)

t	PRESSURE, KB									
(°C)	SAT	0.5	1	2	2.5	3	3.5	4	4.5	5
25	0.05	0.02	(0.00)	(-0.05)	(-0.07)	(-0.09)	(-0.12)	(-0.14)	(-0.16)	(-0.19)
50	-0.01	-0.01	(-0.02)	(-0.03)	(-0.04)	(-0.05)	(-0.06)	(-0.07)	(-0.08)	(-0.09)
75	-0.04	-0.03	(-0.03)	(-0.03)	(-0.03)	(-0.04)	(-0.04)	(-0.04)	(-0.05)	(-0.05)
100	-0.06	-0.05	-0.04	-0.03	-0.03	-0.03	-0.03	-0.04	-0.04	(-0.04)
125	-0.10	-0.07	-0.05	-0.04	-0.03	-0.03	-0.03	-0.03	-0.03	(-0.03)
150	-0.15	-0.10	-0.07	-0.05	-0.04	-0.03	-0.03	-0.03	-0.03	(-0.03)
175	-0.23	-0.13	-0.09	-0.06	-0.05	-0.04	-0.03	-0.03	-0.03	(-0.03)
200	-0.36	-0.19	-0.12	-0.07	-0.05	-0.04	-0.04	-0.03	-0.03	(-0.03)
225	-0.59	-0.27	-0.16	-0.08	-0.06	-0.05	-0.04	-0.03	-0.03	(-0.03)
250	-1.07	-0.40	-0.21	-0.10	-0.07	-0.06	-0.05	-0.04	-0.03	(-0.03)
275	-2.16	-0.62	-0.29	-0.12	-0.09	-0.06	-0.05	-0.04	-0.03	(-0.03)
300	-5.27	-1.00	-0.41	-0.15	-0.10	-0.07	-0.06	-0.04	-0.04	(-0.03)
325	-18.15	-1.74	-0.58	-0.18	-0.12	-0.08	-0.06	-0.05	-0.04	(-0.03)
350	-147.56	-3.25	-0.84	-0.22	-0.14	-0.10	-0.07	-0.05	-0.04	(-0.03)
375		(-6.77)	-1.21	-0.27	-0.17	-0.12	-0.08	-0.06	-0.05	(-0.04)
400		(-16.38)	-1.76	-0.34	-0.21	-0.13	-0.09	-0.07	-0.05	(-0.04)
425			-2.59	-0.43	-0.25	-0.16	-0.10	-0.08	-0.06	(-0.05)
450			-3.63	-0.54	-0.30	-0.19	-0.13	-0.09	-0.07	(-0.05)
475			(-5.10)	(-0.67)	(-0.37)	(-0.23)	(-0.15)	(-0.11)	(-0.08)	(-0.06)
500			(-6.79)	(-0.84)	(-0.45)	(-0.27)	(-0.18)	(-0.12)	(-0.09)	(-0.07)

TABLE 26

Conventional standard partial molal expansibility ($\bar{E}°_x$) of HCO_3^- in cm^3 $mole^{-1}$ $(°K)^{-1}$ computed from equation (41), coefficients in table 18, and values of U given by Helgeson and Kirkham (1974a)

t	PRESSURE, KB									
(°C)	SAT	0.5	1	2	2.5	3	3.5	4	4.5	5
25	0.05	0.04	(0.02)	(-0.02)	(-0.04)	(-0.05)	(-0.07)	(-0.09)	(-0.11)	(-0.13)
50	0.00	0.00	(-0.01)	(-0.02)	(-0.03)	(-0.03)	(-0.04)	(-0.05)	(-0.06)	(-0.07)
75	-0.03	-0.02	(-0.02)	(-0.02)	(-0.03)	(-0.03)	(-0.03)	(-0.04)	(-0.04)	(-0.05)
100	-0.06	-0.04	-0.03	-0.03	-0.03	-0.03	-0.03	-0.03	-0.03	(-0.04)
125	-0.09	-0.06	-0.04	-0.03	-0.03	-0.03	-0.03	-0.03	-0.03	(-0.03)
150	-0.14	-0.09	-0.06	-0.04	-0.04	-0.03	-0.03	-0.03	-0.03	(-0.03)
175	-0.21	-0.12	-0.08	-0.05	-0.04	-0.04	-0.03	-0.03	-0.03	(-0.03)
200	-0.33	-0.17	-0.11	-0.06	-0.05	-0.04	-0.03	-0.03	-0.03	(-0.03)
225	-0.56	-0.25	-0.15	-0.08	-0.06	-0.05	-0.04	-0.03	-0.03	(-0.03)
250	-1.00	-0.38	-0.20	-0.10	-0.07	-0.05	-0.04	-0.04	-0.03	(-0.03)
275	-2.03	-0.58	-0.27	-0.12	-0.08	-0.06	-0.05	-0.04	-0.03	(-0.03)
300	-4.96	-0.95	-0.38	-0.14	-0.10	-0.07	-0.05	-0.04	-0.03	(-0.03)
325	-17.10	-1.64	-0.55	-0.17	-0.11	-0.08	-0.06	-0.05	-0.04	(-0.03)
350	-139.02	-3.06	-0.79	-0.21	-0.14	-0.09	-0.07	-0.05	-0.04	(-0.03)
375		(-6.37)	-1.14	-0.26	-0.16	-0.11	-0.08	-0.06	-0.04	(-0.03)
400		(-15.43)	-1.65	-0.32	-0.19	-0.13	-0.09	-0.06	-0.05	(-0.04)
425			-2.39	-0.40	-0.24	-0.15	-0.10	-0.07	-0.06	(-0.04)
450			-3.42	-0.50	-0.29	-0.18	-0.12	-0.09	-0.06	(-0.05)
475			(-4.80)	(-0.63)	(-0.35)	(-0.22)	(-0.14)	(-0.10)	(-0.07)	(-0.06)
500			(-6.39)	(-0.79)	(-0.42)	(-0.25)	(-0.17)	(-0.12)	(-0.09)	(-0.06)

TABLE 27

Conventional standard partial molal compressibility ($\bar{K}^\circ$) of Ca^{++} (expressed as $-\bar{K}^\circ \times 10^3$) in ($cm^3$ $mole^{-1}$ bar^{-1}) $\times 10^3$ computed from equation (43), coefficients in table 18, and values of N given by Helgeson and Kirkham (1974a)

t (°C)	PRESSURE, KB									
	SAT	0.5	1	2	2.5	3	3.5	4	4.5	5
25	6.6	6.1	(5.9)	(5.9)	(5.8)	(5.8)	(5.8)	(5.7)	(5.7)	(5.6)
50	6.6	5.9	(5.7)	(5.7)	(5.7)	(5.6)	(5.5)	(5.5)	(5.4)	(5.4)
75	7.0	6.1	(5.8)	(5.8)	(5.7)	(5.6)	(5.5)	(5.4)	(5.4)	(5.3)
100	7.9	6.6	6.1	5.9	5.8	5.6	5.5	5.5	5.4	(5.3)
125	9.4	7.4	6.7	6.1	5.9	5.7	5.6	5.5	5.4	(5.4)
150	12.2	8.8	7.5	6.5	6.2	5.9	5.7	5.6	5.5	(5.4)
175	17.1	10.9	8.7	7.0	6.5	6.2	5.9	5.8	5.6	(5.5)
200	26.6	14.3	10.4	7.7	7.0	6.5	6.2	5.9	5.8	(5.6)
225	46.0	20.2	13.1	8.7	7.6	6.9	6.5	6.1	5.9	(5.7)
250	90.0	30.4	17.2	10.0	8.5	7.5	6.8	6.4	6.1	(5.9)
275	206.0	49.5	23.6	11.8	9.6	8.2	7.3	6.7	6.4	(6.1)
300	590.3	87.1	33.9	14.2	11.0	9.1	7.9	7.1	6.6	(6.3)
325	2487.8	168.2	50.4	17.4	12.8	10.1	8.6	7.6	7.0	(6.6)
350	26193.3	362.9	77.6	21.7	15.1	11.5	9.4	8.2	7.4	(6.9)
375		(905.3)	122.5	27.4	18.1	13.2	10.5	8.9	7.9	(7.2)
400		(2734.7)	196.9	35.1	21.9	15.3	11.7	9.7	8.4	(7.6)
425			320.5	45.5	26.8	17.9	13.2	10.7	9.1	(8.1)
450			524.1	59.6	33.0	21.1	15.1	11.8	9.9	(8.7)
475			(847.2)	(78.5)	(41.1)	(25.1)	(17.4)	(13.2)	(10.8)	(9.4)
500			(1313.2)	(103.5)	(51.4)	(30.1)	(20.1)	(14.9)	(11.9)	(10.1)

TABLE 28

Conventional standard partial molal compressibility ($\bar{K}^\circ$) of Na^+ (expressed as $-\bar{K}^\circ \times 10^3$) in ($cm^3$ $mole^{-1}$ bar^{-1}) $\times 10^3$ computed from equation (43), coefficients in table 18, and values of N given by Helgeson and Kirkham (1974a)

t (°C)	PRESSURE, KB									
	SAT	0.5	1	2	2.5	3	3.5	4	4.5	5
25	3.8	3.7	(3.6)	(3.6)	(3.6)	(3.6)	(3.6)	(3.6)	(3.5)	(3.5)
50	3.0	2.8	(2.7)	(2.7)	(2.7)	(2.7)	(2.7)	(2.7)	(2.6)	(2.6)
75	2.5	2.3	(2.2)	(2.2)	(2.2)	(2.1)	(2.1)	(2.1)	(2.1)	(2.1)
100	2.4	2.0	1.9	1.8	1.8	1.8	1.7	1.7	1.7	(1.7)
125	2.5	2.0	1.8	1.6	1.6	1.5	1.5	1.5	1.4	(1.4)
150	3.0	2.1	1.8	1.5	1.4	1.4	1.3	1.3	1.3	(1.2)
175	4.4	2.5	1.9	1.5	1.4	1.3	1.2	1.2	1.1	(1.1)
200	6.6	3.3	2.3	1.5	1.3	1.2	1.1	1.1	1.0	(1.0)
225	11.7	4.8	2.9	1.7	1.4	1.2	1.1	1.0	1.0	(0.9)
250	23.3	7.4	3.9	2.0	1.5	1.3	1.1	1.0	0.9	(0.9)
275	54.3	12.4	5.5	2.4	1.8	1.4	1.2	1.0	0.9	(0.8)
300	156.9	22.4	8.2	2.9	2.1	1.6	1.2	1.0	0.9	(0.8)
325	664.1	44.0	12.6	3.7	2.5	1.8	1.4	1.1	0.9	(0.8)
350	7000.8	96.0	19.8	4.8	3.1	2.1	1.5	1.2	1.0	(0.9)
375		(241.0)	31.7	6.3	3.8	2.5	1.8	1.3	1.1	(0.9)
400		(730.0)	51.6	8.3	4.8	3.0	2.1	1.5	1.2	(1.0)
425			84.6	11.1	6.1	3.7	2.4	1.7	1.3	(1.1)
450			139.0	14.8	7.7	4.5	2.9	2.0	1.5	(1.2)
475			(225.3)	(19.8)	(9.8)	(5.6)	(3.5)	(2.4)	(1.7)	(1.3)
500			(349.9)	(26.5)	(12.5)	(6.8)	(4.2)	(2.8)	(2.0)	(1.5)

TABLE 29

Conventional standard partial molal compressibility ($\bar{K}^\circ$) of Cl^- (expressed as $-\bar{K}^\circ \times 10^3$) in ($cm^3\ mole^{-1}\ bar^{-1}$) $\times 10^3$ computed from equation (43), coefficients in table 18, and values of N given by Helgeson and Kirkham (1974a)

t	PRESSURE, KB									
(°C)	SAT	0.5	1	2	2.5	3	3.5	4	4.5	5
25	0.9	0.3	(0.1)	(0.0)	(0.0)	(0.0)	(-0.1)	(-0.1)	(-0.2)	(-0.2)
50	0.6	-0.2	(-0.5)	(-0.5)	(-0.5)	(-0.6)	(-0.7	(-0.7)	(-0.8)	(-0.8)
75	0.8	-0.2	(-0.6)	(-0.6)	(-0.8)	(-0.9)	(-0.9)	(-1.0)	(-1.1)	(-1.1)
100	1.7	0.2	-0.4	-0.6	-0.8	-0.9	-1.0	-1.1	-1.2	(-1.3)
125	3.4	1.1	0.2	-0.4	-0.7	-0.9	-1.0	-1.2	-1.3	(-1.3)
150	6.6	2.6	1.1	-0.1	-0.5	-0.8	-1.0	-1.1	-1.2	(-1.3)
175	12.4	5.0	2.4	0.4	-0.1	-0.5	-0.8	-1.0	-1.2	(-1.3)
200	23.5	9.0	4.5	1.2	0.4	-0.2	-0.6	-0.8	-1.1	(-1.2)
225	46.3	15.9	7.6	2.4	1.1	0.3	-0.3	-0.6	-0.9	(-1.1)
250	98.0	27.9	12.4	3.9	2.1	0.9	0.2	-0.3	-0.7	(-0.9)
275	234.6	50.3	19.9	6.0	3.4	1.7	0.7	0.0	-0.4	(-0.7)
300	687.1	94.7	31.9	8.8	5.0	2.7	1.3	0.5	-0.1	(-0.5)
325	2921.3	190.1	51.4	12.5	7.1	4.0	2.2	1.0	0.3	(-0.2)
350	30832.9	419.3	83.4	17.6	9.8	5.6	3.1	1.7	0.7	(0.1)
375		(1058.0)	136.2	24.3	13.3	7.5	4.3	2.5	1.3	(0.5)
400		(3212.0)	223.8	33.4	17.8	10.0	5.8	3.4	1.9	(1.0)
425			369.3	45.6	23.5	13.0	7.6	4.5	2.7	(1.5)
450			609.1	62.2	30.9	16.8	9.8	5.9	3.6	(2.2)
475			(989.4)	(84.4)	(40.3)	(21.5)	(12.4)	(7.6)	(4.7)	(3.0)
500			(1538.2)	(113.8)	(52.4)	(27.4)	(15.6)	(9.5)	(6.0)	(3.9)

TABLE 30

Conventional standard partial molal compressibility ($\bar{K}^\circ$) of HCO_3^- (expressed as $-\bar{K}^\circ \times 10^3$) in ($cm^3\ mole^{-1}\ bar^{-1}$) $\times 10^3$ computed from equation (43), coefficients in table 18, and values of N given by Helgeson and Kirkham (1974a)

t	PRESSURE, KB									
(°C)	SAT	0.5	1	2	2.5	3	3.5	4	4.5	5
25	0.4	-0.1	(-0.3)	(-0.4)	(-0.4)	(-0.5)	(-0.5)	(-0.5)	(-0.6)	(-0.6)
50	0.0	-0.7	(-1.0)	(-0.9)	(-1.0)	(-1.1)	(-1.1)	(-1.2)	(-1.2)	(-1.3)
75	0.2	-0.7	(-1.1)	(-1.1	(-1.2)	(-1.3)	(-1.4)	(-1.5)	(-1.5)	(-1.6)
100	1.0	0.4	-0.9	-1.2	-1.3	-1.4	-1.5	-1.6	-1.7	(-1.8)
125	2.5	0.4	-0.5	-1.0	-1.3	-1.4	-1.6	-1.7	-1.8	(-1.8)
150	5.4	1.7	0.3	-0.8	-1.1	-1.3	-1.5	-1.7	-1.8	(-1.9)
175	10.6	3.9	1.5	-0.3	-0.8	-1.2	-1.4	-1.6	-1.7	(-1.9)
200	20.8	7.6	3.4	0.4	-0.3	-0.9	-1.2	-1.5	-1.7	(-1.8)
225	41.5	13.8	6.2	1.4	0.3	-0.4	-0.9	-1.3	-1.5	(-1.7)
250	88.8	24.8	10.6	2.8	1.2	0.1	-0.6	-1.0	-1.4	(-1.6)
275	213.5	45.2	17.5	4.7	2.3	0.8	-0.1	-0.7	-1.1	(-1.4)
300	626.6	85.7	28.4	7.3	3.8	1.7	0.5	-0.3	-0.8	(-1.2)
325	2666.4	172.8	46.2	10.7	5.8	2.9	1.2	0.2	-0.5	(-1.0)
350	28149.5	382.1	75.4	15.3	8.2	4.3	2.1	0.8	-0.1	(-0.7)
375		(965.2)	123.6	21.4	11.4	6.1	3.2	1.5	0.4	(-0.3)
400		(2931.7)	203.6	29.7	15.5	8.4	4.5	2.3	1.0	(0.1)
425			336.4	40.9	20.7	11.1	6.2	3.4	1.7	(0.6)
450			555.3	56.0	27.4	14.6	8.1	4.6	2.5	(1.2)
475			(902.6)	(76.3)	(36.1)	(18.9)	(10.6)	(6.1)	(3.5)	(1.9)
500			(1403.6)	(103.1)	(47.1)	(24.2)	(13.5)	(7.9)	(4.7)	(2.8)

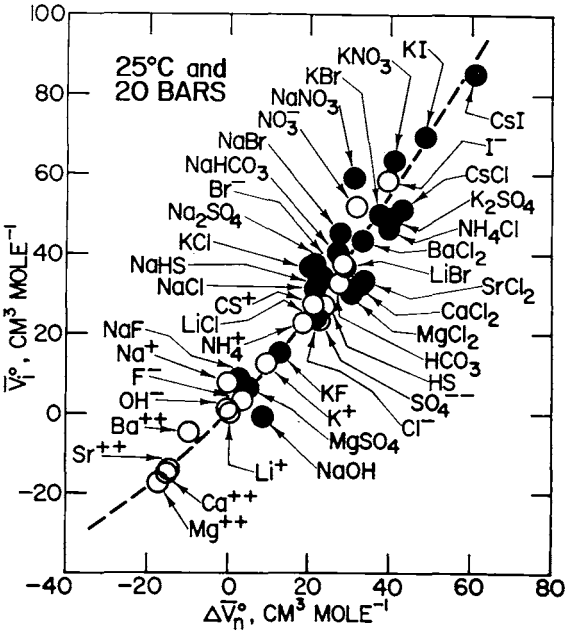

Fig. 54. Correlation of $\bar{V}°_i$ with $\Delta\bar{V}°_n$ for aqueous electrolytes and ionic species at 25°C and 20 bars. The values of $\bar{V}°_i$ and $\Delta\bar{V}°_n$ were computed from equations (26), (30), and (31), coefficients in tables 8, 11, 17, and 18, and (where no a_1 coefficient is available) the approximation, $a_1 \approx \sigma_{20\ bars}$ (see text).

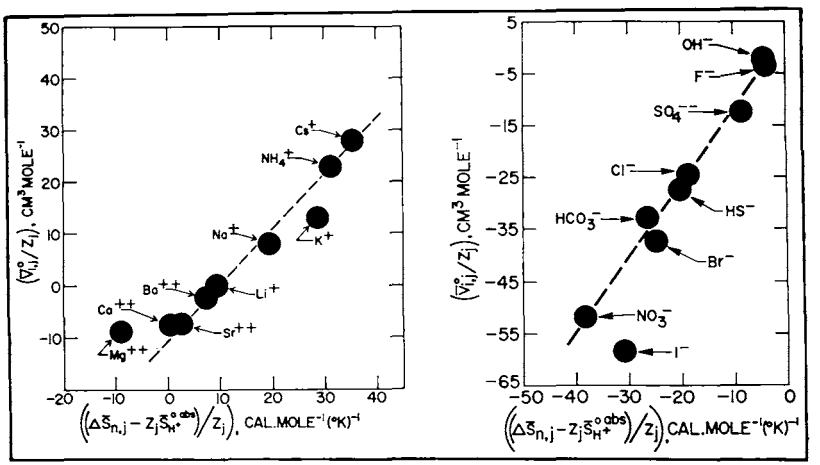

Fig. 55. Correlation of $\bar{V}°_{i,j}$ for aqueous ions with charge Z_j computed from equation (31), coefficients in tables 17 and 18, and (where no a_1 coefficient is available) the approximation, $a_1 \approx \sigma_{20\ bars}$ (see text) with $\Delta\bar{S}°_{n,j} - Z_j\ \bar{S}°_{H^+}{}^{abs}$ (table 7 and eq 67) at 25°C and 1 bar.

coefficients for ionic species in table 18 do not always yield values of $\bar{V}^\circ_j$, $-\bar{\kappa}^\circ_j$, and $\bar{E}^\circ_{x,j}$ at high pressures and temperatures that are exactly consistent with the corresponding values for electrolytes computed from the coefficients in table 11. This is particularly true at pressures $\geq$ 1 kb and temperatures $\leq$ 100°C, which is outside the region of pressure and temperature where values of Q, N, and U can be computed with confidence (Helgeson and Kirkham, 1974a). At pressures $\geq$ 1 kb and temperature $\leq$ 100°C, most of the discrepancies are $\leq$ 1 cm^3 mole^{-1}, but a few are as large as 5 cm^3 mole^{-1}. For the other pressures and temperatures considered in the tables and figures, the discrepancies are $<$ 0.2 cm^3 mole^{-1} for KCl, NaBr, $NaNO_3$, NaCl, KNO_3, and $CaCl_2$, $<$ 0.5 cm^3 mole^{-1} for K_2SO_4, KBr, KF, and $NaHCO_3$, $<$ 1 cm^3 mole^{-1} for $MgSO_4$, and $<$ 3 cm^3 mole^{-1} for NaF, $SrCl_2$, $MgCl_2$, and Na_2SO_4. These discrepancies are remarkably small considering that the equation of state coefficients were obtained by regression of data at temperatures $\leq$ 200°C. Although the values of $\bar{V}^\circ$ generated from the coefficients in table 11 are more accurate than the additivity values computed from $\bar{V}^\circ_j$, differences $\leq$ 3 cm^3 mole^{-1} can be regarded as negligible in most geochemical calculations.

CORRELATIONS AND COEFFICIENT ESTIMATES

Despite the fact that the equation of state derived in the preceding pages is based in part on arithmetic separation of the variables $\bar{V}^\circ_i$, $\Delta\bar{V}^\circ_c$, and $\Delta\bar{V}^\circ_s$, the intrinsic, collapse, and solvation contributions to $\bar{V}^\circ$ are obviously interrelated. For example, it can be seen in figure 54 that $\bar{V}^\circ_i$ correlates with $\Delta\bar{V}^\circ_n$ (and thus with $\Delta\bar{V}^\circ_c$) at 25°C and 1 bar. The scatter in the distribution of the symbols in figure 54 is a consequence of the large uncertainty in the relative values of $\bar{V}^\circ_i$ and $\Delta\bar{V}^\circ_n$ computed from the regression equation (see above) as well as the partial dependence of these variables on other properties.

Entropy, volume, and compressibility.—Although $\bar{V}^\circ_i$ for electrolytes exhibits no simple correlation with its crystalline counterpart ($\bar{V}^\circ_{x,i}$), it can be seen in figure 55 that $\bar{V}^\circ_{i,j}$ for both cations and anions is related at 25°C and 1 bar to $\Delta\bar{S}^\circ_{n,j} - Z_j\bar{S}^\circ_{H^+}{}^{abs}$ (table 7), which is equal to $\bar{S}^\circ_j - \Delta\bar{S}^\circ_{s,j}{}^{abs}$ (eq 67). The linear curves in figure 55 are a consequence of the proportional dependence of $\Delta\bar{V}^\circ_{s,j}$ on $\Delta\bar{S}^\circ_{s,j}$ at constant temperature and pressure and the linear relation of $\bar{V}^\circ_j$ to $\bar{S}^\circ_j$ for similar ions at 25°C and 1 bar (fig. 56). Note that the values of $\bar{V}^\circ_j$ and $\bar{S}^\circ_j$ for aqueous complexes shown in the lower diagram of figure 56 have been "normalized" to the number of moles of ions (mole of complex)$^{-1}$.

The relation of $\bar{V}^\circ_j$ to $\bar{S}^\circ_j$ in figure 56 is similar to that exhibited by the standard partial molal volumes and entropies of dissociation for aqueous complexes at 25°C and 1 bar, which also exhibit a gross linear correlation (Hepler, Stokes, and Stokes, 1965). However, it should be stressed that the scatter in the distribution of the symbols plotted in figure 56 cannot be attributed entirely to errors in $\bar{V}^\circ_j$ and/or $\bar{S}^\circ_j$. Each of these properties depends on other variables, only some of which are directly related. Although correlations of the kind shown in figures 54

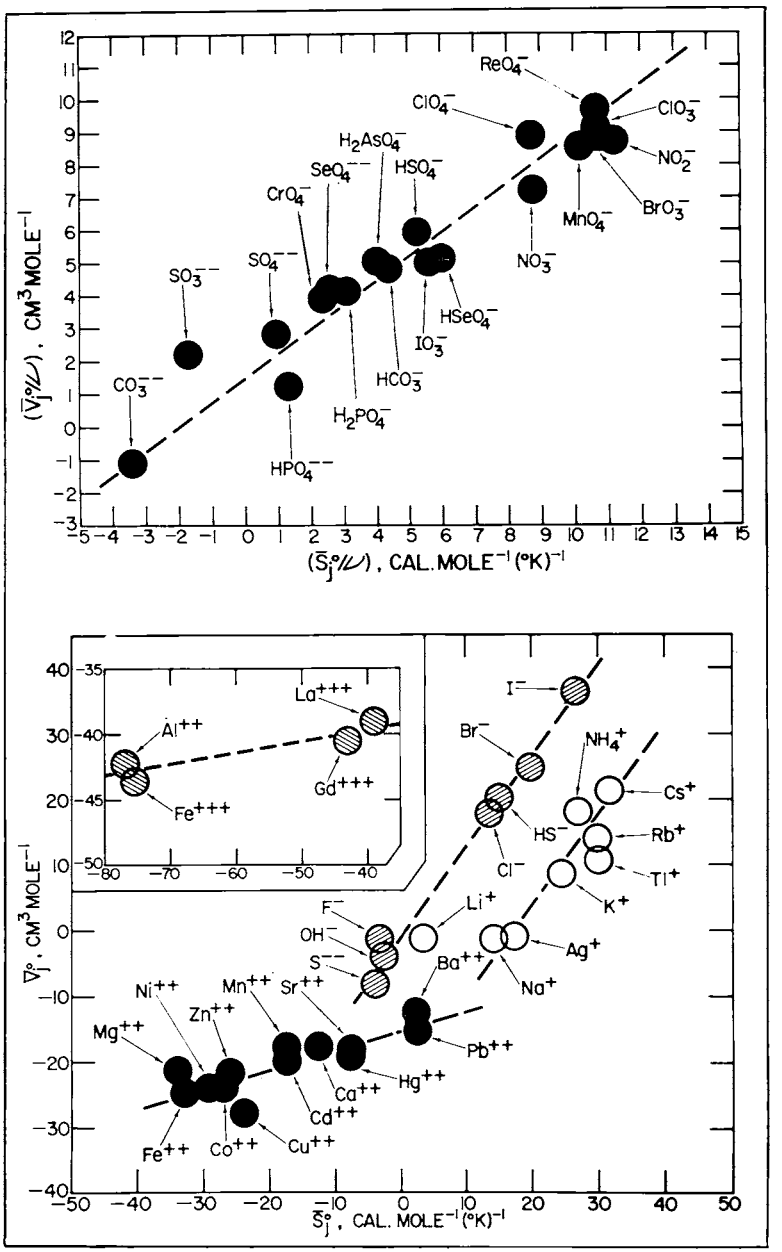

Fig. 56. Correlation of conventional standard partial molal volumes ($\bar{V}^\circ_j$) and entropies ($\bar{S}^\circ_j$) of aqueous species at 25°C and 1 bar. The values of $\bar{V}^\circ$ were taken from Millero (1972a) or computed from equations (39) and (40), coefficients in tables 17 and 18, the appropriate value of Q in table 4, and (where no a_1 or a_3 coefficients are available) the approximations $a_1 \approx \sigma_{20\ bars}$ and $a_3 \approx \xi_{20\ bars}$. The values of $\bar{S}^\circ_j$ shown above are given in table 7 and/or reported by Wagman and others (1968), Wagman and others (1969), Wagman and others (1971), or Parker, Wagman, and Evans (1971). The symbol ν refers to the number of moles of ions (mole of complex)$^{-1}$.

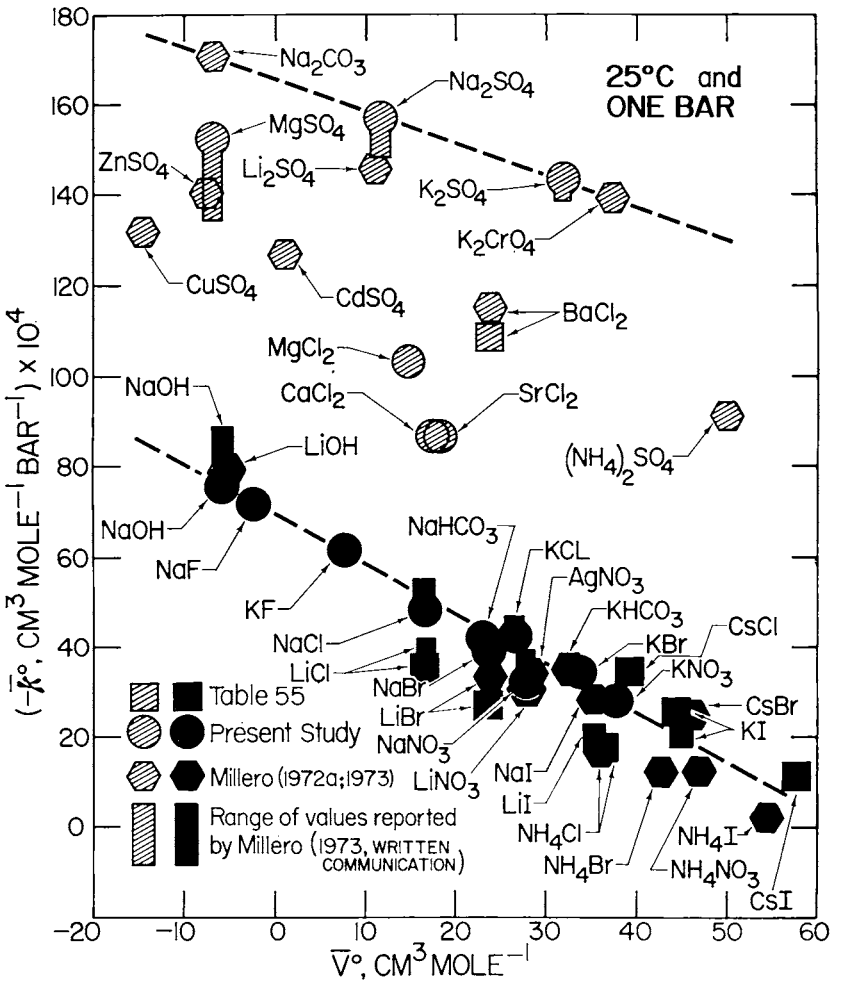

Fig. 57. Correlation of the standard partial molal compressibilities of aqueous electrolytes ($\bar{\kappa}°$) with their standard partial molal volumes ($\bar{V}°$) at 25°C and 1 bar. The values of $\bar{\kappa}°$ were taken from Millero (1973; written commun., 1973) and/or computed from equation (43), coefficients in table 11, and the appropriate value of N in table 4. The values of $\bar{V}°$ were taken from Millero (1972b) or computed from equation (39), coefficients in table 11, and the appropriate value of Q in table 4. The vertical bars represent the range of $\bar{\kappa}°$ values reported in the literature.

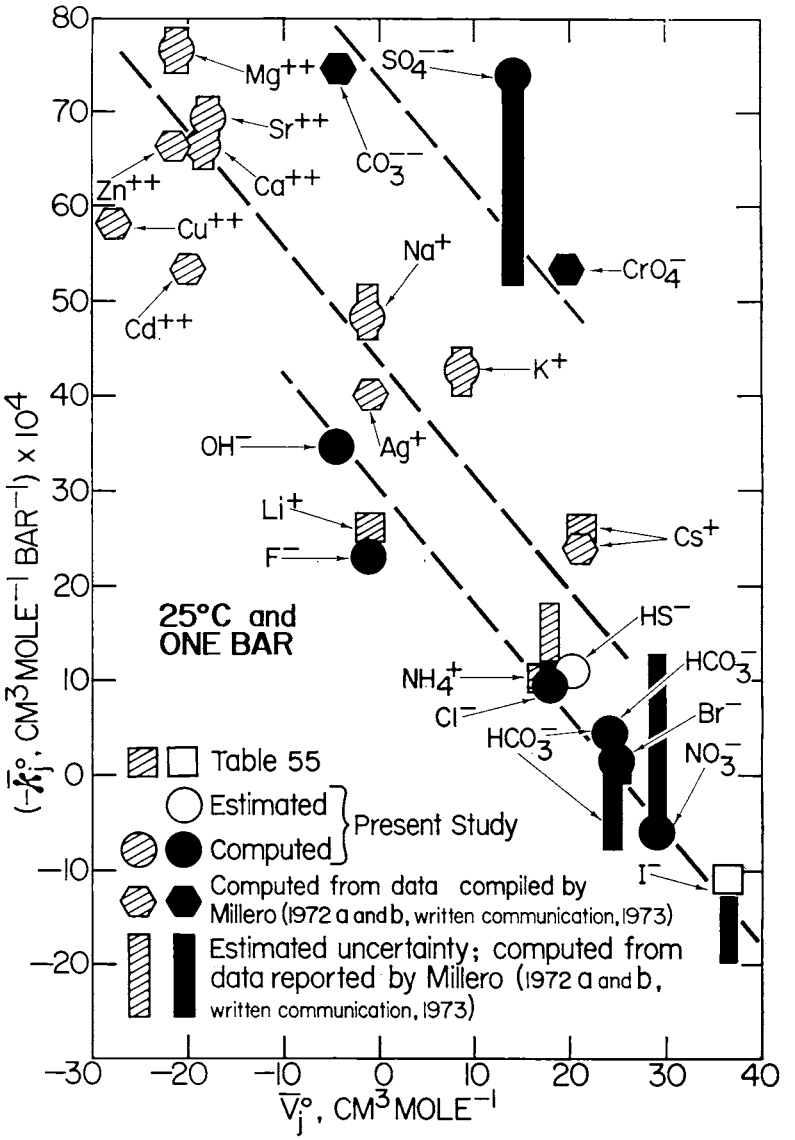

Fig. 58. Correlation of the conventional standard partial molal compressibilities of aqueous ions ($\bar{\kappa}^\circ_j$) with their conventional standard partial molal volumes ($\bar{V}^\circ_j$) at 25°C and 1 bar. The values of $\bar{\kappa}^\circ$ were calculated by additivity from those for electrolytes given by Millero (1973; written commun., 1973) or computed from equation (43), coefficients in tables 18 and 31, and the appropriate value of N in table 4. The values of $\bar{V}^\circ$ were taken from Millero (1972a) or computed from equation (39), coefficients in tables 18 and 31, and the appropriate value of Q in table 4. The vertical bars represent the range of $\bar{\kappa}^\circ$ values reported in the literature.

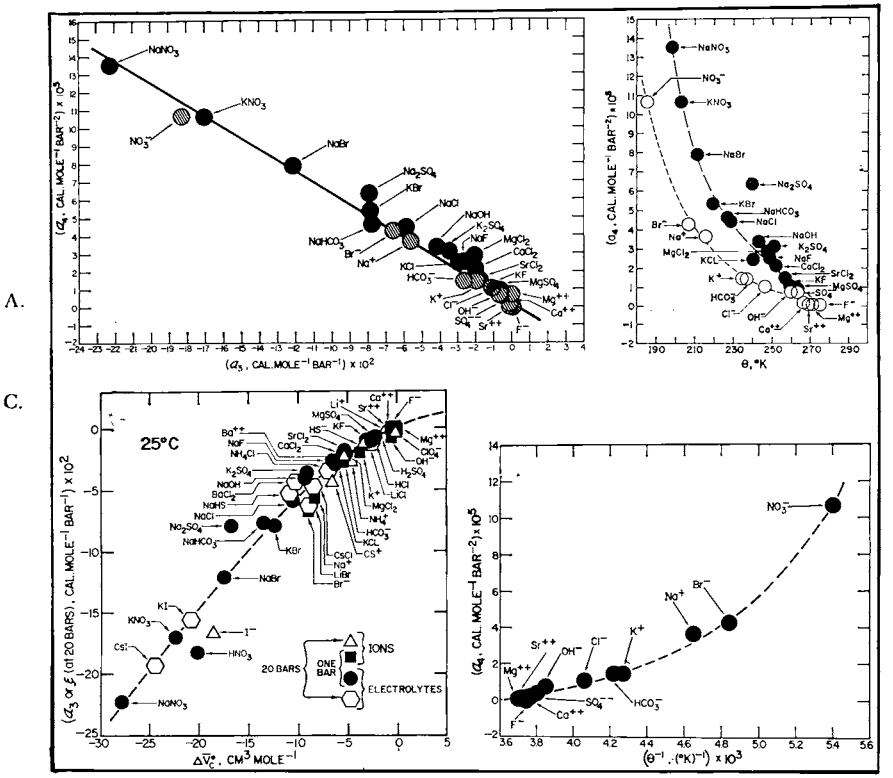

Fig. 59. Correlations among equation of state coefficients for aqueous electrolytes and ionic species (tables 8, 11, 17, and 18).

through 56 afford approximations and estimates of the thermodynamic properties of aqueous species, they should not be considered fundamentally significant.

It can be seen in figure 57 that the standard partial molal compressibilities of 1:1 electrolytes increase as the standard partial molal volume decreases at 25°C and 1 bar. Inconsistencies, discrepancies, and uncertainties in values of $-\bar{K}^\circ$ reported in the literature are primarily responsible for the scattered distribution of the symbols in figure 57. The scatter is magnified in figure 58, where the inconsistencies in $-\bar{K}^\circ$ for electrolytes lead to large discrepancies in corresponding values of $-\bar{K}_j$ for anions. Nevertheless, as suggested by Litvinenko (1963), it appears that $-\bar{K}^\circ$ can be correlated with $\bar{V}^\circ$. The curve for 1:1 electrolytes in figure 57 is consistent with those for the monovalent ions in figure 58.

Various other properties of aqueous electrolytes exhibit correlations of the kind summarized above, some of which afford estimates of the thermodynamic behavior of electrolytes at high pressures and temperatures from data at 25°C and 1 bar (Helgeson and Kirkham, in prepara-

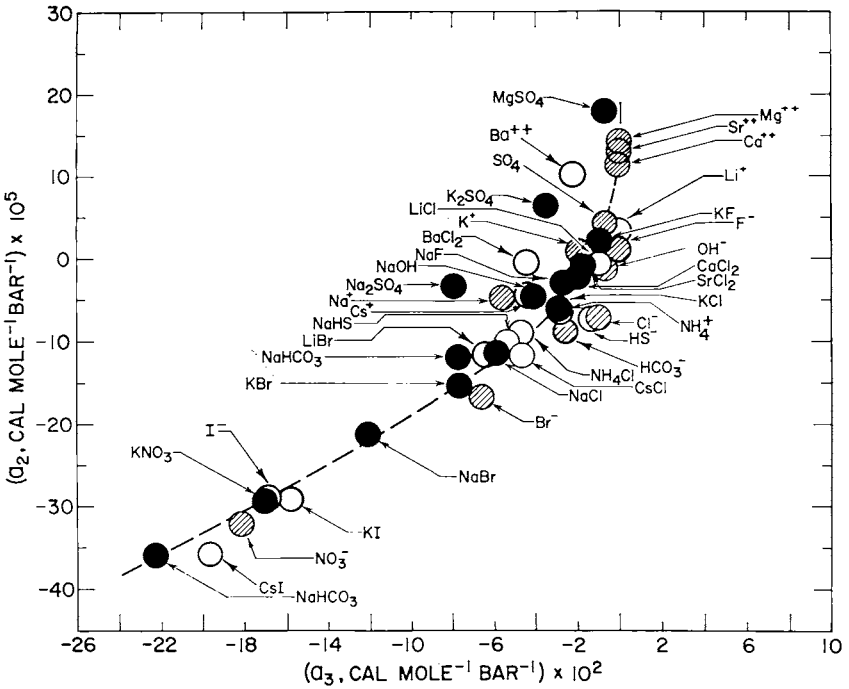

Fig. 60. Correlation of a_2 with a_3 (tables 11 (closed circle), 18 (striped circle), and 55 (open circle).

tion). These correlations in part manifest the interrelation of various coefficients in the equation of state for aqueous electrolytes.

Equation of state coefficients.—Because the regression equation derived from the equation of state is a nonlinear function of a_3, a_4, and θ, these coefficients are interdependent. However, it can be seen in figure 59 that only in the case of a_4 as a function of a_3 is this dependence linear. Because a_3 differs only slightly from ξ at 20 bars, values of the latter variable are also plotted in figure 59 for those electrolytes lacking compressibility data at temperatures > 25°C. The scatter in the distribution of the symbols in figure 59 is a measure of the relative uncertainty in the values of a_3, a_4, and θ obtained from the regression analysis. It can be seen in figure 60 that a_2 exhibits a gross correlation with a_3, but in this case the scatter in the distribution of the symbols is in part a manifestation of the dependence of a_2 on other properties of the aqueous species.

Various algorithms for predicting independently the absolute standard intrinsic partial molal volumes of aqueous ions ($\bar{V}^\circ_{i,j}{}^{abs}$) have been suggested in the literature (for example, see Conway, Verrall, and Desnoyers, 1965, 1966; Pankhurst, 1969; Hepler, 1957; Stokes and Robinson, 1957; Mukerjee, 1961; Glueckauf, 1965; Noyes, 1964; Millero, 1972a), most of which are predicated on spherical ion symmetry. As a rule, the absolute standard intrinsic partial molal volume of an ion at 25°C and 1

bar (where $\bar{V}^\circ_{i,j}{}^{abs} = a_1 + a_2 \approx a_1$) is regarded in theoretical models as the sum of the standard partial molal crystal volume of the species ($\bar{V}^\circ_{x,i,j}$) and an absolute disorder contribution ($\bar{V}^\circ_{d,j}{}^{abs}$) representing void space in its solvation shell; that is,

$$\bar{V}^\circ_{i,j}{}^{abs} = \bar{V}^\circ_{x,i,j} + \bar{V}^\circ_{d,j}{}^{abs} \tag{119}$$

where $\bar{V}^\circ_{x,i,j}$ (in cm^3 mole^{-1}) is given by

$$\bar{V}^\circ_{x,i,j} = 2.5227\ r_{x,j}{}^3 \tag{120}$$

where $r_{x,j}$ stands for the crystal radius of the jth ion in angstroms.

$\bar{V}^\circ_{d,j}{}^{abs}$ in equation (115) has been correlated with various functions of $r_{x,j}$ which purport to represent the intrinsic radius ($r_{i,j}$) of ions in aqueous solution. For example, if $\bar{V}^\circ_{d,j}{}^{abs}$ is proportional to the crystal volume of an ion, it follows that

$$\bar{V}^\circ_{d,j}{}^{abs} = 2.5227\ \hat{a}\ r_{x,j}{}^3 \tag{121}$$

and

$$\bar{V}^\circ_{i,j}{}^{abs} = 2.5227\ r_{x,j}{}^3\ (1 + \hat{a}) \tag{122}$$

where $\hat{a}$ is a constant for a given class of ions. In contrast, if $\bar{V}^\circ_{d,j}{}^{abs}$ is proportional to the surface area of a spherical ion, then

$$\bar{V}^\circ_{d,j}{}^{abs} = 7.568\ \hat{a}\ r_{x,j}{}^2 \tag{123}$$

which implies that $\bar{V}^\circ_{i,j}{}^{abs}$ corresponds to the absolute intrinsic volume of an ellipsoidal ion; that is,

$$\bar{V}^\circ_{i,j}{}^{abs} = 2.5227\ r_{x,j}{}^2\ (r_{x,j} + 3\hat{a}) \tag{124}$$

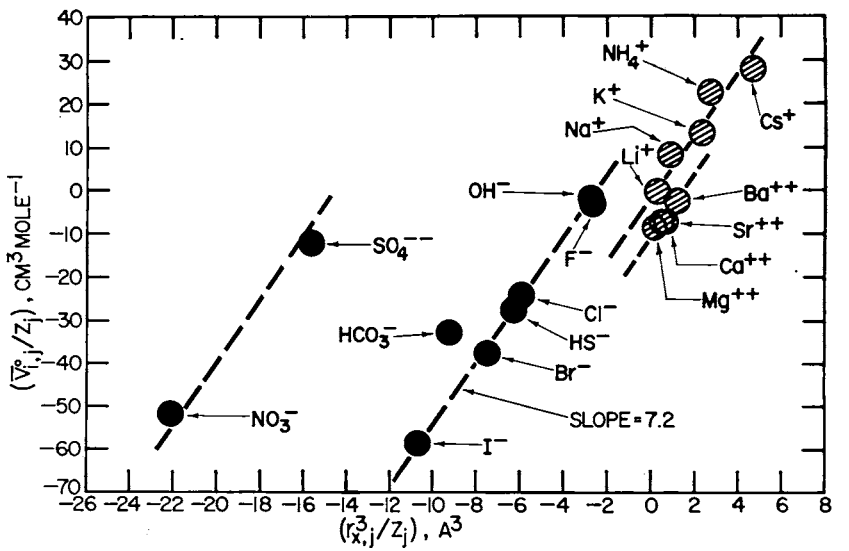

Fig. 61. Correlation of the conventional intrinsic standard partial molal volumes of aqueous ions with the cube of the crystallographic radius of the ions (table 7).

Another assumption commonly made in theoretical calculations of $\bar{V}^{\circ}_{i,j}{}^{abs}$ is that $r_{i,j}$ can be represented by

$$r_{i,j} = r_{x,j} + \hat{a} \tag{125}$$

where â again represents a constant for a given class of ions. Although equation (125) is analogous to equation (61), which represents the effective electrostatic radius of an ion ($r_{e,j}$) as a function of $r_{x,j}$, $r_{e,j}$ and $r_{i,j}$ are not equivalent.

It can be deduced from figure 61 that the conventional counterpart of equation (122) with a finite intercept and a conventional analog of â equal to 1.85 A for both monovalent and divalent cations and anions affords close approximation of nearly all the values of $\bar{V}^{\circ}_{i,j}$ computed in this study ($\bar{V}^{\circ}_{i,j} = a_1 + a_2 \approx a_1 \approx \sigma_{20\ bars}$). The intercepts of the curves for the divalent cations and monovalent anions and cations in figure 61 exhibit a linear dependence on Z_j (fig. 62), which leads to

$$\bar{V}^{\circ}_{i,j} = \bar{V}^{\circ}_{i,j}{}^{abs} - Z_j\bar{V}^{\circ}_{i,H^+}{}^{abs} = 8 - 9.7\ Z_j + 7.2\ r_{x,j}{}^3 \tag{126}$$

Because $\bar{V}^{\circ}_{i,H^-} = 0$, it follows that $r_{x,H^+} = 0.62$A, which differs considerably from the value computed from electrostatic considerations (table 7). In contrast to equation (122), equation (126) requires a linear dependence of $\bar{V}^{\circ}_{d,j}{}^{abs}$ on the crystal volume of an ion, which is consistent with equation (125) to the extent that $\bar{V}^{\circ}_{d,j}{}^{abs}$ is finite at $r_{x,j} = 0$.

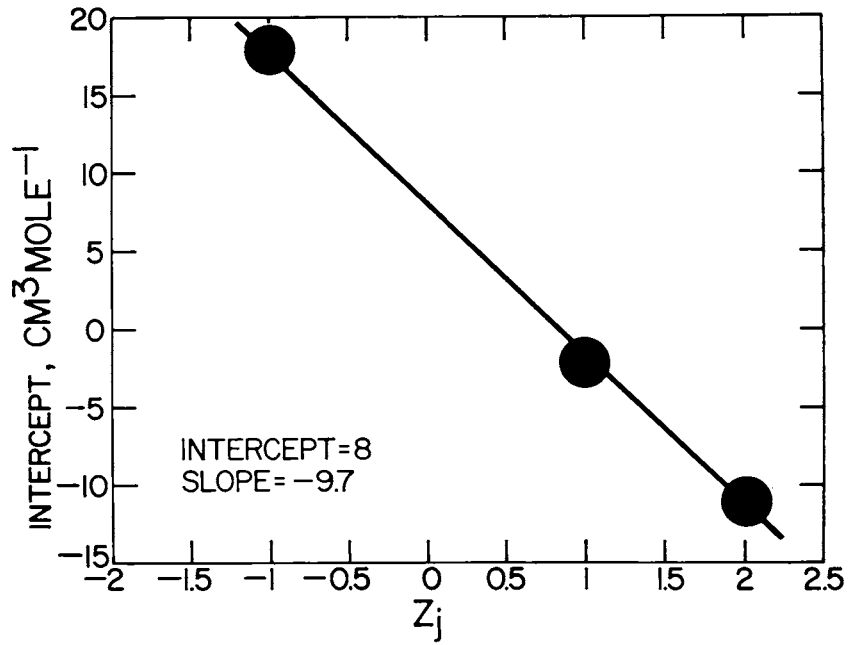

Fig. 62. Intercepts of the curves in figure 61 for monovalent anions and cations and divalent cations as a function of ionic charge (Z_j).

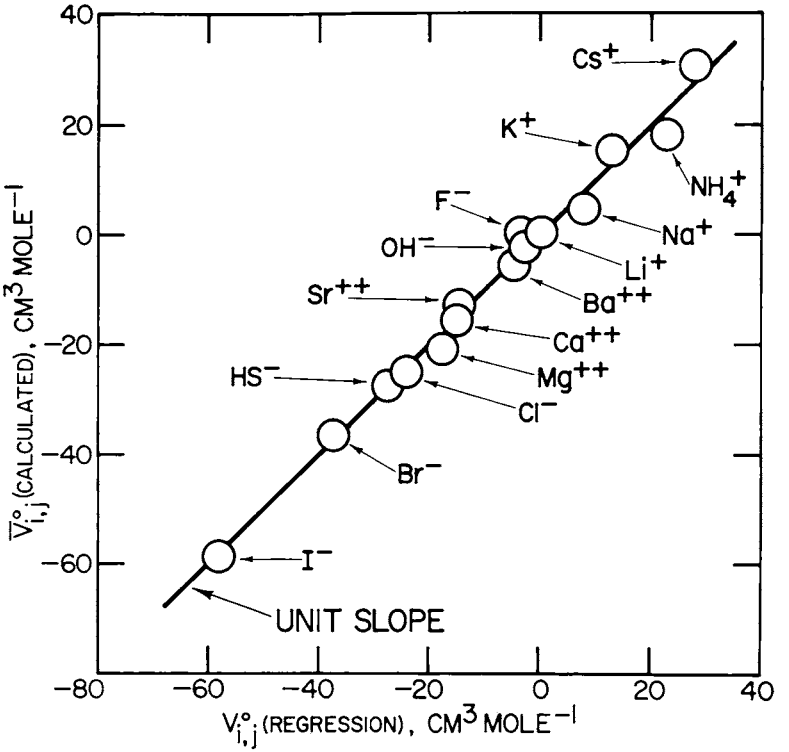

Fig. 63. Correlation of the conventional intrinsic standard partial molal volumes of aqueous ions ($\bar{V}^\circ_{i,j}$) computed from equation (126) with those calculated from equation (31) and values of a_1 or $\sigma_{20\ bars}$ (tables 17 and 18).

Although figure 63 leaves little doubt that equation (126) yields values of $\bar{V}^\circ_{i,j}$ in close agreement with those obtained in the regression analysis described above, it can be deduced from figure 64 that various other algorithms also yield acceptable (but less convincing) representations of $\bar{V}^\circ_{i,j}$ as a function of $r_{x,j}$. The linear relations shown in figure 64 correspond to

$$\bar{V}^\circ_{i,j} = \bar{V}^\circ_{i,j,\, r_{i,j}=0} + 2.5227\, r_{i,j}^3 \tag{127}$$

with $r_{i,j}$ represented by equation (125) and

$$\bar{V}^\circ_{i,j} = \bar{V}^\circ_{x,j} + \bar{V}^\circ_{i,j,\, r_{i,j}=0} + \hat{a}\, r_{i,j}^2 \tag{128}$$

or

$$\bar{V}^\circ_{i,j} = \bar{V}^\circ_{x,j} + \bar{V}^\circ_{i,j,\, r_{i,j}=0} + (\hat{a}\, r_{i,j}^2/|Z_j|) \tag{129}$$

with $r_{i,j}$ represented alternately by $r_{i,j} = r_{x,j}$ and $r_{i,j} = r_{e,j}$. It can also be shown that

$$\bar{V}^\circ_{i,j} = \bar{V}^\circ_{i,j\ r_{e,j}=0} + \hat{a}\, r_{e,j}^3 \tag{130}$$

affords a close approximation of $\bar{V}^\circ_{i,j}$.

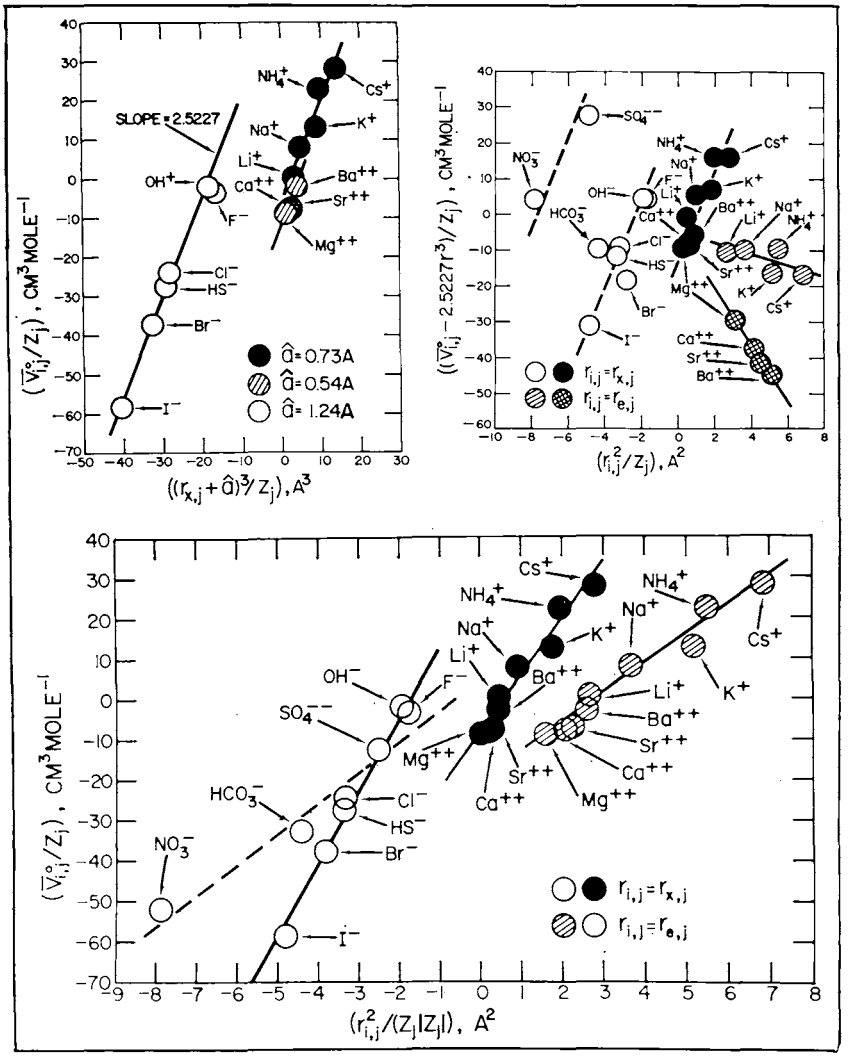

Fig. 64. Correlation of the conventional intrinsic standard partial molal volumes of aqueous ions ($\bar{V}^{\circ}_{i,j}$) with various radius functions (see text and eqs 127 through 132).

TABLE 31

Estimated equation of state coefficients for various ions and electrolytes

Species	σ[a]	$\xi \times 10^2$[a]	θ[b]	$\omega \times 10^{-5}$[c]	a_1[d]	$a_2 \times 10^5$[e]	$a_3 \times 10^2$[f]	$a_4 \times 10^5$[g]	$-\bar{\kappa}^\circ \times 10^4$[h]	$\bar{V}^\circ$[k]
Li^+	0.0052	-0.0379	253.94	0.4862	0.004	3.62	-0.043	0.223	26.0[j]	-1.1
Cs^+	0.6687	-4.2301	217.04	0.0974	0.670	-4.41	-4.286	2.806	25.6[j]	21.2
NH_4^+	0.5540	-2.8468	225.29	0.1791	0.555	-6.08	-2.886	1.954	9.7[j]	17.9
Ba^{++}	-0.1086	-2.2555	245.02	0.9851	-0.111	10.39	-2.287	1.589	90.0[j]	-12.3
I^-	1.3904	-16.6538	186.51	1.2934	1.396	-28.68	-16.863	10.459	-9.0[j]	36.4
HS^-	0.6501	-1.2713	252.19	1.4410	0.651	-6.98	-1.291	0.983	11[j]	20.2
LiCl	0.5798	-1.0827	246.49	1.9421	0.580	-0.89	-1.100	0.867	35.4[l]	16.8
CsCl	1.2339	-4.6499	231.08	1.5534	1.236	-8.76	-4.711	3.064	34.9[m]	39.1
NH_4Cl	1.1258	-3.6962	234.68	1.6351	1.127	-6.45	-3.746	2.477	19.0[l]	35.8
LiBr	0.8928	-6.3724	209.09	1.8719	0.895	-11.45	-6.455	4.125	27.4[l]	23.8
KI	1.6626	-15.6023	204.46	1.4861	1.668	-28.77	-15.799	9.811	24.2[l]	45.1
CsI	2.0408	-19.4275	198.66	1.3908	2.048	-35.61	-19.671	12.167	16.6[m]	57.6
NaHS	0.8168	-5.3073	237.21	1.7716	0.819	-9.23	-5.377	3.469	49[h]	18.9
$BaCl_2$	1.0408	-4.3526	245.52	3.8970	1.041	-0.20	-4.414	3.081	108.7[m]	23.6

[a] cal mole^{-1} bar^{-1} at 20 bars (from tables 8 and 17). [b] °K (from tables 8 and 17). [c] cal mole^{-1} (from tables 8 and 17). [d] cal mole^{-1} bar^{-1} (computed from eq 28 and the values of σ and a_2 shown above). [e] cal mole^{-1} bar^{-2} (computed from eq 43, the values of $-\bar{\kappa}^\circ$, a_4, θ, and ω shown above, and $N = -2.24 \times 10^{-10}$). [f] cal mole^{-1} bar^{-1} (computed from eq 29 using the values of ξ and a_4 shown above). [g] cal mole^{-1} bar^{-2} (computed from eq 131 using the values of ξ shown above for a_3). [h] cm^3 mole^{-1} bar^{-1} at 25°C and 1 bar (computed from equation (132) and the value of $\bar{V}^\circ_{NaHS}$ shown above). [j] cm^3 mole^{-1} bar^{-1} at 25°C and 1 bar (Millero, written communication, 1973). [j] cm^3 mole^{-1} at 25°C and 1 bar (computed from additivity relations using values of $-\bar{\kappa}^\circ$ for ions at 25°C and 1 bar calculated from equation (43) and coefficients in table 18 and those for the electrolytes shown above). [k] cm^3 mole^{-1} at 25°C and 20 bars (from tables 9 and 14). [l] Generated by extrapolation to infinite dilution of apparent molal compressibilities reported by Allam (1963) using the partial derivative of equation (57a) with respect to pressure at constant temperature and theoretical values of $\hat{a}$ (Helgeson and Kirkham, 1976). [m] Mathieson and Conway (1974).

It can be seen in figure 64 that the values of $\hat{a}$ (in eq 125) for cations generated by regression are not greatly different from the value of 0.55A proposed by Glueckauf (1965). In contrast to equations (124) and (126), which are consistent with elliptical and spherical symmetry, respectively, equation (129) implies a cylindrical configuration for solvated ions. Although equation (126) affords accurate calculation of $\bar{V}^\circ_{i,j}$, the partial success of equations (127) through (130) casts considerable doubt on its fundamental significance. None of the algorithms discussed above for computing $\bar{V}^\circ_{i,j}$ is satisfactory in this regard.

Because ξ at 20 bars differs only slightly from a_3, close approximations of a_4 for ions and electrolytes for which compressibilities at temperatures > 25°C are not available can be computed from the equation of the curve in figure 59A and values of ξ obtained by regression of $\bar{V}^\circ$ as a function of temperature at 20 bars. The curve in figure 59A can be represented by

$$a_4 = 2 \times 10^{-6} - 6.16 \times 10^{-4}\, a_3 \qquad (131)$$

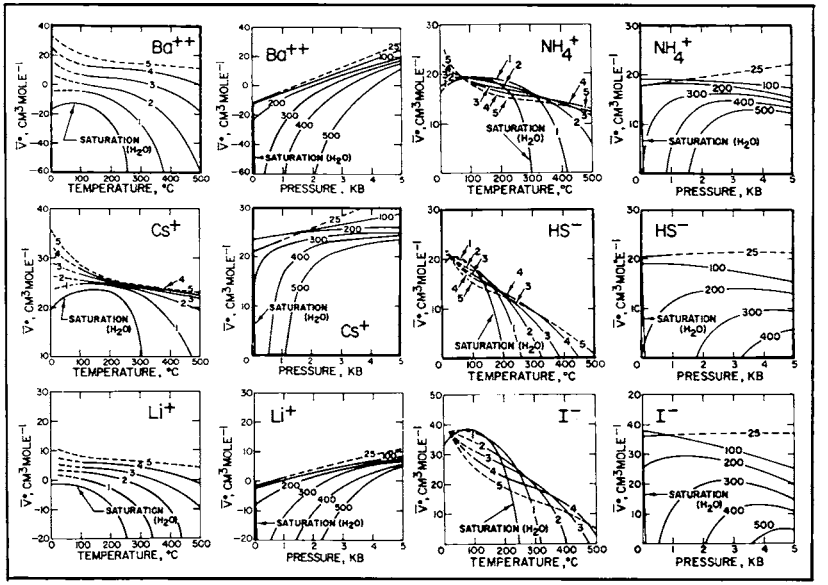

Fig. 65. Conventional standard partial molal volumes ($\bar{V}°$) of aqueous ions as a functions of temperature (in °C) and pressure (in kb) computed from equation (39), coefficients in table 31, and values of Q given by Helgeson and Kirkham (1974a).

where a_3 and a_4 are expressed in cal mole^{-1} bar^{-1}. Combining the values of ξ in table 31 with equation (131) leads to the values of a_j shown in the table. The values of a_3 in the table were computed from the estimated a_4 coefficients with the aid of equation (29). Except for HS^- and NaHS, estimates of a_2 for the ions and electrolytes listed in table 31 were calculated from equation (43) and values of $-\bar{\kappa}°$ at 25°C and 1 bar taken from Mathieson and Conway (1974) or obtained by extrapolating to infinite dilution apparent molal compressibilities reported by Allam (ms) using the partial derivative of equation (57a) with respect to pressure at constant temperature and theoretical values of å (Helgeson and Kirkham, in preparation). Corresponding estimates of a_2 for HS^- and NaHS were generated from equation (43) with the aid of a predicted value of $\bar{\kappa}°$ for NaHS computed from the equation of the curve for 1:1 electrolytes in figure 57. The curve in figure 57 is consistent with

$$-\bar{\kappa}° = 70 \times 10^{-4} - 1.11 \times 10^{-4}\,\bar{V}° \qquad (132)$$

where $\bar{V}°$ and $\bar{\kappa}°$ are expressed in cm^3 mole^{-1} and cm^3 mole^{-1} bar^{-1}, respectively. Combining the computed values of a_2 and the regression values of σ in table 31 with equation (28) generated the values of a_1 in the table.

It can be seen in figure 60 that the estimated values of a_2 in table 31 are consistent with the empirical correlation of the regression values of a_2 with a_3. Similarly, the estimated value of $-\bar{\kappa}°$ for HS^- in the table is compatible with the curve for simple anions in figure 58. High pressure/temperature values of $\bar{V}°_j$, $\bar{E}°_{x,j}$, and $-\bar{\kappa}°_j$ computed from the estimated

coefficients for the ions in table 31 are plotted in figures 65 through 67 and numerical values for HS^- are given in tables 32 through 34. Corresponding numerical values for the other ions shown in the figures can be computed from equations (39), (41), and (43) using the appropriate coefficients in table 31 and the values of Q, U, and N tabulated by Helgeson and Kirkham (1974a).

Differences in additivity values of $\bar{V}°$ for electrolytes computed from the values of $\bar{V}°_j$ plotted in figure 65 and those generated directly from the estimated coefficients for electrolytes in table 31 are comparable to the discrepancies discussed above for the species shown in table 11. It can be seen in figures 65 through 67 that the estimates in table 31 yield values of $\bar{V}°_j$, $\bar{E}°_{x,j}$, and $-\bar{\kappa}°_j$ comparable to those depicted in figures 51 through 53, which were computed directly from the regression coefficients in table 18. Note that the predicted high pressure/temperature behavior of $\bar{V}°_j$, $\bar{E}°_{x,j}$, and $\bar{\kappa}°_j$ for Ba^{++}, Cs^+, and Li^+ in figures 65 through 67 is similar to that for the other cations in figures 51 through 53, but the curves for NH_4^+ are similar to those for HS^- and I^- in figures 65 through 67. The latter curves are comparable to those for Br^-, Cl^-, HCO_3^-, and NO_3^- in figures 51 through 53. NH_4^+ thus appears to exhibit anomalous behavior compared to that of other cations, which is also true of F^-, OH^-, and SO_4^{--} compared to other anions (see above).

Estimates of equation of state coefficients can also be made for ions and electrolytes for which thermodynamic data are available only at 25°C and 1 bar. Such estimates, together with calculation and correlation of

TABLE 32

Conventional standard partial molal volume ($\bar{V}°$) of HS^- in cm^3 $mole^{-1}$ computed from equation (39), coefficients in table 31, and values of Q reported by Helgeson and Kirkham (1974a)

t	PRESSURE, KB									
(°C)	SAT	0.5	1	2	2.5	3	3.5	4	4.5	5
25	20.2	20.6	20.8	(21.1)	(21.2)	(21.2)	(21.3)	(21.3)	(21.3)	(21.3)
50	20.6	20.7	20.5	(20.1)	(19.9)	(19.6)	(19.2)	(18.9)	(18.5)	(18.1)
75	20.1	20.2	20.0	(19.4)	(19.0)	(18.6)	(18.1)	(17.6)	(17.0)	(16.5)
100	18.8	19.2	19.1	18.6	18.2	17.7	17.2	16.6	16.0	(15.4)
125	16.8	17.8	18.0	17.7	17.4	16.9	16.4	15.8	15.2	(14.5)
150	13.8	15.7	16.5	16.6	16.5	16.1	15.6	15.1	14.4	(13.8)
175	9.2	12.9	14.6	15.3	15.4	15.2	14.8	14.3	13.7	(13.1)
200	2.2	9.0	12.0	13.7	14.1	14.1	13.9	13.5	13.0	(12.4)
225	-9.0	3.3	8.6	11.8	12.6	13.0	12.9	12.7	12.2	(11.7)
250	-28.1	-4.9	4.1	9.4	10.9	11.6	11.9	11.8	11.5	(11.0)
275	-63.3	-17.4	-2.1	6.6	8.8	10.1	10.7	10.8	0.7	(10.3)
300	-137.9	-37.3	-10.8	3.2	6.4	8.3	9.3	9.8	9.8	(9.6)
325	-337.0	-70.7	-23.0	-0.9	3.6	6.3	7.8	8.6	8.9	(8.8)
350	-1235.2	-130.7	-40.5	-5.8	0.2	4.0	6.1	7.3	7.9	(8.0)
375		-249.3	-65.8	-12.0	-3.7	1.3	4.2	5.9	6.8	(7.1)
400		-517.7	-102.5	-19.6	-8.4	-1.9	1.9	4.2	5.5	(3.8)
425		(-1216.0)	-155.6	-29.3	-14.2	-5.7	-0.7	2.3	4.1	(5.1)
450		(-2749.9)	-231.9	-41.4	-21.2	-10.2	-3.7	0.1	2.5	(3.8)
475		(-4119.8)	-340.3	-56.8	-29.8	-15.5	-7.3	-2.4	0.6	(2.4)
500		(-4610.0)	-488.7	-76.0	-40.2	-21.8	-11.5	-5.4	-1.6	(0.8)
525			(-677.3)	(-95.7)	(-49.1)	(-29.6)	(-18.2)	(-10.0)	(-4.4)	(-1.1)
550			(-889.3)	(-121.1)	(-62.8)	(-37.8)	(-23.6)	(-13.8)	(-7.1)	(-3.1)
575			(-1090.6)	(-147.7)	(-77.2)	(-46.4)	(-29.2)	(-17.6)	(-9.9)	(-5.2)
600			(-1237.9)	(-172.3)	(-90.6)	(-54.3)	(-34.2)	(-21.1)	(-12.4)	(-7.1)

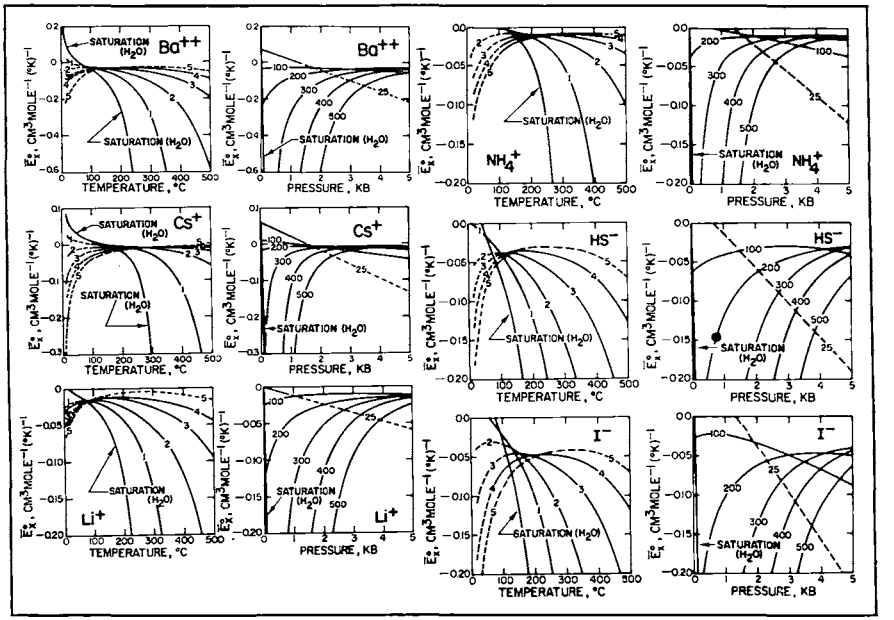

Fig. 66. Conventional standard partial molal expansibilities ($\bar{E}°_x$) of aqueous ions as a function of temperature (in °C) and pressure (in kb) computed from equation (41), coefficients in table 31, and values of U given by Helgeson and Kirkham (1974a).

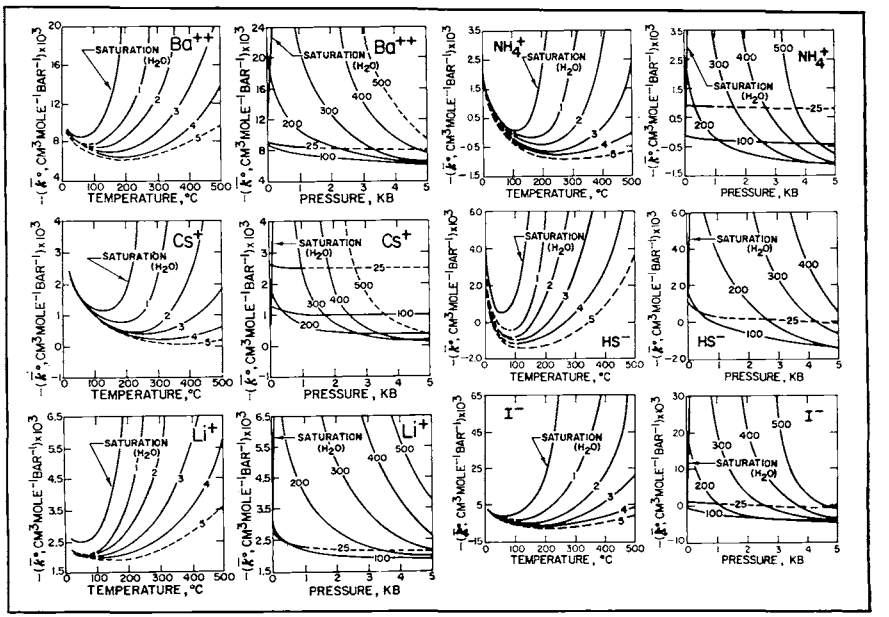

Fig. 67. Conventional standard partial molal compressibilities ($\bar{K}°$) of aqueous ions as a function of temperature (in °C) and pressure (in kb) computed from equation (43), coefficients in table 31, and values of N given by Helgeson and Kirkham (1974a).

osmotic and activity coefficients and the standard and relative partial molal heat capacities, entropies, enthalpies, and Gibbs free energies of aqueous species at high pressures and temperatures are the subject of the fourth (and last) paper in this series of communications (Helgeson and Kirkham, in preparation).

CONCLUDING REMARKS

The equations and coefficients derived above afford a comprehensive basis for quantitative interpretation of phase relations in geologic systems and prediction of the chemical, thermodynamic, and mineralogic consequences of metasomatic reactions in geochemical processes at high pressures and temperatures. For example, isothermal changes in the standard partial molal heat capacity, entropy, Gibbs free energy, and enthalpy of an aqueous electrolyte with increasing pressure can be computed by integrating equations (39), (41), and (42) with respect to pressure at constant temperature, which leads to

$$\bar{C}^\circ_{P,T} - \bar{C}^\circ_{P_r,T} = \left(-T\int_{P_r}^{P}\left(\frac{\partial \Delta \bar{E}^\circ_x}{\partial T}\right)_P dP \right)_T$$

$$= \frac{\theta T\,(2a_3(P - P_r) + a_4(P^2 - P_r^2))}{(T-\theta)^3} + \omega T(X_{P,T} - X_{P_r,T}), \qquad (133)$$

$$\bar{S}^\circ_{P,T} - \bar{S}^\circ_{P_r,T} = -\int_{P_r}^{P} \bar{E}^\circ_{x,T} dP =$$

$$\frac{\theta\left(2a_3(P - P_r) + a_4(P^2 - P_r^2)\right)}{2(T-\theta)^2} + \omega(Y_{P,T} - Y_{P_r,T}), \qquad (134)$$

$$\bar{G}^\circ_{P,T} - \bar{G}^\circ_{P_r,T} = \int_{P_r}^{P} \bar{V}^\circ_T dP =$$

$$\frac{2(a_1 T - a_1\theta + a_3 T)(P - P_r) + (a_2 T - a_2\theta + a_4 T(P^2 - P_r^2))}{2(T-\theta)} + \omega\left(\frac{1}{\varepsilon_{P,T}} - \frac{1}{\varepsilon_{P_r,T}}\right), \qquad (135)$$

TABLE 33

Conventional standard partial molal expansibility ($\bar{E}°_x$) of HS^- in cm^3 $mole^{-1}$ $(°K)^{-1}$ computed from equation (41), coefficients in table 31, and values of U given by Helgeson and Kirkham (1974a)

t	PRESSURE, KB									
(°C)	SAT	0.5	1	2	2.5	3	3.5	4	4.5	5
25	0.02	0.00	(-0.02)	(-0.05)	(-0.07)	(-0.09)	(-0.11)	(-0.13)	(-0.14)	(-0.16)
50	-0.02	-0.02	(-0.02)	(-0.04)	(-0.04)	(-0.05)	(-0.06)	(-0.06)	(-0.07)	(-0.08)
75	-0.04	-0.03	(-0.03)	(-0.03)	(-0.03)	(-0.04)	(-0.04)	(-0.04)	(-0.05)	(-0.05)
100	-0.07	-0.05	-0.04	-0.04	-0.03	-0.03	-0.03	-0.04	-0.04	(-0.04)
125	-0.10	-0.07	-0.05	-0.04	-0.04	-0.03	-0.03	-0.03	-0.03	(-0.03)
150	-0.16	-0.10	-0.07	-0.05	-0.04	-0.04	-0.03	-0.03	-0.03	(-0.03)
175	-0.24	-0.14	-0.09	-0.06	-0.05	-0.04	-0.04	-0.03	-0.03	(-0.03)
200	-0.37	-0.19	-0.12	-0.07	-0.06	-0.05	-0.04	-0.03	-0.03	(-0.03)
225	-0.61	-0.28	-0.16	-0.09	-0.07	-0.05	-0.04	-0.04	-0.03	(-0.03)
250	-1.10	-0.41	-0.22	-0.11	-0.08	-0.06	-0.05	-0.04	-0.03	(-0.03)
275	-2.23	-0.64	-0.30	-0.13	-0.09	-0.07	-0.05	-0.04	-0.03	(-0.03)
300	-5.44	-1.04	-0.42	-0.16	-0.11	-0.08	-0.06	-0.05	-0.04	(-0.03)
325	-18.73	-1.80	-0.60	-0.19	-0.13	-0.09	-0.06	-0.05	-0.04	(-0.03)
350	-152.27	-3.35	-0.86	-0.23	-0.15	-0.10	-0.07	-0.06	-0.04	(-0.03)
375		(-6.98)	-1.25	-0.28	-0.18	-0.12	-0.08	-0.06	-0.05	(-0.04)
400		(-16.90)	-1.81	-0.35	-0.21	-0.14	-0.10	-0.07	-0.05	(-0.04)
425			-2.62	-0.44	-0.26	-0.17	-0.11	-0.08	-0.06	(-0.05)
450			-3.75	-0.55	-0.31	-0.20	-0.13	-0.09	-0.07	(-0.05)
475			(-5.26)	(-0.70)	(-0.38)	(-0.24)	(-0.16)	(-0.11)	(-0.08)	(-0.06)
500			(-7.00)	(-0.87)	(-0.46)	(-0.28)	(-0.18)	(-0.13)	(-0.09)	(-0.07)

TABLE 34

Conventional standard partial molal compressibility ($\bar{\kappa}°$) of HS^- (expressed as $-\bar{\kappa}° \times 10^3$) in $(cm^3\ mole^{-1}\ bar^{-1}) \times 10^3$ computed from equation (43), coefficients in table 31, and values of N given by Helgeson and Kirkham (1974a)

t	PRESSURE, KB									
(°C)	SAT	0.5	1	2	2.5	3	3.5	4	4.5	5
25	1.1	0.5	(0.3)	(0.2)	(0.2)	(0.1)	(0.1)	(0.0)	(0.0)	(0.0)
50	0.6	-0.2	(-0.5)	(-0.5)	(-0.5)	(-0.6)	(-0.7)	(-0.7)	(-0.8)	(-0.8)
75	0.7	-0.2	(-0.6)	(-0.7)	(-0.8)	(-0.9)	(-1.0)	(-1.0)	(-1.1)	(-1.1)
100	1.6	0.2	-0.4	-0.7	-0.8	-1.0	-1.1	-1.2	-1.2	(-1.3)
125	3.3	1.0	0.0	-0.5	-0.8	-0.9	-1.1	-1.2	-1.3	(-1.4)
150	6.3	2.4	0.9	-0.2	-0.5	-0.8	-1.0	-1.2	-1.3	(-1.4)
175	11.9	4.8	2.3	0.3	-0.2	-0.6	-0.9	-1.1	-1.2	(-1.3)
200	22.7	8.7	4.2	1.1	0.3	-0.3	-0.6	-0.9	-1.1	(-1.3)
225	44.7	15.3	7.3	2.2	1.0	0.2	-0.3	-0.7	-1.0	(-1.2)
250	94.9	27.0	11.9	3.7	1.9	0.8	0.1	-0.4	-0.8	(-1.0)
275	227.3	48.7	19.2	5.7	3.2	1.6	0.6	-0.1	-0.5	(-0.8)
300	665.8	91.6	30.8	8.4	4.8	2.5	1.2	0.4	-0.2	(-0.6)
325	2830.9	184.1	49.7	12.1	6.8	3.8	2.0	0.9	0.2	(-0.3)
350	29880.0	406.3	80.7	16.9	9.4	5.3	2.9	1.5	0.6	(0.0)
375		(1025.2)	131.9	23.4	12.8	7.2	4.1	2.3	1.1	(0.4)
400		(3112.6)	216.8	32.2	17.1	9.6	5.5	3.2	1.8	(0.8)
425			357.8	44.1	22.7	12.5	7.3	4.3	2.5	(1.4)
450			590.1	60.1	29.8	16.2	9.4	5.6	3.4	(2.0)
475			(958.8)	(81.7)	(39.0)	(20.8)	(11.9)	(7.2)	(4.5)	(2.8)
500			(1490.6)	(110.2)	(50.7)	(26.4)	(15.0)	(9.1)	(5.7)	(3.7)

and

$$\bar{H}^\circ_{P,T} - \bar{H}^\circ_{P_r,T} = \int_{P_r}^{P} \left(\bar{V}^\circ_T - T\bar{E}^\circ_{x,T} \right) dP =$$

$$\frac{2(a_1(T-\theta)^2 + a_3T^2)\,(P - P_r) + (a_2(T-\theta)^2 + a_4T^2)\,(P^2 - P_r^2)}{2(T-\theta)^2}$$

$$+ \omega \left(\frac{1}{\varepsilon_{P,T}} - \frac{1}{\varepsilon_{P_r,T}} + T(Y_{P,T} - Y_{P_r,T}) \right) \qquad (136)$$

where $\bar{C}^\circ_{P,T}$, $\bar{C}^\circ_{P_r,T}$, $\bar{S}^\circ_{P,T}$, $\bar{S}^\circ_{P_r,T}$, $\bar{G}^\circ_{P,T}$, $\bar{G}^\circ_{P_r,T}$ $\bar{H}^\circ_{P,T}$, and $\bar{H}^\circ_{P_r,T}$ represent the standard partial molal heat capacity, third law entropy, Gibbs free energy, and enthalpy of the electrolyte at the subscripted pressure and temperature. These expressions, together with the corresponding equation for $\bar{C}_{P_r}$ as a function of temperature (Helgeson and Kirkham, in preparation), values of the Born functions for H_2O (Helgeson and Kirkham, 1974a), and the equation of state coefficients derived in the preceding pages permit calculation of the relative stabilities of minerals in hydrothermal systems. However, more data are required to test further the equation of state and confirm and extend its applicability at high pressures and temperatures. Among these, precision measurements of the dielectric constant of H_2O and the dielectric constant and densities of aqueous electrolyte solutions at high pressures and temperatures rank high in priority. Hopefully the theoretical framework summarized here will encourage experimental work in this direction and at the same time provide a comprehensive basis for theoretical interpretation of the data.

ACKNOWLEDGMENTS

The work reported here was supported in part by NSF Grants GA 25314, GA 36023, GA 35888, and DES 74-14280, and the donors of the Petroleum Research Fund administered by the American Chemical Society, under PRF #5356-AC2. Additional funds donated by the Kennecott Copper Corporation, the Anaconda Company, and the Committee on Research at the University of California, Berkeley, are also acknowledged with thanks. We are indebted to Joan Delany, Branch Russell, Ron Stoessell, John Walther, Yoshi Hidaka, David Pitou, Joachim Hampel, Dennis Gin, and Michael Lee for assistance with plotting, drafting, references, proofreading, and reproduction, and to Debbie Aoki for typing and retyping the manuscript. Finally, our gratitude to A. J. Ellis, L. A. Dunn, and F. J. Millero for critical reviews of the manuscript, and to J. B. Thompson, Jr. for reminding one of us (HCH) in the shadow of a statue of John Dalton in Manchester, England, that a dearth of definitive data is not necessarily a malignant obstacle to progress in science.

REFERENCES

Adams, L. H., 1932, Equilibrium in binary systems under pressure. II. The system K_2SO_4–H_2O at 25°: Am. Chem. Soc. Jour., v. 54, p. 2224-2243.

Åkerlöf, G. C., and Bender, P., 1941, The density of aqueous solutions of potassium hydroxide: Am. Chem. Soc. Jour., v. 63, p. 1085-1088.

Åkerlöf, G. C., and Kegeles, G., 1939, The density of aqueous solutions of sodium hydroxide: Am. Chem. Soc. Jour., v. 61, p. 1027-1032.

Åkerlöf, G. C., and Teare, J., 1938, A note on the density of aqueous solutions of hydrochloric acid: Am. Chem. Soc. Jour., v. 60, p. 1226-1228.

Allam, D. S., ms, 1963, Ultrasonic studies in some electrolyte solutions: Ph.D. dissert., Univ. London, 189 p.

Arden, B. W., and Astill, K. N., 1970, Numerical algorithms: origins and applications: Menlo Park, Calif., Addison-Wesley, 308 p.

Barker, J. A., and Henderson, D., 1972, The structure and properties of water and aqueous solutions: Washington, D.C., U.S. Dept. Interior, Office of Saline Water, Research and Devel. Prog. Rept. 773, 41 p.

Batuecas, T., 1946, Partial molecular volumes, at 0°, of water, sodium chloride, and potassium chloride in solutions of these halides: Anales Fisica Quimica (Madrid), v. 42, p. 713-722.

Ben-Naim, A., 1973, Molecular theories and models of water and of dilute aqueous solutions, *in* Franks, F., ed., Water, V. 2, Crystalline hydrates; aqueous solutions of simple nonelectrolytes: New York, Plenum Press, p. 585-624.

Benson, S. W., and Copeland, C. S., 1963, The partial molar volumes of ions: Jour. Phys. Chemistry, v. 67, p. 1194-1197.

Bernal, J. D., and Fowler, R. H., 1933, A theory of water and ionic solution, with particular reference to hydrogen and hydroxyl ions: Jour. Chem. Physics, v. 1, p. 515-548.

Bjerrum, N., 1929, Neuere Anschauungen über Elektrolyte: Deutsche Chem. Gesell. Ber., v. 62, p. 1091-1103.

Bockris, J. O'M., 1949, Ionic Solvation: Quart. Rev. (London), v. 3, p. 173-180.

Bockris, J. O'M., and Saluja, P. P. S., 1972, Approximate calculations of the heats and entropies of hydration according to various models: Jour. Phys. Chemistry, v. 76, p. 2298-2310.

Bockris, J. O'M., Saluja, P. P. S., and Madan, G., 1970, The study of ionic solvation: Washington, D.C., U.S. Dept. Interior, Office of Saline Water, Research, and Devel. Prog. Rept. 569, 155 p.

Bodanszky, A., and Kauzmann, W., 1962, The apparent molar volume of sodium hydroxide at infinite dilution and the volume change accompanying the ionization of water: Jour. Phys. Chemistry, v. 66, p. 177-179.

Booth, F., 1957a, The dielectric constant of water and the saturation effect: Jour. Chem. Physics, v. 19, p. 391-394.

———— 1957b, Errata: The dielectric constant of water and the saturation effect: Jour. Chem. Physics, v. 19, p. 1327-1328.

———— 1957c, Erratum: errata: The dielectric constant of water and the saturation effect: Jour. Chem. Physics, v. 19, p. 1615.

Born, M., 1920, Volumen und Hydratationswärme der Ionen: Zeitschr. Physik, v. 1, p. 45-48.

Brummer, S. B., and Gancy, A. B., 1972, Aqueous solutions under extreme conditions. I. High pressures, *in* Horne, R. A., ed., Water and aqueous solutions: New York, Wiley-Intersci., p. 745-770.

Clark, R. J. H., and Ellis, A. J., 1960, The effect of pressure on the ionization of some benzoic acids: Chem. Soc. [London] Jour., v. 48, p. 247-254.

CODATA, 1975, CODATA recommended key values for thermodynamics: Jour. Chem. Thermodynamics, v. 7, p. 1-3.

Conway, B. E., 1966, Electrolyte solutions: Solvation and structural aspects: Ann. Rev. Phys. Chemistry, v. 17, p. 481-528.

Conway, B. E., and Barradas, R. G., 1966, eds., Chemical physics of ionic solutions: New York, John Wiley & Sons, Inc., 622 p.

Conway, B. E., and Laliberte, L. H., 1968, H_2O–D_2O isotope effect on partial molal volumes of alkali metal and tetraalkylammonium salts: Jour. Phys. Chemistry, v. 72, p. 4317-4320.

Conway, B. E., Desnoyers, J. E., and Smith, A. C., 1964, The hydration of simple ions and polyions: Royal Soc. London Philos. Trans., ser. A 256, p. 389-437.

Conway, B. E., Verrall, R. E., and Desnoyers, J. E., 1965, Specificity in ionic hydration and the evaluation of individual ionic properties: Zeitschr. Phys. Chemie. (Leipzig), v. 230, p. 157-178.

———— 1966, Partial molal volumes of tetraalkylammonium halides and assignment of individual ionic contributions: Faraday Soc. Trans., v. 62, p. 2738-2749.

Copeland, C. S., Silverman, J., and Benson, S. W., 1953, The system NaCl–H_2O at supercritical temperatures and pressures: Jour. Chem. Physics, v. 21, p. 12-16.

Couture, A. M., and Laidler, K. J., 1956, The partial molal volumes of ions in aqueous solution. I. Dependence on charge and radius: Canadian Jour. Chemistry, v. 34, p. 1209-1216.

———— 1957, The entropies of ions in aqueous solution. II. An empirical equation for oxy-anions: Canadian Jour. Chemistry, v. 35, p. 202-210.

Curthoys, G., and Mathieson, J. G., 1970, Partial molal volumes of ions: Faraday Soc. Trans., v. 66, p. 43-51.

Davis, C. M., and Jarzynski, J., 1972, Liquid water—acoustic properties: absorption and relaxation, *in* Franks, F., ed., Water, V. 1, The physics and physical chemistry of water: New York, Plenum Press, p. 443-462.

Desnoyers, J. E., and Arel, M., 1967, Apparent molal volumes of n-alkylamine hydrobromides in water at 25°C· hydrophobic hydration and volume changes: Canadian Jour. Chemistry, v. 45, p. 359-366.

Desnoyers, J. E., Arel, M., Perron, G., and Jolicoeur, C., 1969, Apparent molal volumes of alkali halides in water at 25°. Influence of structural hydration interactions on the concentration dependence: Jour. Phys. Chemistry, v. 73, p. 3346-3351.

Desnoyers, J. E., and Jolicoeur, C., 1969, Hydration effects and thermodynamic properties of ions, *in* Bockris, J. O'M., and Conway, B. E., ed., Modern aspects of electrochemistry, No. 5: New York, Plenum Press, p. 1-89.

Desnoyers, J. E., Verrall, R. E., and Conway, B. E., 1965, Electrostriction in aqueous solutions of electrolytes: Jour. Chem. Physics, v. 43, p. 243-250.

Dibrov, I. A., Mashovets, V. P., and Mateeva, R. P., 1964, The density and compressibility of aqueous sodium hydroxide solutions at high temperature: Jour. Appl. Chemistry USSR (translation), v. 37, p. 38-44.

Dorsey, N. E., 1940, Properties of ordinary water-substance: New York, Reinhold Publishing Corp., 673 p.

Drakin, S. I., and Mikhailov, V. A., 1959, Calculation of the entropy of cation hydration: Russian Jour. Phys. Chemistry, v. 33, p. 45-48.

Drude, P., and Nernst, W., 1894, Über Elektrostriktion durch freie Ionen: Zeitschr. Phys. Chemie, v. 15, p. 79-85.

Duedall, I. W., and Weyl, P. K., 1965, Apparatus for determining the partial equivalent volumes of salts in aqueous solutions: Rev. Sci. Instruments, v. 36, p. 528-531.

Duncan, J. F., and Kepert, D. L., 1959, Aquo-ions and ion pairs, *in* Hamer, W. J., ed., Structure of electrolytic solutions: New York, John Wiley & Sons, Inc., p. 380-400.

Dunn, L. A., 1966, Apparent molar volumes of electrolytes: Faraday Soc. Trans., v. 62, p. 2348-2354.

———— 1968, Apparent molar volumes of electrolytes. III. Some 1-1 and 2-1 electrolytes in aqueous solution at 0, 5, 15, 35, 45, 55 and 65°C: Faraday Soc. Trans., v. 64, p. 2951-2961.

———— 1974, Ion-solvent interactions in aqueous solutions at various temperatures: Jour. Solution Chemistry, v. 3, p. 1-14.

Dunn, L. A., and Marshall, W. L., 1969, Electrical conductances of aqueous sodium iodide and the comparative thermodynamic behavior of aqueous sodium halide solutions to 800° and 4000 bars: Jour. Phys. Chemistry, v. 73, p. 724-728.

Eigen, M., and DeMaeyer, L., 1959, Hydrogen bond structure, proton hydration, and proton transfer in aqueous solution, *in* Hamer, W. J., ed., Structure of electrolytic solutions: New York, John Wiley & Sons, Inc., p. 64-85.

Eisenberg, D., and Kauzmann, W., 1969, The structure and properties of water: London, Oxford Univ. Press, 296 p.

Ellis, A. J., 1959, The effect of pressure on the first dissociation constant of "carbonic acid": Chem. Soc. [London] Jour., v. 750, p. 3689-3699.

———— 1963, The effect of temperature on the ionization of hydrofluoric acid: Chem. Soc. [London] Jour., p. 4300-4304.

———— 1966, Partial molal volumes of alkali chlorides in aqueous solution to 200°: Chem. Soc. [London] Jour. (A), p. 1579-1584.

———— 1967, Partial molal volumes of $MgCl_2$, $CaCl_2$, $SrCl_2$ and $BaCl_2$ in aqueous solution to 200°: Chem. Soc. [London] Jour. (A), p. 660-664.

Ellis, A. J., 1968, Partial molal volumes in high-temperature water. Part III. Halide and oxyanion salts: Chem. Soc. [London] Jour. (A), p. 1138-1143.
Ellis, A. J., and Anderson, D. W., 1961, The first acid dissociation constant of hydrogen sulphide and high pressures: Chem. Soc. [London] Jour., v. 917, p. 4678-4680.
Ellis, A. J., and McFadden, I. M., 1968, The partial molal volume of hydrochloric acid in high temperature water: Chemical Communications, v. 9, p. 516-517.
———— 1972, Partial molal volumes of ions in hydrothermal solutions: Geochim. et Cosmochim. Acta, v. 36, p. 413-426.
Fajans, K., and Johnson, O., 1942, Apparent volumes of individual ions in aqueous solution: Am. Chem. Soc. Jour., v. 64, p. 668-678.
Fisher, J. R., and Barnes, H. L., 1972, The ion-product constant of water to 350°: Jour. Phys. Chemistry, v. 76, p. 90-99.
Fortier, J. L., Leduc, P. A., and Desnoyers, J. E., 1974, Thermodynamic properties of alkali halides. II. Enthalpies of dilution and heat capacities in water at 25°C: Jour. Solution Chemistry, v. 3, p. 323-349.
Franck, E. U., 1956a, Hochverdichteter Wasserdampf I. Elektrolytische Leitfähigkeit in KCl–H_2O—Lösungen bis 750°C: Zeitschr. Phys. Chemie, v. 8, p. 92-106.
———— 1956b, Hochverdichteter Wasserdampf II. Ionendissoziation von KCl in H_2O bis 750°C: Zeitschr. Phys. Chemie, v. 8, p. 107-126.
———— 1956c, Hochverdichteter Wasserdampf III. Ionendissoziation von KCl, KOH und H_2O in überkritischem Wasser: Zeitschr. Phys. Chemie, v. 8, p. 192-206.
———— 1961, Überkritisches Wasser als electrolytisches Lösungsmittel: Angew. Chemie., v. 73, p. 309-322.
———— 1973, Concentrated electrolyte solutions at high temperatures and pressures: Jour. Solution Chemistry, v. 2, p. 339-353.
Frank, H. S., 1955, Thermodynamics of a fluid substance in the electrostatic field: Jour. Chem. Physics, v. 23, p. 2023-2032.
———— 1958, Covalency in the hydrogen bond and the properties of water and ice: Royal Soc. London Proc., A247, p. 481-492.
———— 1963, Single ion activities and ion-solvent interaction in dilute aqueous solutions: Jour. Phys. Chemistry, v. 67, p. 1554-1558.
———— 1965, Structural influences on activity coefficients in aqueous electrolytes: Zeitschr. Phys. Chemie., v. 228, p. 364-372.
———— 1966, Solvent models and the interpretation of ionization and solvation phenomena, *in* Conway, B. E., and Barradas, R. G., eds., Chemical physics of ionic solutions: New York, John Wiley & Sons, Inc., p. 53-66.
———— 1972, Structural models, *in* Franks, F., ed., Water, V. I. The physics and physical chemistry of water: New York, Plenum Press, p. 514-544.
Frank, H. S., and Quist, A. S., 1961, Pauling's model and the thermodynamic properties of water: Jour. Chem. Physics, v. 34, p. 604-611.
Frank, H. S., and Robinson, A. L., 1940, The entropy of dilution of strong electrolytes in aqueous solutions: Jour. Chem. Physics, v. 8, p. 933-938.
Frank, H. S., and Wen, W. Y., 1957, Structural aspects of ion-solvent interaction in aqueous solutions: a suggested picture of water structure: Faraday Soc. Disc., no. 24, p. 133-140.
Franks, F., 1972, Water, V. I. The physics and physical chemistry of water: New York, Plenum Press, 596 p.
———— 1973, Water, V. 3. Aqueous solutions of simple electrolytes: New York, Plenum Press, 472 p.
Franks, F., and Smith, H. T., 1967, Apparent molal volumes and expansibilities of electrolytes in dilute aqueous solutions: Faraday Soc. Trans., v. 63, p. 2586-2598.
Frantz, J. D., and Eugster, H. P., 1973, Acid-base buffers: Use of Ag + AgCl in the experimental control of solution equilibria at elevated pressures and temperatures: Am. Jour. Sci., v. 273, p. 268-286.
Friedman, H. L., and Krishnan, C. V., 1973, Thermodynamics of ionic solvation, *in* Franks, F., ed., Water, V. 3, Aqueous solutions of simple electrolytes: New York, Plenum Press, p. 1-118.
Gancy, A. B., 1972, Aqueous solutions under extreme conditions. II. High Temperatures, *in* Horne, R. A., ed., Water and aqueous solutions: New York, Wiley-Interscience, p. 771-801.
Gardner, W. L., Mitchell, R. E., and Cobble, J. W., 1969, Thermodynamic properties of high temperature aqueous solutions. XI. Calorimetric determination of the standard partial molal heat capacity and entropy of sodium chloride solutions from 100 to 200°: Jour. Phys. Chemistry, v. 73, p. 2025-2032.

Geffcken, W., 1931, The apparent molecular volume of dissolved electrolytes: Zeitschr. Phys. Chemie., A155, p. 1-28.

Geffcken, W., and Price, D., 1934, Refractometric investigations. XXXIX. Dependence on concentration of the apparent molecular volume and refraction in dilute solutions: Zeitschr. Chemie., v. 1326, p. 81-99.

Gibson, R. E., 1935, The influence of the concentration and nature of the solute on the compressions of certain aqueous solutions: Am. Chem. Soc. Jour., v. 57, p. 284-293.

———— 1938, On the effect of pressure on the solubility of solids in liquids: Am. Jour. Sci., 5th ser., v. 35A, p. 49-69.

Giese, K., Kaatz, U., and Pottel, R., 1970, Permittivity and dielectric and proton magnetic relaxation of aqueous solutions of the alkali halides: Jour. Phys. Chemistry, v. 74, p. 3718-3725.

Gilkerson, W. R., 1970, The importance of the effect of the solvent dielectric constant on ion-pair formation in water at high temperatures and pressures: Jour. Phys. Chemistry, v. 74, p. 746-750.

Glueckauf, E., 1964, Heats and entropies of ions in aqueous solution: Faraday Soc. Trans., v. 60, p. 572-577.

———— 1965, Molar volumes of ions: Faraday Soc. Trans., v. 61, p. 914-921.

———— 1966, Effect of dielectric constant changes in the vicinity of ions on the properties of electrolyte solutions, *in* Conway, B. E. and Barradas, R. G., eds., Chemical physics of ionic solutions: New York, John Wiley & Sons, Inc., p. 67-74.

Gourary, B. S., and Adrian, F. J., 1960, Wave functions for electron-excess color centers in alkali halide crystals: Solid State Physics, v. 10, p. 127-247.

Greyson, J., and Snell, H., 1970, A study of a specific influence of dissolved ions on the structure of water: U.S. Dept. Interior, Office of Saline Water, Research and Devel. Prog. Rept. 523, 32 p.

Gucker, F. T., 1933, The apparent molal heat capacity, volume and compressibility of electrolytes: Chem. Rev., v. 13, p. 111-130.

———— 1934, Calculation of partial molal solute quantities as functions of the volume concentration with special reference to the apparent volume: Jour. Phys. Chemistry, v. 38, p. 307-317.

Guggenheim, E. A., 1935, Specific thermodynamic properties of aqueous solutions of strong electrolytes: Philos. Mag., v. 19, p. 588-643.

Guggenheim, E. A., and Stokes, R. H., 1969, Equilibrium properties of aqueous solutions of single strong electrolytes: New York, Pergamon Press, 148 p.

Gurney, R .W., 1953, Ionic processes in solution: New York, McGraw-Hill, 275 p.

Haggis, G. H., Hasted, J. B., and Buchanan, T. J., 1952, The dielectric properties of water in solutions: Jour. Chem. Physics, v. 20, p. 1452-1465.

Halasey, M. E., 1941, Partial molal volumes of potassium salts of the Hofmeister series: Jour. Phys. Chemistry, v. 45, p. 1252-1263.

Hamman, S. D., 1963, Chemical equilibria in condensed systems, *in* Bradley, R. S., ed., High pressure physics and chemistry, V. 2: New York, Academic Press, p. 131-162.

Hamman, S. D., and Lim, S. C., 1954, The volume change on ionization of weak electrolytes: Australian Jour. Chemistry, v. 7, p. 329-334.

Hamman, S. D., and Strauss, W., 1955, The chemical effects of pressure. Pt. 3. Ionization constants at pressures to 12,000 atmospheres: Faraday Soc. Trans., v. 51, p. 1684-1690.

Harris, F. A. ,and O'Konski, C. T., 1957, Dielectric properties of aqueous ionic solutions at microwave frequencies: Jour. Phys. Chemistry, v. 61, p. 310-319.

Hartman, D., and Franck, E. U., 1969, Elektrische Leitfähigkeit wässeriger Lösungen bei hohen Temperaturen und Drucken. III: Ber. Bunsengesell. für Phys. Chemie, v. 73, p. 514-521.

Hasted, J. B., and El Sabeh, S. H. M., 1953, The dielectric properties of water in solutions: Faraday Soc. Trans., v. 49, p. 1003-1011.

Hasted, J. B., Ritson, D. M., and Collie, C. H., 1948, Dielectric properties of aqueous solutions. Pts. I and II: Jour. Chem. Physics, v. 16, p. 1-21.

Hasted, J. B., and Roderick, G. W., 1958, Dielectric properties of aqueous and alcoholic solutions: Jour. Chem. Physics, v. 29, p. 17-26.

Heger, K., ms, 1969, Die statische Dielektrizitätskonstante von Wasser und Methylalkohol im überkritischen Temperatur und Druckbereich: Ph.D. dissert., Univ. Karlsruhe, West Germany, 58 p.

Helgeson, H. C., and Kirkham, D. H., 1974a, Theoretical prediction of the thermodynamic behavior of aqueous electrolytes at high pressures and temperatures: I. Summary of the thermodynamic/electrostatic properties of the solvent: Am. Jour. Sci., v. 274, p. 1089-1198.

Helgeson, H. C., and Kirkham, D. H., 1974b, Theoretical prediction of the thermodynamic behavior of aqueous electrolytes at high pressures and temperatures: II. Debye-Hückel parameters for activity coefficients and relative partial molal properties: Am. Jour. Sci., v. 274, p. 1199-1261.

Hemmes, P., 1972, The volume changes of ionic association reactions: Jour. Phys. Chemistry, v. 76, p. 895-900.

Hepler, L. G., 1957, Partial molal volumes of aqueous ions: Jour. Phys. Chemistry, v. 61, p. 1426-1428.

Hepler, L. G., and Woolley, E. M., 1973, Hydration effects and acid-base equilibria, *in* Franks, F., ed., Water, V. 3, Aqueous solutions of simple electrolytes: New York, Plenum Press, p. 145-172.

Hepler, L. G., Stokes, J. M., and Stokes, R. H., 1965, Dilatometric measurements of apparent molar volumes of dilute aqueous electrolytes: Faraday Soc. Trans., v. 61, p. 20-29.

Holzapfel, W., and Franck, E. U., 1966, Leitfähigkeit und Ionendissoziation des Wassers bis 1000°C und 100 kbar: Ber. Bunsengesell. für Phys. Chemie, v. 70, p. 1106-1112.

Horne, R. A., 1969, Marine chemistry: New York, Wiley-Interscience, 568 p.

Hunt, J. P., 1965, Metal ions in aqueous solutions: New York, W. A. Benjamin Inc., 124 p.

International Critical Tables, V. III, 1928: New York, McGraw-Hill.

Isono, T., and Tamamushi, R., 1967, Relation between the viscosity B-coefficient and the molal volume of electrolytes in aqueous solutions: Electrochim. Acta, v. 12, p. 1479-1482.

Jones, G., and Bickford, C. F., 1934, The conductance of aqueous solutions as a function of concentration. I. Potassium bromide and lanthanum chloride: Am. Chem. Soc. Jour., v. 56, p. 602-611.

Jones, G., and Colvin, J. H., 1940, VIII. Silver nitrate, potassium sulfate and potassium chromate: Am. Chem. Soc. Jour., v. 62, p. 338-340.

Jones, G., and Fornwalt, H. J., 1936, The viscosity of aqueous solutions as a function of the concentration. III. Cesium iodide and potassium permanganate: Am. Chem. Soc. Jour., v. 58, p. 619-625.

Jones, G., and Talley, S. K., 1933a, The viscosity of aqueous solutions as a function of the concentration: Am. Chem. Soc. Jour., v. 55, p. 624-642.

———— 1933b, The viscosity of aqueous solutions as a function of concentration. II. Potassium bromide and potassium chloride: Am. Chem. Soc. Jour., v. 55, p. 4124-4125.

Kapustinski, A. F., Drakin, S. I., and Yakushevskiy, B. M., 1953, Entropies, heats of hydration, and volumes of ions in aqueous solutions in relation to their electrostatic characteristics: Zhur. Fiz. Khimii, v. 27, p. 433-442.

Kavanaugh, J. L., 1964, Water and solute-water interactions: San Francisco, Holden-Day Inc., 101 p.

Kay, R. L., ed., 1973, The physical chemistry of aqueous systems: New York, Plenum Press, 258 p.

Keenan, J. H., Keyes, F. G., Hill, P. G., and Moore, J. G., 1969, Steam tables: New York, John Wiley & Sons, Inc., 162 p.

Kell, G. S., 1972, Precise representation of volume properties of water at one atmosphere: Chem. Eng. Data, v. 12, p. 66-69.

Kell, G. S., and Whalley, E., 1965, The PVT properties of water. I. Liquid water in the temperature range 0 to 150°C and at pressures up to 1 kb: Royal Soc. London Philos. Trans., ser. A, Math. Phys. Sci., v. 258, p. 565-617.

King, E. J., 1969, Volume changes for ionization of formic, acetic, and butyric acids and the glycinium ion in aqueous solution at 25°: Jour. Phys. Chemistry, v. 73, p. 1220-1232.

Klotz, I. M., and Eckert, C. F., 1942, The apparent molal volumes of aqueous solutions of sulphuric acid at 25°: Am. Chem. Soc. Jour., v. 64, p. 1878-1880.

Kohner, H., 1928, The dependence of equivalent refractivity on the concentration of strong electrolytes in solution: Zeitschr. Phys. Chemie., B1, p. 427-455.

Laidler, K. J., 1956, The entropies of ions in aqueous solution. I. Dependence on charge and radius: Canadian Jour. Chemistry, v. 34, p. 1107-1113.

Laidler, K. J., and Pegis, C., 1957, The influence of dielectric saturation on the thermodynamic properties of aqueous ions: Royal Soc. [London] Proc., ser. A, v. 241, p. 80-92.

Lamb, A. B., and Lee, R. E., 1913, New precise method for determining densities of liquids: Am. Chem. Soc. Jour., v. 35, p. 1666-1693.

Latimer, W. M., 1955, Single ion free energies and entropies of aqueous ions: Jour. Chem. Physics, v. 23, p. 90-92.

Latimer, W. M., Pitzer, K. S., and Slansky, C. M., 1939, The free energy of hydration of gaseous ions, and the absolute potential of the normal calomel electrode: Jour. Chem. Physics, v. 7, p. 108-111.

Lee, S., 1966, The apparent and partial molal volumes of electrolytes in water and in aqueous sodium chloride solutions: Ph.D. thesis, Yale Univ., Univ. Microfilms, Order No. 66-4906, dissert. Abs., B27, 141 p.

Lepple, F. K., and Millero, F. J., 1971, The isothermal compressibility of sea water near one atmosphere: Deep-Sea Research, v. 18, p. 1233-1254.

Lindstrom, R. E., and Wirth, H. E., 1969, Estimation of the bisulfate ion dissociation in solutions of sulfuric acid and sodium bisulfate: Jour. Phys. Chemistry, v. 73, p. 218-223.

Litvinenko, I. V., 1963, The compressibility of aqueous solutions of electrolytes and the hydration of anions and cations: Russian Jour. Structural Chemistry, v. 4, p. 768-772.

Longworth, L. G., 1935, Transference numbers of aqueous solutions of some electrolytes at 25° by the moving boundary method: Am. Chem. Soc. Jour., v. 57, p. 1185-1191.

Lown, D. A., and Thirsk, H. R., 1972, Effect of the solution vapour pressure on temperature dependence of the dissociation constant of acetic acid in water: Faraday Soc. Trans., v. 68, p. 1982-1986.

Lown, D .A., Thirsk, H. R., and Lord Wynne-Jones, 1968, Effect of pressure on ionization equilibria in water at 25°C: Faraday Soc. Trans., v. 64, p. 2073-2080.

———— 1970, Temperature and pressure dependence of the volume of the ionization of acetic acid in water from 25-225°C and 1-3000 bars: Faraday Soc. Trans., v. 66, p. 51-73.

Lucas, M., 1973, Thermodynamic properties of a hard-sphere solute in aqueous solution at various temperatures in relation with hydrophobic hydration: Jour. Phys. Chemistry, v. 77, p. 2479-2483.

Mangold, K., and Franck, E. U., 1969, Elektrische Leitfähigkeit wässeriger Lösungen bei hohen Temperaturen und Drucken. II: Ber. Bunsengesell. für Phys. Chemie, v. 73, p. 21-27.

Marshall, W. L., 1968, Conductances and equilibria of aqueous electrolytes over extreme ranges of temperature and pressure: Rev. Pure and Appl. Chemistry, v. 18, p. 167-186.

———— 1969, Correlations in aqueous electrolyte behavior to high temperatures and pressures: Rec. Chem. Prog., v. 30, p. 61-84.

———— 1970, Complete equilibrium constants, electrolyte equilibria, and reaction rates: Jour. Phys. Chemistry, v. 74, p. 346-355.

———— 1972, Predictions of the geochemical behavior of aqueous electrolytes at high temperatures and pressures: Chem. Geology, v. 10, p. 59-68.

Masson, D. O., 1929, Solute molecular volumes in relation to solvation and ionization: Philos. Mag., v. 8, p. 218-235.

Matheson, R. A., 1969, The thermodynamics of electrolyte equilibria in media of variable water composition: Jour. Phys. Chemistry, v. 73, p. 3635-3642.

Mathieson, J. G., and Conway, B. E., 1974, Partial molal compressibilities of salts in aqueous solution and assignment of ionic contributions: Jour. Solution Chemistry, v. 3, p. 455-477.

Mikhailov, V. A., and Drakin, S. I., 1960, Mechanism of the solvation of ions: Akad. Nauk SSSR Izv. Sibirsk. Otd., v. 6, p. 44-52.

Millero, F. J., 1967, Apparent molal volumes of sodium fluoride in aqueous solutions at 25°C: Jour. Phys. Chemistry, v. 71, p. 4567-4569.

———— 1970, The apparent and partial molal volume of aqueous sodium chloride solutions at various temperatures: Jour. Phys. Chemistry, v. 74, p. 356-362.

———— 1971, The molal volumes of electrolytes: Chem. Rev., v. 71, p. 147-176.

———— 1972a, The partial molal volumes of electrolytes in aqueous solutions, *in* Horne, R. A., ed., Water and aqueous solutions: New York, John Wiley & Sons, Inc., p. 519-564.

Millero, F. J., 1972b, Compilation of the partial molal volumes of electrolytes at infinite dilution, $\bar{V}^\circ$, and the apparent molal volume concentration dependence constants, S_V^* and b_V, at various temperatures, *in* Horne, R. A., ed., Water and aqueous solutions: New York, John Wiley & Sons, Inc., p. 565-595.

———— 1973, Theoretical estimates of the isothermal compressibility of sea water: Deep-Sea Research, v. 20, p. 101-105.

Millero, F. J., Hoff, E. V., and Kahn, L., 1972, The effect of pressure on the ionization of water at various temperatures from molal-volume data: Jour. Solution Chemistry, v. 1, p. 309-327.

Millero, F. J., Knox, J. H., and Emmet, R. T., 1972, A high-precision, variable-pressure magnetic float densimeter: Jour. Solution Chemistry, v. 1, p. 173-186.

Mukerjee, P., 1961, On ion-solvent interactions. Part I. Partial molal volumes of ions in aqueous solution: Jour. Phys. Chemistry, v. 65, p. 740-744.

———— 1966, Ionic partial molal volumes and electrostrictions in aqueous solution: Jour. Phys. Chemistry, v. 70, p. 2708.

North, N. A., 1973, Pressure dependence of equilibrium constants in aqueous solutions: Jour. Phys. Chemistry, v. 77, p. 931-940.

Noyes, A. A., 1907, The electrical conductivity of aqueous solutions: Carnegie Inst. Washington, Pub. 63, p. 1-352.

Noyes, A. A., Kato, Y., and Sosman, R. B., 1910, The hydrolysis of ammonium acetate and the ionization of water at high temperatures: Am. Chem. Soc. Jour., v. 32, p. 159-178.

Noyes, R. M., 1962, Thermodynamics of ion hydration as a measure of effective dielectric properties of water: Am. Chem. Soc. Jour., v. 84, p. 513-521.

———— 1964, Assignment of individual ionic contributions to properties of aqueous ions: Am. Chem. Soc. Jour., v. 86, p. 971-979.

Olofsson, G., and Hepler, L. G., 1975, Thermodynamics of ionization of water over wide ranges of temperature and pressure: Jour. Solution Chemistry, v. 4, p. 127-143.

Oshry, H. I., ms, 1949, The dielectric constant of saturated water from the boiling point to the critical point: Ph.D. dissert., Univ. Pittsburgh, Pittsburgh, Pa., 13 p.

Ostapenko, G. T., and Samoilovich, L. A., 1971, Partial and apparent molar volumes in aqueous lithium chloride, sodium chloride, and potassium chloride solutions at high temperature and pressures: Russian Jour. Phys. Chemistry, v. 45, p. 1198-1199.

Owen, B. B., and Brinkley, S. R., 1942, Calculation of the effect of pressure upon ionic equilibria in pure water and in salt solutions: Chem. Rev., v. 29, p. 461-474.

Owen, B. B., Miller, R. C., Milner, C. E., and Cogan, H. L., 1961, The dielectric constant of water as a function of temperature and pressure: Jour. Phys. Chemistry, v. 65, p. 2065-2070.

Padova, J., 1963, Ion-solvent interaction. II. Partial molar volume and electrostriction: a thermodynamic approach: Jour. Chem. Physics, v. 39, p. 1552-1560.

Pankhurst, M. H., 1969, The determination and interpretation of absolute partial molal ionic volumes: Rev. Pure Appl. Chemistry, v. 19, p. 45-59.

Parker, V. B., Wagman, D. D., and Evans, W. H., 1971, Selected values of chemical thermodynamic properties. Tables for the alkaline earth elements: Natl. Bur. Standards. Tech. Note 270-6, 106 p.

Pauling, L., 1948, The nature of the chemical bond: Ithaca, New York, Cornell Univ. Press, 450 p.

Pearson, D., Copeland, C. S., and Benson, S. W., 1963a, The electrical conductance of aqueous sodium chloride in the range 300 to 383°: Am. Chem. Soc. Jour., v. 85, p. 1044-1047.

———— 1963b, The electrical conductance of aqueous hydrochloric acid in the range 300 to 383°: Am. Chem. Soc. Jour., v. 85, p. 1047-1049.

Pesce, G., 1932, Variation with concentration of equivalent refraction of dissolved electrolytes: Zeitschr. phys. Chemie., A160, p. 295-300.

Pottel, R., 1969, The complex dielectric constant of some aqueous electrolyte solutions in a wide frequency range, *in* Conway, B. E. and Barradas, R. G., ed., Chemical physics of ionic solutions: New York, John Wiley & Sons, Inc., p. 581-596.

———— 1973, Dielectric Properties, *in* Franks, F., ed., Water, V. 3, Aqueous solutions of simple electrolytes: New York, Plenum Press, p. 401-431.

Powell, R. E., and Latimer, W. M., 1951, The entropy of aqueous solutes: Jour. Chem. Physics, v. 19, p. 1139-1141.

Quist, A. S., 1970, The ionization constant of water to 800° and 4000 bars: Jour. Phys. Chemistry, v. 74, p. 3396-3402.

Quist, A. S., Franck, E. U., Jolley, H. R., and Marshall, W. L., 1963, Electrical conductances of aqueous solutions at high temperatures and pressure. I. The conductances of potassium sulfate-water solutions from 25 to 800° and at pressures up to 4000 bars: Jour. Phys. Chemistry, v. 67, p. 2453-2459.

Quist, A. S., and Marshall, W. L., 1965, Estimation of the dielectric constant of water to 800°: Jour. Phys. Chemistry, v. 69, p. 3165-3167.

———— 1966, Electrical conductances of aqueous solutions at high temperatures and pressures. III. The conductances of potassium bisulfate solutions from 0-700° and at pressures to 4000 bars: Jour. Phys. Chemistry, v. 70, p. 3714-3725.

———— 1968a, Electrical conductances of aqueous sodium chloride solutions from 0-800° and at pressures to 4000 bars: Jour. Phys. Chemistry, v. 72, p. 684-703.

———— 1968b, Electrical conductances of aqueous hydrogen bromide solutions from 0-800°C and at pressures to 4000 bars: Jour. Phys. Chemistry, v. 72, p. 1545-1552.

———— 1968c, Ionization equilibria in ammonia-water solutions to 700° and to 4000 bars of pressure: Jour. Phys. Chemistry, v. 72, p. 3123-3128.

———— 1968d, Electrical conductances of aqueous sodium bromide solutions from 0 to 800° and at pressures to 4000 bars: Jour. Phys. Chemistry, v. 72, p. 2100-2105.

———— 1969, The electrical conductances of some alkali metal halides in aqueous solutions from 0-800° and at pressures to 4000 bars: Jour. Phys. Chemistry, v. 73, p. 978-985.

Quist, A. S., Marshall, W. L., and Jolley, H. R., 1965, Electrical conductances of aqueous solutions at high temperatures and pressure. II. The conductances and ionization constants of sulfuric acid-water solutions from 0-800° and at pressures up to 4000 bars: Jour. Phys. Chemistry, v. 69, p. 2726-2735.

Ravich, M. I., and Borovaya, F. E., 1971, Volume properties of aqueous solutions of potassium sulphate at elevated pressures in the temperature range 300-500°C: Russian Jour. Inorganic Chemistry, v. 16, p. 1662-1666.

Redlich, O., 1940, Molal volumes of solutes. IV: Jour. Phys. Chemistry, v. 44, p. 619-629.

Redlich, O., and Biegeleisen, J., 1942a, Molal volumes of solutes. VI. Potassium chlorate and hydrochloric acid: Am. Chem. Soc. Jour., v. 64, p. 758-760.

———— 1942b, Molal volumes. V. Thermodynamic properties of electrolytes at infinite dilution: Chem. Rev., v. 30, p. 171-179.

Redlich, O., and Meyer, D. M., 1964, The molal volumes of electrolytes: Chem. Rev., v. 64, p. 221-227.

Redlich, O., and Rosenfeld, P., 1931, The theory of the molal volume of a dissolved electrolyte. II: Zeitschr. Elektrochemie, v. 37, p. 705-711.

Renkert, H., and Franck, E. U., 1969, Elektrische Leitfähigkeit wässeriger Lösungen bei hohen Temperaturen und hohen Drucken. IV. Kaliumchlorid bis 350°C und 8 kbar: Ber. Bunsengesell. für Phys. Chemie, v. 74, p. 40-42.

Ritzert, G., and Franck, E. U., 1968, Elektrische Leitfähigkeit wasseriger Lösungen bei hohen Temperaturen und Drucken. I. KCl, $BaCl_2$, $Ba(OH)_2$, und $MgSO_4$ bis 750°C und 6 kbar: Ber. Bunsengesell. für Phys. Chemie, v. 72, p. 798-808.

Robinson, R. A., 1937, The osmotic and activity coefficient data of some aqueous salt solutions from vapor-pressure measurements: Am. Chem. Soc. Jour., v. 59, p. 84-90.

Robertson, R. E., Sugamori, S. E., Tse, R., and Wu, C. Y., 1966, The solvent isotope effect and the partial molar volume of ions: Canadian Jour. Chemistry, v. 44, p. 487-494.

Root, C. W., ms, 1932, II. The volume of salts in aqueous solution: Ph.D. thesis, Harvard Univ., Cambridge, Mass.

Rosseinsky, D. R., 1965, Electrode potentials and hydration energies. Theories and Correlations: Jour. Chem. Eng. Data, v. 10, p. 467-490.

Ryzhenko, B., ms, 1974, Regularities of the thermodynamic process of electrolytic dissociation of inorganic substances and evaluation of the form of transport of chemical elements in hydrothermal solutions: Ph.D. dissert., submitted to the Order of Lenin Inst. Geochemistry and Analytic Chemistry, Moscow, USSR, 51 p.

Samoilov, O. Y., 1957, Structure of aqueous electrolyte solutions and the hydration of ions [translated by D. J. G. Ives]: Faraday Soc. Disc., v. 24, 141 p.

———— 1965, Structure of aqueous electrolyte solutions and the hydration of ions [translated by D. J. Ives]: New York, Consultants Bur., 185 p.

———— 1972, Residence times of ionic hydration, *in* Horne, R. A., ed., Water and aqueous solutions: New York, Wiley-Interscience, p. 597-610.

Schmidt, E., 1969, Properties of water and steam in SI-units: New York, Springer-Verlag, 205 p.

Schumm, R. H., Wagman, D. D., Bailey, S., Evans, W. H., and Parker, V. B., 1973, Selected values of chemical thermodynamic properties: Natl. Bur. Standards Tech. Note 270-7, 76 p.

Scott, A. F., 1931, The apparent volumes of salts in solution. I. A test of the empirical rule of Masson: Jour. Phys. Chemistry, v. 35, 2315-2329.

Scott, A. F., and Wilson, R. W., 1934, The apparent volumes of salts in solution and their compressibilities: Jour. Phys. Chemistry, v. 38, p. 951-977.

Shedlovsky, T., and Brown, A. S., 1934, Electrolytic conductivity of alkaline earth chlorides in water at 25°: Am. Chem. Soc. Jour., v. 56, p. 1066-1071.

Sienko, M. J., and Plane, R. A., 1963, Physical inorganic chemistry: New York, W. A. Benjamin Inc., 166 p.

Stokes, R. H., 1964, The van der Waals radii of gaseous ions of the noble gas structure in relation to hydration energies: Am. Chem. Soc. Jour., v. 86, p. 979-982.

Stokes, R. H., and Robinson, R. A., 1957, Application of volume-fraction statistics to the calculation of activities of hydrated electrolytes: Faraday Soc. Trans., v. 53, p. 301-304.

———— 1973, Solvation equilibria in very concentrated electrolyte solutions: Jour. Solution Chemistry, v. 2, p. 173-184.

Tait, P. G., 1889, Report on some physical properties of fresh water and of sea-water, *in* Thomson, Sir Charles Wyville, Physics and Chemistry Series, v. 2, Report on the Scientific Results of the Voyage of HMS Challenger during the years 1873-1876: London, The Stationery Office, p. 1-76.

Tammann, G., 1893, Über die Binnendrucke in Lösungen: Zeitschr. Phys. Chemie, v. 11, p. 676-693.

———— 1895, Über die volumen Veränderungen bei der Neutralisation verdünnter Lösungen: Zeitschr. Phys. Chemie, v. 16, p. 91-96.

Tham, M. K., Gubbins, K. E., and Walker, R .D., 1967, Densities of potassium hydroxide solutions: Jour. Chem. Eng. Data, v. 12, p. 525-526.

Tödheide, K., 1972, Water at high temperatures and pressures, *in* Franks, F., ed., Water, V. I. The physics and physical chemistry of water: New York, Plenum Press, p. 463-514.

Vaslow, F., 1966, The apparent molal volumes of the alkali metal chlorides in aqueous solution and evidence for salt-induced structure transitions: Jour. Phys. Chemistry, v. 70, p. 2286-2294.

———— 1969, Apparent molal volumes of the lithium and sodium halides. Critical-type transitions in aqueous solution: Jour. Phys. Chemistry, v. 73, p. 3745-3750.

———— 1972, Thermodynamics of solutions of electrolytes, in Horne, R. A., ed., Water and aqueous solutions: New York, Wiley-Interscience, p. 465-518.

Voet, A., 1936, Ionic radii and heat of hydration: Faraday Soc. Trans., v. 32, p. 1301-1304.

Wagman, D. D., Evans, W. H., Halow, I., Parker, V. B., Bailey, S. M., and Schumm, R. H., 1968, Selected values of chemical thermodynamic properties. Part 3: Natl. Bur. Standards Tech. Note 270-3, 264 p.

Wagman, D. D., Evans, W. H., Parker, V. B., Halow, I., Bailey, S. M., and Schumm, R. H., 1968, Selected values of chemical thermodynamic properties. Pt. 3: Natl. ments 35 through 53 in the standard order of arrangement: Natl. Bur. Standards Tech. Note 270-4, 152 p.

Wagman, D. D., Evans, W. H., Parker, V. B., Halow, I., Bailey, S. M., Schumm, R. H., and Churney, K. L., 1971, Selected values of chemical thermodynamic properties. Tables for elements 54 through 61 in the standard order of arrangement: Natl. Bur. Standards Tech. Note 270-5, 37 p.

Whalley, E., 1963, Some comments on electrostatic volumes and entropies of solvation: Jour. Chem. Physics, v. 38, p. 1400-1405.

Whitfield, M., 1972, Self-ionization of water in dilute sodium chloride solutions from 5-35°C and 1-2000 bars: Jour. Chem. Eng. Data, v. 17, p. 124-128.

Wicke, E., 1966, Structure formation and molecular mobility in water and aqueous solutions: Angew. Chemie, Internat. Ed., v. 5, p. 106-122.

Wicke, E., Eigen, M., and Ackerman, Th., 1954, Über den Zustand des Protons (Hydroniumions) in wässeriger Lösungen: Zeitschr. Phys. Chemie, p. 340-364.

Wirth, H. E., 1937, The partial molal volumes of potassium chloride, potassium bromide and potassium sulfate in sodium chloride solutions: Am. Chem. Soc. Jour., v. 59, p. 2549-2554.

———— 1940, Density of sea water: Jour. Marine Research, v. 3, p. 230-247.

Wirth, H. E., and Collier, F. N., 1950, Apparent and partial molal volumes of sodium perchlorate and perchloric acid in mixed solutions: Am. Chem. Soc. Jour., v. 72, p. 5292-5296.

Wright, J. M., Lindsay, W. T., and Druga, T. R., 1961, The behavior of electrolyte solutions at elevated temperatures as dervied from conductance measurements: Washington, D.C., U.S. Atomic Energy Comm., WAPD-TM-204.

Wulff, C. A., 1967, Entropies of the aqueous Zn^{+2}, Cd^{+2}, Hg^{-2} and Hg_2^{+2} ions: Jour. Chem. Eng. Data, v. 12, p. 82-85.

Zen, E-an, 1957, Partial molar volumes of some salts in aqueous solutions: Geochim. et Cosmochim. Acta, v. 12, p. 103-122.